The University of Nottingham

UNITED KINGDOM · CHINA · MALAYSIA

Development of Biomimetic Platforms to Investigate the Influence of the Extra-Cellular Environment on Immunological Responses

Amy Rose Donaldson

Thesis submitted to the University of Nottingham for the degree of Doctor of Philosophy

Immunology Department, School of Life Sciences,
University of Nottingham

August 2016

Abstract

The immune system comprises highly sophisticated networks of cells and signalling molecules which function in concert to protect the body against pathogens. Within this system a role for the extra-cellular microenvironment as a crucial mediator of immune responses is becoming increasingly apparent.

Conventional *in vitro* cultures lack physiologically relevant extra-cellular cues, such as extracellular matrix (ECM) and shear flow. Tissue engineering can be used to simulate features of the natural microenvironment for the development of biologically relevant platforms. It is anticipated that this will enable the study of the influence of the extra-cellular environment on immune responses.

This thesis describes the development and characterisation of tissue-engineered platforms for immune cell culture which incorporate the ECM and shear flow. This work goes on to apply these platforms for the study of the effect of the extra-cellular environment on dendritic cells and their interactions with T cells in the context of immunological stimulation.

The ECM defines the three-dimensional architecture of the natural microenvironment. It provides structural support and also promotes cell motility in tissues. This is important for the function of the immune system as it directs the organisation and interactions of immune cells which ultimately contributes to the modulation of immune responses.

Candidate synthetic and natural biomaterials were assessed for their suitability to provide an *in vitro* extracellular matrix (ECM) platform for human immune cell culture. The suitability of these materials to provide an artificial ECM platform was based on the viability, resting immune state and immune competence of the cells.

The synthetic biomaterials tested were a thermo-responsive colloidal gel and electrospun PET and PLGA scaffolds coated with a thermo-responsive polymer. An important finding from the work done with the colloidal gel was that the human dendritic cells, which were incorporated into the gel at the beginning of the experiment, could not be separated from the material for flow cytometric analysis. Therefore, characterisation of the colloidal gel for immune cell culture could not be completed. Regarding the characterisation of the electrospun PET and PLGA scaffolds, although they did not significantly impair cell viability of dendritic cells they were found to induce cell maturation. As a result, none of the synthetic biomaterials were found to be a suitable ECM surrogate.

A semi-natural biomaterial, gelatin methacryloyl (GelMA) hydrogel, was included in the investigation. The results from the characterisation of GelMA for human immune cell culture indicated that the hydrogel induced a pro-inflammatory immune response due to the profile of secreted cytokines. Based on this, GelMA was also discounted as an appropriate material for the development of the ECM platform.

The final ECM candidate was a collagen hydrogel, which is a naturally-derived biomaterial. The collagen hydrogel was shown to support immune cell survival and human dendritic cells maintained an immature phenotype in culture. In addition, typical responses to immunological stimuli by human dendritic cells and T cells were observed in collagen hydrogel cultures. This work demonstrated that out of the biomaterials which were characterised, the collagen hydrogel was the most suitable biomaterial for the development of the ECM platform.

The influence of the collagen hydrogel ECM platform on antigen-specific immune responses was investigated in the context of autologous human dendritic cell and T cell co-cultures stimulated with the model antigen *Mycobacterium tuberculosis* purified protein derivative, also referred to as PPD. The results from these experiments indicated that the presence of the collagen hydrogel increased the sensitivity and specificity of the immune response, compared to conventional tissue culture conditions.

An attempt was made at utilising the ECM platform to investigate immune responses to chemical sensitisers to address the requirement for *in vitro* alternatives to replace current animal testing methods. In this work, innate and adaptive immune responses to sensitisers were detected using the ECM platform. However, the reproducibility of these experiments was low due to large donor variation. Therefore the effect of the ECM platform on immune responses to sensitisers could not be evaluated. This difficulty likely reflects the complexity of the molecular and cellular mechanisms which lead to the acquisition of chemical sensitisation.

Shear flow is a type of physiological stress to which immune cells are exposed *in vivo* due to the movement of blood and lymph fluid. Recent studies have implicated flow as an immunologically relevant stimulus, capable of inducing changes in the expression of receptors and chemokines involved in regulating immune cell migration, and activating immune receptor signalling.

A fluidic cell culture platform was developed to recapitulate the effect of shear flow. Two different prototypes were constructed, one of which was taken forward and characterised for immune cell culture applications.

The fluidic platform taken forward had a paper-based cell culture scaffold which was coated with collagen hydrogel. The scaffold was found to induce maturation of human dendritic cells which was attributed to the possibility of incomplete coverage of the scaffold by the collagen hydrogel. The viability of dendritic cells was slightly impaired by flow, however not significantly. Interestingly, when exposed to shear flow, dendritic cells maintained a less mature phenotype compared to their static counterparts.

Antigen-specific immune responses were studied on the fluidic platform by setting up co-cultures comprising PPD-stimulated autologous human dendritic cells and T cells. Typical T cell activation was observed on the platform and the sensitivity and specificity of immune responses was found to be greater under flow conditions, compared with static cultures.

In conclusion, this thesis demonstrates the value of developing biomimetic platforms for studying the influence of the extra-cellular environment on immune responses.

Finally, the ability to mimic extra-cellular cues to which cells are exposed *in vivo* has the potential to generate more realistic immune responses in the lab. This presents huge opportunities for advancing understanding in immunology. It also has implications for methods used in research, drug discovery and safety testing, where currently only animals provide a representative system for the study of immune reactions. It is anticipated that enhancing the physiological relevance of *in vitro* cell culture will ultimately contribute to the reduction of animals used in research and testing.

Acknowledgements

To begin, I would like to thank my academic supervisors, particularly Professor Amir Ghaemmaghami for giving me the opportunity to work under his supervision and for his support throughout my PhD. Many thanks also to my co-supervisors Professor Cameron Alexander and Doctor Felicity Rose for their expert opinions on and guidance of my research.

I would like to acknowledge those who have assisted me with my experimental work. Thanks to Doctor David Onion and Nikki Croxall for their support in flow cytometry; Laurence Hall for his contribution to the gene expression studies; Christie Grainger-Boultby for her help with SEM; Doctor Tim Self for training and advice on the confocal microscope, and to all of the members of the Polymer Therapeutics Group at the University of Nottingham, particularly Afnan Aladdad and Shwana Braim for providing some of the materials for my work.

I wish to acknowledge the external collaborators from the Ziaie Biomedical Microdevices Lab, Perdue, USA, particularly Rahim Rahimi for the fluidic devices and technical guidance he provided.

I am grateful for the opportunities I have had had during my PhD. Particularly the valuable experience I gained from my visits to the Khademhosseini Lab, MIT, Boston, USA. I would like to thank Doctors Mehdhi Nikkhah and Waseem Asghar for their support during the time I spent there.

I would like to acknowledge the NC3Rs for providing the financial support which made this project possible.

I wish to thank all of the past and present members of the Allergy and Tissue Modelling Group. In particular Doctor Fabian Salazar, Doctor Sonali Singh, Doctor Wejdan Aldajani, Su Su Htwe, Raudzah Kamal, Asha Hassan, Shehnaz Ahmed, Hassan Rostam and Doctor Paul Cato. You've all been a constant source of support and inspiration.

Thank you to my friends Ellie, Nicola, Laura and Lucinda for your support and for persuading me to occasionally take a break from work!

To all of my family, the biggest thank you, especially to my grandparents who have done so much for me and to my sister and best friend Kate, who has been there for me through all of the highs and lows.

Last, but not least, to my parents, for your unconditional love and support, thank you. Without your belief in me I would never have achieved what I have.

I wish to dedicate this thesis to my uncle Andy, I miss you every day and hope you would have been proud. Lots of love.

Contents

Table of Figures

Table of Tables

Abbreviations

(A)MLR – (autologous) mixed lymphocyte reaction

(d)H_2O – (deionized) water

2D – two dimensional

3D – three dimensional

Ab\Am – antibiotic\antimycotic

ACD – allergic contact dermatitis

AF – *Aspergillus fumigatus*

APC – antigen presenting cell

ARE – antioxidant response element

ATP – adenosine triphosphate

BCG – Bacillus Calmette-Guérin

BrdU – 5-bromo-2'-deoxyuridine

BSA – bovine serum albumin

CCL – C-C motif chemokine ligand

CCR – C-C chemokine receptor

CD – cluster of differentiation

CHS – contact hypersensitivity

CiGiP – cells-in-gels-in-paper

CFSE – carboxyfluorescein succinimidyl ester

DAMP – danger-associated molecular pattern

DAPI – 4',6-Diamidino-2-phenylindole

DC – dendritic cell

DNA – deoxyribonucleic acid

DNCB – 2,4-Dinitrochlorobenzene

DTH – delayed-type hypersensitivity

ECM – extracellular matrix

ELISA – enzyme-linked immunosorbent assay

FACS – fluorescence-activated cell sorting

FCS – foetal calf serum

FDA – Food and Drug Administration

FITC – fluorescein isothiocyanate

FS – forward scatter

GAPDH – glyceraldehyde 3-phosphate dehydrogenase

GelMA – gelatin methacryloyl

GMC-SF – granulocyte macrophage colony-stimulating factor

HEV – high endothelial vessel

ICAM-1 – Intercellular Adhesion Molecule 1

IFN-γ – interferon-gamma

IgG – immunoglobulin G

IL – interleukin

ITAM – immunoreceptor tyrosine-based activation motif

ITS – integrated test strategy

Keap1 – Kelch-like ECH-associated protein

LFA-1 – lymphocyte function-associated antigen-1

LLNA – local lymph node assay

LMW – low molecular weight

LN – lymph node

LPS – lipopolysaccharide

LTBI – latent TB infection

MFI – median fluorescence intensity

MHC – major histocompatibility complex

moDC – monocyte-derived dendritic cell

moDC – monocyte-derived dendritic cells

mRNA – messenger ribonucleic acid

Mtb – *Mycobacterium tuberculosis*

NHP – non-human primate

NLR – nucleotide binding and oligomerization domain-like receptor

Nrf2 – nuclear factor erythroid 2–related factor 2

OSCAR – osteoclast-associated receptor

PAMP – pathogen-associated molecular pattern

PBMC – peripheral blood mononuclear cells

PBS – phosphate-buffered saline

PCL – polycaprolactone

PCR – polymerase chain reaction

pDC – plasmacytoid dendritic cell

PDMS – polydimethylsiloxane

PE – phycoerythrin

PEGMA – poly(polyethylene glycol methacrylate

PET – polyethylene terephthalate

PI – propidium iodide

PLGA – poly(lactic-co-glycolic acid)

PMB – polymyxin B

pMHC – peptide-loaded MHC

PMMA – poly(methyl methacrylate)

PPD – purified protein derivative

PRR – pattern recognition receptor

PS – phosphatidylserine

RLR – RIG-I-like receptor

ROS – reactive oxygen species

rpm – revolutions per minute

RT-PCR – reverse transcription PCR

SD – standard deviation

SEM – scanning electron microscopy

SLS – sodium lauryl sulphate

SS – side scatter

TB – tuberculosis

TC\TCP – tissue culture plastic

TCR – T cell receptor

TLR – Toll-like receptor

TMSPMA – 3-(Trimethoxysilyl)propyl methacrylate

TNF-α – Tumour necrosis factor-alpha

TRC – T cell zone fibroblastic reticular cell

TST – Tuberculin skin test

UV – ultraviolet

v/v % – volume per volume percent

w/v % – weight per volume percent

Chapter 1

Introduction

1.1. Considering how the microenvironment influences immunity

Dendritic cells (DCs) are strategically positioned at the interface of the innate and adaptive immune systems (Steinman, 1991). They patrol peripheral tissues, such as, the skin, gut, lung and genito-urinary tract, which are common routes for the entry of pathogens into the body (Caux et al., 1995, Austyn, 1996).

DCs actively scavenge both host and pathogen-derived material from their local environment. They migrate from sites of inflammation to secondary lymphoid organs, via the lymphatic system. This mechanism enables the delivery of peripheral antigen to naïve T cells, which are restricted to lymphoid tissues. Induction of adaptive immunity depends on efficient T cell activation, which requires antigen-specific recognition in conjunction with co-stimulatory factors produced by DCs (Cella et al., 1997b, Hart, 1997).

In vivo, DCs interact with the extracellular matrix (ECM), within a 3D environment (Garcia-Nieto et al., 2010, Gunzer et al., 2004). In addition, they are likely to be subject to physical stimuli, for example, shear flow (Previtera, 2014, Swartz et al., 2008).

The profound influence of the extra-cellular environment on the biological function of DCs, and the outcome of interactions between DCs and T cells, is becoming apparent based on findings from recent studies. However, most of the current understanding of DC biology comes from *in vitro* cultures, which are performed in the absence of extra-cellular cues.

Assays which comprise DCs are valuable tools in areas of research, drug development and safety testing. The requirement and usage of *in vitro* assays is increasing due to restrictions on animal testing methods. However, these methods are currently limited by their lack of biological relevance.

Enhancing the biological relevance of immune cell assays is anticipated to provide a more realistic representation of immune responses and thus more accurately predict the immunological outcomes of drug and chemical exposure in humans.

Tissue engineering enables recapitulation of features and functions of natural tissues through the combination of cells and scaffolds and appropriate biological, chemical or physical signals. Thus, tissue engineering technologies can be used to address the simplistic, artificial nature of conventional immunological assays by simulating certain aspects of the *in vivo* microenvironment (Pampaloni et al., 2007).

1.2. Introducing Dendritic Cells

Dendritic cells were identified by Ralph Steinman and Zanvil Cohn in the late 1970s. They have since been proven to be highly specialised antigen presenting

cells (APCs), due to their dedicated role in the induction of specific adaptive immunity against foreign antigen (Steinman, 1991). Broadly speaking, DCs reside within peripheral tissues and upon recognition of 'danger' signals they are capable of directing the induction of the adaptive immune system.

As illustrated in Figure 1, DCs originate from a common progenitor in the bone marrow. A major distinction in the DC family can be made between classical and plasmacytoid DCs (pDCs). Although they have similar origins, pDCs differ in that they predominately partition to the blood and lymphoid tissues. pDCs are responsive to virus-derived stimuli, and as a result, produce large amounts of IFN-γ. Following viral stimulation, pDCs differentiate, thereby acquiring a mature phenotype which allows them to activate specific T cells effectively (Liu, 2005, Reizis et al., 2011).

Classical DCs describe the cells discovered by Steinman and include all DCs, apart from pDCs. For the purposes of this thesis, further discussions relate only to the function of classical DCs.

There are several developmentally and functionally distinct subsets of DCs. In the last fifteen years, the scope of DC diversity, and the biological significance of this, has become apparent (Merad et al., 2013). The different DC subsets arise through complex developmental programmes determined by cytokine signalling and transcriptional control. Depending on the subset, DCs reside throughout the body in lymphoid and non-lymphoid tissues.

One DC subset which is set apart from the rest is the epidermal Langerhans cells. These cells reside in the epidermal layer of the skin and represent 3-5% of epidermal cells. They are unlike other DC subsets as they have to capacity to self-renew. Langerhans cells have distinct characteristics, including the presence of Birbeck granules, and expression of cluster of differentiation (CD) 1a and langerin (Ginhoux and Merad, 2010).

During times of tissue injury and infection, it is likely that tissue-resident DCs, such as Langerhans cells, become depleted. Therefore monocytes can be recruited to sites of inflammation and subsequently differentiate to become monocyte-derived DCs (moDCs) (Leon and Ardavin, 2008).

The study of DCs *in vitro* has been facilitated by the ability to isolate monocytes. DCs are commonly generated through the culture of monocytes in the presence of interleukin (IL)-4 and granulocyte macrophage colony-stimulating factor (GM-CSF), which leads to the differentiation of monocyte-derived DCs (moDCs). moDCs have comparable phenotypic and functional characteristics to their *in vivo* counterparts (Sallusto and Lanzavecchia, 1994, Horlock et al., 2007).

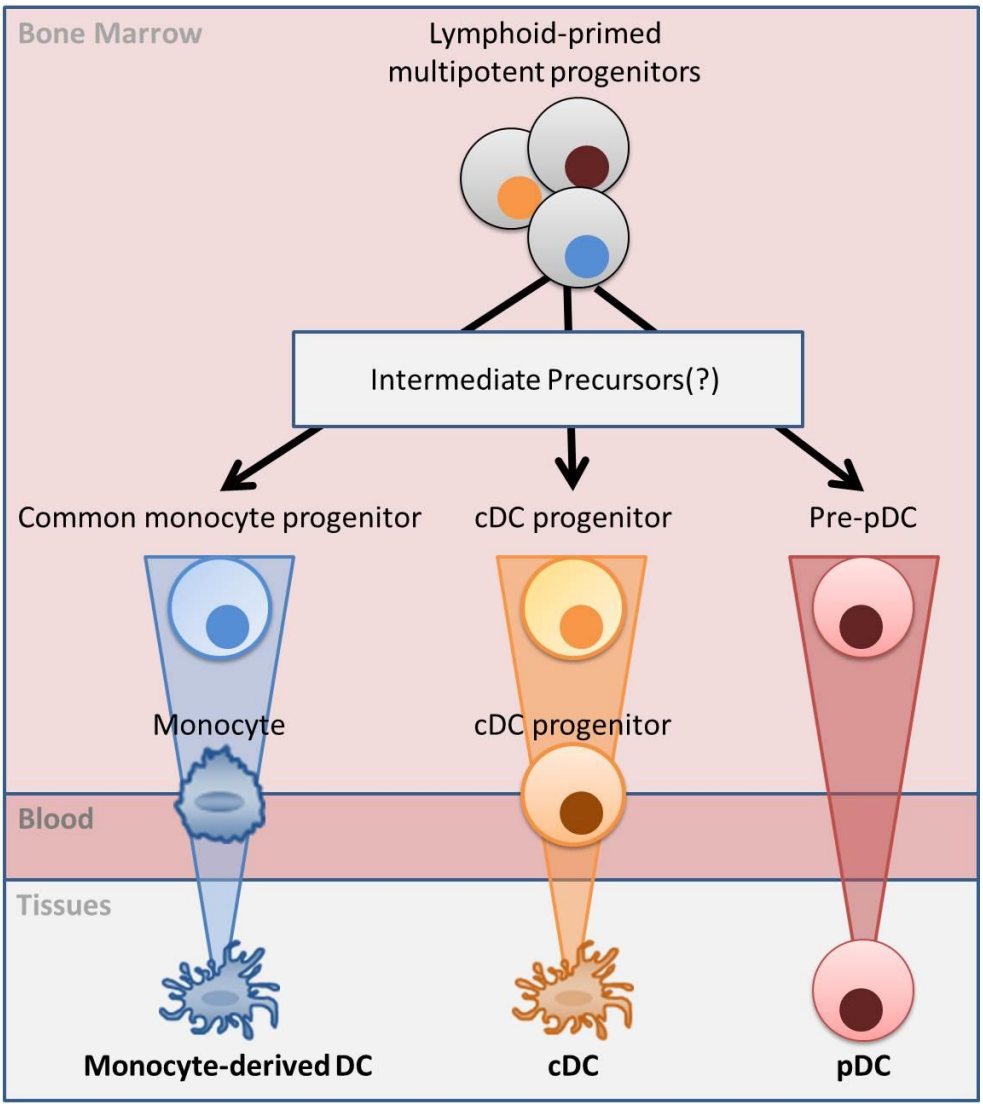

Figure 1. Dendritic cell development.
Dendritic cells originate from common bone marrow precursors, named lymphoid-primed multipotent progenitors. The existence of intermediate precursors is controversial, it has been suggested that a macrophage and DC precursor, which differentiates into a common DC precursor may exist. Classical DC (cDC) progenitors can be distinguished from pre-plasmacytoid DCs (pDCs). cDC progenitors give rise to subsets of cDCs. Pre-pDCs are restricted to pDC differentiation. Monocytes arise from common monocyte progenitors and can differentiate in response to inflammatory signals from the environment into monocyte-derived DCs ((Schraml and Reis e Sousa, 2015, Poltorak and Schraml, 2015).

The Role of Dendritic Cells in Immunity

DCs provide a mechanism for the transport of peripheral antigens to naïve T cells for the induction of adaptive immune responses. This is important as naïve T cells are restricted to lymphoid tissues. DCs do not have a passive role in this process, they direct appropriate immune responses depending on the

immunological context of the tissue from which they originate (Flores-Romo, 2001).

The plasticity of the phenotype and function of DCs contributes to their specialised role as APCs for the modulation of adaptive immunity (Lanzavecchia and Sallusto, 2001). In the steady-state, DCs are classed as 'immature'. These cells can be identified based on their high endocytic activity, which allows efficient antigen sampling, and absence, or low-level expression of cell-surface co-stimulatory molecules and inflammatory cytokines (Lutz and Schuler, 2002, Banchereau et al., 2000).

Pathogen Recognition

DC maturation can be induced as a result of exposure to microbes (bacteria, fungi, viruses and parasites), certain chemicals, or tissue injury. Activation of DCs in response to these stimuli occurs through pattern recognition receptors (PRRs). These receptors are expressed by APCs to ensure the rapid activation of protective pathways of the innate immune system in response to potential pathogens and tissue damage (Gordon, 2002).

Several different groups have been identified which make up the PRR family, including Toll-like receptors (TLRs), nucleotide binding and oligomerization domain (NOD)-like receptors (NLRs) and RIG-I-like receptors (RLRs) (Jeong and Lee, 2011).

The recognition of microbial products by PRRs is based on conserved molecular structures, such as lipids, lipoproteins, lipopolysaccharide,

glycoproteins and nucleic acids. Together, these ligands are known as pathogen-associated molecular patterns (PAMPs) (Akira et al., 2006).

PRRs also sense host-derived products which are generated as a result of tissue damage, for example, adenosine triphosphate (ATP), low molecular weight (LMW) extracellular matrix fragments and reactive oxygen species (ROS). These ligands are collectively termed damage-associated molecular patterns (DAMPs) (Beg, 2002).

Engagement of PPRs by PAMPs or DAMPs activates signal transduction pathways which involve adaptor molecules, kinases and transcription factors. This leads to the expression of a multitude of pro-inflammatory cytokines, chemokines and cell-surface molecules which are essential for instructing the immediate innate response and, crucially, the elicitation of adaptive immunity (Mogensen, 2009, Takeuchi and Akira, 2010).

Antigen Presentation

As DCs mature, their antigen capture function is lost. Instead, their ability to present antigen is enhanced (Banchereau et al., 2000). As a rule, for the elicitation of adaptive immune responses, DCs present antigen to T cells bound to major histocompatibility complex (MHC) molecules (Guermonprez et al., 2002).

There are two classes of MHC molecule. Antigens presented via MHC class-I molecules usually derive from the cytosol, this mechanism of activation

principally targets intracellular infection or malignant cells by direct cell killing (Théry and Amigorena, 2001, Germain, 1994).

Antigens obtained though endocytic pathways are presented in association with MHC class-II molecules (ten Broeke et al., 2013). When DCs mature, transfer of peptide-loaded MCH-II to the cell membrane is increased. This leads to an accumulation of MHC-II on the cell surface, thus enhancing antigen presentation for the successful activation of naïve T cells (Cella et al., 1997a, de Saint-Vis et al.).

Migration

Increased expression of the chemokine receptor CCR7 promotes DC migration to lymphoid organs. Cell migration is directed by gradients of the chemokines CCL21 and CCL19, which are expressed by the lymphatic endothelium.

Co-stimulation

Mature DCs also express high levels of cell-surface co-stimulatory molecules, CD80, CD83, CD86 and CD40, and inflammatory cytokines, TNF-α and IL-12, which are essential for T cell activation (Flores-Romo, 2001).

DC maturation depends on the extent of the inflammatory response in the native tissue. DCs which are not fully mature lack the full complement of co-stimulatory molecules, and are therefore unable to activate T cells efficiently. Semi-mature DCs are associated with the maintenance of peripheral tolerance through the induction of regulatory T cells, T cell anergy or apoptosis (Moser, 2003).

Dendritic Cells in Contact Allergy

Inappropriate induction of adaptive immunity by non-pathogenic or host-derived products can result in devastating pathology, such as allergy or autoimmune disease. This is exemplified by the development of a severe allergic condition, known as allergic contact dermatitis (ACD), which occurs as a result of repeated skin contact with certain organic chemicals, or metal ions.

ACD, or contact hypersensitivity (CHS), is typical of a delayed type IV hypersensitivity response. As depicted in Figure 2, this develops via a well-defined series of events. The first time the sensitiser comes into contact with the skin, the induction phase is initiated, this culminates in the acquisition of specific immune sensitisation. Subsequent exposures to the same sensitising agent elicit cell-mediated immune responses, resulting in severe dermatological inflammation at the site of contact (Vocanson et al., 2009).

The development of ACD depends on the relay of immunogenic sensitiser-modified peptides from the skin, to T cells residing within draining lymph nodes, by dendritic cells. An appreciation of the mechanisms involved is useful in order to understand the role of DCs in this complex immunopathology.

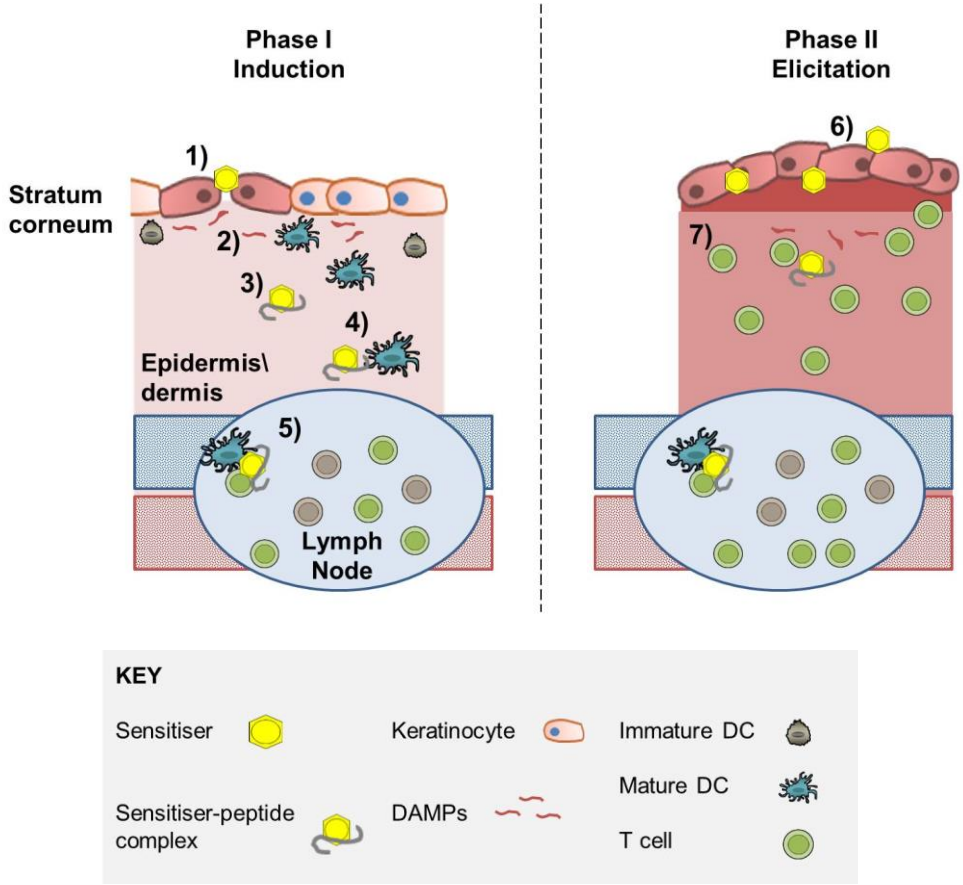

Figure 2. Development of Contact Hypersensitivity.
Induction phase: 1) Sensitiser penetration of the stratum corneum. 2) Activation of stress and innate immune responses in the skin. 3) Peptide haptenisation by sensitiser. 4) Dendritic cell activation and sensitiser-modified peptide processing. 5) Dendritic cell migration and T cell activation within lymph nodes. Elicitation phase: 6) Repeated chemical exposure. 7) Rapid T cell-mediated response directed to skin, resulting in severe inflammation and eczematous lesions. (Vocanson et al., 2009).

Key Tissues and Events in the Induction of Contact Hypersensitivity

The skin

The skin is the first hurdle for chemical sensitisers to overcome in the induction of CHS. The outer protective keratinous layer, the stratum corneum, provides a physical barrier to entry of environmental pathogens into the body (Menon et al., 2012). Genomic profiling studies have linked weakness in the skin barrier function with increased susceptibility to allergic disease, such as

ACD (Schnuch et al., 2011, Thyssen et al., 2013). However, the low molecular weight of haptens, less than 500 Daltons (Da), generally facilitates their penetration despite the integrity of the skin (Bos and Meinardi, 2000).

The epidermis is largely populated by keratinocytes and resident epidermal dendritic cells, known as Langerhans cells. Separated by the basement membrane is the dermis, which is home to subsets of dermal DCs. As the first cells to encounter environmental insults, keratinocytes are key players in initial stress and innate immune responses to sensitisers, for example, through the expression of antioxidant response genes, production of pro-inflammatory cytokines and recruitment of immune cells (van der Veen, 2011).

Keratinocytes produce metabolically active enzymes, such as cytochrome P450 isoenzymes. The metabolic activity of keratinocytes converts certain inert chemicals into reactive species able to haptenate peptides. Sensitisers which require activation via enzymatic processes are also referred to as pro-haptens (Gelardi et al., 2001).

Formation of sensitiser-modified peptide

A crucial aspect of CHS reactions is the specificity of the immune response towards the sensitising agent.

Due to the low molecular weight (LMW) and polarity of chemical sensitisers, they cannot elicit an immune response unless associated with a carrier molecule, usually a peptide. In the field of Immunology, such agents are classed as haptens (half antigens) (Martin, 2004).

Haptenisation, which was first postulated by Landsteiner and Jacobs in 1935, describes the hapten-peptide reaction which gives rise to an immunologically recognisable complex. It is widely accepted that the interaction between sensitiser and host peptide is the principle mechanism by which immunogenic products are formed (Aptula et al., 2007). The generation of sensitiser-specific determinants is fundamental to immune sensitisation.

Activation of Innate Immunity

The inherently reactive nature of chemical sensitisers causes them to act as adjuvants through the oxidative damage and cell stress they cause in the skin. This results in the production of DAMPs, which activate the innate immune system by acting as ligands for PRRs (Kaplan et al., 2012, Sloane et al., 2010).

Two groups of PRRs, Toll-like receptors (TLR) and NOD-like receptors (NLR) have been implicated in the progression of sensitisation (Martin et al., 2008, Watanabe et al., 2008). Current research is beginning to elucidate the mechanisms by which sensitiser-induced DAMP production activates innate immunity. TLR activation by LMW hyaluronic acid (HA) has been demonstrated to occur as a consequence of sensitiser-dependent ROS production (Esser et al., 2012). Also, nickel ions (Ni^{2+}), which are well-known contact sensitisers, are able to directly bind TLR4 in humans to activate the innate immune system. This mechanism could not be identified using animal models, as murine TLR4 lacks two histidine residues which define the binding site for Ni^{2+} in the human receptor (Schmidt et al., 2010).

Oxidative stress experienced by the skin-resident cells, DCs and keratinocytes, caused by the application of contact sensitisers is evident by the up-regulation of antioxidant response genes (van der Veen, 2011). The central players in the oxidative stress response are the members of the nuclear factor-κB (NF-κB) family of transcription factors (Morgan and Liu, 2011).

NF-κB proteins exist as homo- or heterodimers which bind a 10-base pair κB site within a promoter/enhancer sequence for a specific gene. Within the cytoplasm, NF-κB dimers form a complex with Inhibitor of κB (IκB) proteins; IκB proteins inhibit the transcriptional activity of NF-κB by blocking the DNA binding site. Upon stimulation of pro-inflammatory receptors, IκB is phosphorylated by IκB kinase (IKK) which targets it for proteasomal degradation. As a result, the NF-κB dimer is released and translocates to the nucleus where it regulates the expression of its associated genes (Hayden and Ghosh, 2008, Vallabhapurapu and Karin, 2009).

In the context of excessive ROS, caused by contact sensitiser exposure, NF-κB modulates the amount of ROS by inducing the expression of antioxidant genes. This ultimately reduces the ROS concentration and promotes cell survival (Morgan and Liu, 2011).

An additional mechanism for the transcriptional regulation of antioxidant genes is the Keap1-Nrf2 pathway; under steady state conditions, Keap1 (Kelch-like ECH-associated protein) complexes with Nrf2 (nuclear factor erythroid 2–related factor 2). Oxidative stress causes Nrf2 to dissociate and translocate to the nucleus, where it acts as a transcription factor for genes with antioxidant

response elements (ARE) in their promoter (Natsch, 2010, Natsch and Emter, 2008).

Activation of the innate immune system causes inflammation of the affected tissue and induction of dendritic cell maturation. The inflammatory setting experienced by DCs in the local tissue environment is important in determining the extent of the T cell response (Tuschl et al., 2000, Reiser and Schneeberger, 1996).

Induction of Specific Immunity

Dendritic cells are the link to the elicitation of the sensitiser-specific cell response. They present skin-derived haptenated peptides to naïve T cells within draining lymph nodes (LNs) (Vocanson et al., 2009, Xu et al., 1996). There is evidence for the contribution of several DC subsets in the development of ACD. Untangling their roles is complex and made difficult by the limitations of experimental models of DC depletion. However, it is likely that both skin-resident DCs, such as Langerhans cells, and peripherally-recruited moDCs play a role in T cell priming (Vocanson et al., 2009, Honda et al., 2010, Noordegraaf et al., 2010).

CHS is governed by a cell-mediated adaptive immune response, which means T cells have a key role in determining the pathology of this condition. Therefore, T cell priming by DCs in the LN is arguably one of the most important events in the induction of chemical sensitisation. Recognition of cognate antigen through the antigen presenting function of DCs results in T cell activation and clonal expansion.

Sensitiser-primed T cells subsequently migrate from LNs and circulate peripheral and lymphoid tissues. Upon re-exposure to the sensitiser, effector T cells exert a cytotoxic response at the site of chemical contact. This reaction constitutes the elicitation phase, which presents as severe dermatological inflammation (Vocanson et al., 2009).

1.3. Lymph Nodes are Specialised to Choreograph Interactions Between Dendritic Cells and T Cells

Secondary lymphoid organs, including lymph nodes (LNs), are essential for the orchestration of adaptive immunity. They provide sites for the coordination of immune cells, antigen and inflammatory signals. This increases the efficiency of immune responses, as lymphocytes do not have to navigate the entire periphery to encounter their antigen.

Lymph nodes contain a wealth of information with regards to the immunological status of peripheral tissues. Following exposure to pathogen or chemical sensitiser, lymph fluid brings antigen-loaded DCs, free antigen and inflammatory cytokines, to LNs via the lymphatic system (Randolph et al., 2005). Lymph fluid is transported to LNs by afferent vessels and then driven through sinuses which extend through the organ. It is subsequently drained by the efferent vessel.

The circulatory system is closely associated with LNs, which provides a point for naïve T cell entry. As an artery penetrates the LN, it differentiates into a

high endothelial vessel (HEV). The squamous endothelium and expression of specific cell-surface markers promotes the migration of lymphocytes from the blood into the LN through a defined multi-step adhesion cascade (von Andrian and Mempel, 2003). In this process, lymphocytes initially become loosely tethered to the wall of the HEV through L-selectin and the endothelial-expressed L-selectin ligand, PNAD. They roll slowly until integrin leukocyte function-associated antigen 1 (LFA 1) interacts with intercellular adhesion molecules (ICAM) 1 and 2 to mediate their arrest. This is dependent on integrin activation by the constitutively expressed endothelial CC-chemokine ligand 21 (CCL21) binding CC-chemokine receptor 7 (CCR7) on T cells. Subsequently, T cells are able to transmigrate through the wall of the HEV into the LN.

Lymph nodes have three functionally distinct compartments reflected by the cellular constituents of each, as illustrated in Figure 3 (Willard-Mack, 2006). The cortex is largely populated by B cells and follicular DCs providing a well-adapted environment for the mediation of humoral immunity. The paracortex, or ‘T cell zone’, located beneath the cortex, is populated by T cells and DCs and is the centre for T cell priming. The medulla is understood to be a zone for plasma cell proliferation and differentiation, thereby contributing to antibody production (Harry L. Ioachim, 2009).

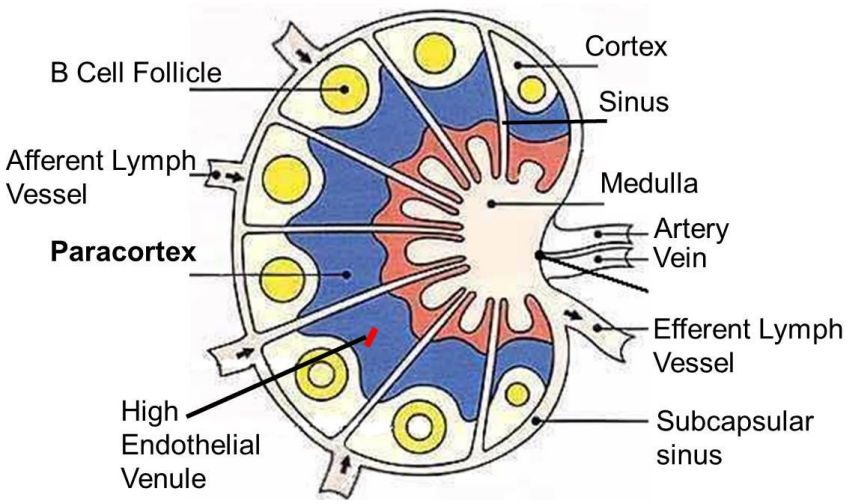

Figure 3. The Lymph Node.
The lymph node structure is well-adapted to its function in facilitating efficient immune responses. Schematic re-annotated and adapted from Janeway's Immunobiology 7th Ed. (Murphy et al., 2008)

The architectural features of the paracortex create an ideal microenvironment for T cell priming. The ECM of the paracortex is a 3-dimensional (3D) network of collagen fibres. This is covered by T cell zone fibroblastic reticular cells (TRCs) which express ligands, such as fibronectin and podoplanin (gp38), to direct the migration of T cells and DCs (Stranford and Ruddle, 2012, Gretz et al., 1997).

Homing of naïve T cells and DCs to the paracortical area is crucially mediated by the TRC- expressed chemokines, CCL21 and CCL19, for which DCs and T cells express the receptor, CCR7.

The TRC-lined collagen fibres are proposed to have an internal space, called a conduit. This provides a structure for the selective movement of lymph fluid carrying DCs and soluble factors from the sinuses into the paracortex. Therefore, TRCs do not only provide structural support, but also direct cellular organisation and interactions within the paracortex.

The paracortex can be broken down into functional units, named paracortical cords, depicted in Figure 4 (Gretz et al., 1997). These microchannel structures can be visualised as a set of spiralling, incomplete rings centred on an HEV. T cells move out from the HEV, following corridors formed by collagen fibres. The corridors have a diameter of 10-25μm and are densely packed with T cells and immobilised DCs.

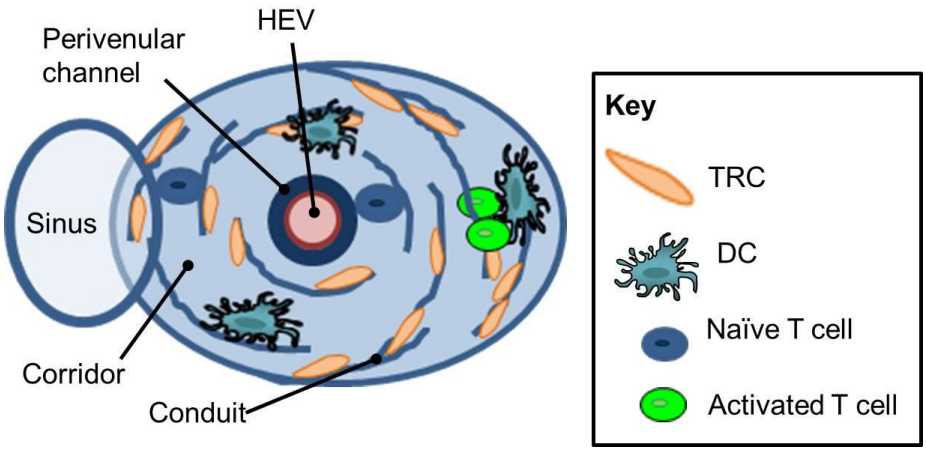

Figure 4. The Paracortical Cord.
Cross-section of the paracortical cord. Centred on an HEV, T lymphocytes move across the perivenular channel, then through spiralling corridors lined with TRCs, where interactions with DCs occur. DCs and soluble factors from the sinus are transported into the paracortex via conduits. (Katakai et al., 2004, Gretz et al., 1997)

1.4. Extra-cellular Influences on Dendritic Cells

In vitro study of DC biology has provided valuable insights into their role as professional APCs in terms of DC responses to pathogen extracts, chemical sensitisers and interactions with T cells. However, the limitations of such studies are becoming increasingly apparent due to the artificial nature of conventional *in vitro* cell culture.

In vivo, the surrounding environmental conditions can significantly influence DC function. Factors including, the extracellular matrix (ECM), 3D

environment and mechanical stimuli can have profound effects on DC survival, maturation and capability to elicit T cell activation (Garcia-Nieto et al., 2010, Gunzer et al., 2004, Lewis et al., 2013, Miteva et al., 2010, Swartz et al., 2008).

Recent research is beginning to elucidate the influence of ECM components on phenotypic and functional characteristics of DCs *in vitro*. Garcia-Nieto et al. showed that moDCs cultured in the presence of the ECM components, laminin or fibronectin, maintained a more immature cell phenotype, including enhanced endocytic activity, compared to a bovine serum albumin control. This work went on to demonstrate that moDCs were responsive to immunological stimulation and able to induce T cell activation with high efficiency in the presence of ECM (Garcia-Nieto et al., 2010).

The influence of the highly abundant ECM protein, collagen, on DC maturation has been the subject of *in vitro* investigation. However, the results from the work in this area are conflicting. In a recent study, human collagen types I and II were shown to provide an activating signal to DCs as ligands for the FcRgamma-associated receptor, osteoclast-associated receptor (OSCAR). Collagen-induced DC maturation was demonstrated by increased production of inflammatory cytokines, up-regulation of maturation markers and efficient elicitation of T cell proliferation (Schultz et al., 2015). In contrast, it had previously been demonstrated that type I collagen from porcine, bovine and human sources did not induce DC maturation, based on cell-surface expression of maturation markers and TNF-α secretion (Bayrak et al., 2013). This may illustrate the variability in the immunogenicity between different sources of

collagen depending on method of purification, species of origin and collagen type.

The DC-ECM interaction is crucial for their capacity to migrate to LNs. The integrins (VLA-4 and VLA-5) were identified for the adhesion of DCs to the ECM component, fibronectin, and are likely to be involved in the complex molecular mechanisms of DC trafficking *in vivo* (D'Amico et al., 1998).

The 3D structural framework formed by the ECM in the LN is important in DC-T cell interactions. It provides a network which promotes T cell crawling, allowing dynamic antigen presentation which is likely to be more representative of the events leading to T cell activation *in vivo* (Gunzer et al., 2000). T cells are likely to experience cues from the ECM, simultaneously to those from DCs, which contribute to their activation.

In addition to the cues imparted by the ECM, other extracellular biophysical factors have been found to impact DC function and APC-induced T cell activation (Lewis et al., 2013, Tomei et al., 2009, Li et al., 2010, Previtera, 2014). Physiological stress induced by shear flow is particularly relevant, since DCs are exposed to the effects of flow as they travel in the lymphatics and by slow interstitial flow through non-lymphoid and lymphoid tissues. *In vivo*, flow promotes DC migration towards the lymphatics through changes in the expression of adhesion molecules on the lymphatic endothelium and it also likely physically directs DC movement towards LNs (Swartz et al., 2008). Finally, Li et al. demonstrated that shear flow triggered the activation of T cells bound to artificial APCs (Li et al., 2010).

1.5. Applying Tissue Engineering to Safety Testing

Animal models and *in vitro* cell-based assays are currently the most widely used and well-recognised methods for safety testing in industry.

Animal models provide a physiologically relevant system to assess multiple safety parameters, such as toxicity, reproductive toxicity, carcinogenicity and hypersensitivity. Despite this, they are sometimes limited in terms of translation to humans due to fundamental biological differences. This was demonstrated by the 2006 TeGenero clinical trial, where the administration of TGN1412, a CD28 superagonist monoclonal antibody, caused a life-threatening 'cytokine storm' in human volunteers (Goodyear, 2006). Pre-clinical data, generated from non-human primate (NHP) models, failed to predict this (Stebbings et al., 2009). Differences in the pattern of expression of the target molecule on effector cells of the immune systems of the two species accounted for the disastrous translation from NHP to humans in this trial (Eastwood et al., 2010).

In vitro immune cell assays are useful tools for research and safety testing since they:

1. Use cells derived from human tissues, therefore issues relating to translation of animal to human immunology can be overcome.

2. Provide a defined environment to enable the study of specific biological pathways.

3. Are amenable to high throughput screening, allowing thousands of pathogen\allergen extracts, drugs or chemicals to be assessed, saving time and costs compared to animal testing.

The simplicity of such assays is not always an advantage since they cannot capture the complexity of biological mechanisms and extra-cellular factors that occur in whole tissues. *In vitro* monolayer, or two-dimensional (2D), culture often results in cells losing their native tissue phenotype and therefore do not have the same functionality as *in vivo* counterparts, which limits them for certain applications (Gomez-Lechon et al., 1998).

An emerging solution to reconcile the limitations associated with the artificial nature of conventional *in vitro* cell culture methods lies in tissue engineering. Tissue engineering aims to recapitulate the structure and function of living tissues. The field has made significant advances, with the main focus being on clinical applications to replace, repair or enhance damaged tissues.

It has been recognised that artificial tissues with biological function also have a place outside of the clinic. This has already been demonstrated through the development of a range of artificial tissue models including skin, liver and lungs, with potential applications in drug and chemical safety testing (Kandarova et al., 2005, Chang et al., 2010, Harrington et al., 2014).

Increasing attention is being given to the development of artificial tissue models which simulate immunological events, such as lymph nodes (Cupedo et al., 2012). Progress has been relatively slow in this area, perhaps due to the complexity of the immune system. However, studies have been published to demonstrate proof of concept of artificial immune-competent systems.

Giese et al. described an approach for the construction of an artificial lymph node (aLN) model. It was centred on a 3D matrix-assisted culture of DCs in a bioreactor system which was perfused with lymphocytes (Giese et al., 2006). The immunological capabilities of the model were investigated by antigenic stimulation with human cytomegalovirus lysate and a commercially available Hepatitis A vaccine, HavrixTM (GSK) (Giese et al., 2010). The longevity and immune reactivity of the model was supported by the evaluation of cytokine production, including IL-2, IL-4, IL-5, IL-6, IL-10, IL-1β, interferon-gamma (IFN-γ) and tumour necrosis factor-alpha (TNF-α).

Methods for Predicting Chemical Sensitisation

Allergic conditions which manifest as a result of exposure to chemical products is a growing public health concern. Repeated skin contact with certain organic chemicals, or metal ions, can lead to the development of a severe allergic condition, known as allergic contact dermatitis (ACD).

A recent epidemiological review estimated the prevalence of chemical contact allergy to be around 20% for Western European and North American populations (Thyssen et al., 2007). The occurrence of ACD is not significantly affected by age, genetic background or geographical location, thus it affects a

wide range of individuals, including young children. In the work place, ACD accounts for 70-90% of reported occupational skin disease. It carries a heavy financial burden in terms of loss of productivity and medical costs (Peiser et al., 2012).

ACD is highly distressing for patients and treatment is only symptomatic. It can also be debilitating, since avoidance of the chemical involved is the only option for preventing reoccurrence of the condition. This may require drastic changes to occupation and lifestyle. Therefore, methods to predict the potential of chemicals to induce sensitisation are essential to prevent the occurrence of adverse immune reactions.

Animal Safety Testing – The 'gold standard'

Historically, the principle chemical safety tests recognised by regulatory bodies for the prediction of sensitisation have been based on animal models. The first test methods approved in the Organisation for Economic Co-operation and Development (OECD) guidelines for the evaluation of chemical sensitisation included the guinea pig maximisation test (GPMT) and Buehler's occluded patch test (Botham et al., 1991). In these tests, animals are subject to an initial chemical exposure. After 10-14 days, they are re-challenged and quantification of sensitisation is based on the resultant skin reaction.

In the last decade, the murine local lymph node assay (LLNA) has taken precedence over the guinea pig tests (GPTs). The LLNA was accepted as the first standalone test for the prediction of chemical sensitisation following

evaluation by the Interagency Coordinating Committee on the Validation of Alternative Methods (ICCVAM).

In contrast to the GPTs, the LLNA assesses immune activation during the induction phase of sensitisation at a cellular level. This is done by measuring the magnitude of T cell proliferation in the LN following chemical exposure. Briefly, the chemical is applied behind the ears of the mice. Five days later, mice are injected with a radioactive tracer which labels proliferating T cells. The mice are euthanized and LNs are excised to harvest the LN-resident cells. The magnitude of the proliferative T cell response is measured by the level of radioactivity detected (Kimber et al., 2002).

The LLNA also has the capability to establish a chemical's sensitising potency. This is the dose which produces a certain level of response sufficient for the acquisition of skin sensitisation. The potency value commonly derived from the LLNA is the EC3, this is the concentration required to cause a 3-fold increase in T cell proliferation compared to un-treated animals (Kimber et al., 2002). This feature gives the LLNA added value over GPTs and current non-animal alternatives.

At the time of implementation, the LLNA fulfilled regulatory, animal welfare and scientific requirements more satisfactorily than the GPT methods. Although the LLNA is sufficient for the assessment of the safety of most chemicals, there remain some discrepancies. The occurrence of false-positives to the non-sensitising irritant sodium lauryl sulphate (SLS) and the failure to

detect responses to Ni^{2+}, a prevalent human contact allergen, limits the reliability of the assay (Kimber et al., 2002).

Routine use of the LLNA in industry continues to raise ethical concerns regarding the welfare of animals used in research. This is in accordance with the long-running 3Rs campaign; advocating the Replacement, Reduction and Refinement of animals in research for the improvement of animal welfare (Mehling et al., 2012).

Recent legislation has also put pressure on finding alternatives to animals for chemical safety testing. For instance, the 7th Amendment to the European Union Cosmetics Directive recently banned the testing of cosmetic products on animals. Also, testing for human hazardous effects of chemicals, produced or imported within the European Union at quantities greater than 1 ton per year, is now required according to the Registration, Evaluation, Authorisation and Restriction of Chemicals (REACH) guidelines.

Animal models have proved to be useful tools for chemical safety testing and given some insight into the molecular and cellular basis of CHS. However, in the light of the ethical, scientific and regulatory limitations associated with animal testing, validated non-animal tests for the identification of chemical sensitisers are now highly sought after.

Non-Animal Alternatives: State of the Art

A wealth of funding has been put into research and development of alternative tests (Aeby et al., 2010). Some of the key methods currently being developed to replace animal testing are summarised in Table 1.

For the development of alternative methods, the immunological mechanisms involved in the development of CHS have been put into an adverse outcome pathway (AOP) framework (OECD, 2012). Assessing the performance of a chemical at each step in the AOP is important for determining sensitising potential using non-animal methods.

The main requirements of alternative tests are the reliability and accuracy of predicting chemical sensitisation in humans. This includes ascertaining the relative sensitising potency of a chemical to allow the classification of sensitisers into strong, moderate and weak categories. This is likely to become a critical aspect of the modern risk assessment for the characterisation of sensitisers, according to an amendment in the regulations for the Globally Harmonized System of Classification and Labelling (GHS).

Table 1. Summary of Alternative Methods for the Prediction of Chemical Sensitisation.

Method Summary		Step in the development of CHS (refer to Figure 2 in this chapter)
***In vitro* cell assays**		
Keratinocytes	KeratinoSens Up-regulation of anti-oxidant response genes. (Andreas et al., 2011) NCTC 2544 IL-18 test Increase in IL-18 production. (Corsini et al., 2013)	Stress & innate immune responses
Dendritic Cells	human-Cell Line Activation Test (h-CLAT) \ monocyte-derived DCs (PBMDC) Up-regulation of CD86 or CD54 expression. (Nukada et al., 2012, Tuschl et al., 2000) Genomic Allergen Rapid Detection (GARD)	

Artificial skin	Transcriptional profiling MUTZ-3 metabolic, cell cycling and oxidative stress responses.(Albrekt et al., 2014) Dendritic cell - keratinocyte co-culture Up-regulation of DC markers CD86 and CD54. (Cao et al., 2012) Sens-IS Keratinocyte activation. (Cottrez, 2011) 3D artificial skin with DC co-culture. DC migration, CD86\CD54 expression and cytokine production. (Uchino et al., 2009, Chau et al., 2013)	Specific immune response
T cells	Human T cell priming assay. T cell proliferation and IFN-γ production. (Richter et al., 2012)	

Chemistry		
Cell-free	Direct Peptide Reactivity Assay (DPRA)\ Peroxidase Peptide Reactivity Assay (PPRA) Peptide depletion. (Gerberick et al., 2004, Gerberick et al., 2009)	Chemical reactivity
Computational modelling		
Cell-free	Quantitative-Structure Activity Relationship models Databases of chemical information and data generated from *in vivo* sensitisation models. (Golla et al., 2009). Expert Systems Correlation of chemical structure with peptide haptenation associated with sensitisation. (Patlewicz et al., 2007)	Chemical reactivity\biological activity relationship

In vitro cell assays

Keratinocytes

Induction of oxidative stress response gene expression by sensitisers, through the Keap1-Nrf2-ARE regulatory pathway, has been exploited to develop a keratinocyte reporter cell line. Natsch et al. generated an assay using the human keratinocyte cell line, HaCaT, with the stable insertion of a luciferase reporter construct under the transcriptional control of the ARE-element of a sensitiser-inducible human gene. Evaluation of luciferase expression and cytotoxicity is performed to assess sensitisation potential. This tool is more widely known as the KeratinoSens assay (Natsch and Emter, 2008). An inter-laboratory study to test the ability of the KeratinoSens assay to predict skin sensitisers indicated a high level of reproducibility, accurate for 26 out of the 28 chemicals tested (Andreas et al., 2011).

The up-regulation of IL-18, associated with exposure to sensitisers, has been utilised in a keratinocyte assay by Corsini et al. The keratinocyte cell line, NCTC2544, showed a specific, dose-dependent increase in intracellular IL-18 to skin sensitising chemicals, in comparison to respiratory sensitisers and non-sensitisers (Corsini et al., 2009).

Dendritic Cells

DCs have a central role in sensitiser-specific T cell activation. Therefore, they have been the focus in the development of many assays for the identification of sensitisers.

The induction of DC maturation by sensitisers provides a useful target for the development of alternative tests. The human cell line activation test (h-CLAT) was developed using a human monocytic leukemia cell line, THP-1. The expression of DC maturation markers, CD86 and CD54, are measured following exposure to the test substance. Evaluation of the h-CLAT for predicting chemical sensitisers highlighted the promise of this test, as it was found to have an accuracy of 84% against the LLNA (Nukada et al., 2012).

In addition to the DC-like cell line assays, there is also a PBMDC (peripheral blood mononuclear DC) assay. Here, sensitisers can be identified based on the increased expression of CD86 (Reuter et al., 2011)

A genomic biomarker signature of 200 genes for the human myeloid leukemia-derived cell line, MUTZ-3, has recently been described for the identification of sensitisers. The Genomic Allergen Rapid Detection (GARD) assay revealed changes in the regulation of pathways associated with cell cycle, oxidative stress, metabolism and biosynthesis which correlated with sensitiser treatment (Albrekt et al., 2014, Johansson et al., 2013).

The biological relevance of co-culturing DCs with keratinocytes has also been considered. The metabolic capacity of keratinocytes is likely to give such assays an advantage, particularly for the detection of pro-haptens. Co-cultures have shown potential for increased sensitivity over mono-cultures for identifying contact sensitisers based on markers of DC maturation (Wanner and Schreiner, 2008, Cao et al., 2012).

Dendritic cell-T cell co-culture

The sensitiser-specific T cell response holds great value for the development of *in vitro* tests which predict sensitisation, since it ultimately determines the elicitation of ACD (Kimber et al., 2012). This is reflected in the LLNA, where the proliferative T cell response accurately predicts sensitisation.

This aspect of sensitisation is vastly outweighed by the focus on innate responses to sensitisers. However, the importance of the sensitiser-specific DC-T cell interaction is gaining more appreciation. This is evident from the focus on the development of the Human T cell priming assay (hTCPA), a co-culture of naïve T cells, sensitiser-pulsed monocyte derived DCs (moDC) and a feeder cell line with the addition of co-stimulatory signals (Richter et al., 2012). Successful T cell priming is measured by flow cytometry to determine sensitiser-specific T cell frequency and cytokine production.

Artificial Skin

The surface area of the skin exposed to the sensitising chemical, rather than the absolute concentration applied, appears to be the more important factor in determining sensitisation (Kimber et al., 2001). Conventional *in vitro* cell assays do not have the capacity to measure this element of skin sensitisation.

This has been addressed through the construction of 3D human epidermal tissue models. The Sens-IS method exposes a 3D artificial epidermal tissue (EpiSkin) to test substances to address cytotoxicity and activation of keratinocytes based on the induction of antioxidant gene expression (Cottrez, 2011).

Other models have the advantage of the incorporation of DCs. An immune-competent 3D human skin model was developed by Chau et al. which was shown to be responsive to the strong sensitiser 2,4-Dinitrochlorobenzene (DNCB), based on DC movement towards the bottom layer of the construct (Chau et al., 2013). Another artificial 3D skin construct (VG-KDF-Skin) showed evidence of sensitiser-specific up-regulation of CD86 expression and cytokine release by DCs (Uchino et al., 2009).

Cell-Free Methods

Chemical Reactivity Assays

Contact allergens, or haptens, have unique properties which allow them to react with peptides to produce immunogenic epitopes. As a result, there has been interest in measuring this interaction for the prediction of sensitisation. This led to the development of the direct peptide reactivity assay (DPRA), and the peroxidase peptide reactivity assay (PPRA) (Gerberick et al., 2004, Gerberick et al., 2009). Both measure chemical reactivity based on the depletion of synthetic model peptides containing a lysine or cysteine residue. However, the PPRA may be better at predicting pro and pre-haptens due to the incubation step with horseradish peroxidase, or hydrogen peroxide.

Computer Modelling

Finally, computational models have been developed, including Quantitative Structure Activity Relationship (QSAR) models, and expert systems to identify sensitising chemicals. These methods integrate sensitisation data from animal

models and sensitiser chemistry with algorithms to predict the reactivity and biological activity of a chemical entity *in vivo* (Golla et al., 2009).

Perspective on Alternative Methods

Alternative methods necessitate the breakdown of the complex process of skin sensitisation into isolated components. Taking these steps out of context in an experimental setting is not necessarily predictive of a chemical's sensitising potential. Therefore no single alternative method can be used as a standalone test for predicting sensitisation. This has resulted in the development of integrated test strategies (ITS), whereby panels of alternative tests are implemented to cover the spectrum of events which lead to sensitisation (Sharma et al., 2011).

Promising progress has been made in the field, with the h-CLAT and DPRA being entered into pre-validation studies by the European Centre for the Validation of Alternative Methods (ECVAM). However, the majority of alternative tests currently focus on the immediate stress and innate cell responses to sensitisers. Looking forward, a validated assay which indicates sensitisation based on the outcome of DC-T cell interactions is required to complete the picture in ITS.

The artificial nature of alternative methods cannot be overlooked. The skin tissue models overcome this to some extent by the co-culture of multiple cell types in a 3D setting. However, conventional *in vitro* methods make it difficult to capture the complexity of the *in vivo* conditions during sensitisation.

The application of tissue engineered constructs, such as artificial skin and aLNs, to model immune cell responses shows great promise. The development of tools for the prediction of sensitisation is one area which could benefit from such an approach. It is anticipated that a biologically relevant *in vitro* platform for DCs and DC-T cell co-cultures would produce more realistic cell responses to sensitisers, thus enhancing the accuracy in predicting sensitisation. This system would also have potential applications in, but not limited to, immunology research, vaccine development and drug discovery.

1.6. Thesis plan

The overall aim of the research presented in this thesis was to investigate the influence of the extra-cellular environment on human immune cells. Biomimetic platforms were used to simulate biologically relevant features of the *in vivo* microenvironment, including ECM and shear flow. The immune response generated on these platforms was compared to that elicited under conventional cell culture conditions.

Chapter 2 describes the characterisation of synthetic and naturally-derived biomaterials to develop an ECM platform for immune cell culture. **Chapter 3** describes the construction of fluidic systems and characterisation of a fluidic platform for immune cell culture. **Chapters 4 and 5** examine the application of the ECM and fluidic platforms for investigating the influence of the extra-cellular environment on specific immune responses. An overview of the aims for each chapter is given here and these are reiterated at the start of each chapter.

The aim of the work described in **Chapter 2** was to investigate how human immune cells interacted with the candidate biomaterials including a colloidal gel, electrospun scaffolds, GelMA and collagen hydrogels. This was done by assessing immune cell viability, phenotype and response to immunological stimuli when cultured in the presence of the biomaterials.

In **Chapter 3**, the aim of the work was to develop a fluidic cell culture platform in order to investigate the effect of shear flow on immune responses. This was achieved by first developing a robust fluidic system. Then, the fluidic

platform was utilised to characterise the effect of shear flow on immune cells based on human dendritic cell viability, maturation and response to immunological stimulation.

The aim of **Chapter 4** was to investigate the influence of the extracellular environment on antigen-specific dendritic cell interactions with T cells by using the ECM and fluidic platforms previously characterised in Chapters 2 and 3 of this thesis. This was done by comparing the antigen-specific T cell response induced on the biomimetic platforms with that generated under conventional cell culture conditions.

The aim of the work described in **Chapter 5** was to study the effect of the ECM on immune responses to chemical sensitisers. Using the ECM platform, dendritic cell maturation and T cell activation in response to chemical sensitisers was compared with a conventional cell culture method.

Chapter 6 summarises the results of the research conducted and provides a conclusion for this thesis.

Chapter 2

Characterisation of the Immune-Compatibility of Biomaterials

2.1. Introduction

Chapter Overview

Biomaterials can be distinguished from other materials in terms of their ability to 'exist in contact with tissues of the body without causing an unacceptable degree of harm…' (Williams, 2008).

The field of biomaterials has advanced significantly in the last 50 years. This has made a great contribution to tissue engineering in terms of allowing the fabrication of increasingly complex constructs for transplantation *in vivo*, in addition to research and safety testing *in vitro* (Place et al., 2009, Cosson et al., 2015).

It is recognised that when cultured as a monolayer, i.e. in two-dimensions (2D), cells often lose their native tissue phenotype. This limits traditional biological assays in terms of their physiological relevance. For example, in hepatocyte drug toxicity assays, monolayer cultures rapidly become undifferentiated and

lose their drug metabolising activity. This impairs the predictive power of the assay, thus many drug candidates fail (Gomez-Lechon et al., 1998).

In vivo, cells reside within a densely populated, extracellular matrix (ECM). This three-dimensional (3D) network provides cellular, biochemical and mechanical cues which direct cell functions, such as apoptosis, differentiation and migration (Kleinman et al., 2003). Tissue engineers use biomaterials to recapitulate the natural microenvironment in order to maintain physiologically relevant cell differentiation and function *in vitro* (Pampaloni et al., 2007).

Biomaterials may consist of natural or synthetic material, or combinations of both. The inherent nature of the biomaterial, along with the fabrication method and further (chemical) modifications, determines its suitability for applications in tissue engineering.

Biomaterial selection depends on the requirements of the bioengineered construct. Factors including mechanical strength, degradability, micro-, or nano-architecture and biological activity influence the choice of biomaterial (Lee et al., 2014, Chan and Leong, 2008, Dhandayuthapani, 2011, Kohane and Langer, 2008).

Assessment of biomaterial 'biocompatibility' is usually based on the cellular response, including cell viability, phenotype and function. Crucially, the cell-biomaterial interaction can vary between cell types and tissue locations. Therefore, the biocompatibility of biomaterials should be characterised on an

individual basis, in terms of the tissue-specific application and desired outcome (Williams, 2014).

This chapter describes the work carried out to characterise, *in vitro*, the suitability of biomaterials for the development of an ECM-supported platform for immune cell culture. The candidates for testing were:

Synthetic

1. Thermo-responsive particle gel.

2. PET and PLGA thermo-responsive electrospun scaffolds.

Semi-Natural

Gelatin methacryloyl (GelMA) hydrogel.

Natural

Collagen hydrogel.

Immune Responses to Biomaterials

The importance of understanding how immune cells interact with a biomaterial was highlighted over 20 years ago by Remes (Remes and Williams, 1992). However, this has only been fully appreciated in the last few years with the increasing use of biomaterials for *in vivo* applications (Johnson et al., 2007). Many biomaterials have been extensively studied using well-established cells lines and thus termed 'biocompatible'. However, comprehensive study

regarding their interaction with and impact on cells of the immune system is a relatively recent focus.

The foreign body reaction is a well-known physiological phenomenon. It describes the natural propensity of immune cells to mount responses against foreign bodies, which extends to biomaterials. Briefly, upon recognition of foreign material, cells of the immune system, namely monocytes, become activated in order to attempt to eradicate it by phagocytosis (Anderson et al., 2008, Ekdahl et al., 2011). Production of cytokines, including tumour necrosis factor (TNF)-α, IL-1β, IL-6 and IL-8 (Gretzer et al., 2003), by activated cells are characteristic of this response and mediate inflammation and wound healing *in vivo* (Chang et al., 2008).

Certain biomaterials have been shown to have profound effects in terms of modulating the immune system (Silva et al., 2015, Yoshida and Babensee, 2004). These properties can be harnessed in areas such as vaccine delivery, autoimmune disease and cancer therapeutics to direct appropriate immune responses (Swartz et al., 2012). In the development of vaccines, for example, adjuvant effects of certain biomaterials can be used to enhance the induction of adaptive immune responses, thereby potentially increasing the level of protection offered by the vaccine (Lewis et al., 2014).

On the other hand, for applications where the purpose of the biomaterial is to contribute to the biological physiological relevance of the construct, it is not desirable for the material to directly affect the immunological status of the system, for example when investigating antigen-specific immune responses.

Therefore thorough characterisation of biomaterials for specific applications in immunology is important.

Biomaterials for Tissue Engineering

Synthetic Polymers

Advances in polymer chemistry have sparked a huge increase in the use of synthetic polymeric biomaterials in tissue engineering. Synthetic polymers are non-biological materials which can be designed to have properties which make them potentially suitable for cell culture (Guo and Ma, 2014, Bajaj et al., 2014). The advantage of such materials is that they may be functionalised to promote cell interactions, for example by the incorporation of ECM-mimic peptides (Zhu, 2010). Also, their physical and chemical properties, e.g. degradability and stiffness, can be tailored to a specific application (Guo and Ma, 2014). Since synthetic polymers generally have well-defined constituents, issues related to batch-to-batch variability and immunogenicity are greatly reduced (Bajaj et al., 2014, El-Sherbiny and Yacoub, 2013, Hughes et al., 2010).

The development of stimuli-responsive synthetic polymers offers further flexibility to tissue engineers. Changes in pH, temperature, light and other biochemical stimuli can be used to modulate the material properties, e.g. hydrophobicity\hydrophilicity, degradability (Hoffman, 2013, Huang et al., 2011). Such properties are useful for *in situ* biomaterial assembly and non-enzymatic cell passage (Al Ghanami et al., 2010, Takahashi et al., 2012).

In this work, two formats of synthetic biomaterial were employed, these being a particulate gel and electrospun fibrous scaffolds. Both of these types of material had thermo-responsive properties which were exploited to enhance cell recovery for analysis and downstream applications.

Thermo-responsive particulate gel

A new family of thermo-responsive particulate gels are showing promise in the field of tissue engineering. These materials have been demonstrated to form gels reversibly near human body temperature (37°C), have a porous 3D matrix structure and support multiple rounds of cell passage (Wang et al., 2009).

This technology combines a thermo-responsive polymer, poly(polyethylene glycol methacrylate) (usually denoted as PEGMA or pPEGMA), with polycaprolactone (PCL) or poly(lactide-glycolide) (PLGA) micro-particles, which have hydrophobic surface properties. The structures of these components are depicted in Figure 5.

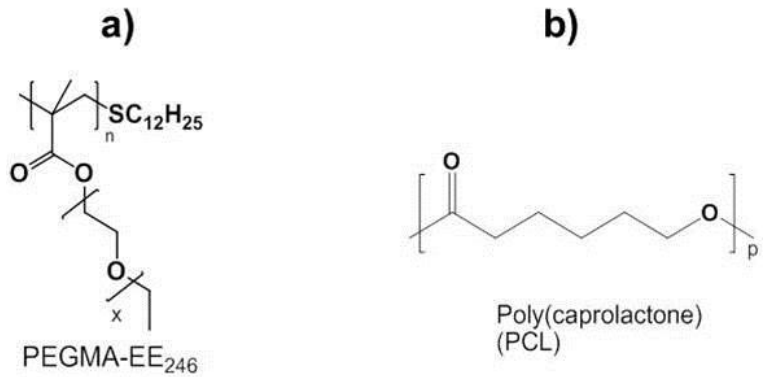

Figure 5. Structures of thermo-responsive pPEGMA (a) and PCL particles (b).

A temperature-responsive particulate dispersion is generated by mixing pPEGMA and PCL particles. Upon mixing, the thermo-responsive polymer is adsorbed onto the surface of the particles, illustrated in Figure 6. At temperatures below 37°C, the pPEGMA chains are strongly hydrated and extend in aqueous solution to provide a steric barrier to particle aggregation, giving rise to a free-flowing suspension. When the temperature is increased to 37°C, the pPEGMA chains dehydrate and collapse to self-associating globule this increases the hydrophobicity of each particle, leading to inter-particle aggregation and entrapment of cells within the 3D matrix (Al Ghanami et al., 2010).

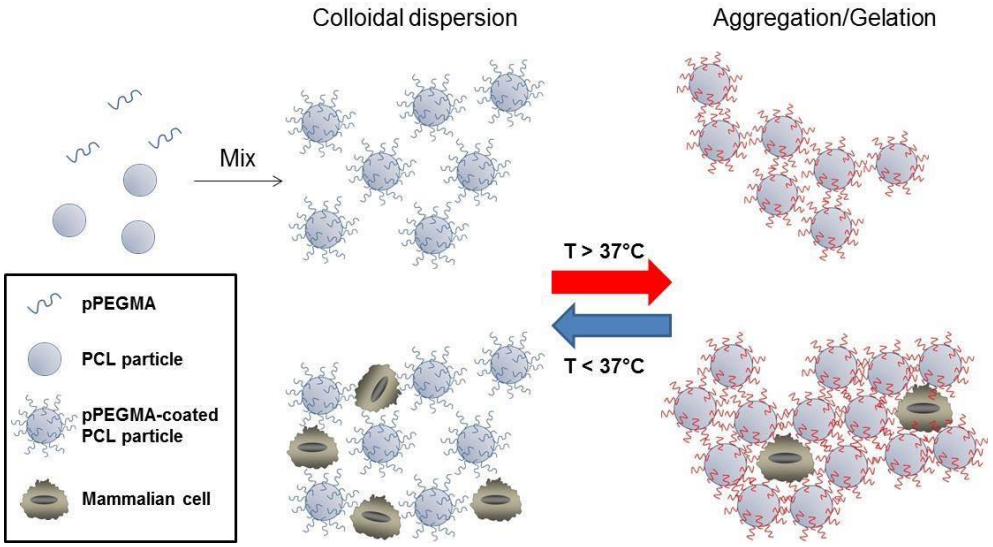

Figure 6. Schematic illustration of temperature-responsive particulate gel matrix formation.
PCL particles and pPEGMA are mixed to generate a colloidal dispersion. Below 37°C PEGMA chains are extended causing repulsive interactions between particles. Above 37°C PEGMA chains collapse and particles aggregate. Cells are dispersed in a free-flowing particle suspension below 37°C. An increase in temperature, above 37°C, causes particles to form a gel which encapsulates the cells within the 3D matrix.

Thermo-responsive electrospun scaffolds

Electrospinning is a popular technique for generating biomaterials for tissue culture (Sill and von Recum, 2008). It is applicable to a range of natural and synthetic polymers. Electrospun scaffolds are composed of micro-, or nano-meter sized fibres, which form a mesh-like structure reflective of the architecture of some natural tissues (Agarwal et al., 2008).

Electrospinning can be performed under ambient conditions. Briefly, the electrospinning rig comprises 1) a high voltage power supply, 2) a syringe and needle, and 3) a grounded collector plate. A high voltage is applied to the needle containing the polymer solution (which has been prepared using an appropriate solvent). The repulsive forces within the polymer solution overcome the surface tension resulting in the expulsion of a jet of polymer solution from the needle tip. The charged solution is attracted to the grounded collector plate. A whipping motion caused by the instability of the polymer stream dries the polymer fibres and creates a fibrous mesh which is deposited on the collector plate (Sill and von Recum, 2008).

For this work, polymers were used which are regulated by the Food and Drug Administration (FDA) and regarded as safe, namely, polyethylene terephthalate (PET) and poly(lactic-co-glycolic acid) (PLGA). The molecular structures for these polymers are shown in **Figure 7**. It is important to note that PLGA degrades over time, the stability and therefore the degradation rate of PLGA depends of the ratio of glycol to lactic acid used (Shin et al., 2006). In this work, a fresh batch of electrospun PLGA was used in each experiment and was

only required to support cell cultures for a maximum of 6 days, therefore characterisation of degradation was not necessary.

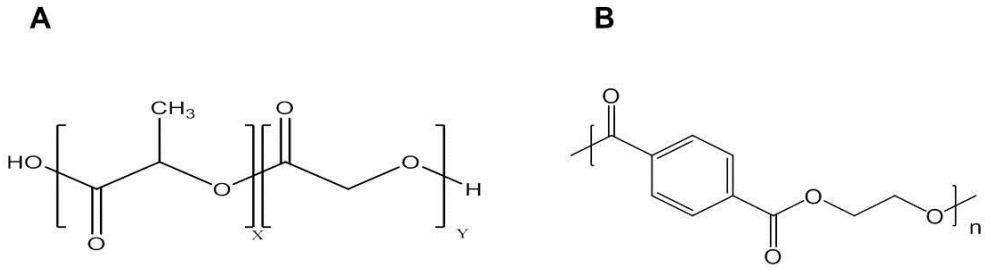

Figure 7. Molecular structure of A) poly (lactic-co-glycolic acid) (x = number of lactic acid units and y = number of glycolic acid units), and B) poly (ethylene terephthalate) (PET), (n = the number of repeating units in the PET polymer). Credit for illustration to Afnan Aladdad, PhD.

PET or PLGA were co-spun with the thermo-responsive polymer PEGMA to achieve thermo-sensitive electrospun scaffolds. The molecular structure for polyPEGMA188 used in this work is depicted in **Figure 8**.

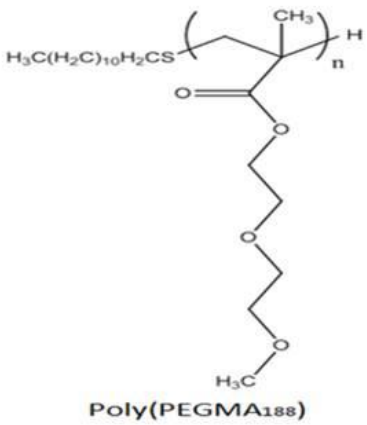

Figure 8. Molecular structure of Poly (PEGMA188). Credit for schematic to Afnan Aladdad, PhD.

As shown in Figure 9, the PEGMA chains collapse at body temperature and the hydrophobicity of the collapsed polymer structure allows protein adsorption onto the surface of the fibres. This in turn provides a matrix which facilitates cell adhesion. Upon cooling, the polymer chains open up, causing repulsive

forces between the fibres in a hydrated environment, thereby releasing cells which are attached to the scaffold.

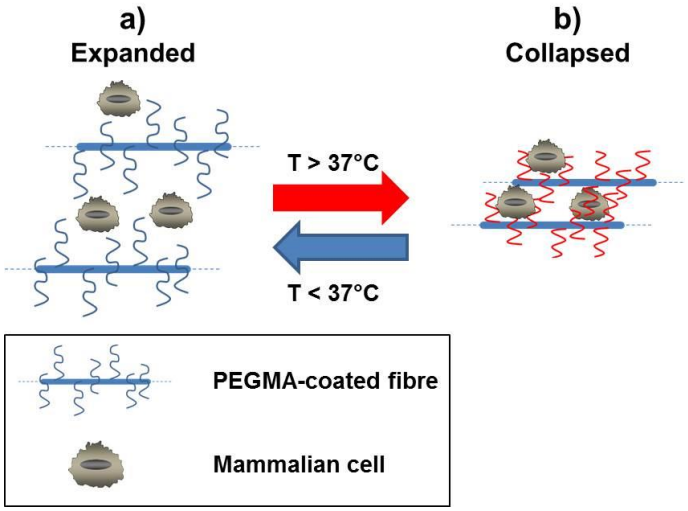

Figure 9. Schematic representation of thermo-responsive electro-spun scaffolds.
a) Below 37°C PEGMA chains exist in an extended conformation with repulsive forces acting between the fibres resulting in cell release. b) At 37°C, the extended chain structure collapses, resulting in attractive interactions between the fibres and facilitating cell attachment to the scaffold.

Naturally-derived Polymers

Biomaterials are also derived from a range of polymers found in nature. They have their own advantages in terms of being biodegradable and biologically active. However, they can have immunogenic effects due to their origin and their molecular constituents can be difficult to standardise due to variation between batches (Tibbitt and Anseth, 2009).

In this work, two collagen-based hydrogels were investigated. Hydrogels are widely used in the field of tissue engineering and regenerative medicine (El-Sherbiny and Yacoub, 2013). They are an attractive class of biomaterial since their highly hydrated, porous structure closely resembles the natural extracellular matrix (ECM) of soft tissues (Slaughter et al., 2009).

Collagen & Gelatin methacryloyl (GelMA)

Collagen is a highly abundant natural protein, distributed in the extracellular matrix of all animal tissues. It can be isolated from tissue by neutral salt-solubilisation, acid-solubilisation or pepsin-solubilisation (Mocan et al., 2011). Collagen is present *in vivo* in a variety of forms, including types I, II, III, V and XI which form fibres.

As depicted in Figure 10, the collagen molecule is formed from three α chains. The repeating amino acid sequence, -Gly-X-Y- allows the tight assembly of the chains to form the collagen molecule. Triple helix collagen molecules go on to self-assemble into fibrils (van der Rest and Garrone, 1991, Knupp and Squire, 2003).

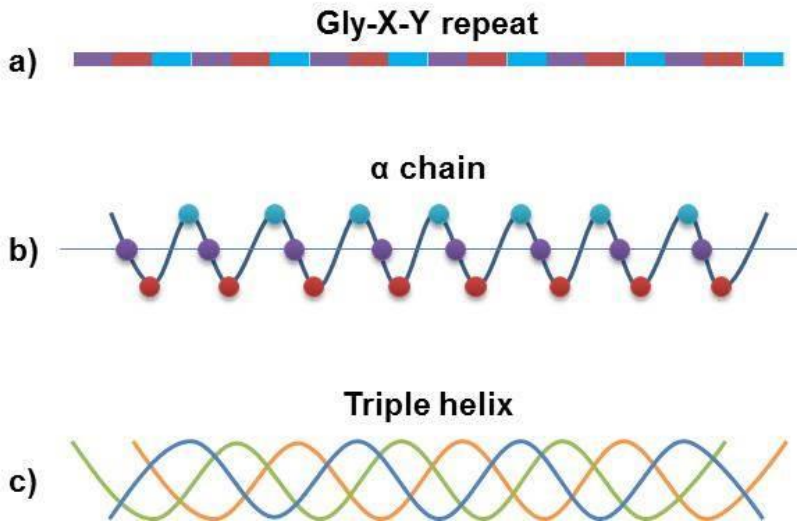

Figure 10. Schematic of collagen molecular structure.
a) Repeating amino acid sequence, glycine-X-Y, with X and Y usually being proline and hydroxyproline. b) The collagen α chain subunit. c) Three α chains intertwine to form the characteristic triple helix of the collagen molecule. Diagram modified from Knupp and Squire 2003.

Collagen generally possesses properties associated with good biocompatibility. This includes features such as cell adhesion motifs. These are specific

sequences of amino acids that are recognised by various cell-surface ECM receptors, such as integrins (Knight et al., 2000, Parenteau-Bareil et al., 2010), and which mediate cell attachment, motility, survival, and differentiation (Rosso et al., 2004). In most instances, collagen is not significantly immunogenic. Its ubiquitous presence in the body normally results in the development of immune tolerance and therefore the frequency of immunological responses towards collagen products is low (Lynn et al., 2004). Collagen also demonstrates minimal cytotoxicity and is biodegradable (Khan and Khan, 2013).

Collagen has been successfully used for a range of tissue engineering applications both *in vivo* and *in vitro*, with type I collagen being the most widely used (Glowacki and Mizuno, 2008). For example, collagen hydrogels have been used extensively to provide 3D scaffolds for the study of fibroblast wound healing behaviour (Kanta, 2015), tumour progression (Szot et al., 2011) and hepatocyte culture (Gomez-Lechon et al., 1998). In addition, collagen has previously been shown to be an appropriate biomaterial for immune cell culture applications, for example in the development of a tissue-engineered platform for immuno-therapy (Stachowiak and Irvine, 2008).

Gelatin methacryloyl (GelMA) is a collagen-derived hydrogel. The synthesis of GelMA involves chemical modification of the hydrolysed form of collagen, gelatin. The reaction of gelatin with methacryloyl derivatives results in the formation of polymerisable methacrylate side groups, as shown in Figure 11. These side-chains enable tuning of the physical properties of GelMA derivatives in a way not possible for its unmodified counterparts, collagen and

gelatin. Thus, the mechanical strength and degradability of GelMA hydrogels may be controlled depending on the desired application (Van Den Bulcke et al., 2000). Methacrylate-functionalised gelatin retains properties similar to unmodified gelatin, however, polymerisation gives rise to a highly cross linked, rigid hydrogel (Van Den Bulcke et al., 2000). For example, with the addition of a photo initiator, GelMA is photo-polymerisable upon exposure to an ultra violet (UV) light source.

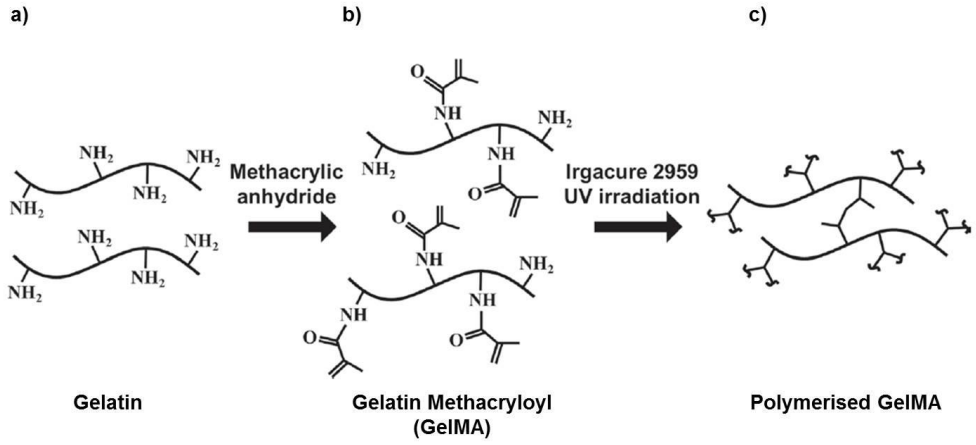

Figure 11. Schematic to demonstrate synthesis and photo-polymerisation of GelMA. Unmodified gelatin (a) is reacted with methacrylic anhydride resulting in the synthesis of gelatin methacryloyl (b). In the presence of a photoinitiator (Irgacure 2959) GelMA can be photo-polymerised thereby forming a stable, porous hydrogel (c). Modified from (Jung and Oh, 2014).

GelMA retains biocompatible features, including the preservation of cell adhesion motifs (Hutson et al., 2011). It has been used successfully as a biomaterial for various applications in tissue engineering, including cardiac (Shin et al., 2013, Saini et al., 2015) , bone (Ovsianikov et al., 2011, Dolatshahi-Pirouz et al., 2014) and vascularization (Chen et al., 2012, Bertassoni et al., 2014), as well as development of tumour microenvironment models (Peela et al., 2016).

Due to its mechanical stability, GelMA is an attractive material for incorporation into microfluidic systems. This has been successfully implemented by Chen et al. in the development of a microfluidic device which models the heart valve microenvironment (Chen et al., 2013). Although GelMA is evidently compatible with a range of cell types, based on the current available literature, the immunological properties of GelMA have not yet been characterised.

Chapter aims

This chapter describes the characterisation of synthetic and naturally derived biomaterials to develop an ECM platform for immune cell culture. The aim of the work in this chapter was to investigate how human immune cells interacted with the candidate biomaterials including a colloidal gel system, electrospun scaffolds, GelMA and collagen hydrogels. This was done by assessing immune cell viability, phenotype and response to immunological stimuli when cultured in the presence of the biomaterials.

2.2. Materials and Methods

PBMC Isolation from Peripheral Blood

Heparinised blood (buffy coats) from healthy donors obtained from the National Blood Service following ethics committee approval (National Blood Services, Sheffield, UK: 2009/D055). PBMCs were separated by density gradient centrifugation on Histopaque-1077 (Sigma Aldrich) as described before (Garcia-Nieto et al., 2010).

Generation of Monocyte-Derived Dendritic Cells

Monocytes were purified by $CD14^+$ selection from PBMCs using a magnetic cell separation method (kit purchased from Miltenyi Biotech) as previously described (Royer et al., 2010, Ghaemmaghami, 2002). The $CD14^+$ cells (>95% purity) were plated ($1x10^6$ cells\well) in a 24-well tissue culture-treated plate in 500µL complete RPMI-1640 medium containing 10% foetal bovine serum (FBS) , 100U\mL penicillin, 100mg\mL streptomycin and 2mM L-glutamine (all purchased from Sigma Aldrich). The media was supplemented with GM-CSF (50ng/mL) and IL-4 (250U/mL) (cytokines purchased from Miltenti Biotech). Cells were maintained under standard tissue culture conditions (37°C, 5% CO_2) for 6 days. An additional 500µL complete RPMI-1640 media containing GM-CSF and IL-4 was added on day 3.

Thermo-Responsive Particulate Gels

The materials were kindly donated for experiments by Shwana Braim, Polymer Therapeutics Group, University of Nottingham.

Synthesis of polyPEGMA

As previously described by Al Ghanami et al, the polymer was prepared by free radical polymerisation. The monomer (in the case of polyPEGMA-EE_{246} PEGMA (M_n =246, 10 g, 40 mmoles) was weighed into a round bottom flask to which 1-dodecanethiol (0.05 g, 0.25 mmoles) and butanone (15ml) were added. AIBN (0.05 g, 0.3 mmoles) was added last, and the mixture was degassed with argon for 15 minutes. The flask was then immersed in an oil bath, and the polymerization was conducted at 70°C for 1 hour. PolyPEGMA-EE_{246} was precipitated into a large excess (10 fold) of hexane. The polymer was further purified by dialysis against deionised water for 7 days in a cold room (5°C; dialysis membrane of a molecular weight cut off: 6000), then freeze dried for 2 days and stored at 8°C.

Preparation of Polycaprolactone microparticles

As described by Al Ghanami, the single emulsion solvent evaporation method was used. Poly(caprolactone)(M_n=10000, 300mg) dissolved in dichloromethane (DCM, 10ml) was added to a 100ml of 0.3wt% polyvinylalcohol (PVA, Mw=13-23 kDa) solution in water. The mixture was homogenised at 24000rpm for 2 minutes and then left to stir at 400 rpm for 6 hours, for DCM evaporation and microparticles hardening. The microparticles were collected by centrifugation at 3000 rpm for 4 minutes, and then freeze dried.

Preparation of the Particulate Gel (illustrated in Figure 5 of this chapter).

The colloidal gels were made according to the protocol set out by Al Ghanami et al. with minor modifications (Al Ghanami et al., 2010).

To sterilise the particles, the required weight was measured into a transparent glass container. Large clumps were crushed to a fine powder using a spatula. The container was then set on a roller under a UV bar (245nm) for 30 minutes in order to sterilise the particles.

pPEGMA 188 was dissolved in complete RPMI-1640 media to achieve a 4% (w/v) solution. The solution was sterilised by filtering it through a 0.2µm filter.

The pre-gel mixture was prepared by mixing 300mg particle with 1mL 4% (w/v) pPEGMA 188 (which had been dissolved in complete RMPI-1640 media).The mixture was kept on ice, it was vortexed and sonicated to obtain a smooth, milky suspension.

Encapsulation of Cells Within Particulate Gels

Based on a cell density of $5x10^5$ cells/50µL particulate gel, the required number of monocyte-derived dendritic cells was pelleted in a 1.6mL sterile Eppendorf, then re-suspended in the appropriate volume of gel mixture. A 48 well tissue culture plate containing 500µL complete RPMI-1640 media per well was prepared and transferred to the incubator. When required, the plate was removed from the incubator and placed on a heat block (set at 37°C). Under sterile conditions, 50µL of the cell-laden particulate gel suspension was

slowly and gently pipetted into each well forming a droplet-like gel matrix. The plate was carefully transferred back to the incubator and maintained under standard tissue culture conditions for 24 hours (37°C, 5% CO_2).

Retrieval of Cells from Particulate Gels

The plate containing the gels was transferred to the refrigerator (4°C) for 10 minutes. The dispersed gel\cell mixture was collected using ice cold PBS and passed through a 40μM filter to remove large particles. The suspension was divided between FACS tubes and washed with cold PBS before proceeding with staining methods for phenotypic analysis and the Annexin V cell viability assay.

Electrospun Scaffolds

Materials for this work were kindly provided by Afnan Aladdad, Polymer Therapeutics Group, University of Nottingham.

Preparation of PLGA and PET polymer solutions

The PLGA polymer (Sigma-Aldrich, lactide/glycolide ratio 75/25, Mn [gel permeation chromatography, GPC] = 68 kDa, Đ = 1.7) was prepared as a 18.5% (w/v) solution in 5mL dichloromethane (DCM). This was done by stirring continuously at room temperature for 24 hours.

The PET polymer (sigma, molecular weight of repeating unit: 192.2g/mole) was prepared as a 30% (w/v) solution in a mixture of DCM and trifluoroacetic

acid (TFA). Complete dissolution was achieved by continuous stirring at room temperature for 24 hours.

Synthesis of the thermo-responsive polymer poly (poly (ethylene glycol) methacrylate), poly (PEGMA188)

Poly (PEGMA188) was prepared by free radical polymerization following a published method (Al Ghanami et al., 2010). Di (ethylene glycol) methyl ether methacrylate (98%, Sigma, 188), (22 g, 0.12 moles) was weighed into a round-bottom flask, to which 1-dodecanethiol (chain transfer agent; 98%, Sigma; 0.225 g, 0.001 moles) and 15 mL of 2-butanone were added. Azobisisobutyronitrile (AIBN; 0.15 g, 0.001 moles) was added last and the mixture was degassed with nitrogen for 15 minutes. The flask was then placed on a hot plate (Stuart®) and the polymerization reaction was conducted at 70°C for 1 h. The prepared poly (PEGMA188) was precipitated three times in 500 mL of hexane and re-dissolved in 50 mL of 2-butanone to remove any residual PEGMA188 monomer. The precipitated poly (PEGMA188) was placed in a desiccator for 48 h to remove any remaining solvent.

Preparation of the co-polymer solutions

The PLGA co polymer solution was prepared as 20% (w/v) with 1% (w/v) poly (PEGMA188). The PET co polymer solution was prepared as 30% (w/v) with 2% poly (PEGMA188).

Electrospinning

10mL plastic syringes, fitted with an 18-gauge blunt needle, were loaded with 5mL polymer/ co polymer solution which had been prepared as described above. The syringes were mounted onto a syringe pump (Harvard) and the flow rate set to 4mL/hour for the PLGA polymer solution and 0.5mL/hour for the PET polymer solution. A voltage of 14 or 19kV was applied to the needle tip for PET or PLGA polymer solutions repectively using a high-voltage unit (Glassman High Voltage Inc). The solution was spun onto a 6cm2 stainless-steel grounded collector plate. The working distance between the needle and collector plate was approximately 15cm. The electrospinning process was performed at room temperature, the entire 5mL polymer solution was spun and the collector plate was rotated every 20 minutes. Finally, the electrospun mats were air0dried for 48 hours at room temperature, manually peeled off the plate and stored at room temperature.

Preparation of Scaffolds for Cell Culture

$1cm^2$ sections of electrospun scaffolds were cut and sterilised under a UV bar (245nm) for 20 minutes each side. Steel rings, which had been sterilised by autoclaving, were used to hold the scaffolds in place in a sterile, non-tissue culture treated 24-well plate. A 20% v/v antibiotic\antimycotic (Ab/Am) solution was prepared by diluting Antibiotic Antimycotic Solution 100X (purchased from Sigma) in PBS. Scaffolds were immersed in the 20% v/v Ab/Am solution overnight. The next day, the Ab\Am solution was removed and scaffolds were washed in complete RPMI-1640 media. The scaffolds were soaked in the media for at least 2 hours before cell seeding.

Dendritic Cell Culture on Electrospun Scaffolds

Monocyte-derived dendritic cells were seeded onto scaffolds at a density of $5x10^5$ cells in 300µL cytokine-free complete RPMI-1640 media. Cells were maintained under standard tissue culture conditions (37°C, 5% CO_2) for 24 hours. Cells were harvested from scaffolds by washing in ice cold PBS. The PEGMA-coated scaffolds were incubated at 4°C for 10 minutes to facilitate the release of cells from the scaffolds. Samples were divided between FACS tubes for staining for phenotypic analysis and the Annexin V cytotoxicity assay.

Endotoxin neutralisation was done using Polymyxin B sulphate (PMB) (purchased from Sigma). A 50µg/mL solution was prepared in sterile PBS. Scaffolds were incubated with the PMB solution for 45 minutes and washed thoroughly with media before cell seeding.

Preparation of Gelatin Methacryloyl (GelMA) Hydrogels

The GelMA foam was synthesised as described previously (Van Den Bulcke et al., 2000) and kindly provided by the Khademhosseini Lab, Massachusetts Institute of Technology, USA.

The photoinitiator, 2-Hydroxy-4′-(2-hydroxyethoxy)-2-methylpropiophenone (Irgacure 2959) (purchased from Sigma) was dissolved in PBS to make a 0.25% (w/v) solution.

A 5% (w/v) GelMA pre-polymer solution was prepared by dissolving GelMA into 0.25% photoinitiator solution at 60°C.

100µL of pre-polymer GelMA solution was added per well of a 48-well tissue culture plate and photo-cross linked by UV exposure (40 seconds, 800mW, 8cm). Hydrogels were washed in PBS and sterilised by submersion in a 20% v/v Ab\Am solution overnight. A final wash was done with sterile PBS before cell seeding.

PBMC Culture on GelMA Hydrogels

$5x10^5$ PBMCs were seeded per gel in 500µL complete RPMI-1640 media. For the LPS-simulated conditions, 0.1µg/mL *E. coli* LPS (0111:B4) (purchased from Sigma) was added to the appropriate wells. Plates were transferred to a humidified incubator (37°C, 5% CO_2). Cultures were maintained for 5 days to assess cell viability. Supernatant was sampled after 4 and 24 hours for cytokine and gene expression analysis.

TNF-α Depletion on GelMA Hydrogels

Recombinant human TNF-α protein (purchased from Invitrogen) was added to complete RPMI-1640 media at 5 or 2.5ng/mL. GelMA hydrogels were made as described above in *Preparation of GelMA hydrogels*. 500µL of media with or without TNF-α was incubated with the GelMA hydrogels for 4 hours in a humidified incubator (37°C, 5% CO_2). Supernatant was collected and stored at -80°C for analysis of TNF-α by ELISA.

Preparation of Thin-Layer GelMA Hydrogels (for immuno-fluorescent staining)

GelMA was photo-polymerised on surface-treated glass slides. The glass slides were coated with 3-(Trimethoxysilyl) propyl methacrylate (TMSPMA) in order to functionalise the surface to enhance hydrogel attachment. Briefly, glass microscope slides were submerged in a 10% (w/v) sodium hydroxide solution overnight. Slides were thoroughly rinsed and soaked overnight in dH_2O. They were washed 3 times in 100% ethanol and air-dried. Slides were then stacked in a beaker and wetted with TMSPMA. The beaker was covered with aluminium foil and the slides were baked at 80°C overnight. Finally, slides were washed in 100% ethanol 3 times, wrapped in aluminium foil and baked for a further 2 hours at 80°C. The glass slides were then cut into chips of $1cm^2$.

A 5% (w/v) pre-polymer GelMA solution was prepared, as described previously in *Preparation of GelMA hydrogels*. 5µL of GelMA pre-polymer solution was dispensed onto a glass chip, a spacer with a depth of 100µm was placed on top to form an even layer and then the gel was crosslinked for 8.5 seconds (Nikkhah et al., 2012). The glass chips were transferred to a 24 well plate and washed with PBS. Then gels were submerged in control RPMI-media or media containing recombinant human TNF-α and incubated for 4 hours in a humidified incubator (37°C, 5% CO_2).

Immuno-Fluorescent Staining GelMA Hydrogels for TNF-α

Following the incubation with or without TNF-α-containing media, the supernatant was removed and the GelMA hydrogels were washed in PBS. The samples were blocked for 30 minutes with 5% (w/v) FBS in PBS. A 1:200 dilution in 5% (w/v) FBS in PBS was made for the mouse anti-human TNF-α monoclonal antibody, clone 2C8 (purchased from abcam) and samples were incubated overnight at 4°C. Samples were washed 3 times in PBS, then incubated for 1 hour at room temperature with a Rhodamine red-conjugated goat anti-mouse secondary antibody (purchased from Life Technologies) diluted 1:250 with 5% (w/v) FBS in PBS. Samples were washed in PBS and mounted on cover glass for imaging. A Zeiss LSM710 confocal microscope system, with a 20X objective, was used to image the GelMA hydrogels.

Image analysis

ImageJ was used for the analysis of fluorescent images (Schneider et al., 2012).

Preparation of Collagen Hydrogels

Collagen, Type I, derived from rat tail (3mg/mL) (purchased from Life Technologies).

0.5mg/mL collagen hydrogels were prepared using the following calculation:

Vt = Total volume of collagen hydrogel needed

Volume of collagen needed (V1) =

$$\frac{(Final\ conc.of\ collagen)x\ \left(Total\ Volume(Vt)\right)}{Initial\ conc.of\ collagen}$$

Volume of 10X PBS needed (V2) =

$$\frac{Total\ volume\ (Vt)}{10}$$

Volume of 1N NaOH needed (V3) = (V1) x 0.025

Volume of dH_2O needed (V4) = (Vt)-(V1 + V2 + V3)

Cell Culture on Collagen Hydrogels

100µL of collagen hydrogel solution was added per well of a 48-well tissue culture plate and incubated at 37°C for 40 minutes to polymerise. $5x10^5$ cells were seeded per gel in 500µL complete RPMI-1640 media. For the LPS-simulated conditions, 0.1µg/mL *E. coli* LPS (0111:B4) (purchased from Sigma) was added to the appropriate wells. Plates were transferred to a

humidified incubator (37°C, 5% CO_2). Cultures were maintained for 5 days to assess cell viability. Supernatant was sampled after 24 hours for cytokine analysis.

Annexin-V-FITC\Propidium Iodide Cytotoxicity assay

The Annexin V-FITC cell viability kit (purchased from Beckman Coulter) was used for the assessment of cell viability. This assay is based on the principle that in early apoptosis cells lose the asymmetry of the plasma membrane. Thus, phosphatidylserine (PS), normally located on the inside of the cell membrane, appears on the outer surface. Annexin V has a high affinity for PS, therefore when conjugated with a fluorochrome (e.g. FITC), can be used to label cells in early apoptosis. During late apoptosis, the integrity of the cell membrane is lost allowing penetration of propidium iodide (PI), which intercalates DNA. Upon DNA binding, PI fluoresces allowing detection of dead cells.

To perform the assay, harvested cells were immediately placed on ice. After washing in PBS, cells were re-suspended in 1X Annexin V binding buffer and the staining method was carried out according to manufacturer's instructions. Samples were analysed immediately on the Beckman Coulter FC500.

Dendritic Cell Phenotypic Analysis

Harvested cells were washed twice in ice cold PBS (supplemented with 0.5% bovine serum albumin (BSA) and 0.1% sodium azide). Cells were immuno-fluorescently stained for CD11c (clone MJ4-27G12, PE, IgG2b, Miltenyi Biotech), CD40 (clone HB14, PE, IgG1, Miltenyi Biotech), CD83 (clone

HB15e, FITC, IgG1, eBioscience) CD86 (clone FM95, PE, IgG1, Miltenyi Biotech), CD54 (clone 84H10, FITC, IgG1, Beckman Coulter) for 20 min at 4°C. Relevant isotype matched control antibodies were used (all purchased from Miltenyi Biotech). The cells were then washed twice in ice cold PBS (with 0.5% BSA and 0.1% sodium azide) and fixed in 0.5% formaldehyde in PBS. Cells were analysed within 2 days.

Flow Cytometric Analysis

Flow cytometry was performed using a Beckman Coulter FC500 and 30,000 events were collected per sample.

Data were analysed using the flow cytometry WEASEL software. For phenotypic analysis, dead cells were excluded by forward and side scatter characteristics. For cell viability, no exclusion gate was applied.

Scanning Electron Microscopy

Scaffolds were fixed in 4% (v/v) paraformaldehyde (Electron Microscopy Sciences, United Kingdom) overnight at 4°C and then dehydrated through an ascending series of ethanol concentrations. The scaffolds were then placed onto carbon-coated electron microscope stubs and sputter-coated with gold (3 min, Blazers SCD 030 Blazers Union Ltd., Liechtenstein) under an argon atmosphere (BOC, U.K.) prior to analysis. Samples were kindly imaged by Christine Grainger-Boultby using SEM (Scanning Electron Microscopy) analysis (JEOL JMS-6060 LV microscope, JEOL Ltd., U.K.) operating at an accelerating voltage of 10 kV (Harrington et al., 2014).

Cytokine Detection

Interleukin 1β, interleukin 6, interleukin 8 and tumour necrosis factor-α were measured using a multiplex bead-based analyte detection system according to manufacturer's instructions (Procartaplex) (purchased from eBioscience) as described by (Sharquie et al., 2013).

Supernatants from cell-free TNF-α and IFN-γ depletion experiments were analysed by ELISA following manufacturer's instructions (kits for TNF-α and IFN-γ purchased from R&D systems).

PCR

Preparation of cell lysate for mRNA isolation

Cells were harvested from GelMA hydrogels by washing with cold PBS and immediately transferred to a Falcon tube on ice. Cells were washed twice in PBS, then 1mL of MACS lysis/ re-suspension buffer was added to 10^7 cells and mixed until lysate was clear.

mRNA isolation and cDNA synthesis

mRNA purification and cDNA synthesis were carried out using the μMACS one-step cDNA kit (Miltenyi Biotech) following the manufacturer`s instructions. The purity and quantity of the cDNA was assessed with a NanoDrop 1000 Spectrophotometer (Thermo Scientific).

Primer Design

The primers for TNF-α that were used in this work for both conventional and quantitative real-time PCR TNF-α were originally described by Breen et al. 2000 (Breen et al., 2000). To check primer specificity, the sequences were mapped with NCBI Reference Sequence: NM:000594.3. For both the forward and reverse primer, the homology was shown to be 100% over the full length of the primers. Mapping to the reference sequence showed that the TNF-α forward primer spans exon 1 and exon 2. The TNF-α reverse primer is non exon spanning and internal to exon 4. The amplicon size for these primers is 325bp. Primers were obtained from Eurofin, UK: TNF-α Forward (5'–CAGAGGGAAGAGTTCCCCAG-3'), TNF-α Reverse (5'-CCTTGGTCTGGTAGGAGACG-3').

The primers for Glyceraldehyde-3-phosphate dehydrogenase (GAPDH) were kindly provided by Fabian Salazar, Immunology and Allergy Tissue Modelling Group, University of Nottingham. The specificity of the primers was checked by mapping the sequences with NCBI Reference Sequence: NM_001289746.1. The homology was shown to be 100% for both the forward and reverse primers. The GAPDH forward primer spans exon 1 and exon 2, the reverse primer is non exon spanning. The amplicon size for these primers is 185bp. Primers were obtained from Eurofin, UK, Glyceraldehyde 3-phosphate dehydrogenase (GAPDH) Forward (5`-GAGTCAACGGATTTGGTCGT-3`), GAPDH Reverse (5`-GACAAGCTTCCCGTTCTCAG-3`).

Conventional PCR

Conventional PCR was carried out in a TC-312 PCR Thermocycler (Bibby Scientific Ltd, UK) using the Phusion Flash High-Fidelity PCR Master Mix (Thermo Fisher Scientific) and 20ng of μMACS cDNA per reaction..

PCR was carried out with an initial denaturation at 98°C for 10 seconds, followed by 32 cycles of denaturation (98°C, 0-1 seconds), annealing (62°C, 30 seconds), extension (72°C, 30 seconds), final extension was performed at 72°C for 60 seconds. Then, the PCR products were analysed in an E-gel pre-cast 2% agarose electrophoresis system (Thermo Fisher Scientific) and the molecular weight of the bands were calculated with a standard 100bp Directload DNA ladder (Sigma-Aldrich).

Quantitative real-time PCR analysis

Real time PCR was performed in a Stratagene MxPro 3005P qPCR System with the Brilliant III Ultra-Fast SYBR Green qPCR Master Mix (Agilent Technologies, USA). Primers were obtained from Eurofin, details for GAPDH and TNF-α as above. Cycling was initiated at 95°C for 3 minutes, followed by 45 cycles of 95°C for 20 seconds and 62°C for 30 seconds. Melt curves were performed at the end in order to show the presence of a single, specific product, representative melt curves from these experiments are shown in Appendix I.

Samples were run in triplicates and relative expression calculated using comparative threshold cycle method normalized to GAPDH (Livak and

Schmittgen, 2001). This method is commonly referred to as the ΔΔCt method and uses the following equation:

Relative quantity to the calibrator = 2-(ΔΔCt)

Where Δ ΔCt =

(CtTNF-α – CtGAPDH)calibrator – (CtTNF-α – CtGAPDH)unknown

Statistical Analysis

One-way ANOVA or t-tests were performed in the statistical analysis. The analysis was carried out using GraphPad Prism version 6.00 for Windows, GraphPad Software, La Jolla California USA (www.graphpad.com).

2.3. Results and Discussion

Investigating Synthetic Biomaterials for Immune Cell Culture

Thermo-Responsive Particulate Gel

Formation of cell-laden thermo-responsive particulate gels

The immune cells used for this work were human monocyte-derived dendritic cells (moDCs), generated from peripheral blood mononuclear cells (PBMCs). To establish cell densities which were compatible with gel formation, a range of densities were tested from 5 x 10^4 – 5 x 10^5 cells\50µL matrix. Figure 12A illustrates the thermo-responsive generation of the particulate gels at 37°C and their dispersal after a 10 minute incubation at 4°C. Figure 12B shows the formation of the particulate gels laden with moDCs. Gels were produced successfullywith the highest cell density of 5 x 10^5 cells\50µL gel in a reproducible manner at 37°C.

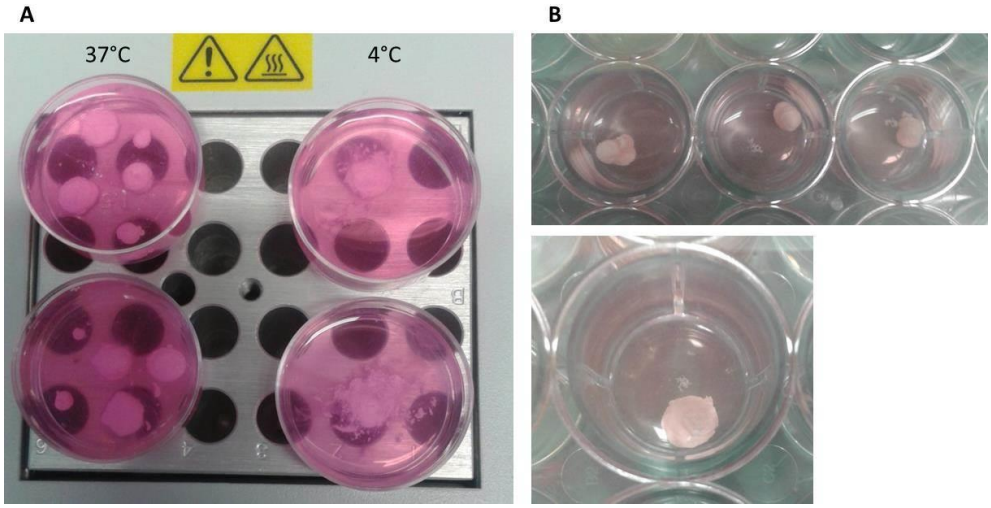

Figure 12. Thermo-responsive formation of particulate gels with dendritic cells.
A. Formation of a robust particulate gel matrix at 37°C and dispersal following incubation at 4°C. B. Generation of reproducible droplet-like 3D gels with encapsulated moDCs.

This work established that 5 x 10^5 cells could be incorporated into the matrix without affecting the integrity of the gel. Although the formation of gels with encapsulated cells has previously been described by Al Ghanami et al., it was important to optimise the protocol specifically for moDCs. The reason for this is that, 3T3 fibroblasts used in the study by Al Ghanami are larger cells (18µm) compared with moDCs (10µm)., It was found that the number of moDCs that could be encapsulated was higher compared to the number of 3T3 cells used in Al Ghanami's work (Al Ghanami et al., 2010). It was also important to determine that sufficient numbers of moDCs could be incorporated into the gels so that they could be collected for analysis.

moDC analysis after 24 hours in culture with particulate gels

The gels, containing 5 x 10^5 moDCs\50µL matrix, were maintained under standard tissue culture conditions (37°C, 5% CO_2) for 24 hours. The temperature-sensitive property of the material was used in order to disassemble the gels for cell retrieval and analysis by flow cytometry.

The results from the flow cytometry analysis are displayed in Figure 13. The dot plots show forward scatter (FS) and side scatter (SS) cell properties, expression of the moDC marker CD11c and Annexin V-FITC\propidium iodide (PI) staining for cell viability of the moDCs harvested from tissue culture plastic (TCP) and particulate gel.

The FS\SS profile gives an indication of the size and granularity of a population of cells. Based on the profile of the cells collected from TCP, a region was drawn to indicate the moDC population. When this region was

transposed onto the FS\SS dot plots for the particle gel samples, it was difficult to detect moDCs due to the large number of events representing particles from the gel. As labelled on the dot plot, this population is likely to be a mixture of particles, cells and debris.

One explanation for the difference in the distribution of cells in the FS\SS dot plots could be due to cell attachment to, or cells taking up, the particles. In terms of the latter, this is highly likely due to the actively endocytic nature of unstimulated moDCs (Garcia-Nieto et al., 2010). This would alter the size and granularity properties of the cells, therefore they wouldn't fall in the same region as cells from TCP.

Samples collected from the particulate gels were also fluorescently stained for CD11c. A distinct population of cells, >90%, was $CD11c^+$ in samples harvested from TCP. For gel samples, a population of cells, 6%, was detected which expressed CD11c. Labelling cells for CD11c was useful to differentiate the moDC population from the particulate material, which could not be done based on FS\SS.

Finally, cell viability was measured using the Annexin V-FITC\PI cytotoxicity assay. This is a flow cytometric-based assay, which distinguishes between live cells (Annexin V^-\ PI^-), apoptotic cells (Annexin V^+\ PI^-) and dead cells (Annexin V^+\PI^+). Analysis of Annexin V-FITC\PI staining allows quantitative determination of the level of cytotoxicity.

The viability of moDCs harvested from TCP was >80%. In the samples from the gel, the proportion of viable cells could not be distinguished from the particles and debris, which also feature in the Annexin V^{-}\PI^{-} quadrant. Therefore determination of cytotoxicity was difficult since the particulate material could not be differentiated from unstained (viable) cells in the lower left quadrant of the dot plots. Overall, the flow cytometric approach used for the analysis of cells collected from the particulate gel was limited by the inability to separate\distinguish cells from the particulate gel material.

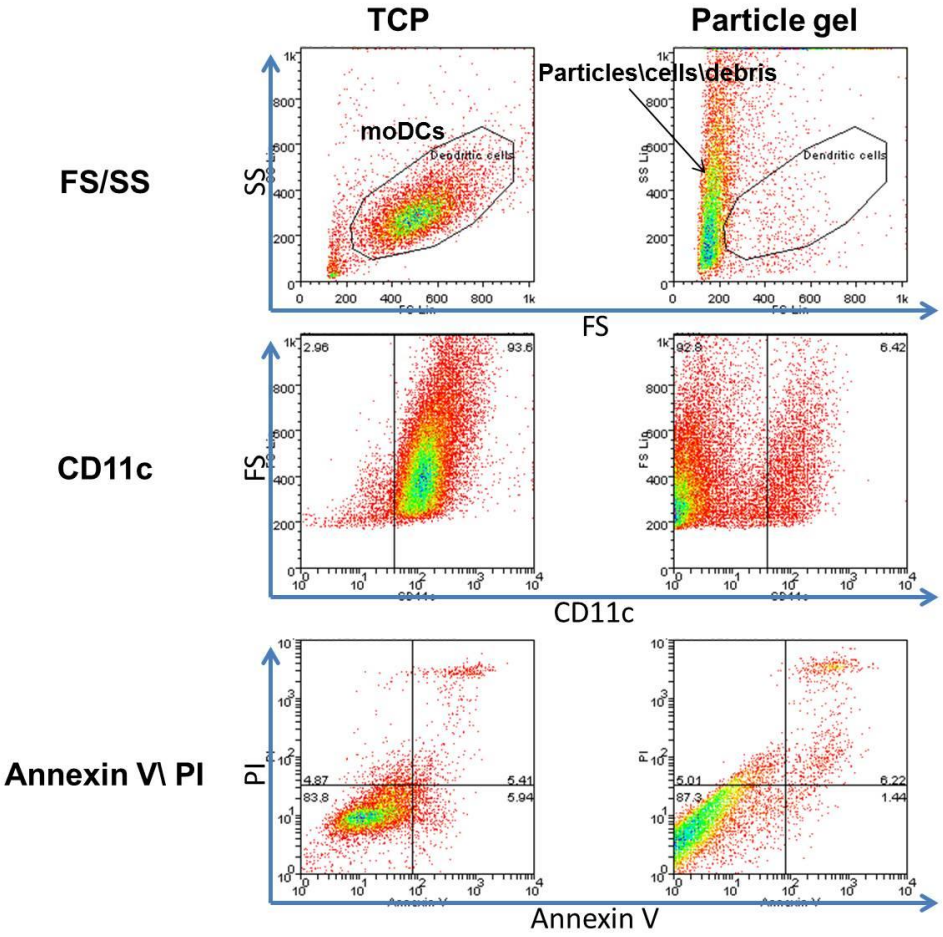

Figure 13. Flow cytometric analysis of moDCs following culture with particulate gel. FS/SS: A distinct population of moDCs was detected based on FS/SS properties of the cells collected from TCP. A discreet cell population could not be distinguished based on FS/SS profile of cells collected from the particulate gel. CD11c: The population of cells harvested from TCP was 93.6% positive for CD11c. In the particulate gel samples, a population of 6% CD11c expressing cells was identified. Annexin V\PI: Cell viability of moDCs harvested from TCP was >80%. The cytotoxicity couldn't be determined for the particulate gel samples (n = 3 independent experiments).

PET-based Electrospun Scaffolds

In the work performed to characterise electrospun PET scaffolds for immune cell culture applications, human moDCs were used for all experiments. Cells were seeded on to sterilised uncoated PET and PEGMA-coated PET (PET\PEGMA) scaffolds, then, they were maintained under standard tissue culture conditions for 24 hours (37°C, 5% CO_2). Cells were harvested from the scaffolds for analysis of viability and phenotype by flow cytometry. The temperature-sensitive properties of PET\PEGMA scaffolds were taken advantage of for cell retrieval by incubating at 4°C for 10 minutes before washing with ice cold PBS to collect the cells.

Electrospun PET scaffold cytotoxicity

Cell viability was measured using the Annexin V\PI cytotoxicity assay. Figure 14 shows the results from this. It was found that the proportions of viable cells collected from PET (88.8%) and PET\PEGMA (83.0%) scaffolds were not significantly different ($P \geq 0.05$) from TCP (88.0%). There was no significant difference in the percentage of non-viable cells collected from uncoated PET (9.2%) or PET\PEGMA (15.7%) with respect to TCP (10.2%). This data suggested that moDC viability was not impaired by PET-based electrospun scaffolds.

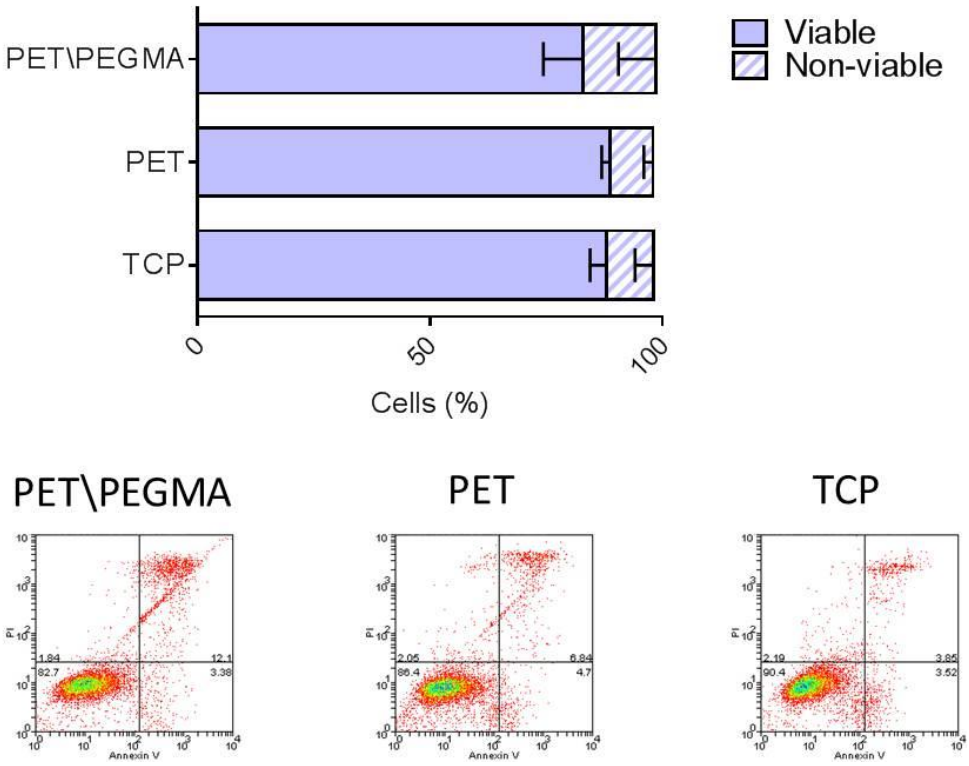

Figure 14. PET-based electrospun scaffolds are not cytotoxic to moDCs.
Viability of moDCs was not significantly affected after 24 hours in culture with PET or PET\PEGMA scaffolds. One-way ANOVAs performed to determine significant differences in the proportion of viable\non-viable cells collected from each of the conditions respectively. No significant differences found for either non-viable or viable ($P>0.05$) ($n = 3$ independent experiments). Error bars represent standard deviation. Representative dot plots of Annexin V/PI staining profile shown below.

Induction of moDC maturation by PET electrospun scaffolds

The phenotype of moDCs seeded on the scaffolds was assessed by the expression of the dendritic cell maturation marker, CD83. Immuno-fluorescent staining of cells was performed for analysis of CD83 expression by flow cytometry.

Figure 15 shows the expression of CD83, presented as the percentage of CD83 positive cells, of moDCs harvested from uncoated PET (56.4%), PET\PEGMA (62.7%) and TCP (3.25%). Statistical analysis revealed that CD83 expression was significantly increased by cells when cultured on uncoated PET and

PET\PEGMA scaffolds (P≤0.05, *). The increase in CD83 was indicative that the PET-based scaffolds caused the maturation of moDCs.

Due to the methods involved in the synthesis of electrospun materials, the potential of endotoxin contamination causing cell maturation could not be overlooked. A further experiment was performed to control for this using the antibiotic polymyxin B (PMB). Scaffolds were incubated with PMB to neutralise endotoxin prior to cell seeding. Since moDC activation was also induced on PMB-treated scaffolds, the results indicated that endotoxin contamination was not responsible for the induction of moDC maturation on PET scaffolds (data not shown).

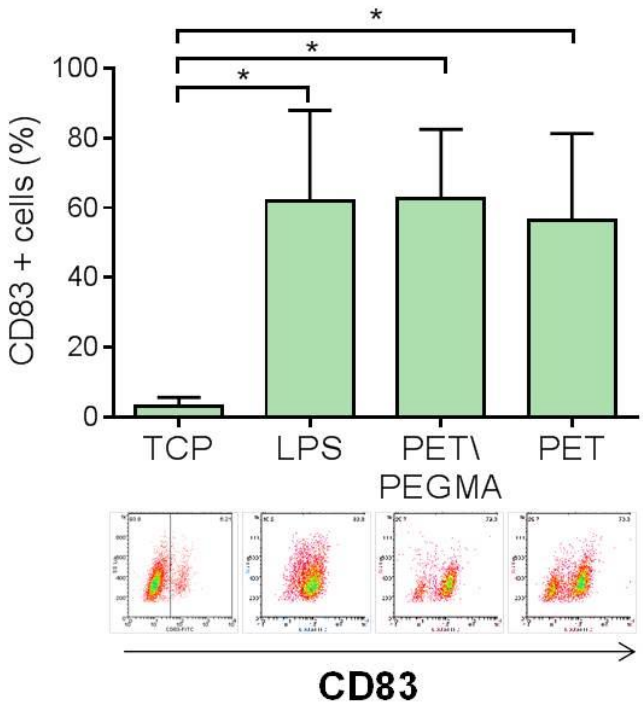

Figure 15. PET scaffolds induce moDC maturation.
moDC maturation was elicited in culture on PET electrospun scaffolds. Expression of CD83 was significantly increased with both PET and PET\PEGMA scaffolds after 24 hours of culture. One-way ANOVA used to test for significance (P≤ 0.05, *) (n = 3 independent experiments). Error bars represent standard deviation.

Weak attachment of moDCs on PET scaffolds

To visualise the interaction and attachment of moDCs with the scaffolds, samples were prepared for scanning electron microscopy (SEM). Figure 16 shows representative micrographs of the samples.

Attachment of moDCs on uncoated PET scaffolds was sparse, cells present on the scaffolds had a rounded morphology and occurred in clumps. moDCs that had attached to PET\PEGMA scaffolds could be seen stretched across the fibres, and cells were distributed unevenly. These observations indicated moDCs did not interact strongly with the materials; low adhesion likely led to cells being lost during the fixation and dehydration steps of SEM sample preparation.

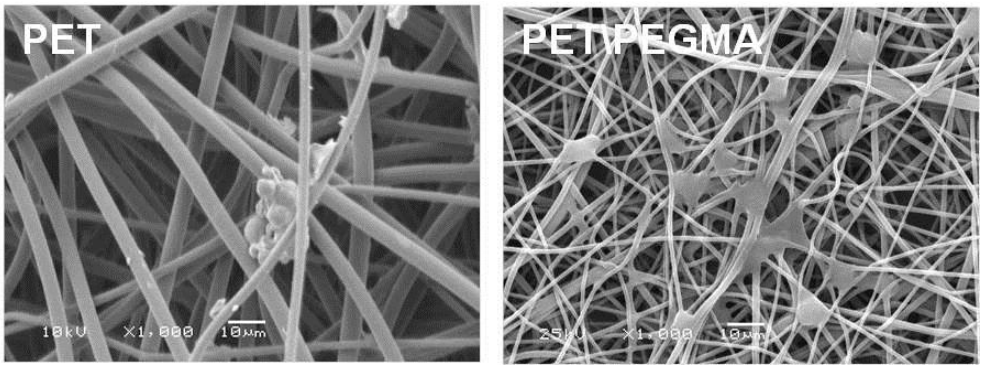

Figure 16. moDCs interact weakly with PET electrospun scaffolds.
Scanning electron microscopy of PET scaffolds seeded with dendritic cells. On PET scaffolds, moDC attachment was sparse and cells occured in clumps. Slightly more cells were attached on PET\PEGMA scaffolds, cells appeared stretched across the fibres but cell distribution was uneven. 1,000X magnification was used to acquire the images. Scale bars represent 10µm.

PLGA-based Electrospun Scaffolds

To characterise uncoated PLGA and PEGMA-coated PLGA (PLGA\PEGMA) electrospun scaffolds for immune cell culture, all experiments were performed with human moDCs. The thermo-sensitive properties of PLGA\PEGMA scaffolds were utilised by incubating for 10 minutes at 4°C before cell collection.

Cytotoxicity of PLGA electrospun scaffolds

Figure 17 shows the results from the Annexin V\PI viability assay carried out to assess the cytotoxicity of the PLGA-based scaffolds on moDCs. The percentages of non-viable moDCs collected from uncoated PLGA (27.6%) and PLGA\PEGMA (18.2%) scaffolds were slightly increased compared to cells harvested from TCP (10.2%), however, no significant differences were found ($P>0.05$). Also, there was no significant difference between the proportions of viable cells collected from uncoated PLGA (70.4%), or PLGA\PEGMA (78.9%) with TCP (88.0%). These results suggested that PLGA-based scaffolds may have had a long term detrimental effect on cell health but in a 24 hour period, levels of cytotoxicity were not significant.

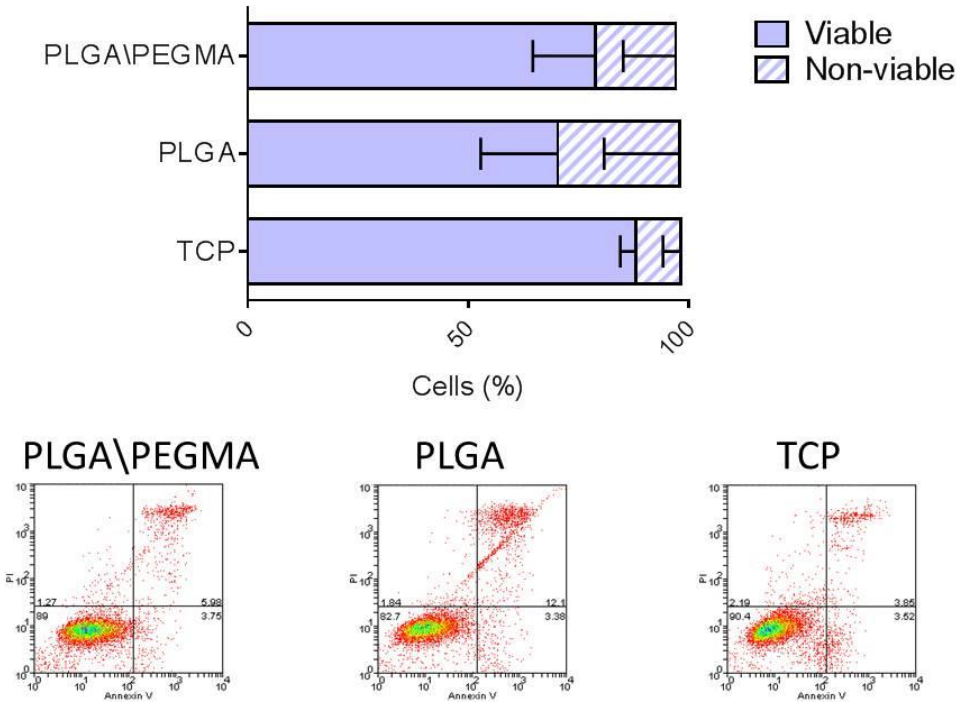

Figure 17. Electrospun PLGA scaffolds do not significantly impair the viability of moDCs.
Cell viability was slightly reduced after 24 hours of culture in the presence of PLGA and PLGA\PEGMA scaffolds. However, one-way ANOVAs of viable\non-viable cells did not reveal any significant differences compared to TCP ($P>0.05$) ($n = 3$ independent experiments). Error bars represent standard deviation.

Induction of moDC maturation by PLGA electrospun scaffolds

The effect of PLGA scaffolds on moDC phenotype is shown in Figure 18, presented as the percentage of CD83 positive cells. Expression of CD83 was increased by cells cultured with uncoated PLGA scaffolds (53.9%), however, this was not found to be significant ($P>0.05$). Seventy percent of cells collected from PLGA\PEGMA scaffolds were CD83 positive, which was significantly higher ($P\leq0.05$, *) compared with TCP (3.3%). The increased expression of CD83 by moDCs cultured on PLGA scaffolds suggested that the material induced cell maturation.

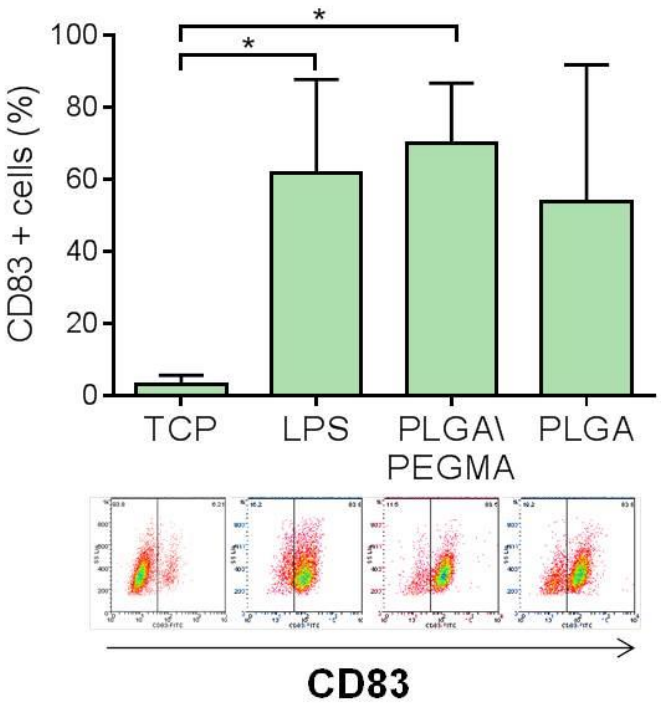

Figure 18. PLGA electrospun scaffolds induce moDC maturation.
Maturation of moDCs was seen after 24 hours of culture with thermo-responsive PLGA\PEGMA scaffolds. One-way ANOVA determined a statistically significant increase of CD83 expression in moDCs harvested from PLGA\PEGMA scaffolds ($P \leq 0.05$, *) (n = 3 independent experiments). Error bars represent standard deviation.

As previously described for PET scaffolds, an experiment to test for the effects of endotoxin contamination was carried out by treating the scaffolds with polymyxin B (PMB) prior to cell seeding. PMB was not found to affect the expression of CD83, thereby ruling out endotoxin contamination as a cause for cell maturation (data not shown).

moDCs attach weakly to PLGA scaffolds

SEM was performed to visualise moDC interaction with the scaffolds, as shown in Figure 19. Few cells were found attached to the PLGA scaffolds, this suggested weak attachment and cells were most likely lost during the washing, fixing and dehydration steps involved in SEM sample preparation. Clumps of

cells were found to be attached on PLGA\PEGMA scaffolds, although these were relatively few and far between.

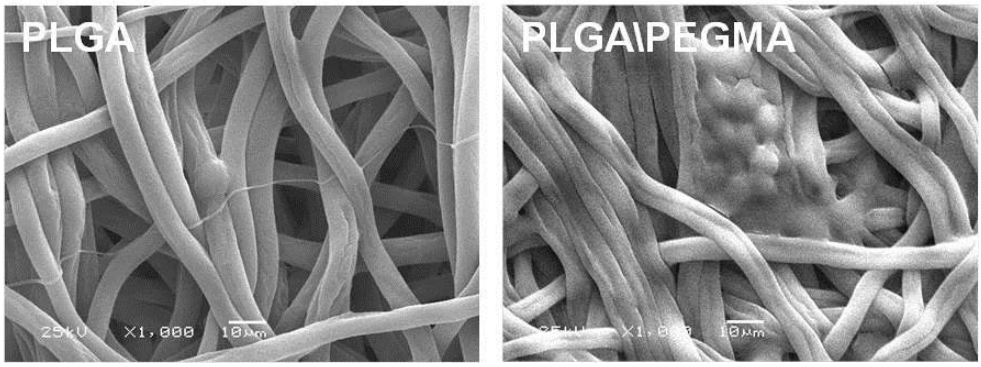

Figure 19. moDCs interact weakly with PLGA electrospun scaffolds.
Scanning electron microscopy of PLGA electrospun scaffolds seeded with moDCs. Very few cells were attached to PLGA scaffolds. Cells attached to PLGA\PEGMA scaffolds were in clumps and few and far between. The magnification used was 1,000X. The scale bars represent 10µm.

Naturally-derived Biomaterials

Gelatin Methacryloyl Hydrogel

Viability of immune cells harvested from GelMA

Peripheral blood mononuclear cells (PBMCs), isolated from the blood of healthy donors, were used as a source of primary human immune cells in these experiments. The cellular composition of PBMCs is 70-90% lymphocytes (T cells, B cells and natural killer (NK) cells), 10-30% monocytes, 1-2% dendritic cells and small numbers of basophils. The total PBMC population was used in these experiments since it comprises the cell types of interest for this work and requires minimal processing following the initial purification step performed by density centrifugation.

To set up these experiments, PBMCs were seeded onto a pre-photo-polymerised GelMA hydrogel layer. After 5 days in culture, cell viability was assessed by Annexin V\PI staining.

Figure 20 shows the results from the cytotoxicity assay, A and B illustrate representative dot plots of Annexin V\PI stained cells harvested from TC (tissue culture plastic) and GelMA respectively. As shown by the graph in C, after 5 days in culture, the proportions of live cells collected from GelMA hydrogels (mean = 67%) were not found to be significantly different compared to TC (mean = 76%). Apoptotic and dead cells were combined to determine the amount of non-viable cells for GelMA (mean = 33%) and TC (mean = 24%). No significant difference was found between the percentages of non-viable cells harvested from GelMA, compared to TC.

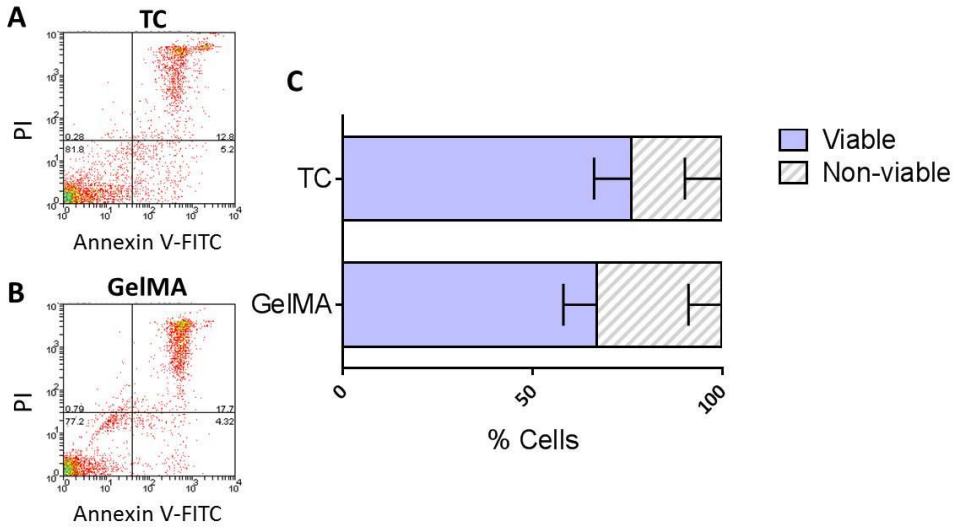

Figure 20. PBMC viability is not impaired by culture with GelMA hydrogels.
A & B. Annexin V\PI staining profiles of cells harvested from TC and GelMA cultures respectively. C. Percentage of viable (solid bar) and non-viable (striped bar) cells collected from GelMA and TC. Two-tailed t tests determined that there were no significant differences ($P > 0.05$) in the proportion of viable cells, or non-viable cells harvested from GelMA cultures compared to TC (n=3). Error bars represent standard deviation.

Cell health is a critical parameter when assessing the suitability of a biomaterial for *in vivo* and *in vitro* applications (Williams, 2008). This encompasses several cell functions, including cell death. With regards to the method of polymerisation, the photoinitiator can potentially have detrimental impacts on cell survival. Although in this experiment GelMA hydrogels were photo-polymerised prior to cell seeding, persisting free radical species, produced as a result of the photoinitiator being exposed to UV, have the potential to cause oxidative damage to the cells, leading to cell death (Mironi-Harpaz et al., 2012, Williams et al., 2005). Based on the findings from these experiments, however, the photoinitiator did not appear to induce cell death.

Immune-modulatory effect of GelMA on the production of inflammatory cytokines

To characterise the immune-modulatory properties of GelMA, the responsiveness of PBMCs to immunological manipulation in the presence of GelMA was investigated. This was done by assessing the response of PBMCs to lipopolysaccharide (LPS).

PBMCs were cultured on GelMA hydrogels, with or without LPS stimulation for 4 hours. Secretion of a panel of inflammatory cytokines (IL-1β, IL-6, IL-8 and TNF-α) was used to determine the immune response. In Figure 21, graphs A-D show the production of TNF-α, IL-1β, IL-6 and IL-8 respectively following immunogenic stimulation with LPS.

In the TC condition, levels of all cytokines increased significantly in response to LPS. Within the PBMC population, monocytes are the main responders to

LPS (Tazi et al., 2006) and are largely accountable for the production of pro-inflammatory cytokines, including IL-1β, IL-6, IL-8 and TNF-α. In the presence of GelMA hydrogels, background levels of all inflammatory cytokines were raised and there was large variation in the response to LPS between donors. This may account for there being no significant up-regulation for any of the cytokines upon stimulation with LPS. Interestingly, there was a significant difference in the concentration of TNF-α detected in GelMA+LPS cultures compared with TC+LPS cultures, with higher levels of TNF-α in TC+LPS samples.

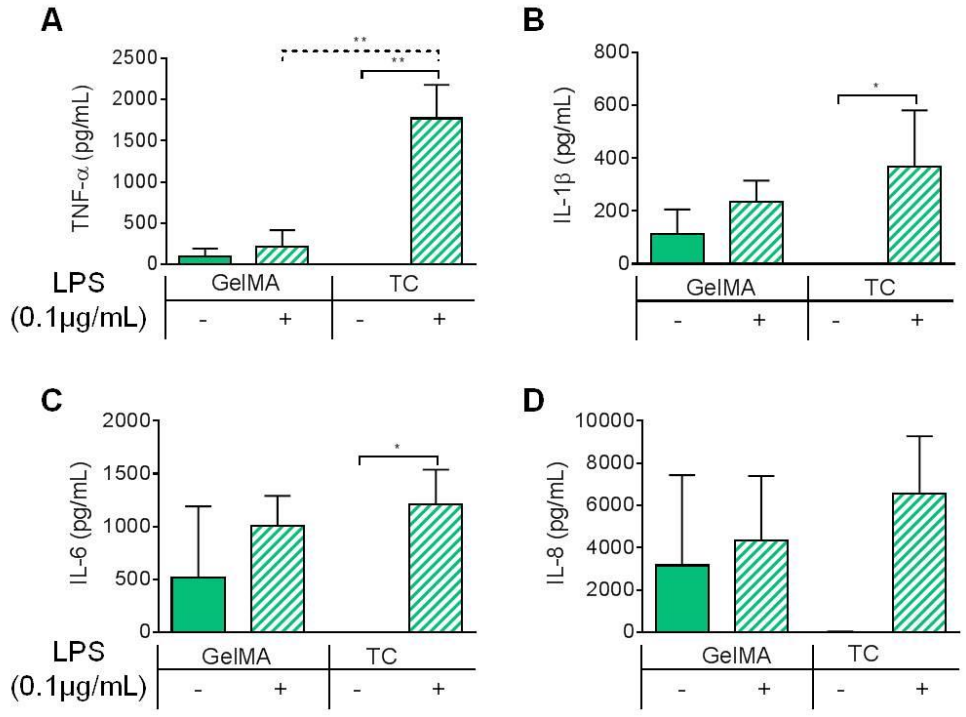

Figure 21. Modulatory effect of GelMA on inflammatory cytokine production, with and without LPS stimulation.
Cytokine production after 4 hours by PBMCs cultured on GelMA hydrogels or TC, with (+) or without (-) LPS stimulation. A. TNF-α was not significantly increased following LPS stimulation in GelMA cultures. Secretion of TNF-α was found to increase significantly in the LPS-stimulated TC control ($P \leq 0.0001$, ****). A significant difference in the level of LPS-induced TNF-α production was found between GelMA and TC conditions ($P \leq 0.001$, ***). B. Production of IL-1β was not significantly increased with LPS stimulation in the presence of GelMA, whereas in TC it was ($P \leq 0.05$, *). C. IL-6 secretion was not significantly increased in GelMA cultures following LPS stimulation, this was found to be significant in TC ($P \leq 0.05$, *). D. No significant rise in IL-8 production with LPS stimulation in GelMA or TC cultures ($P \geq 0.05$). One-way ANOVA performed to determine statistically significant differences in cytokine production (n = 3 independent donors). Error bars represent standard deviation.

The possibility of endotoxin contamination causing the induction of inflammatory cytokine production was ruled out by incubating the GelMA hydrogel with PBM prior to cell culture (data not shown). Immunogenicity is a common problem with natural biomaterials. Since the origin of the gelatin used for the synthesis of GelMA was porcine, the elicitation of a pro-inflammatory cytokine response may be explained by the antigenicity caused through the use of a xenogenic source of gelatin (Chan and Leong, 2008).

Given that TNF-α is a key inflammatory cytokine, it was surprising to find that the levels detected were not increased upon LPS stimulation in the presence of GelMA. In terms of its induction in response to LPS, under standard culture conditions, secretion of TNF-α by monocytes is rapidly increased, generally peaking around 4 hours after immunogenic stimulation (Tazi et al., 2006). The observations for TNF-α were particularly striking since the three other pro-inflammatory cytokines did increase to some extent with LPS stimulation in the presence of GelMA, although not significantly.

TNF-α has diverse roles in the function and regulation of the immune system, dependent on tissue type, immunological context and timing (Wajant et al., 2003). It predominantly has pro-inflammatory effects in affected tissues and can exacerbate disease states such as, rheumatoid arthritis and chronic wounds (Albillos et al., 2004).

GelMA suppresses LPS-induced TNF-α gene expression in PBMCs.

Given the observation that GelMA potentially diminished the levels of TNF-α, further investigation at the level of gene expression was carried out. In these experiments, PBMCs were cultured on photopolymerised GelMA hydrogel layers, with and without LPS stimulation. Then, they were harvested for analysis of TNF-α gene expression after 30 minutes and 4 hours of culture.

TNF-α gene expression by PBMCs in culture with GelMA hydrogels was measured by reverse transcription PCR. Both conventional gel-based PCR and quantitative real-time PCR were used to analyse TNF-α mRNA.

Figure 22A and B show the results obtained by conventional gel-based PCR and quantitative PCR respectively. Levels of TNF-α mRNA increased after 30 minutes with LPS stimulation, this indicated that TNF-α gene expression was up-regulated both in TC and GelMA cultures in response to LPS. After four hours, the quantity of TNF-α mRNA in PBMCs cultured on GelMA hydrogels was reduced, suggesting TNF-α gene expression had been suppressed. In contrast, LPS-stimulated PBMCs cultured in the TC condition maintained expression of TNF-α.

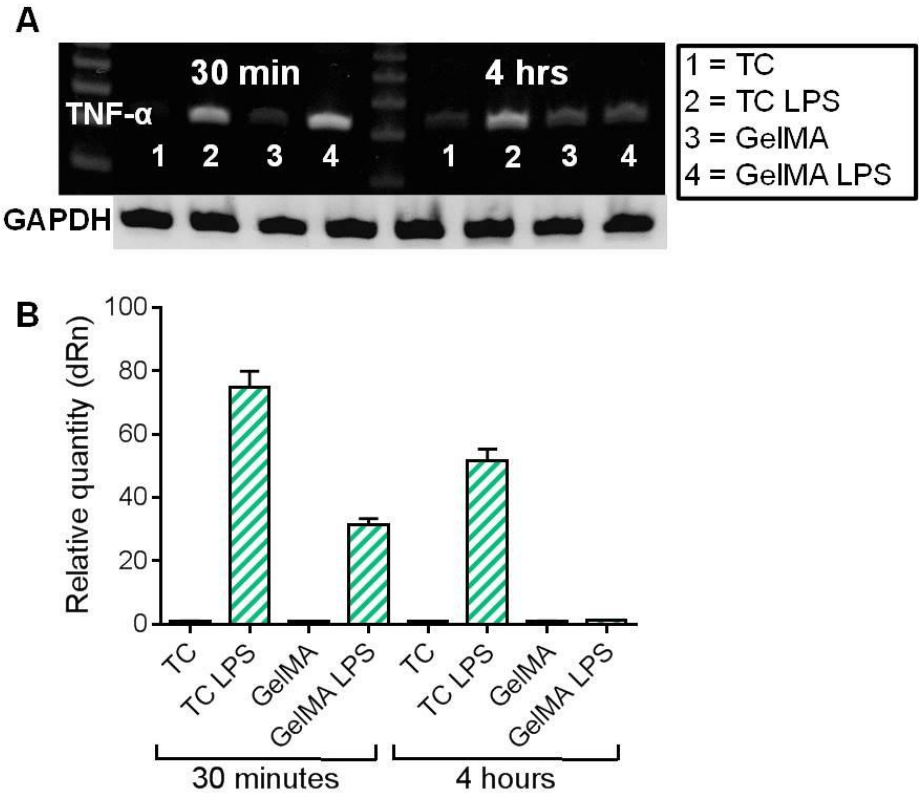

Figure 22. LPS-induced TNF-α gene expression is down-regulated in PBMCs cultured on GelMA.
A. Measurement of TNF-α gene expression by conventional ethidium bromide gel-based RT PCR: after 30 minutes in culture, the band intensity indicates TNF-α gene expression had increased as a result of LPS stimulation in both GelMA and TC cultures. At 4 hours, expression of TNF-α was maintained in the TC control, however, it was down-regulated in the GelMA condition. B. Analysis of TNF-α gene expression by real time quantitative PCR: 30 minutes after LPS stimulation the relative quantity of TNF-α expression increased in GelMA and TC cultures. After 4 hours, up-regulation of TNF-α gene expression was maintained in TC cultures, however, LPS-induced TNF-α gene expression was attenuated in the presence of GelMA. ΔΔ Ct Analysis normalised against GapDH. Error bars represent standard error. Data shown is from one donor but is representative of results from 3 independent donors. Refer to Appendix I for supplementary data.

GelMA hydrogels 'mop up' TNF-α

A cell-free system was used to determine whether levels of soluble TNF-α protein were depleted by GelMA. In these experiments, recombinant human TNF-α was added to the tissue culture media and incubated with GelMA hydrogels. After 4 hours, the supernatants were collected for cytokine analysis by ELISA.

As shown in Figure 23A, there was a large reduction in soluble TNF-α detected in supernatants collected from GelMA, compared to TC. This was shown over a titration of concentrations of TNF-α in Graph 1 of Figure 23A. By calculating the residual TNF-α in the media collected from GelMA (30%), relative to TC (100%), a significant reduction of TNF-α recovered from GelMA was determined ($P = 0.0006$, **), as shown in Graph 2 of Figure 23A.

To confirm the fate of the TNF-α protein, GelMA was incubated with TNF-α-containing media for 4 hours. Immuno-fluorescent staining of the gel was performed for TNF-α in order to determine whether it was bound within the gel. As shown in Figure 23B, GelMA hydrogels which had been incubated with TNF-α were positively and specifically stained for human TNF-α, indicating the presence of TNF-α bound within the hydrogel.

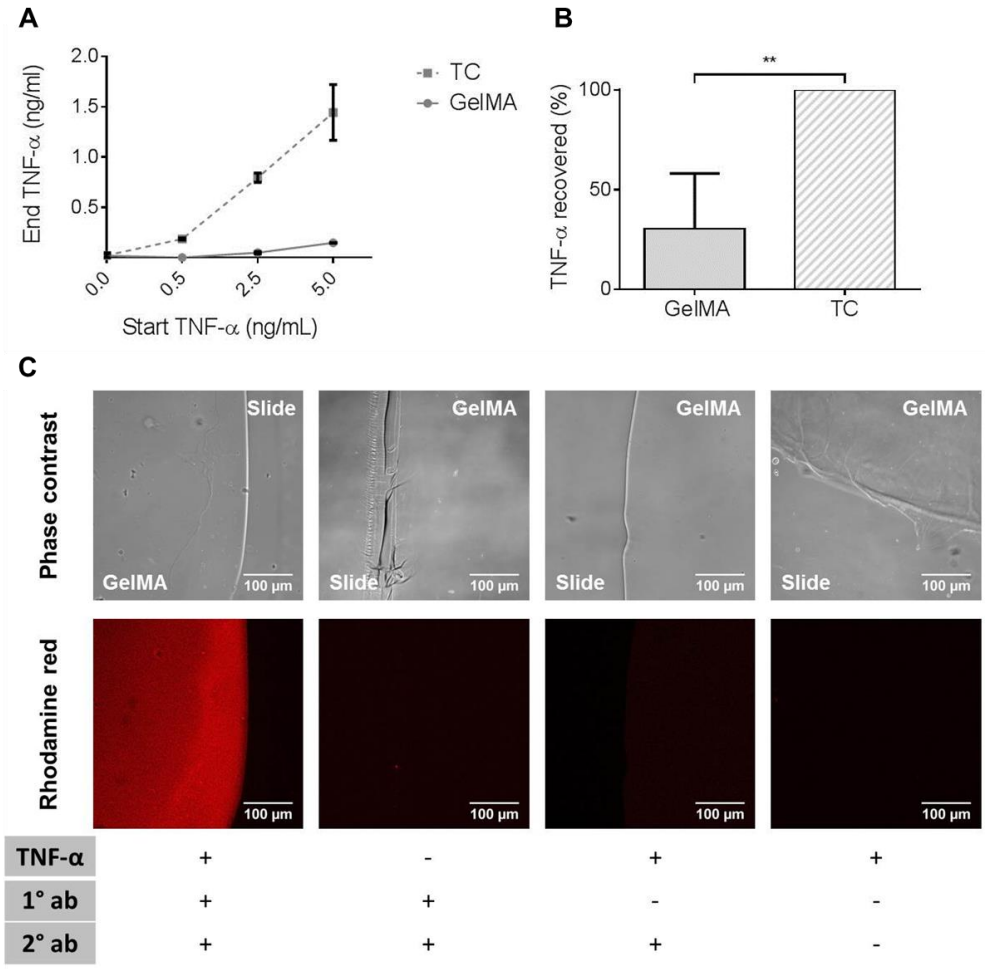

Figure 23. Depletion of soluble TNF-α by GelMA hydrogels.
A. Residual TNF-α detected after incubation of GelMA hydrogels in media containing 0.5, 2.5 and 5ng/mL recombinant TNF-α. Error bars represent standard error of the mean. B. TNF-α recovered from TC (100%) and GelMA (30%), a significant reduction in residual TNF-α recovered from GelMA was found relative to TC (P = 0.0006, **). A two-tailed t test was performed to determine statistical significance (n = 3 independent experiments). Error bars represent standard deviation. C. TNF-α-treated GelMA, labelled with mouse anti-human TNF-α (primary) and rhodamine red goat anti-mouse (secondary) antibodies. Untreated GelMA, stained with primary and secondary antibodies. GelMA, secondary antibody control. GelMA, unlabelled. Images acquired on an LSM710 META Zeiss confocal system, using a 20X objective. Scale bars represent 100µm.

It is plausible that GelMA exhibits the ability to adsorb certain polypeptides and proteins, including some cytokines. Gelatin has a repeating amino acid sequence of Gly-Pro-X but does include other amino acids with a range of side chains (Van Den Bulcke et al., 2000). It may be possible that GelMA based on the specific gelatin source displayed sufficient functional groups able to interact non-covalently with TNF-α, as has been noted for a variety of small

molecules, providing a potential cytokine sequestration mechanism (Nezu and Winnik, 2000, Taravel and Domard, 1993, Vaidyanathan et al., 2003). In addition, the 3D, porous nature of the GelMA hydrogel could also assist in the wicking away of cytokines (Benton et al., 2009).

Characterisation of Collagen Hydrogel

Both human PBMCs and moDCs were used in the experiments to characterise collagen for immune cell culture. Collagen hydrogel layers were formed under sterile conditions before seeding cells and maintained under standard tissue culture conditions (37°C, 5% CO_2).

Cell health is not impaired by collagen hydrogels

For cell viability studies, PBMCs were cultured on collagen hydrogel layers for 5 days. The Annexin V\PI cytotoxicity assay was performed to analyse cell viability by flow cytometry.

Representative dot plots for Annexin V\PI-stained cells harvested from TCP and collagen hydrogels are illustrated in Figure 24A and B respectively. As shown in Figure 24C, the percentages of viable (79.4%) and non-viable (20.6%) cells collected from collagen hydrogels were not found to be significantly different from those collected from TCP, 76.0% viable and 24.0% non-viable cells ($P>0.05$). These results suggest that collagen hydrogels do not impair immune cell health.

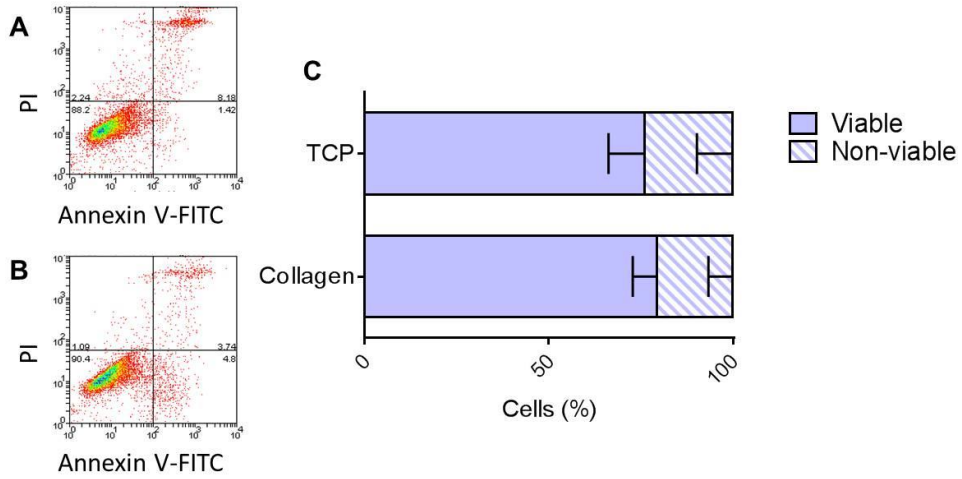

Figure 24. Collagen hydrogels are not detrimental to PBMC viability.
Annexin-V\PI profiles of cells harvested from TCP (A) and collagen hydrogels (B). C. Percentage of viable (solid bars) and non-viable (striped bars) cells collected from TCP and collagen hydrogel. No significant differences were found using two-tailed t-tests to compare the proportions of viable or non-viable cells collected from each condition ($P>0.05$) ($n = 3$ independent experiments). Error bars represent standard deviation.

Collagen hydrogels support PBMC immune responses

PBMCs were used to investigate immunological responsiveness in the presence of collagen hydrogels. LPS was used to stimulate a pro-inflammatory response, which was assessed by the production of a panel of cytokines including IL-1β, IL-6, IL-8 and TNF-α. Supernatants were collected for cytokine analysis by a multiplex bead array method.

The results from this experiment are shown in Figure 25. Graphs A-D show the production of IL-1β, IL-6, IL-8 and TNF-α respectively. IL-1β was significantly upregulated by PBMCs cultured on collagen hydrogels following LPS stimulation ($P = 0.0128$, *). There was also a significant increase in IL-6 upon LPS stimulation in collagen hydrogel cultures ($P = 0.0048$, **). Production of IL-8 was raised, with respect to TCP, in unstimulated collagen hydrogel cultures and there was no augmentation with LPS. Production of

TNF-α was increased following stimulation by LPS in collagen hydrogel cultures, however, this was not found to be statistically significant (P≥0.05).

Overall, the increase in the production of inflammatory cytokines in collagen cultures with LPS stimulation indicated the induction of a typical immune response to such an immunogenic agent by PBMCs cultured in the presence of collagen hydrogels.

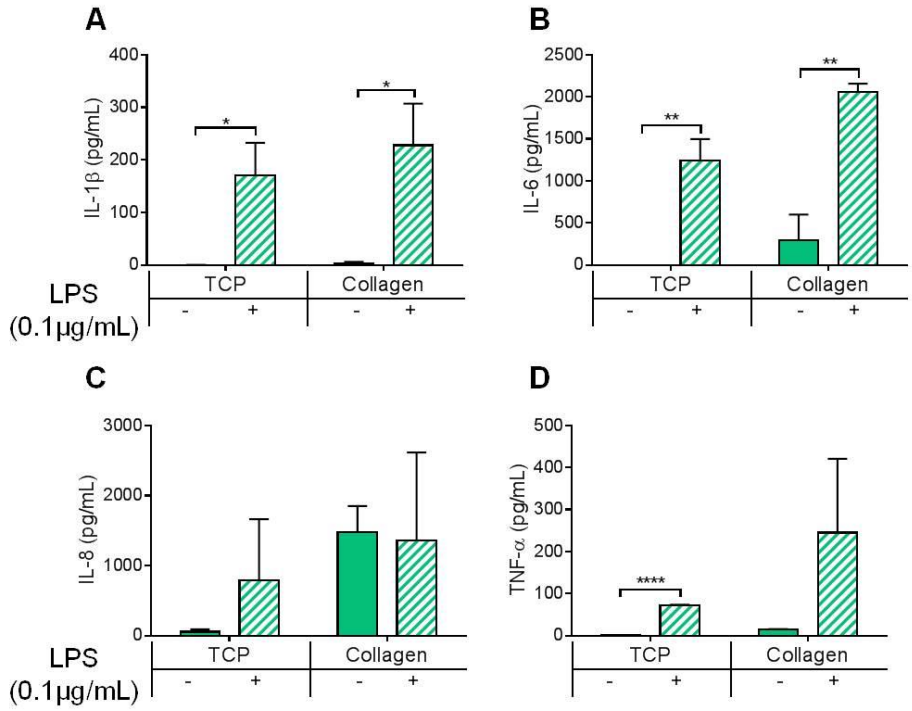

Figure 25. PBMC inflammatory cytokine response is supported by collagen hydrogels.
A. IL-1β production by PBMCs increased significantly in TCP (P = 0.0134, t=5.263, df=3) and collagen hydrogel cultures (P=0.0128, t=5.343, df=3) with LPS stimulation. B. Levels of IL-6 significantly increased with LPS stimulation for TCP (P=0.0026, t=9.331, df=3) and collagen hydrogels (P=0.0048, t=7.569, df=3). C. Increased IL-8 production in LPS-stimulated TCP cultures but this was not found to be significant. Levels of IL-8 increased in unstimulated collagen cultures, no effect seen +LPS. D. TNF-α production increased with LPS stimulation, this was significant for TCP (P=<0.001, t=63.00, df=3) but not collagen hydrogel cultures. T tests were used to determine significant differences (n = 3 independent experiments). Error bars represent standard deviation.

Phenotypic maturity of dendritic cells is not affected in culture with collagen hydrogels

To confirm the suitability of collagen for immune cell culture, the interaction with a purified cell type, moDC, was investigated. In these experiments moDC were seeded on collagen hydrogels and cultured for 24 hours before harvesting for phenotypic analysis. The phenotype of moDCs was assessed by staining for CD40, CD54, CD83 and CD86. These markers of moDC maturation include co-stimulatory and adhesion molecules. The level of expression of each marker was used to judge the maturation state of the cells.

Figure 26 shows the expression of these markers under resting conditions on the collagen hydrogels. Graphs A-D represent the expression of CD40, CD54, CD83 and CD83 respectively presented as median fluorescence intensity (MFI). Reassuringly, collagen hydrogels did not cause any significant changes in the expression of the four markers ($P \geq 0.05$). This indicated that collagen hydrogels did not affect the maturation state of moDCs.

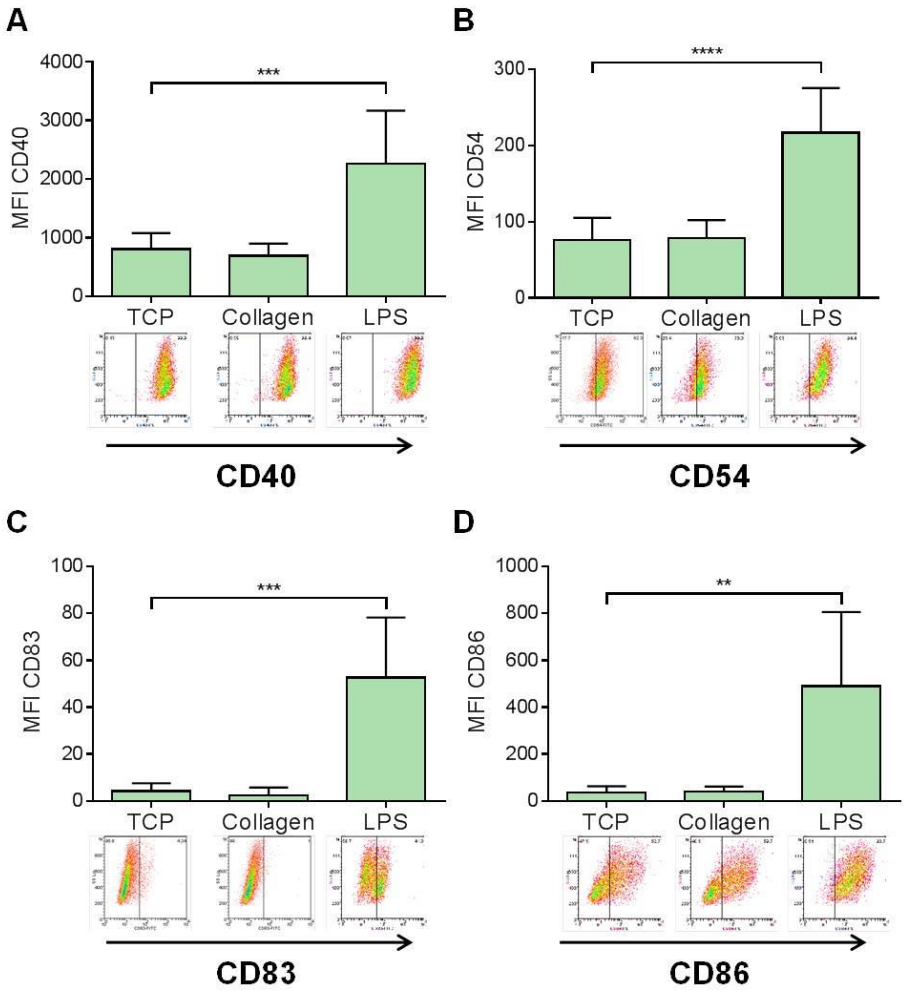

Figure 26. Dendritic cell maturity is unchanged in culture with collagen hydrogels.
A, B, C & D show expression of CD40, CD50, CD83 and CD86 by dendritic cells is not affected by culture with collagen hydrogels. One-way ANOVA used to determine statistical significance (P≤0.001, ***), (P≤0.0001, ****), (P≤0.01, **) (n = 3 independent experiments). Error bars represent standard deviation. MFI = median fluorescence intensity.

Dendritic cells are responsive to immunological stimulation in collagen hydrogel cultures

LPS-stimulations were performed to check whether moDCs were still responsive to an immunogenic stimulus when cultured on collagen hydrogels. Cells were stimulated for 24 hours and then collected for phenotypic analysis.

In Figure 27, graphs A-D show the expression of CD40, CD54, CD83 and CD86 as MFI. Expression of CD40 is increased with LPS stimulation in the

context of collagen, although this was not found to be statistically significant. There was a significant increase in the expression of CD54 (P = 0.0071, **), CD83 (P = 0.0199, *) and CD86 (0.0466, *) by moDCs following LPS stimulation in the presence of collagen. These results suggested that moDCs were immunologically competent when cultured in the presence of a collagen hydrogel.

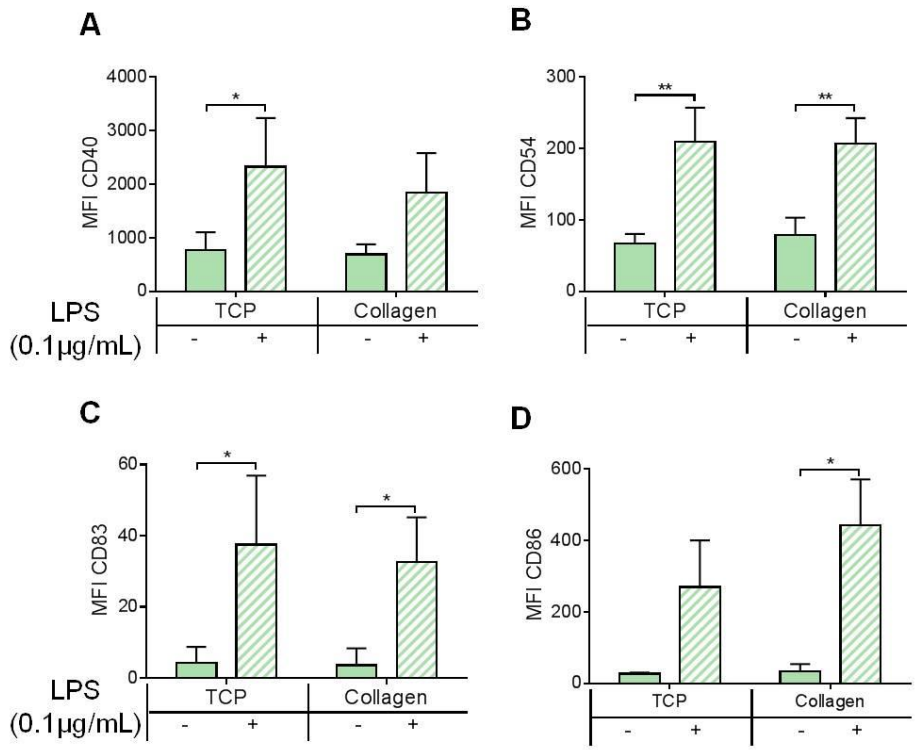

Figure 27. Dendritic cells are responsive to LPS stimulation in culture with collagen hydrogels.
The response of collagen-cultured moDCs upon LPS stimulation was assessed by expression of cell surface maturation markers. A. CD40 expression increaseed with LPS stimulation, this was found to be significant for TCP-cultured dendritic cells (P=0.0493, t=2.791 df=4) but not for collagen hydrogels. B. Expression of CD54 increased significantly by both TCP (P=0.0074, t=5.020 df=4) and collagen-cultured (P=0.0071, t=5.071 df=4) dendritic cells. C. CD83 expression was significantly up-regulated in response to LPS by dendritic cells cultured on TCP (P=0.0444, t=2.894 df=4) and collagen hydrogel (P=0.0199, t=3.750 df=4). Expression of CD86 is increased following stimulation by LPS stimulated, this was significant for collagen-cultured cells (P=0.0466, t=4.469 df=2) but not TCP. T tests used to determine significance (n = 3 independent experiments). Error bars represent standard deviation.

Depletion of the soluble cytokine, IFN-γ, by collagen hydrogels

As noted in this work and by others, certain ECM-derived biomaterials, including collagen, can bind cytokines with potentially immune-modulatory effects (Wiegand et al., 2010, Lortat-Jacob et al., 1991).

For the purposes of this thesis, interferon (IFN)-γ was an important readout for the down-stream assessment of antigen-specific T cell activation, as described in Chapter 4 of this thesis (Xu et al., 1996).

To determine whether the collagen hydrogel dramatically affects levels of soluble IFN-γ, a cell-free system was used. Collagen hydrogels were prepared at two different concentrations, 1.7mg/mL and 0.5mg/mL. At time zero (T0) the concentration of IFN-γ in the media was 500pg/mL. This was incubated with the collagen hydrogels under standard conditions (37°C, 5% CO_2) and sampled after 30 minutes, 1 hour, 2 hours and 4 hours.

The results from this experiment are shown in Figure 28. Graphs A-B represent the IFN-γ concentration detected after 30 minutes, 1 hour, 2 hours and 4 hours respectively. The concentration of IFN-γ decreased rapidly over the 4 hour time course in all conditions. There was an indication that the rate of depletion was only slightly faster in the presence of the collagen hydrogels, with no effect of collagen concentration, compared to TCP.

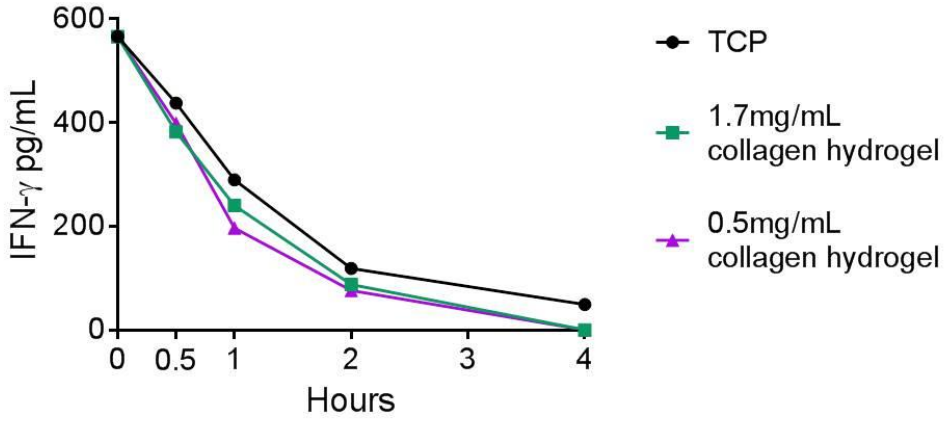

Figure 28. IFN-γ depletion with collagen hydrogels.
IFN-γ depletion over 4 hours on TCP and two collagen hydrogels at different concentrations, 0.5mg/mL and 1.7mg/mL.

2.4. Conclusions and Further Work

Characterisation of biomaterials is an important step in the development of tissue-engineered immune-competent constructs. The thermo-responsive particulate gel showed promise in terms of creating a porous matrix to mimic the ECM of the natural LN tissue. This was the first time primary human immune cells have been cultured within a thermo-responsive particulate gel. The temperature-sensitive properties allowed *in situ* gelation under mild, physiological conditions creating a robust, cell-laden matrix.

Based on the FS\SS properties, the moDC population could not be easily discriminated from the particulate material of the gel. One reason for this could have been that moDCs either stuck to, or engulfed the particles, thereby altering their size and granularity. To investigate this further, fluorescently labelled particles could be used, then, fluorescent imaging could be performed to determine the localisation of the particles with respect to the cells.

Fluorescent labelling for specific markers, such as CD11c, allowed moDCs to be distinguished from the gel material. This showed the potential for a wider array of markers to be used, for example, to assess the effect of the colloidal gel on moDC maturation. It is important to bear in mind that due to the large number of events that account for the particulate material, the sensitivity in terms of detecting markers which are expressed at relatively low levels may be limited.

Flow cytometry was also used to assess cell viability by Annexin V\PI staining. In the analysis, it was impossible to determine the number of viable cells since

they could not be distinguished from the particulate material. Alternative methods to measure cell death, which would not require cell separation from the particles, could include the lactate dehydrogenase (LDH) or MTT assays.

Overall, analysis of the cells by flow cytometry was limited since the material derived from the gel could not be separated. To assess the effect of the colloidal gel on moDC biology, without the need to separate the cells from the particles, alternative methods such as, cytokine production and gene expression, would be appropriate.

The inability to separate moDCs from the particulate material would also be preventative of downstream applications, such as co-culture with T cells. The use of magnetic particles could be explored in order to purify the cells from the gel material to increase the potential for downstream applications. Due to a shortage of time and resources it was decided not to pursue studies of this biomaterial in this work.

Electrospinning offers a convenient method to produce scaffolds for cell culture. The fibrous structure of these materials reflects the ECM network, which guides cell motility and interactions *in vivo*. The PEGMA-coated PET and PLGA scaffolds provided further benefit since their temperature-sensitive properties were used to facilitate the collection of cells. The results from the cell viability assay were encouraging since none of the electrospun scaffolds tested caused a significant level of cell death.

Dendritic cell maturation marker, CD83, was used to assess the effect of the scaffold on the maturation state of moDCs. The significant increase in expression of CD83 on cells harvested from the electrospun materials was indicative that the scaffolds induced cell maturation. SEM revealed that cell coverage on the scaffolds was sparse, suggesting that the cells had not attached strongly and had easily been displaced during sample preparation.

Although the scaffolds demonstrated compatible architectural features and low cytotoxicity, the induction of DC maturation was not a desirable effect for the purposes of this work since it may have potentially affected the immunological specificity of the system.

Investigation of the effect of the fibre diameter and different coatings on DC maturation and attachment would be interesting to determine whether the immunogenicity and immune cell-responsiveness of electrospun scaffolds can be modified.

Hydrogels have a highly hydrated, porous structure which closely resembles the ECM of soft tissues and are therefore popular candidates for tissue engineering purposes. GelMA has been used successfully in a variety of bioengineering applications, it has advantages over unmodified counterparts due to its mechanical stability and flexibility in fabrication methods.

This was the first time GelMA had been characterised for its compatibility with immune cells. The initial results from the cell viability assay were encouraging, since GelMA did not significantly impair cell viability. However, background

levels of inflammatory cytokines were raised in GelMA cultures, indicating it had immunogenic properties. Also, when immune cells were tested for their ability to mount an inflammatory response to LPS, there was little enhancement of inflammatory cytokines.

The species from which natural biomaterials are sourced can have implications on immunogenicity. It would be worth testing the immunogenicity of GelMA synthesised from gelatin derived from other species.

Also, this work was done with the total PBMC population. It would be informative to study the cell-material interaction in more detail using purified populations of immune cells, i.e. monocytes, DCs, T cells and B cells.

TNF-α was the subject of particular attention in this work due to its key role in modulating inflammatory responses *in vivo*. GelMA was found to deplete levels of soluble TNF-α, presumably though adsorption. GelMA is likely to have greater potential for protein interactions, compared with collagen. As it has undergone chemical modification, there are likely to be more chemically reactive groups exposed which may be involved in protein binding. Properties of the cytokines measured in this experiment, including protein size and isoelectric point, were compared and no striking differences were identified. Therefore, it is not clear what property sets TNF-α apart from the other cytokines, IL-1β, IL-6 and IL-8, which caused it to preferentially bind GelMA.

Gene expression studies showed that GelMA suppressed of LPS-induced TNF-α gene expression. TNF-α is under strict regulatory mechanisms which control

its expression. LPS induces TNF-α expression in monocytes through Toll-like receptor 4 (TLR4). The signalling pathways involved in TNF-α production include MAP kinases (ERK1/2, p38 and JNK) and NF-kappaB (Tazi et al., 2006). Soluble TNF-α signals through the receptor TNF-R1, which in turn activates a variety of signal transduction pathways, including MAP kinases and NF-kappaB. These regulate transcription factors involved in the production of inflammatory cytokines (MacEwan, 2002, Ronkina et al., 2010). It is feasible that TNF-α provides positive feedback to cells via paracrine or autocrine signalling in order to maintain its own expression.

In the context of the observations made in this work, a mechanism for the suppression of the expression of TNF-α can be postulated, whereby, the GelMA hydrogel sequesters TNF-α. This would deplete the soluble signal (TNF-α) required for maintaining TNF-α gene expression, which would presumably result in switching off the positive feedback mechanism, as depicted in Figure 29.

The mechanism by which GelMA influences the expression of LPS-induced TNF-α requires deeper investigation in order to confirm the suppressive effect seen at the level of gene expression. This could be done by assessing the effect of GelMA on components of the pathways involved in the regulation of TNF-α gene expression.

Although GelMA was shown to deplete soluble TNF-α and suppress gene expression, it was not clear whether this actually translated into a reduction in cytokine secretion. This could be confirmed by measuring the amount of TNF-

α present in the supernatant and bound in the hydrogel following PBMC stimulation by LPS. It would also be worth testing whether there would be normal activation in response to LPS if GelMA was already saturated with TNF-α.

Finally, further work into the long-term effects of TNF-α sequestration would be interesting to determine what the implications of TNF-α leaching back out of the GelMA hydrogel would be for the inflammatory status of immune cells in the proximity

Since GelMA was observed to have potentially both immunogenic and immune-modulatory effects, it was not considered appropriate as a platform for immune cell culture applications in this work.

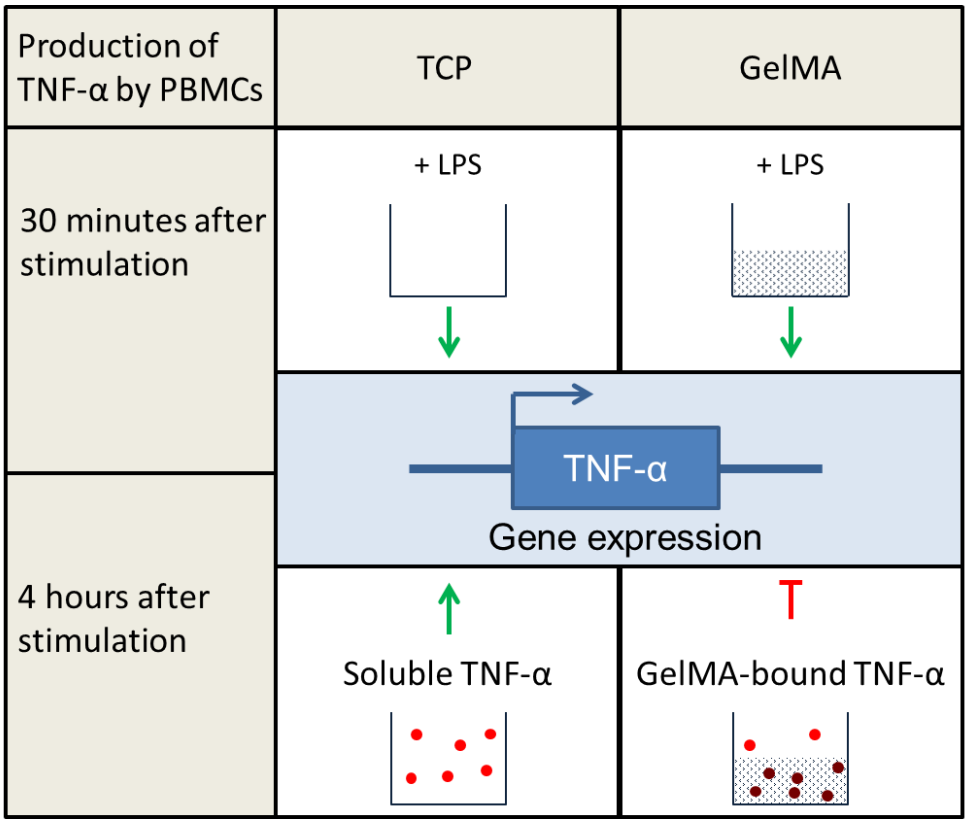

Figure 29. A role for GelMA in the modulation of TNF-α.
TNF-α gene expression increased within 30 minutes of LPS stimulation in both TCP and GelMA conditions. After 4 hours, LPS-induced TNF-α expression is maintained through a positive feedback mechanism and levels of secreted TNF-α peak in TCP. Whereas the GelMA hydrogel sequesters secreted TNF-α protein, thereby effectively removing it from solution. This disrupts the relay of positive feedback signals to the cell for the maintenance of TNF-α expression. Thus, by 4 hours, there is no detectable increase in soluble TNF-α and gene expression is suppressed in the context of GelMA.

Collagen has already been used successfully to engineer immune-competent constructs. To characterise it in terms of this study, assays to determine cell viability and immune responses with mixed (PBMCs) and purified (moDCs) primary human immune cell populations were carried out.

The collagen hydrogel did not induce significant cytotoxicity. Upon stimulation with LPS, PBMCs cultured on collagen hydrogels mounted typical inflammatory responses based on cytokine secretion.

The resting moDC phenotype was not affected in the presence of collagen hydrogels, since there was no significant change in the expression of moDC activation markers, CD40, CD54, CD83 or CD86. In culture with collagen hydrogels, moDCs responded appropriately to immunogenic stimulation by LPS, demonstrated by a significant increase in expression of activation markers.

Future work could focus on the effect of encapsulating immune cells within the hydrogel. This would expose the cells to a truly 3D environment.

In a cell-free system, levels of soluble IFN-γ were depleted marginally faster in the presence of collagen hydrogel, compared to TCP. This is likely to be partly due to adsorption of IFN-γ by collagen, as previously described. This experiment was a snapshot of the fate of one dose of IFN-γ *in vitro*. Fluorescent labelling of the hydrogel for IFN-γ, or digesting the gel and measuring the levels of IFN-γ recovered would also help to give a deeper insight.

In vivo, IFN-γ has important physiological roles in terms of modulating immune responses, therefore its production is under tight regulatory mechanisms (Philip and Epstein, 1986, Arai et al., 1990, Younes and Amsden, 2002). It has a very short half-life, presumably to allow the rapid cessation of its potent immunological effects (Miyakawa et al., 2011).

Activation of a robust T cell response in a biological assay would result in the continuous and increased production of IFN-γ. It was therefore anticipated that

the slight depletion in IFN-γ concentration would not be of significant consequence in terms of using IFN-γ secretion as a readout for T cell activation in collagen hydrogel cultures.

In conclusion, the work in this chapter has described the characterisation of synthetic and natural biomaterials for immune cell culture. This is the first time a particulate gel and GelMA hydrogel, have been cultured with immune cells.

Finally, this study highlighted the importance of investigating biomaterial biocompatibility based on cell function, in this case immune cell function, for specific applications. It has also generated some new, useful information regarding the interaction of biomaterials with immune cells. This contributes to the current trend in the field in establishing the immune-compatibility of biomaterials to ensure scaffolds are appropriate for particular purposes.

Chapter 3

Design, Fabrication & Characterisation of a Fluidic Platform for Immune Cell Culture

3.1. Introduction

Chapter Overview

The development of fluidic platforms for the culture of cells has revolutionised the field of tissue engineering. Such systems are intended to expose cells, either directly or indirectly, to the physical forces of shear fluid stress, also referred to as flow (Inamdar and Borenstein, 2011). In addition to removing waste and providing nutrients, flow is also a physiological mechanical stimulus which has crucial roles in modulating the function of a variety of cells and tissues *in vivo*.

The application of fluidics to *in vitro* cell culture is anticipated to have a number of advantages through increasing the physiological relevance of tissue engineered constructs. Exposure to flow may help to promote *in vivo*-like cell phenotypes and prevent de- differentiation, which is a common problem associated with *in vitro* culture of certain cell types (Goral et al., 2010).

Flow also allows the formation of gradients, this is useful for studying the effects of concentration gradients of factors such as oxygen, growth factors, chemokine and cytokines on cell behaviour (Cimetta et al., 2010).

Three-dimensional (3D) *in vitro* cell culture is often limited by the delivery of nutrients to the centre of the construct and removal of waste products. Flow facilitates mass transport of these factors; increasing the availability of nutrients and preventing the accumulation of toxic waste products improves the viability and longevity of 3D tissue-engineered constructs (van Duinen et al., 2015).

Fluidic systems are now being designed for a wide variety of applications in tissue engineering, including disease models, drug discovery and safety testing (Inamdar and Borenstein, 2011). This chapter describes the work involved in the design, development and characterisation of a novel fluidic platform suitable for the culture of immune cells.

Immune Modulation by Fluid Shear Stress

Evidence for the effect of mechanical forces on modulating the immune system is growing, although research into elucidating the mechanisms is still in the early stages. Based on recent findings, inflammatory responses are suppressed by 'normal' mechanical physiological stimuli, whereas physical stimuli outside of this range can elicit inflammation (Previtera, 2014).

Flow is a particularly relevant mechanical stimulus in the study of immune function since immune cells are exposed to the effects of fluid shear stress in

various anatomical sites. For example, immune cells within the vessels of circulatory and lymphatic systems will be exposed to the flow of blood and lymph respectively. The magnitude of the force depends on vessel type, location and the position of the cell within the lumen (Previtera, 2014, Makino et al., 2007).

Cells residing within tissues, including lymph nodes, are subject to interstitial flow which is caused by the movement of fluid in the extracellular space around cells (Previtera, 2014). Interstitial flow is driven by systemic hydrostatic and osmotic pressure differences. It is generally slow and heterogeneous making flow rate quantification almost impossible. Although exact velocities are unknown, interstitial flow increases in the context of inflammation (Swartz and Fleury, 2007). Recent research has highlighted an important role for fluid shear stress in the maintenance and regulation of the immune system.

Non-immune cells of lymphatic tissues have been shown to be responsive to flow with immunologically relevant effects. Stromal cells within the lymph node paracortex, known as T zone fibroblastic reticular cells (TRCs), express the chemokines CCL21 and CCL19. These chemokines are ligands for the receptor CCR7, which is expressed on DCs and T cells. CCL21 and CCL19 are required to guide cell migration to and within lymph nodes (Comerford et al., 2013). Disruption of CCR7 binding leads to impaired immune responses (Förster et al., 1999).

Tomei et el. showed that slow interstitial flow was required to maintain TRC expression of CCL21 in a tissue-engineered lymph node microenvironment. The study also suggested that CCL21 expression is up-regulated in response to increased flow. Change in flow may therefore provide an early inflammatory signal which prepares secondary lymphoid organs, such as lymph nodes, for cell trafficking and the induction of efficient immune responses (Tomei et al., 2009).

The functions of the lymphatic endothelium include the transport of lymph fluid, containing antigen and cytokines, and antigen presenting cells from peripheral sites to lymph nodes. Fluid shear stress has been found to increase the expression of CCL21, as well as molecules involved in cell adhesion and transmigration, ICAM-1 and E-selectin, on lymphatic epithelial tissue. The modulation of the expression profile of these molecules by flow contributes to effective DC migration and homing to the lymph node (Miteva et al., 2010).

It is likely that the physical action of flow is also involved in directing DC migration. This is because the distances from peripheral tissues to lymph nodes are too large for chemokine concentration gradients alone to be efficient, particularly as the direction of flow goes against the gradient (Swartz et al., 2008).

The motility of T lymphocytes has been shown to be modulated by flow. The interaction of CCL21\CCL19 with CCR7 supports T cell entry into lymph nodes and promotes their ‘random walk’ within the T cell zone. T cell arrest is mediated by these chemokines in synergy with ligands for integrin LFA-1,

expressed on DCs and TRCs. Woolf et al. demonstrated that shear flow was required to activate lymphocyte integrins to allow them to efficiently adhere to their ligands, in conjunction with chemokine priming. In the absence of shear forces, integrin adhesiveness was 'silenced' (Woolf et al., 2007).

Finally, mild shear stress has been shown to initiate T cell signalling. In an elegant study, Li et al. generated artificial antigen presenting cells by coupling CD3 ligands to the surface of 3T3 fibroblasts. Elongated CD3 ligands bound but did not activate T cells via the T cell receptor complex. When shear stress was applied to the cells, there was an increase in calcium mobilisation in T cells bound to the extended CD3 ligands. Calcium signalling is an early indicator of T cell activation and this suggested that T cells were mechanically sensitive to physical forces, with the TCR acting as a mechanosensor (Li et al., 2010).

The implication of these observations is that flow has various roles in regulating immune function. Some of these include providing an early indication of inflammation to prime the lymphatic tissues, modulating migration of immune cells to and within lymph nodes and contributing to the induction of T cell activation (Miteva et al., 2010). These effects ultimately contribute to ensuring appropriate and effective immune responses.

Considerations for the Design & Development of Fluidic Platforms

The design and development of fluidic platforms for cell culture applications requires the specialist knowledge of engineers and biologists in order to

produce a robust system that suits the intended application. There are numerous factors to consider in this process, the key elements are outlined here.

Materials and Machining

Materials commonly used for the fabrication of fluidic systems for tissue engineering include polydimethylsiloxane (PDMS) and poly(methyl methacrylate) (PMMA). PDMS is a silicone-based polymer, it is an attractive material due to its oxygen permeability, and amenability to fabrication methods and patterning techniques. One limitation of PDMS, however, is its capacity to bind proteins, an effect which has largely been ignored in the development of fluidic systems. PMMA is a rigid, thermoplastic polymer, which is often chosen for its mechanical and chemical stability (Inamdar and Borenstein, 2011).

Materials such as PDMS and PMMA are amenable to routine engineering methods, such as laser cutting. The majority of methods involved in the manufacture of the components for fluidic systems can be done in standard labs and are scalable to allow high volume output of the devices. PDMS and PMMA are relatively inexpensive and are generally re-usable. Accessibility of materials and transferability of fabrication methods are important in enabling the widespread use of fluidic technologies by researchers around the world (Rizvi et al., 2013).

Cell Culture Substrate

A variety of synthetic and natural biomaterials have been shown to provide suitable cell culture substrates for fluidic systems, some of these are described in more detail in Chapter 2, *Biomaterials for Tissue Engineering*, of this thesis.

In addition to the range of biomaterials already described, paper-based scaffolds are starting to show promise in tissue engineering. Several applications, published and unpublished, have demonstrated good compatibility with cell culture and fluidic systems. Rahimi et al. successfully combined a microfluidic system with a hydrogel-coated paper-based scaffold to generate an air-liquid-interface for epithelial cell culture (Rahim et al., 2015). A novel method, named cells-in-gels-in-paper (CiGiP), has recently been described by Camci-Unal et al. This involved stacking paper scaffolds, embedded with cell-laden hydrogel, to assemble 3D co-cultures of human lung cancer cells and fibroblasts (Camci-Unal et al., 2016).

Pumping System

Pumping systems used in fluidics are usually commercially available syringe or peristaltic pumps. Syringe pumps provide a steady (non-pulsatile) flow and are usually used in one-pass systems. This means media does not recirculate and requires large volumes of reagents. It also prevents the accumulation of soluble signalling molecules, such as cytokines, which provide important feedback to cells.

Peristaltic pumps generate a pulsatile flow. They allow continuous perfusion of media, therefore secreted factors recirculate, which may be more representative

of the *in vivo* microenvironment. These systems require much lower volumes of media.

The importance of pulsatile versus non-pulsatile flow for *in vitro* cell culture applications has not yet been fully determined. Research in the field indicates the nature of the flow has more significant effects on certain cell types than others. This could be partially dependent on the flow conditions in the native tissue from which the cells are originally derived (Balcells et al., 2005, Abe et al., 2013).

Data Collection

The device must be accessible for sampling, the application and type of samples will determine the design for this. For example, optical transparency would be a requirement for a platform where imaging methods are central in the experimental approach. Likewise, the addition of ports for the collection of supernatant and cells would facilitate sample collection over a time course study without interrupting the experiment.

Interpretation of data obtained from fluidic platforms may be limited in terms of its comparability to conventional methods. Due to the novelty of such techniques, incorporating relevant controls into experiments is essential since the field is in its infancy and such information does not yet exist.

Operator

Following initial optimisation, fluidic platforms must be suitable for use in a tissue culture lab. A general method can be outlined and applied to the setup of

a range of fluidic platforms as follows. First, the components are sterilised, then, the platform is assembled and seeded with cells under sterile conditions. Finally, it is transferred to an incubator and connected to the pumping system. These steps have the potential to be fraught with operational barriers, such as keeping the components sterile, tubing attachment, accessibility for cell seeding and leakage or evaporation of media. Careful planning during the design process can avoid this.

Chapter Aims

This chapter describes the construction of fluidic systems and characterisation of a fluidic platform for immune cell culture. In this chapter, the aim of the work was to develop a cell culture platform to investigate the effects of shear flow on immune cells in vitro. This was achieved by first developing a robust fluidic system. Then, the platform was utilised to characterise the effect of shear flow on human immune cells based on dendritic cell viability, maturation and response to immunological stimulation.

3.2. Materials and Methods

Fluidic Platform Assembly

Three-channel microfluidic device

The device was constructed from 3.175mm-thick PMMA, which was cut to 24 x 40mm, with inlet and outlet ports 2.2mm in diameter, using a laser cutter (VersaLASER, Universal Laser Systems Inc.). Double-sided adhesive (DSA) films were cut to the same dimensions, then, three channels were cut out of the centre measuring 4mm wide. Six DSA films were stacked to give the channels a depth of 3mm. The DSA stack was stuck down on to a #1.5 thickness cover glass slide.

The surface of the glass slide was plasma etched under the following conditions to increase the hydrophilicity of the surface for subsequent collagen hydrogel coating, time = 60, seconds, power = 40 watts, pressure = 300 mTorr.

The devices were sterilised by UV irradiation (245nm) for 15 minutes. 10µL collagen hydrogel (0.5mg/mL), prepared according to the method described in Chapter 2 of this thesis, 2.4. Materials and Methods: *Preparation of Collagen Hydrogels*, was then spread evenly over each channel, then transferred to the incubator for 40 minutes to allow the hydrogel to set.

The PMMA sheet was attached to the top layer of DSA and the inlet and outlet tubing (TYGON 3350 silicone; Cole Parmer) was glued in place using 5 minute epoxy (Devcon). Tubing was attached to syringes loaded on the syringe

pump (Harvard Appartus PHD 2000 Syringe Pump) with 18G blunt fill needles. A flow rate of 2µL/minute was used to test the device.

Fluidic device with paper-based scaffold

The platform was fabricated using 2mm-thick polymethyl methacrylate (PMMA) and 1mm-thick PDMS. A CO_2 laser system (Universal Laser Systems Inc., Scottsdale, AZ) was used to cut all components to required dimensions. The PMMA was cut to 5cm(L) by 3.5cm(W), with 8 holes (5mmø) around the perimeter, 2mm from the edge, for the insertion of bolts.

Inlet and outlet ports were bored into the sheets of PMMA which formed the top of the flow platform.

For static platform, central channels were cut out of PMMA sheets. Two of these sheets were glued together to form the cell culture chamber.

The PDMS was cut to 5cm(L) by 3.5cm(W), with 8 5mmø holes. PDMS sheets had channels cut out, 2cm (L) by 5mm(W), to form cell culture chambers which were used for static and flow devices.

The silicone-coated cellulose based paper scaffold (purchased from Reynolds Kitchens, Reynolds® parchment paper roll) was cut to 5cm(L) by 3.5cm(W). The surface of the paper treated using a CO_2 laser, where the power was 10W and scanning speed was 35mm/second, to achieve a hydrophilic surface.

Components were sterilised by UV irradiation (245nm), followed by submersion in a 20% antibiotic\ antimycotic solution overnight, then they were washed PBS and air-dried under sterile conditions.

Assembly of the platform was conducted in a laminar flow hood. Static device: Paper scaffold interleaved between PDMS films, upper film with channel cut out. Two layers of PMMA glued together, centre channel cut out to create cell culture chamber. Sheets of PMMA enclosed the device. Flow platform: Paper scaffold inserted between PDMS films, channel cut out of upper film. Sheets of PMMA encased device, upper sheet with inlet and outlet ports for fluidic tubing to be attached. PVC double manifold tubing (purchased from Watson Marlow) was attached to the inlet port and a gas-permeable silicone tubing (TYGON) was connected to the outlet port using epoxy glue (5-minute epoxy, Devcon) to fix the tubing in place. 5mm nuts and bolts used to hold components together.

A peristaltic pump, 323S Drive 400rpm, fitted with a 314MC five channel, four roller microcassette pumphead (Watson-Marlow) was used as the pumping system for this device.

Flow rate calibration (µL\min) was performed by measuring the volume of buffered saline solution that passed through the platform in 5 minutes. This was done for the following settings for the peristaltic pump: 3rpm, 5rpm and 10 rpm. Each measurement was repeated 3 times and the average volume collected was calculated.

The volume capacity of the flow platform, including tubing but not the reservoir, was 200µL.

Collagen Hydrogel-Coated Paper Scaffold

The collagen hydrogel was prepared according to the method described in Chapter 2 of this thesis, 2.4. Materials and Methods: *Preparation of Collagen Hydrogels*. The collagen solution was retained on ice until required.

10µL of the collagen hydrogel was evenly spread over the hydrophilic surface of the paper scaffold. It was then transferred to the incubator for 40 minutes to set.

Generation of Monocyte-Derived Dendritic Cells

This was done according to the method described in Chapter 2 of this thesis, 2.4. Materials and Methods: *Generation of Monocyte-Derived Dendritic Cells*.

Dendritic Cell Culture on Collagen Hydrogel-Coated Paper Scaffolds

5 x 10^5 monocyte-derived dendritic cells were seeded per scaffold and transferred to the incubator for 2 hours to allow cells to adhere. For flow platforms, 500µL complete RPMI media was contained in the reservoir. The manifold tubing was connected to the peristaltic pump and a flow rate of 5µL\min (3rpm) was used for all experiments. For static platforms, 500µL media was added directly to the cell culture chamber. Flow and static platforms

were maintained under standard tissue culture conditions (5% CO_2, 37°C) for the duration of the experiment.

Dendritic cell stimulation was performed using *E. coli* lipopolysaccharide (LPS) (0111:B4) (purchased from Sigma) at a concentration of 0.1µg/mL for 24 hours.

Endotoxin neutralisation was done using Polymyxin B sulphate (PMB) (purchased from Sigma). A 50µg/mL solution was prepared in sterile PBS. Scaffolds were incubated with the PMB solution for 45 minutes and washed thoroughly with media before cell seeding.

Annexin-V\Propidium Iodide Cytotoxicity assay

This was done according to the method described in Chapter 2 of this thesis, 2.4. Materials and Methods: *Annexin-V\Propidium Iodide Cytotoxicity assay*.

Dendritic Cell Phenotypic Analysis

This was done according to the method described in Chapter 2 of this thesis, 2.4. Materials and Methods: *Dendritic Cell Phenotypic Analysis*.

Flow cytometric analysis

This was done according to the method described in Chapter 2 of this thesis, 2.4. Materials and Methods: *Flow Cytometric Analysis*.

Immuno-Fluorescent Staining moDCs with Phalloidin Alexa Fluor-488 and DAPI

Samples were gently washed in PBS then fixed in 4% paraformaldehyde for 20 minutes at room temperature. They were then washed twice with PBS before permeablising cells with 0.15% Triton X for 20 minutes. Samples were washed twice in PBS, then blocked using a 5% solution of goat serum for 30 minutes. Samples were washed three times in PBS. A 1:20 dilution of Phalloidin Alexa Fluor-488 (Life technologies) was made and incubated with samples for 20 minutes, in the dark, at room temperature. They were washed three times in PBS. 4',6-Diamidino-2-Phenylindole (DAPI) was diluted 1 : 20,000 and added to samples for 5 minutes. Samples were washed three times in PBS and then mounted using #1.5 thickness cover slips.

Confocal microscopy

Samples were imaged using a Zeiss LSM710 confocal microscope. 10X and 20X objectives were used. Lasers 405 and 488 were selected for DAPI (Excitation\Emission: 358\461) and Phalloidin Alexa Fluor 488 (Ex\Em: 490\525) respectively.

Image analysis

ImageJ was used for the analysis of fluorescent images (Schneider et al., 2012).

Statistical analysis

Analysis was carried out using GraphPad Prism version 6.00 for Windows, GraphPad Software, La Jolla California USA (www.graphpad.com)

3.3. Results and Discussion

Construction of Fluidic Platforms for Cell Culture

A three-channel microfluidic device

Two different fluidic platform designs were tested to determine their suitability for this work. The first was based on a microfluidic device originally described by Rizvi et al. with minor modifications (Rizvi et al., 2013). As illustrated in Figure 30, the device had 3 channels which were created by stacking layers of medical-grade double sided adhesive (DSA) onto a cover glass slide. Three channels were laser cut out of the DSA films and 6 films were stacked together to give the channels depth. A sheet of PMMA with inlet and outlet ports bored into it was attached to the top layer of DSA film. The fluidic tubing was then glued into the inlet and outlet ports.

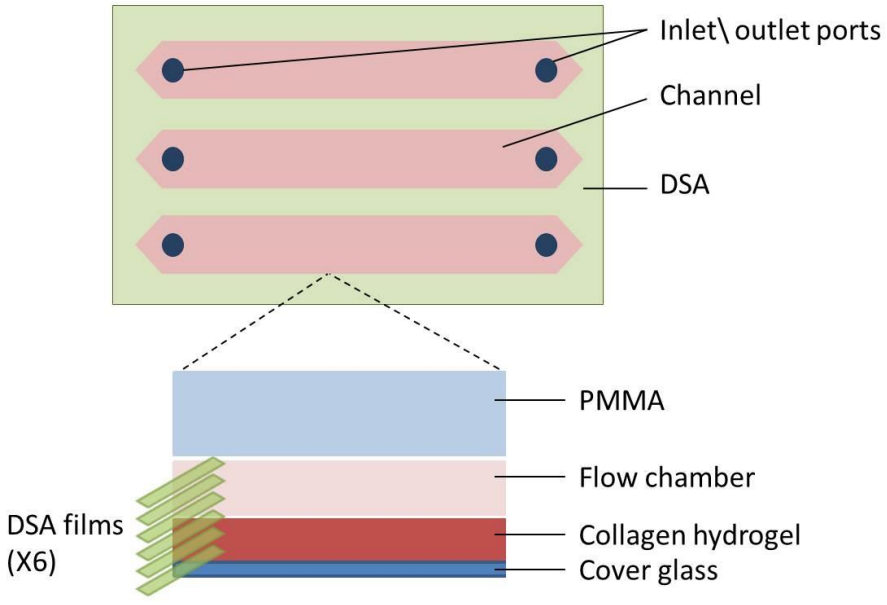

Figure 30. Diagram to show assembly of the three-channel microfluidic device.
Stack of 6 DSA films, with 3 channels cut out, assembled on cover glass slide. Channels coated with collagen hydrogel, then device enclosed by PMMA sheet with inlet and outlet ports. Tubing glued into ports and system attached to syringe pump.

Before assembly, the channels were coated with a collagen hydrogel to provide a substrate for cell culture. First, the channels were plasma etched to increase the hydrophilicity of the glass surface. Then, the device was sterilised by UV exposure at 245nm and collagen hydrogel was spread evenly over the channels.

The pumping system used for the optimisation of this device was a syringe pump. This meant that it was a one-pass flow system.

There were numerous advantages of the design of this device for cell culture applications. It was fabricated from inexpensive and widely available components. The channel coating was not limited to collagen, other ECM substrates, such as Matrigel™, could be used. The cover glass base meant it was optically transparent, which gave it the potential for *in situ* real-time imaging of cells within the channels at high resolution. The continuous flow of media through the system enabled sequential cell seeding.

However, several limitations were identified during assembly and optimisation:

- The cover glass base meant that devices were very fragile and easily fractured.
- One-time use device.
- Manually stacking 6 films of DSA led to difficulties in lining up the films evenly.
    - Leakage and air bubbles occurred due to gaps between layers of DSA films.
- The design lacked flexibility in terms of the construction, therefore no opportunity to make modifications.
- One-pass system used large volume of media.

Despite the efforts to optimise this device, it was not reliable or robust enough to withstand the duration, 3 – 6 days, of the cell culture studies. In light of the drawbacks of the device, it was not pursued for this work.

Fluidic device with a paper-based scaffold

The design of the second device was based on a removable paper insert, which provided the scaffold for cell culture. The paper scaffold was a cellulose-based paper with a silicon coating. The paper was surface treated using a CO_2 laser to increase its hydrophilicity. Paper scaffolds were coated with a collagen hydrogel to provide an appropriate substrate for immune cell culture.

The fluidic platform and the static counterpart are illustrated in the diagram in Figure 31. For both configurations, the paper scaffold was sandwiched between two films of PDMS. The upper film had a channel cut out of the centre to create the cell culture chamber.

Sheets of PMMA were used to give the devices structural support. Uniquely to the flow device, the top sheet of PMMA had two ports to allow for the insertion of inlet and outlet tubing. For the static device, double layered PMMA, with a central channel cut out, was used to form the cell culture chamber. Uncut sheets of PMMA were used as the base for the devices and to seal the static chamber.

For both devices, nuts and bolts were used to hold the components in place. This allowed easy assembly and disassembly of the devices without destroying the components so that they were re-usable.

To ensure the static and flow platforms were comparable, the total volume of media supplied to each system was the same - 500µL. For the static device, this was added directly to the cell culture chamber. The flow system had a reservoir to allow the collection and re-circulation of the media.

A peristaltic pump was used to achieve continuous perfusion of the flow system. The flow rate (µL/min) was calibrated using the Watson-Marlow peristaltic pump, summarised in Table 2. A flow rate of 5µL/min was selected for all cell culture studies to mimic interstitial flow.

The advantage of the modular nature of the device described here was the flexibility it allowed in the assembly. Various configurations of the components were tested to establish a robust setup. The ability to make adjustments was useful in troubleshooting, as specific changes to address leakage and evaporation could be made. The compact design of the devices meant that several platforms, along with the pump, could be set up on a single shelf of a standard tissue culture incubator. Overall, this design was found to provide a sturdy, flexible and user-friendly fluidic platform with potential for cell culture applications.

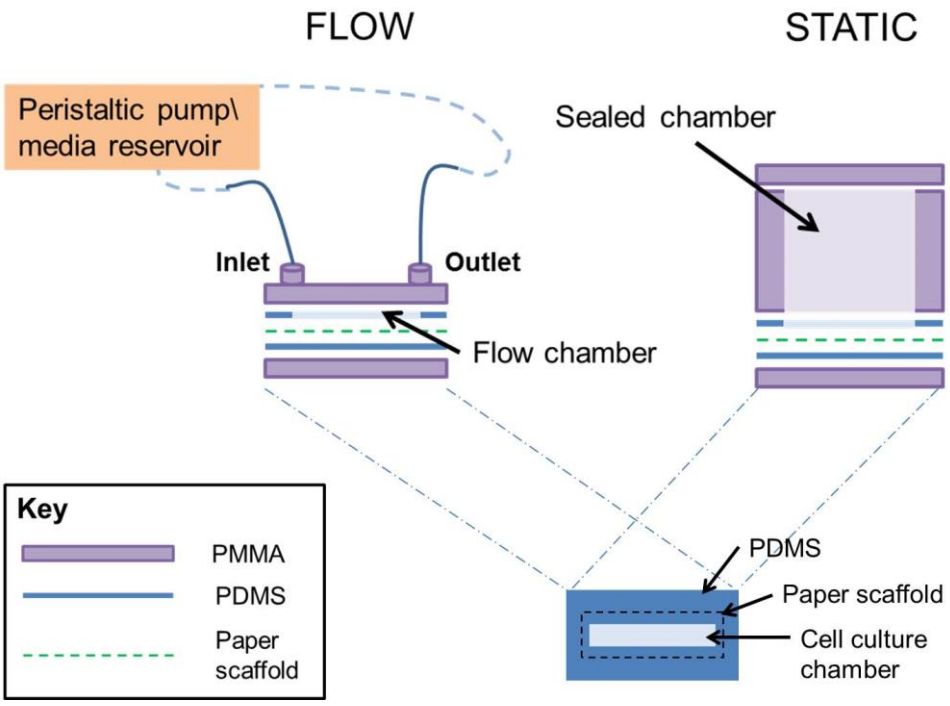

Figure 31. Schematic representation of flow and static paper-based platforms.
Flow device: Paper scaffold inserted between PDMS films, channel cut into centre of top film creates cell culture chamber. Sheets of PMMA encase device, upper sheet with inlet and outlet ports for attachment of fluidic tubing.
Static device: Paper scaffold interleaved between PDMS films, upper film with central channel cut out. Double layer of PMMA with centre channel cut out. Sheets of PMMA enclose the device.

Table 2. Calibration of flow rate for fluidic platform using Watson-Marlow peristaltic pump.

W-M peristaltic pump (rpm)	Fluidic Platform (µL/min)
3	5
5	8
10	15

Characterisation of a Paper-Based Scaffold for Immune Cell Culture

All of the work for the characterisation of the paper-based scaffold for immune cell culture was performed using human moDCs. Cells were seeded onto sterilised, collagen hydrogel-coated paper scaffolds at a density of 5 x 10^5 and maintained under standard tissue culture conditions (5% CO_2, 37°C).

Dendritic cell viability is not impaired by paper scaffolds

The viability of moDCs cultured on the scaffold was established using the setup described for the static platform. Cell viability was determined by flow cytometric analysis of cells stained with Annexin V\ PI.

Figure 32 shows the results from this experiment, the dot plots in Figure 32A and B show the Annexin-V\ PI staining profile of cells collected from TCP and the paper scaffold respectively. Figure 32C compares the proportions of viable and non-viable cells quantified by the assay. The percentage of viable cells harvested from the paper scaffold (71%) was not found to be significantly different to that collected from TCP (79%). Also, numbers of non-viable cells were not significantly different, with 28% and 20% for the paper scaffold and TCP respectively. The results from this experiment confirmed that the collagen hydrogel-coated paper scaffold did not impair moDC viability.

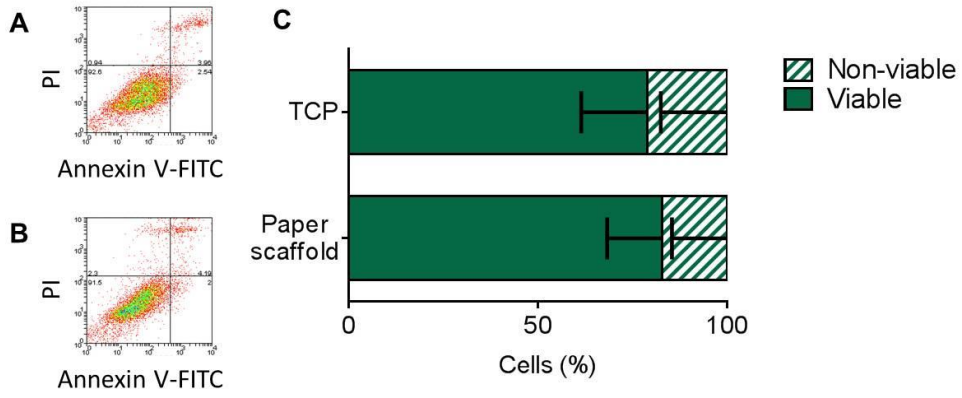

Figure 32. Dendritic cell viability is not impaired by paper scaffolds.
Cell viability after 24 hours in culture with paper scaffolds assessed by the Annexin-V\ PI cytotoxicity assay. A & B: Dot plots of Annexin V\ PI-stained cells harvested from TCP and paper scaffold respectively. C. Graph presenting the percentages of viable (solid colour) and non-viable (striped) cells harvested from each condition. There was no significant difference in the proportion of viable cells collected from the scaffold (71%), compared to TCP (79%). The percentages of non-viable cells for scaffold (28%) and TCP (20%) cultures were not found to be significantly different. T tests were used to determine significance. Difference not significant if $P \geq 0.05$ ($n = 3$). Error bars represent standard deviation.

The paper scaffold induces a mature dendritic cell phenotype

The effect of the scaffold on the phenotype of moDCs was assessed based on the expression of the cell-surface maturation markers, CD40, CD54, CD83 and CD86. After 24 hours in culture, cells were harvested and immunofluorescent staining was performed. Phenotypic analysis of the cells was then done by flow cytometry.

The results from this experiment are shown in Figure 33. Graphs A, B, C and D represent the expression of CD40, CD54, CD83 and CD86 respectively, presented as median fluorescence intensity (MFI). There was a tendency towards an increase in the expression of all markers by moDCs collected from paper scaffolds. This was not found to be significant for CD40, CD83 or CD86 compared to TCP. However, the level of expression of CD54 was found to be significantly higher on cells harvested from the paper platform ($P \leq 0.05$, *) as

opposed to those from TCP. Overall, the data indicate the paper scaffold induced the maturation of moDCs.

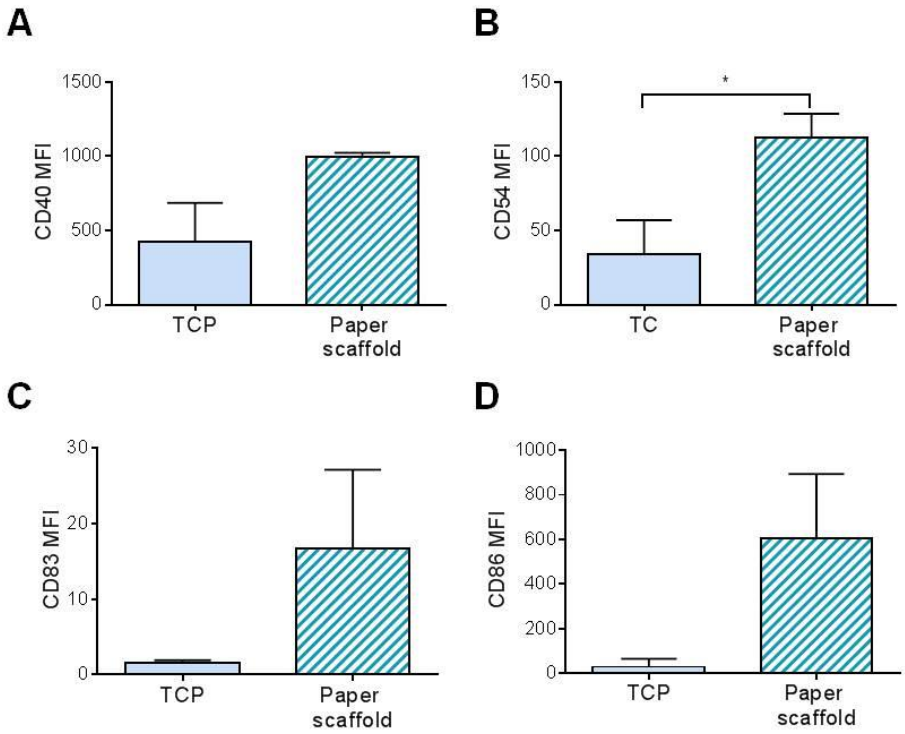

Figure 33. Dendritic cells collected from paper scaffolds have a mature phenotype. Phenotypic analysis of moDCs after 24 hours in culture with paper scaffold. A. Expression of CD40 was raised by cells collected from scaffolds. B. CD54 expression was significantly increased on cells harvested from scaffolds ($P = 0.0341$, *, $t = 5.276$, $df = 2$). C & D. Levels of CD83 and CD86 respectively were higher for cells cultured on paper scaffolds but not found to be significant. T tests were performed to determine statistical significance. Not significant if $P \geq 0.05$ ($n = 3$). Error bars represent standard deviation.

Due to the methods of manufacturing and handling of the paper scaffold, the possibility of endotoxin contamination was examined as an explanation for the maturation of moDCs. An experiment whereby scaffolds were pre-incubated with Polymyxin B sulphate (PMB) to neutralise endotoxin was carried out (data not shown).

The results from this experiment demonstrated that incubation of the scaffold with PMB had no effect on the expression of maturation markers. This ruled out endotoxin as a cause for the maturation of moDCs.

Since the collagen hydrogel had already been well-characterised for immune cell culture (see Chapter 2 of this thesis), the effect of coating the paper scaffold was anticipated to be minimal and not to significantly affect the phenotype of the moDCs. It is possible that the collagen coating was not efficient and uneven coverage led to direct cell exposure to the paper scaffold. In this case, it is likely that some property of the paper scaffold itself was responsible for the raised maturation state of moDCs. Others have demonstrated that antigen presenting cells (APCs) are sensitive to a multitude of substrate properties, including topography, surface chemistry and substrate stiffness (Rostam et al., 2015). These variables can determine the functional activity of APCs and the outcome of immune responses.

Phenotypic response of dendritic cells to LPS is limited in cultures with paper scaffolds

To determine whether moDCs were responsive to an immunogenic challenge when cultured on paper scaffolds, they were stimulated with LPS for 24 hours. Phenotypic analysis was performed to determine the response based on the expression of maturation markers.

The results of the analysis are displayed in Figure 34. Graphs A, B, C and D represent CD40, CD54, CD83 and CD86 expression, plotted as MFI. There was a slight increase in the expression of the markers following stimulation by LPS by cells harvested from paper scaffolds. However, none were found to change significantly ($P \geq 0.05$).

When cultured on paper scaffolds, the phenotype of unstimulated moDCs was barely discernible from those stimulated with LPS. This is likely due to an intrinsic property of the scaffold which caused the increased expression of maturation markers under resting conditions. Therefore, the extent to which expression could be further up-regulated upon immunogenic stimulation was limited.

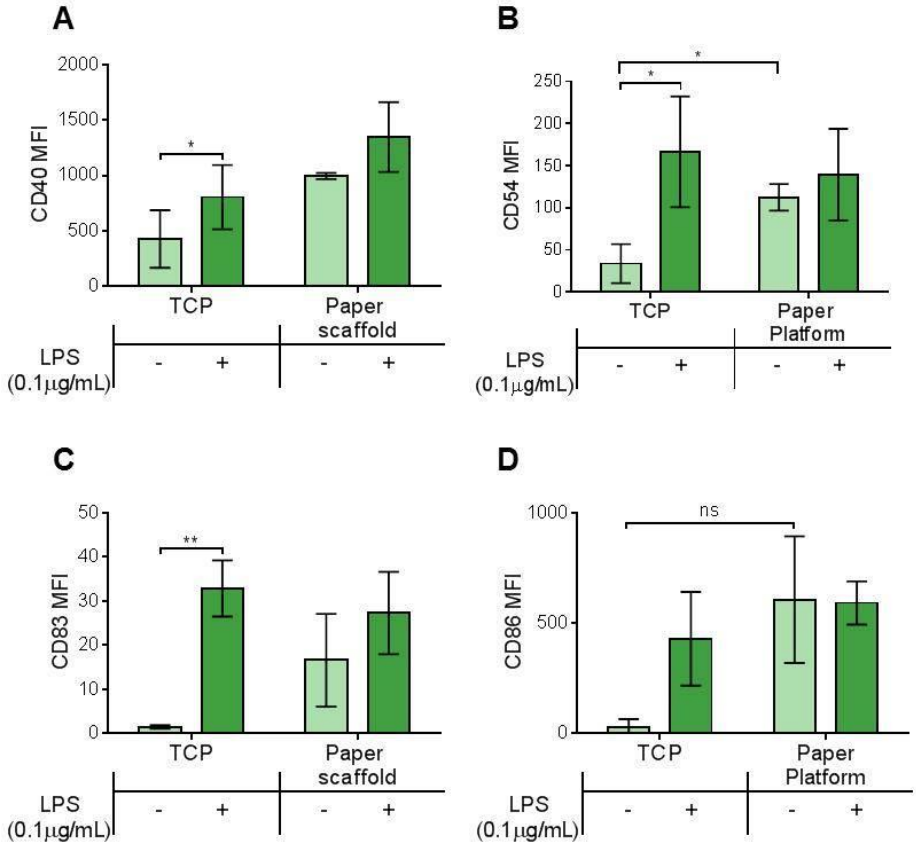

Figure 34. Limited moDC phenotypic response to LPS on paper scaffolds.
Expression of maturation markers after 24 hours of LPS stimulation by cells cultured on paper scaffolds. A. Significant increase in CD40 expression with LPS in TCP ($P = 0.0121$, *, $t = 9.012$, $df = 2$). CD40 expression also raised following stimulation by LPS in cells harvested from paper scaffolds but not significantly. B. Significant difference between CD54 background expression in TCP and paper scaffold ($P = 0.0341$, *, $t = 5.276$, $df = 2$). CD54 expression significantly increased in TCP with LPS ($P = 0.0414$, *, $t = 3.433$, $df = 3$, slight increase in CD54 expression by cells stimulated with LPS on paper scaffolds, not found to be significant. C. CD83 expression increased in response to LPS on paper scaffolds, however not found to be significant. Expression of CD83 increased significantly in TCP with LPS stimulation ($P = 0.0026$, **, $t = 9.314$, $df = 3$). D. No distinct change in CD86 expression by cells cultured on paper scaffolds when stimulated by LPS. Significance determined using t tests, not significant if $P \geq 0.05$ ($n=3$). Error bars represent standard deviation.

Change in dendritic cell morphology with LPS stimulation on paper scaffolds

Immunofluorescent staining of moDCs cultured on the paper platforms was performed to visually examine how the cells responded to LPS stimulation. DAPI and Alexa Fluor 488 Phalloidin were used to visualise the nuclear and cytoskeletal aspects of the cells. The images acquired in these experiments are shown in Figure 35. Unstimulated moDCs were found to be evenly spread over the scaffold and exhibited a rounded morphology, characteristic of resting dendritic cells. With LPS stimulation, cell clustering and elongated cell morphologies, indicative of activation, were seen.

Observations from fluorescent microscopy suggest that moDCs cultured paper scaffolds were responsive to immunological stimulation. The changes observed for cell organisation and morphology were consistent with the induction of inflammatory responses to LPS. This indicated that despite the poorly defined LPS response in the phenotypic analysis, moDCs cultured on the paper scaffold were immune competent. This highlights the need to investigate more than one feature of the cell response.

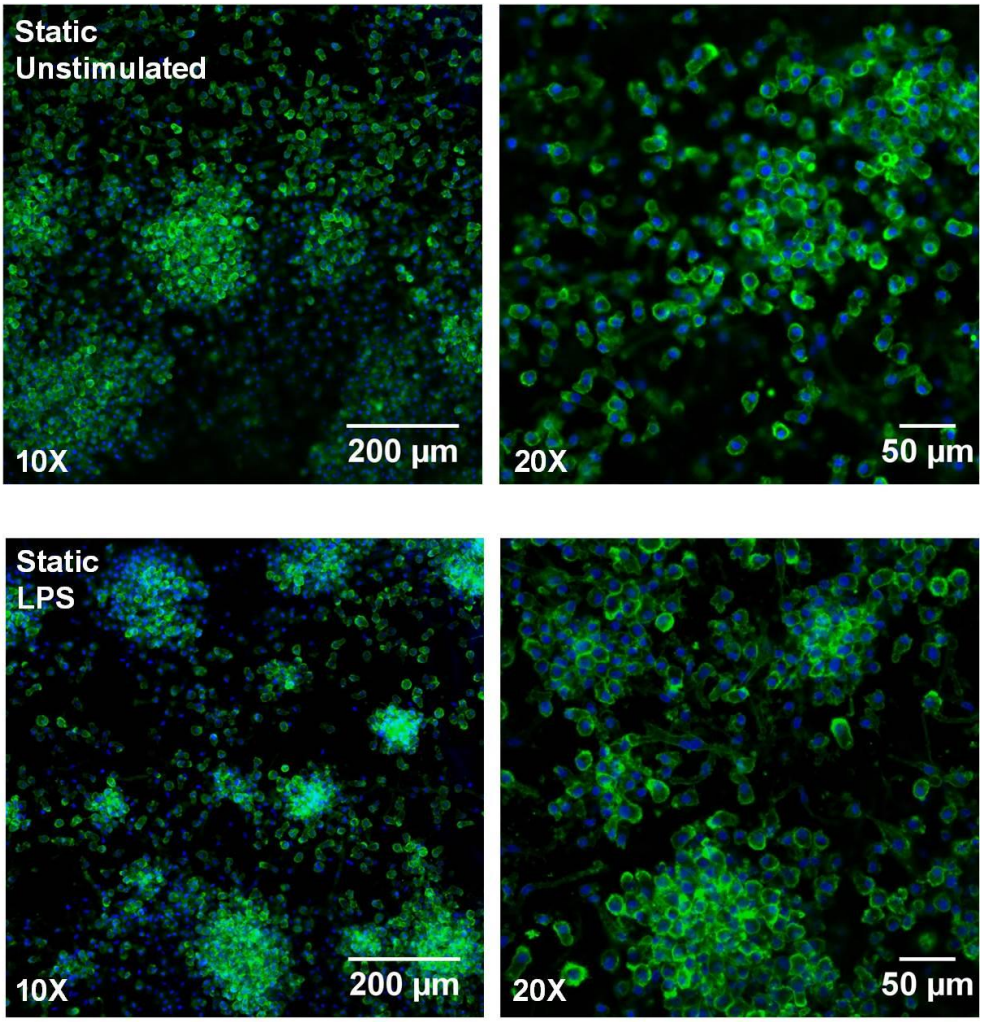

Figure 35. Visualisation of moDC response to LPS paper scaffolds.
moDCs cultured on collagen hydrogel-coated paper scaffolds for 24 hours under resting or LPS-stimulated conditions. Cells fluorescently labelled using Phalloidin Alexa-Fluor488 and DAPI to visualise the actin cytoskeleton and nuclei of the cells. Cells were unevenly distributed over the scaffolds. Unstimulated cells had a rounded morphology. LPS-stimulated cells formed concentrated clusters and some cells were elongated. Images acquired using 10X and 20X objectives on a LSM710 confocal system.

Characterisation of Fluidic Platform with a Paper Scaffold for Immune Cell Culture

Flow does not significantly impair dendritic cell viability

The viability of moDCs was assessed after 24 hours of culture on paper scaffolds under flow conditions. Annexin-V\ PI staining was used to quantitatively measure cell death. The results from the viability assay are shown in Figure 36. Figures A and B are dot plots showing the Annexin-V\ PI staining of moDCs harvested from flow and static devices respectively. The proportions of viable and non-viable cells are presented in the graph in Figure 36C. Numbers of viable cells harvested from the flow device (64%) were slightly lower than those from the static device (71%) but this reduction was not found to be significant. Accordingly, the proportion of non-viable cells was slightly increased under flow conditions (36%), compared to static samples (28%), however this was not found to be statistically significant. It is perhaps not surprising that cell viability is slightly reduced under flow due to the fragility of mammalian cells (Tirella et al., 2008).

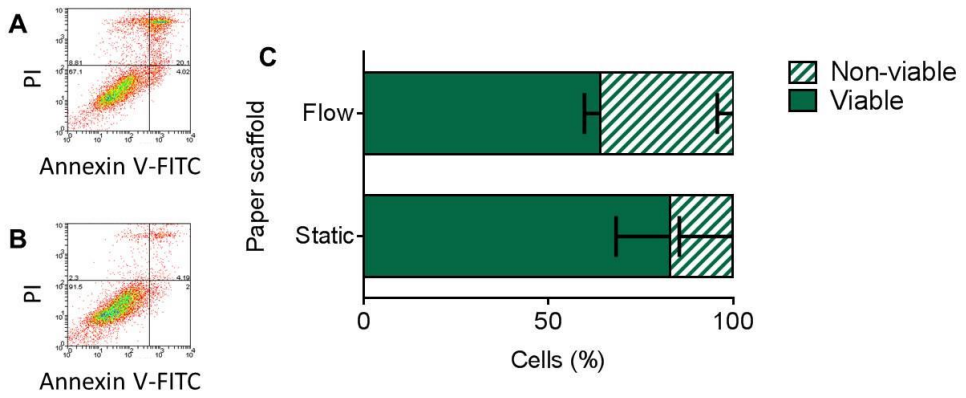

Figure 36. Flow does not significantly impair dendritic cell viability.
Analysis of the viability of moDCs harvested from flow and static platforms after 24 hours. A & B. Dot plots of Annexin-V\ PI-stained cells from flow and static devices respectively. C. Percentage of viable (solid colour) and non-viable (striped) cells collected from flow and static cultures. Numbers of viable cells were slightly reduced in samples collected from flow devices (64%), compared to static (71%), however, this difference was not found to be significant. In concurrence, the proportion of non-viable cells increased under flow conditions (36%) but not significantly to static (28%). Statistical analysis was performed using t tests, differences were not significant if $P \geq 0.05$ ($n = 3$). Error bars represent standard deviation.

Dendritic cells attach to the paper scaffold under flow

Fluorescent staining was used to assess moDC attachment to the collagen-coated paper scaffold under flow conditions after 24 hours. The fluorescent images taken are displayed in Figure 37. The cell distribution and density across the scaffolds was found to be comparable between static and flow platforms. The results suggest that moDCs interact with the scaffold sufficiently to remain attached under the flow rate, 5µL/min, used in this study.

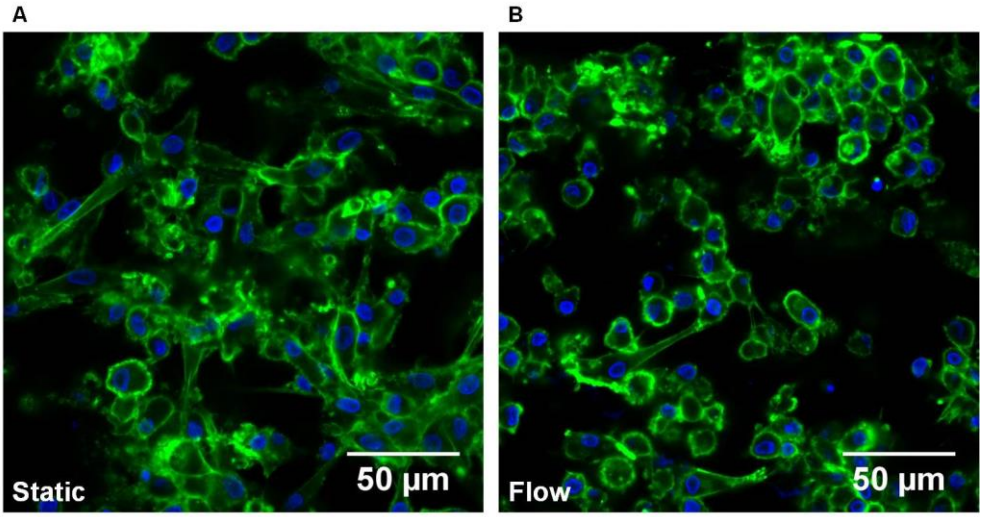

Figure 37. Dendritic cell attachment to paper scaffolds on static and flow platforms. Confocal microscopy was performed to visualise cells stained with Phalloidin Alexa-Fluor488 and DAPI. moDCs were seeded on paper scaffolds coated with collagen hydrogels and maintained under flow or static conditions for 24 hours. The distribution and density of cells attached on the paper scaffolds under flow was similar to that observed for static cultures. Images acquired using a LSM710 confocal system with a 20X objective (n = 2).

Dendritic cells exhibit a less mature phenotype under flow

The effect of flow on the phenotype of moDCs cultured on paper scaffolds was compared to that of their counterparts cultured under static conditions. Cell phenotype was assessed based on the expression of the panel of markers associated with moDC maturation.

The analysis from this experiment is shown in Figure 38; graphs A, B, C and D represent the expression of CD40, CD54, CD83 and CD86 respectively. Data is presented as MFI. Expression of CD40 and CD54 were found to be significantly decreased on cells cultured under flow compared to static. CD83 and CD86 were slightly decreased in cells harvested from flow platforms, however, no significant differences were found compared to static cultures. Overall, the trend in the reduction of the expression of all markers under flow was indicative that cells had a less mature phenotype.

Local cell density is a key regulator of a variety of cell behaviours, such as proliferation, differentiation, motility and survival (Snijder and Pelkmans, 2011). Therefore, the phenotype of dendritic cells will be dependent on cell concentration to some extent. Although the same number of cells was seeded on flow and static platforms at the start, there is the possibility for a greater reduction in the number of cells on the flow platform as a result of cell death, or washing away.

An alternative reason for the lower levels of expression of activation markers under flow conditions could be due to the dilution of inflammatory mediators throughout the system. As shown previously, the paper scaffold induced moDC maturation which likely resulted in the production of inflammatory cytokines, such as TNF-α, IL-1β and IL-6 (Schildberger et al., 2013). These cytokines promote pro-inflammatory responses, including the up-regulation of maturation markers by dendritic cells (Zou and Tam, 2002, Motta and Rumjanek, 2016). Under static conditions, a concentrated extracellular milieu of soluble inflammatory factors may build up, which in turn would enhance pro-inflammatory responses, including DC maturation. Continuous perfusion would reduce the concentration of cytokines to which the cells are directly exposed. The dilution effect would dampen pro-inflammatory cytokine feedback and cells would not be activated as strongly, hence the less matured phenotype observed on the flow platform.

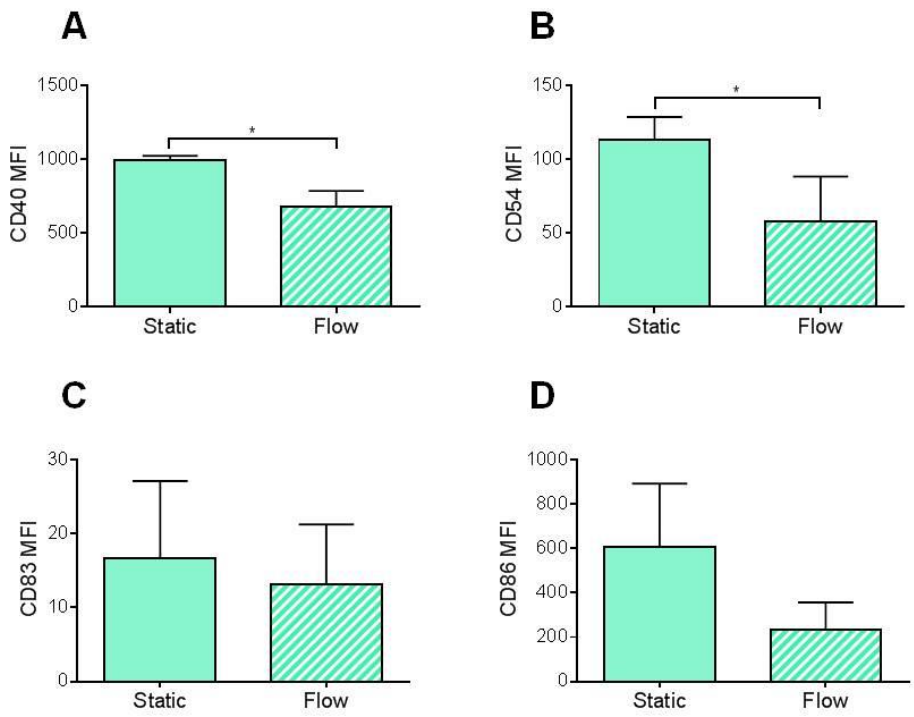

Figure 38. Dendritic cells maintain a less mature phenotype under flow.
moDCs were cultured on flow or static platforms for 24 hours before collection for phenotypic analysis. A. CD40 expression was significantly reduced under flow ($P = 0.0135$, *, $t = 5.247$, $df = 3$). B. Expression of CD54 was found to be significantly lower in flow conditions ($P = 0.0270$, *, $t = 5.960$, $df = 2$). C. No change in expression of CD83 under flow. D. Reduction in expression of CD86 under flow. Statistical analysis was performed using t tests. Differences not significant if $P \geq 0.05$ ($n = 3$). Error bars represent standard deviation.

Dendritic cells mount appropriate responses to LPS under flow

Maturation of moDCs harvested from the paper scaffold following LPS stimulation was compared between static and flow platforms. The moDC markers, CD40, CD54, CD83 and CD86 were included in the phenotypic analysis. The cells were cultured for 24 hours on paper scaffolds under static or flow conditions, with or with LPS stimulation.

The results from this study are displayed in Figure 39, graphs A, B, C and D show the expression of CD40, CD54, CD83 and CD86 respectively, plotted as MFI. The results from the stimulation of moDCs on the static platform have

already been described in this chapter, and so will not be repeated here. For the cells collected from the flow platform, expression of all of the maturation markers was slightly increased upon LPS stimulation. However, no significant differences in expression between unstimulated and stimulated conditions were found. Although the response to LPS was not well defined under flow, the pattern of marker expression observed was indicative of LPS-induced cell maturation. The level of expression of all the markers was slightly lower under flow conditions, however, the trend with and without LPS stimulation was similar to static platforms. The effect of the paper scaffold in spontaneously eliciting moDC maturation is most likely the cause for the poor definition of the LPS response, not the effect of flow.

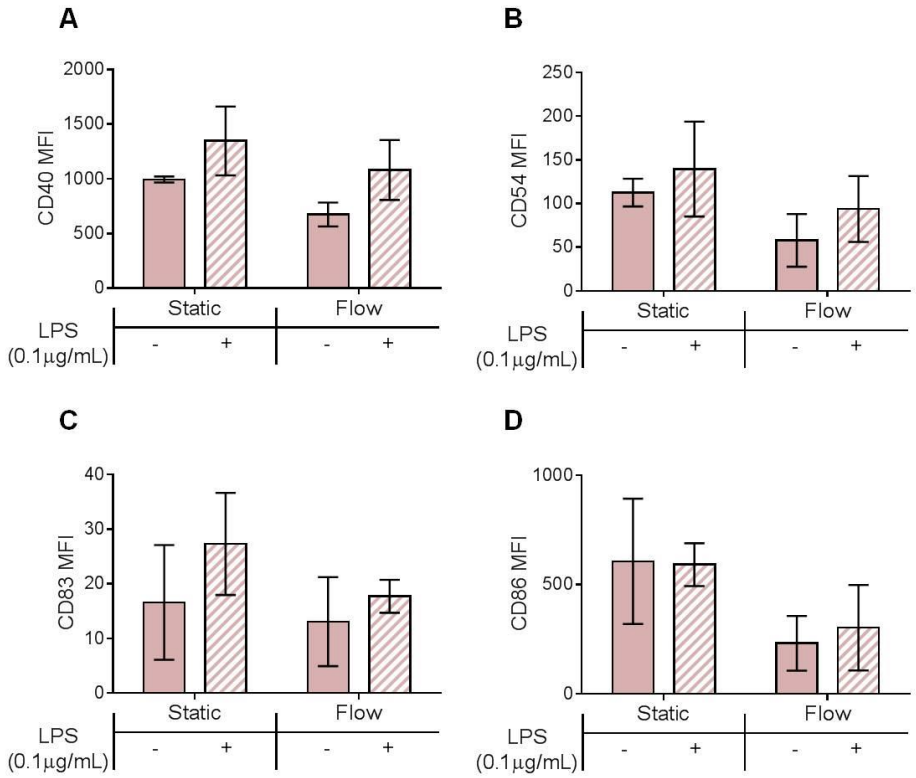

Figure 39. The phenotype of moDCs cultured on flow platforms shifts towards a more mature state with LPS stimulation.
Dendritic cells collected for phenotypic analysis after 24 hours of culture on paper scaffolds from static and flow devices, with or without LPS stimulation. The cells harvested from the flow platforms showed a slight increase in CD40 (A), CD54 (B) and CD83 expression (C) but no effect was seen on CD86 expression (D). T tests were performed to determine statistical significance, if $P \geq 0.05$ result was not significant ($n = 3$). Error bars represent standard deviation.

Fluorescent microscopy was performed to visualise the moDCs cultured on static and flow platforms, with or without LPS stimulation. Cells were fluorescently stained with phalloidin and DAPI. Representative images from these experiments are displayed in Figure 40. Unstimulated cells cultured under static conditions were distributed evenly over the paper scaffold. They had a rounded shape, a morphology typically associated with immature moDCs. Unstimulated moDCs cultured under flow had comparable features to their static counterparts. In the static device, LPS-stimulated moDCs were observed to form cell clusters and some cells took on an elongated morphology, which is characteristic of activated moDCs. Similar observations

were made for the distribution and morphology of LPS-stimulated cells cultured under flow.

Overall, the visual appearance of moDCs cultured on paper scaffolds was comparable between flow and static platforms. Resting moDCs displayed characteristic features of cells which have not experienced immunological stimulation. Cells under both static and flow conditions appeared responsive to LPS stimulation due to changes in their spatial organisation and morphology. Based on the observations made here, the mechanical impact of flow did not seem to have an effect on cell distribution or morphology on the paper scaffold in the context of immune stimulation.

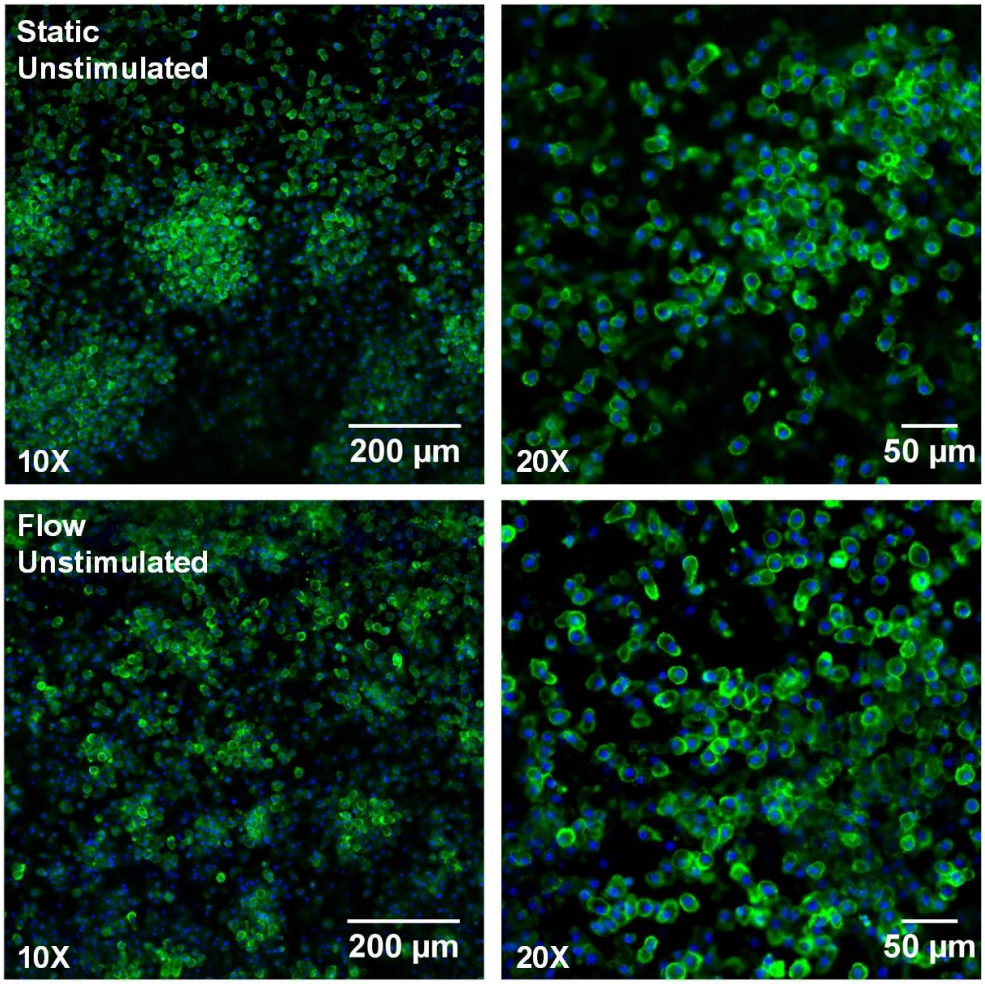
Static
Unstimulated
10X
200 µm
20X
50 µm
Flow
Unstimulated
10X
200 µm
20X
50 µm

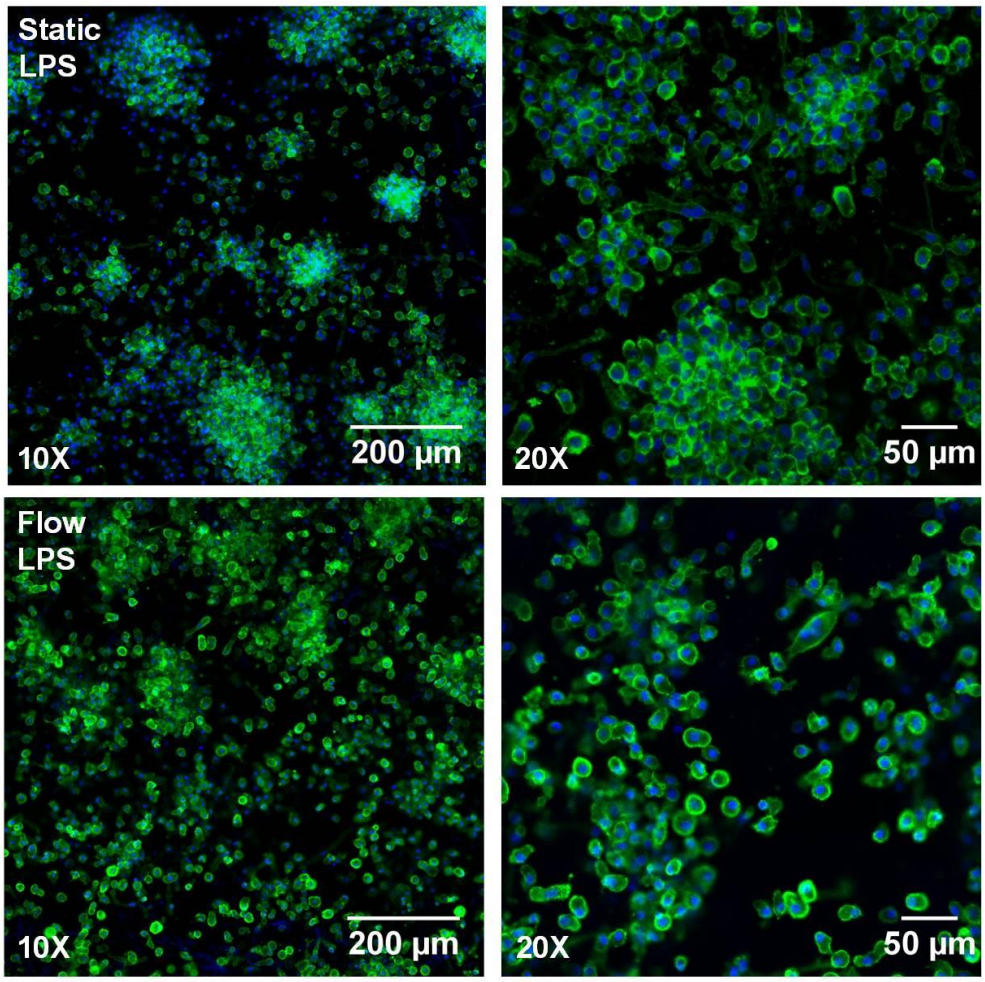

Figure 40. Visualisation of moDC response to LPS on static and flow platforms.
moDCs were cultured on collagen hydrogel-coated paper scaffolds for 24 hours under static and flow conditions, with or without LPS stimulation. Cells were fluorescently stained with Phalloidin Alexa Fluor 488 and DAPI. For unstimulated static and flow samples, cell distribution over the scaffolds was comparable and cells had rounded morphologies. With LPS-stimulation, formation of cell clusters was seen and cell elongation was apparent in static and flow platforms. Images were acquired using the LSM710 confocal system with 10X and 20X objectives (n = 2).

3.4. Conclusions and Further Work

The development of *in vitro* fluidic cell culture platforms is useful to simulate the mechanical forces cells experience in natural tissues. This chapter has described the construction of two different devices and the characterisation of one of these platforms for the culture of immune cells under flow.

The first microfluidic device described, fabricated from DSA film, cover glass and PMMA had a number of advantages. In particular, its optical properties, which suited the platform to applications requiring high resolution *in situ* imaging. However, a number of significant limitations, which could not be overcome with minor troubleshooting, prevented further study.

The fluidic device with a paper-based scaffold showed promise as an accessible and appropriate platform for cell culture. The modular design allowed convenient adjustment of the configuration to suit the requirements for this work. The numerous advantages of this platform, including not having a fixed design, have been demonstrated in this study and also by others in our group in the generation of air-liquid interface cultures (personal communication).

A removable paper insert provided the basis of the cell culture scaffold. The advantage of this was that it increased the options in terms of cell seeding methods, which could be done on or off the platform. The paper scaffold was also amenable to a variety of surface treatments and coatings. This allowed the incorporation of a collagen hydrogel, previously characterised for immune cell culture in Chapter 2 of this thesis.

The paper scaffold was characterised for its compatibility with moDCs, this was the first time it had been used for the culture of immune cells. moDCs cultured on the paper scaffolds exhibited good viability, however, the phenotype of moDCs harvested from the scaffolds was indicative of their maturation. Endotoxin contamination was ruled out as an explanation for this by pre-treating scaffolds with PMB.

It was anticipated that the paper scaffold would have minimal impact on the moDCs as it was coated with collagen hydrogel. It is possible that there were limitations with the efficiency of the coating, which would have caused some of the cells to be directly exposed to the paper scaffold. Therefore, an inherent property of the paper, such as topography, surface chemistry or substrate stiffness, may be responsible for inducing the up-regulation of the markers (Rostam et al., 2015).

To determine whether this was the case, collagen-coated scaffolds could be fluorescently stained for collagen in order to visualise the coverage of the hydrogel on the scaffold by confocal microscopy. Further to this, moDC responses on uncoated and collagen-coated scaffolds would provide useful information on the direct effect of the paper on cell maturation.

moDCs cultured on paper scaffolds were tested to determine whether they were immunologically responsive to LPS. The trend in the expression of maturation markers and changes in the distribution and morphology of cells following stimulation by LPS were suggestive of their immunological responsiveness.

In hindsight, the range of readouts selected for this experiment was probably insufficient to conclusively determine the immune-competence of moDCs cultured on paper scaffolds. Including other measures of biological function, such as, cytokine production and endocytic activity, would be informative for future studies.

The fluidic device with the paper scaffold was characterised for dendritic cell culture. Encouragingly, cell viability was only slightly reduced under flow conditions. Also, the density of cells that remained attached on the scaffold under flow was comparable with that under static conditions.

Phenotypic analysis of moDCs indicated that they maintained a less mature phenotype in the context of flow. It has been suggested that, physical stimuli, such as flow, can modulate immune responses. Due to the heterogeneous nature of interstitial flow it is difficult to compare the flow rate used in these experiments with *in vivo* conditions. However, owing to the maintenance of an immature phenotype by moDCs under flow, it could indicate that the flow rate used in these experiments was representative of physiological conditions which contribute to the suppression of the inflammation. By testing the effect of a range of different flow rates on moDC maturation, it may be possible tell whether the flow rate used here specifically contributed to the maintenance of the immature moDC phenotype.

Alternatively, the increased maturation state of moDCs cultured under static conditions may have been due to the build-up of inflammatory cytokines in the

cell culture chamber. On the flow platform the effect of the cytokines may have been diluted by their circulation throughout the system.

Another factor which should be noted is the potential for the silicone tubing, which was only used for the flow platform, to absorb proteins. This could immobilise inflammatory cytokines circulating in the media, thereby removing the positive feedback for cell activation and suppressing the induction of moDC maturation.

The immunological competence of moDCs was assessed on the fluidic platform. The pattern of increased expression of activation markers following LPS stimulation indicated cells cultured under flow were responsive. This was supported by fluorescent microscopy, whereby the effect of LPS was apparent on the spatial organisation and morphology of the cells.

No significant effect of the introduction of flow was seen on moDC responses to LPS, compared to static. As mentioned previously, the readouts used in this work may not have been sufficient to pull apart differences between static and flow cultures. It would also be interesting to investigate the effect of the rate of flow on moDC responses in the context of immunological stimulation.

In conclusion, the work in this chapter has described the development and characterisation of a fluidic platform with a paper-based scaffold for immune cell culture. This fluidic platform showed promise for the study of the effect of flow on immune responses. However, it was important to take in to account the

limitations identified with regards to the influence of the scaffold and flow on the phenotype of the cells in further studies.

Chapter 4

Application of Physiologically Relevant Platforms for the Study of Antigen-Specific Dendritic Cell – T Cell Interactions

4.1. Introduction

Chapter Overview

T cell activation underpins efficient adaptive immunity. To date, much research has been undertaken to elucidate the mechanisms involved in both protective and pathological T cell-mediated immune responses.

Mixed lymphocyte reactions (MLRs) are useful *in vitro* tools for studying T cell activation in disease, drug development and safety testing (Kashipaz et al., 2002). Traditionally these assays are performed in static 2D cultures and in the absence of ECM. They often involve the co-culture of purified T cell populations with antigen presenting cells, such as DCs or irradiated PBMCs. In addition to the biological or chemical entity being tested, co-stimulatory

factors, including cocktails of cytokines or antibodies, are also frequently added.

These assays provide important insights into immunological mechanisms, however, the immunological reactions take place under artificial conditions and the outcome may be biased by the cellular or biochemical composition. This limits their translation for predicting immune responses (Pörtner and Giese, 2006, Giese and Marx, 2014).

In vivo, induction of adaptive immunity occurs in the complex microenvironment of secondary lymphoid tissues, such as the lymph node. Here, a variety of cues such as, cellular and extracellular matrix components, mechanical forces and biochemical signals, provide a balance of stimulatory and regulatory cues to ensure the induction of appropriate T cell responses (Gasteiger et al., 2016).

This chapter describes the work carried out to investigate the effect of incorporating physiologically relevant features into MLRs for antigen-specific T cell activation.

Physiological relevance was incorporated into this work by the application of:

1. A collagen hydrogel ECM platform.
    a. Also combined with the chemokine, CCL21.
2. A paper scaffold-based fluidic platform.

Cell-Mediated Adaptive Immunity

All cells of the immune system originate from pluripotent hematopoietic stem cells in the bone marrow. From these cells, lymphoid-primed multipotent progenitors give rise to the cells that comprise the adaptive immune system, namely T and B cells (Bhandoola and Sambandam, 2006).

The fundamental features of the adaptive immune system are antigen specificity and immunological memory. This enables the generation of targeted immune responses to rapidly eliminate pathogens, to which an individual has been previously exposed (Murphy et al., 2008).

Cell-mediated adaptive immunity is imparted by the functions of T lymphocytes (Murphy et al., 2008). There are two key subsets within the T lymphocyte population, distinguished by the expression of CD8 or CD4 (Germain, 2002). These markers reflect the effector function of the cell, as illustrated in Figure 41. CD8 is found on cytotoxic T cells, which directly kill cells harbouring a cytosolic viral or bacterial infection (Harty et al., 2000). $CD4^+$ T cells have the potential to differentiate to carry out different types of effector activity, termed Th1, Th2 and Th17 (Annunziato et al., 2015b).

Th1 cells help control intracellular bacterial, parasitic and viral infection through the activation of the programme of cell death of the antigen presenting cell. Th1 cells also have a role in stimulating antibody production. Th2 effector cells activate B cells into producing antibodies to help eliminate toxins or extracellular pathogens. Finally, Th17 responses provide defence against extracellular bacteria and fungi. Th1\Th2\Th17 polarisation depends on the

combination of antigen, co-stimulatory molecules and cytokines during antigen presentation (Annunziato et al., 2015a).

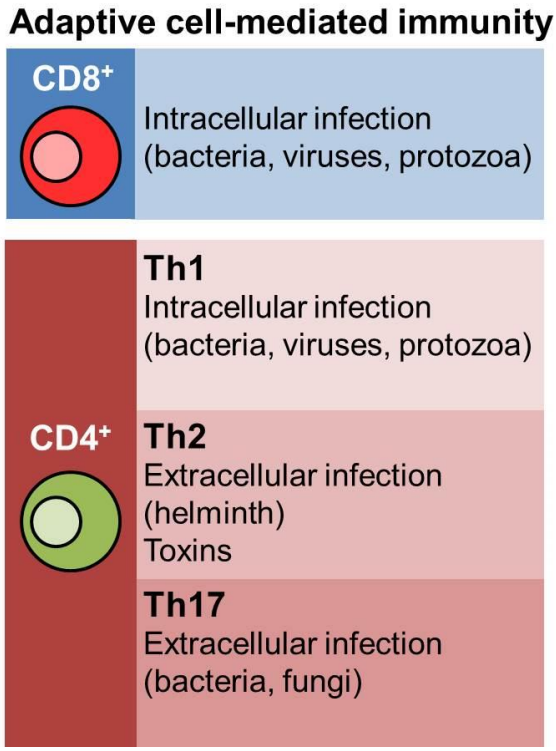

Figure 41. Effector functions of T cells in cell-mediated adaptive immune responses.
T cell effector function targets pathogens based on location. $CD8^+$ T cells have cytotoxic effects on cells presenting antigen derived from the cytosol. $CD4^+$ T cells differentiate to carry out a variety of effector functions depending on the nature of the pathogen; Th1 contributes to killing cells harbouring intracellular pathogen, Th2 stimulates antibody production by B cells to combat extracellular pathogens and Th17 produces cytokines which promote an inflammatory tissue response to eliminate extracellular infections.

T Cell Activation

The molecules involved in the recognition of specific antigen which are expressed by T cells are known as T cell receptors (TCRs). As depicted in Figure 42, the TCR is membrane-bound and composed of two chains, α and β, each with a variable and a constant region. The variable regions of the α and β chains combine to give rise to the antigen binding site. During development within the thymus, a programme of genetic re-arrangement of the α and β chains results in each cell having a unique TCR. This generates a T cell

repertoire capable of recognising a phenomenal number of antigenic peptides (Zuniga-Pflucker and Lenardo, 1996).

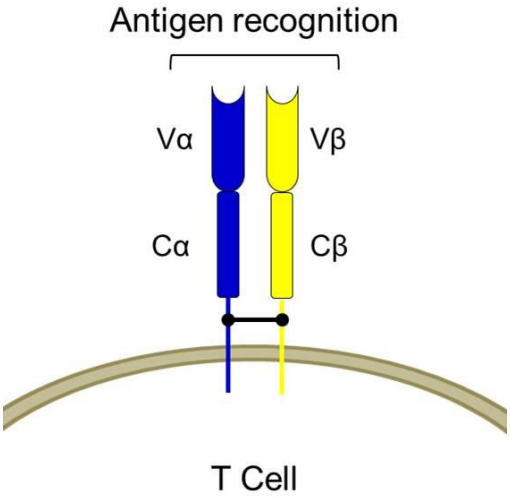

Figure 42. The T Cell Receptor.
The TCR is membrane-bound and composed of α and β chains linked by a disulphide bond. Each chain has a constant (C) and a variable (V) region. The variable region forms the antigen-specific binding site.

Typically, the TCR only recognises antigen bound to major histocompatibility complex (MHC) molecules (Rudolph et al., 2006). The principle classes of MHC molecules are MHC-I and MHC-II which are preferentially bound by the T cell co-receptors, CD8 and CD4 respectively. As a rule, MHC-I displays antigen derived from the cytosol, indicative of an intracellular infection, which elicits CD8 T cell-mediated immunity. Dendritic cells are also able to present exogenous peptides through MHC-I, a mechanism known as cross presentation (Ackerman and Cresswell, 2004, Williams et al., 2002). Peptides originating from extracellular sources are presented by dendritic cells through MHC-II, this cues $CD4^+$ T cell effector functions (Villadangos, 2001).

The TCR alone does not have signalling capability. As shown in Figure 43, association with the accessory molecules CD4 or CD8, CD3 complexes and the

ζ chain, is required for optimal signalling. The CD3 complex is comprised of dimers of CD3γ, CD3δ and CD3ε, which interact with the α and β chains of the TCR (Kane et al., 2000). Signalling comes about through immunoreceptor tyrosine-based activation motifs (ITAMs) present in the cytoplasmic tails of the CD3 complexes and the ζ chain. Phosphorylation of ITAM sequences initiates a cascade of intracellular signalling pathways which directs the specific cellular response.

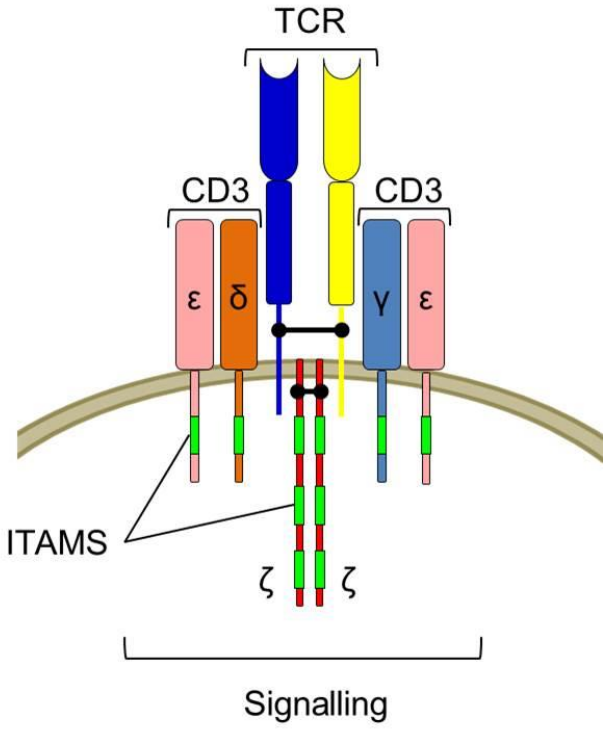

Figure 43. The TCR signalling complex.
The α:β TCR heterodimer provides the antigen-specific binding site. The CD3 complex, comprised of ε, δ and γ chains, stabilises the TCR and allows signalling via ITAMs upon antigen recognition. The ζ chain homodimer contains ITAMs and is also involved in signalling following antigen binding. Diagram adapted from Murphy et al. 2008.

Recognition of peptide-loaded MHC (pMHC) by the TCR in conjunction with its accessory molecules is required for efficient T cell activation, as shown in Figure 44. The antigen-specific interaction is known as Signal 1. In conjunction with the antigen-specific interaction, efficient T cell activation requires additional signals. This includes co-stimulation through CD28, or

CD28-related molecules, termed Signal 2. Finally, the third signal is provided by cytokines (Tseng and Dustin, 2002, Gonzalo et al., 2001, Curtsinger and Mescher, 2010).

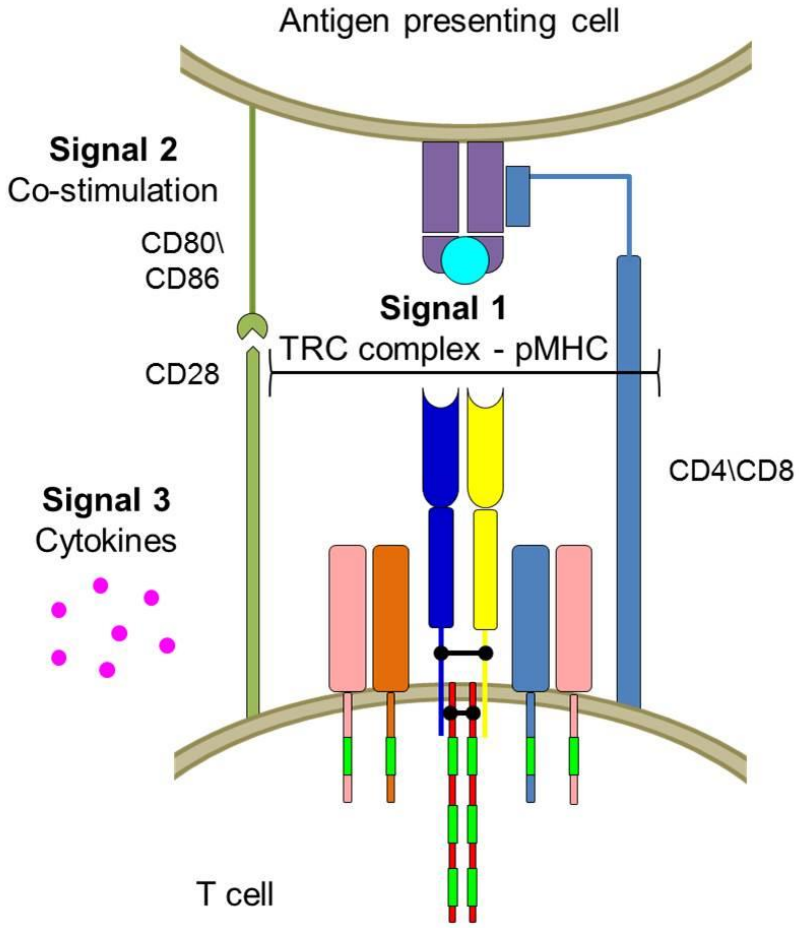

Figure 44. Efficient T cell activation via the TCR requires 3 signals.
Signal 1. The antigen-specific induction of the TCR complex through the recognition of peptide-loaded MHC (pMHC). Signal 2. Co-stimulation through molecules expressed on surface of antigen-presenting cell. Signal 3. Extracellular milieu of soluble factors, e.g. cytokines, which provide co-simulation and contribute to T cell polarisation. Schematic modified from Murphy et al. 2008.

This is a brief overview intending to illuminate the key aspects involved in T cell activation. In reality, it is a highly complex immunological event with multiple levels of regulation. In normal circumstances, T cell-mediated immune responses effectively protect the body from pathogens. Dysregulation of T cell activation and resultant inappropriate responses can lead to pathology, such as uncontrolled infection, allergy, autoimmunity and cancer.

T Cell Activation In Vitro

Modelling antigen-specific T cell activation *in vitro* has many useful applications in areas of immunology research, therapeutic development, diagnostic and immunotoxicology screening. Activation of T cells via the TCR complex can be achieved through the application of a variety of antigenic entities, including pathogen or allergen-derived extracts and antibodies.

Purified protein derivative (PPD) from *Mycobacterium tuberculosis* (Mtb) is an example of a pathogen-derived agent used to stimulate T cells. PPD is derived from Mtb cultures through purification by ammonium sulphate precipitation. The resulting preparation has high protein content and is low in polysaccharides, nucleic acids and lipids (Yang et al., 2012). Currently, preparations contain a mixture of peptides, however, work is underway to identify individual peptides with the most potent antigenic activity (Cho et al., 2012, Brusasca et al., 2001).

PPD is considered as the tuberculin standard by the World Health Organisation (Guld et al., 1958). It is used for the tuberculin skin test (TST) for the identification of individuals with asymptomatic tuberculosis (TB), known as latent TB infection (LTBI).

Mtb is an intracellular pathogen and it is able to persist in macrophages at the site of infection, usually the lungs, without causing clinical symptoms of TB. The protective response against Mtb infection is principally mediated by cellular immunity, involving Th1-polarised $CD4^+$ T cells and $CD8^+$ T cells (Flynn and Chan, 2001).

The TST is performed by intradermal injection of PPD into the forearm, followed by monitoring for the onset of a delayed-type hypersensitivity (DTH) response within 48-72 hours (Mackin, 1998). The DTH response indicates an individual's immune system has been sensitised to the antigen and is suggestive of LTBI, or previous vaccination against Mtb with the Bacillus Calmette-Guérin (BCG) vaccine.

PPD has also been used to stimulate immune cells *in vitro* for diagnosis of Mtb infection with some success (Katial et al., 2001, Lein and Von Reyn, 1997). Individuals who have been vaccinated against Mtb with the BCG vaccine will also respond to PPD in these assays. T cell proliferation and IFN-γ production demonstrate the induction of T cell-mediated responses as a result of PPD stimulation.

The wealth of information available regarding the immunology and antigenic properties underlying the activity of PPD make it a useful tool for the study of antigen-specific T cell responses in cell-mediated immunity.

Physiological Considerations for T Cell Activation

Extracellular Matrix

The ECM can have profound effects on the function of immune cells. As discussed in more detail in Chapter 2 of this thesis, a number of studies have highlighted the role of ECM components in potentially determining the outcome of immune responses.

Three-dimensional (3D) collagen hydrogels have previously been used to study T cell motility and interaction with APCs in order to provide an environment more representative of the lymph node (Gunzer et al., 2000, Gunzer et al., 2004). T cell behaviour in 3D collagen hydrogels was found to reflect *in vivo* observations in terms of the dynamics of interactions with APCs and formation of small cell aggregates. This is in contrast to the cell behaviour seen in conventional liquid culture, where large cell aggregates occur.

Therefore, through introducing components of the natural tissue, the T cell response to antigen *in vitro* may be more representative of that in secondary lymphoid organs. This may be achieved by employing biomaterials, such as collagen hydrogels, in artificial ECM platforms for modelling T cell activation.

Biochemical Cues

The biochemical milieu is critical for T cell activation and polarises the effector activity of immune cells *in vivo*. Cytokines are often added to *in vitro* assays to provide co-stimulatory signals to T cells.

Chemokines also have important functions in directing immune cell responses. The chemokine, CCL21, is important in terms of its role in facilitating efficient immune responses *in vivo*. It is expressed within the lymph node on T cell zone fibroblastic reticular cells. CCL21 is a ligand for the receptor CCR7, which is found on DCs and T cells. CCL21 is required for T cell and DC homing to lymph nodes and cell motility within the paracortex.

Studies are emerging which demonstrate CCL21 may have further functional roles in the induction of immune responses (Forster et al., 2008). It has been suggested that CCL21 may act as a natural adjuvant. Marsland et al. demonstrated it induced DC maturation, resulting in the enhanced ability to prime T cells (Marsland et al.). Interestingly, CCL21 induced endocytosis in mature DCs but not immature DCs (Yanagawa and Onoe, 2003). These studies indicate CCL21 may modulate DC antigen presenting efficiency with important implications for T cell activation.

With regards to the functional effects of CCL21 on T cells, there is evidence to suggest it is an early co-stimulatory molecule during T cell priming. CCL21 induced proliferation of $CD8^+$ and $CD4^+$ T cells and promoted Th1 differentiation (Flanagan et al., 2004). This work implicated CCL21 as a significant molecule for T cell activation.

Since CCL21 has been observed to have profound effects on immune cell behaviour *in vivo* and *in vitro*, it has the potential to contribute to the enhancement of the physiological relevance of DC-T cell interaction studies *in vitro*.

Shear Flow

The effect of extra-cellular mechanical forces on immune cell behaviour is gaining increasing attention (Previtera, 2014). As highlighted in Chapter 3 of this thesis, the influence of shear flow has been shown to have a role in the modulation of immune responses.

Physical extra-cellular forces can exert their effects on cells through the activation of cell-surface receptors. This has implications on the regulation of phosphorylation and kinase signalling (Giannone and Sheetz, 2006). CD3 complexes, associated with the TCR, carry out signalling functions upon pMHC recognition through the phosphorylation of tyrosine residues within the ITAM. An elegant study carried out by Li et al. demonstrated that mechanical forces acting via the TCR complex caused T cell signalling (Li et al., 2010).

T cells are exposed to the physical effects of interstitial flow within the lymph node. Based on the accumulating evidence that mechanical forces modulate immune cell responses, flow is likely to be a physiologically relevant influence on the elicitation of T cell activation. Thus, it is reasonable for flow to be incorporated into *in vitro* T cell assays in order to simulate the mechanical stress T cells experience during antigen presentation.

Chapter Aims

This chapter seeks to examine how the extra-cellular environment affects the outcome of antigen-specific DC-T cell interactions *in vitro* through the application of the ECM and fluidic platforms developed in Chapters 2 and 3 of this thesis. This was done by comparing the antigen-specific T cell response induced on the biomimetic platforms with that generated under conventional cell culture conditions.

4.2. Materials and Methods

Generation of Monocyte-Derived Dendritic Cells

This was done according to the method described in Chapter 2 of this thesis, 2.4. Materials and Methods: *Generation of Monocyte-Derived Dendritic Cells.*

Isolation of T Cells

T cells were isolated from PBMCs by negative selection. Pan T cell isolation (kit purchased from Miltenyi Biotech) by magnetic cell separation was performed, as previously described (Horlock et al., 2007). The purity of isolated T cells was typically >95%.

Autologous Mixed Lymphocyte Reaction

Immature moDCs and T cells, obtained from the same donor, were co-cultured at a ratio of 10 T cells to 1 moDC. Cells were stimulated with 5µg/mL tuberculin PPD (Statens Serum Institut) and maintained in a humidified incubator (37°C, 5% CO_2) for 6 days. For the tissue culture control, cells were seeded in a U-bottom 96-well TCP plate. Collagen cultures were set up in flat 96-well plates which had been prepared with 100µL of a 0.5mg/mL collagen hydrogel, onto which the cells were seeded.

Preparation of Collagen Hydrogels

The collagen hydrogel was prepared according to the method described in Chapter 2 of this thesis, 2.4. Materials and Methods: *Preparation of Collagen Hydrogels*. The collagen solution was retained on ice until required.

Paper-Based Fluidic Platforms (static & flow)

Platforms were assembled according to the method described in Chapter 3 of this thesis, 3.4 Materials and Methods: *Fluidic platform assembly, Paper-based fluidic device*.

IFN-γ Detection

Enzyme-linked immunosorbant assays (ELISAs) were used to detect IFN-γ in the supernatants collected from AMLRs. The IFN-γ Duo-set ELISA kit (purchased from R&D systems) was used according to manufacturer's instructions.

Light Microscopy

Brightfield images were acquired on an Olympus CRX 41 microscope using a 4X objective with Infinity Analyse Lumenera software.

Image analysis

ImageJ was used for the analysis of fluorescent images (Schneider et al., 2012).

Statistical analysis

Analysis was carried out using GraphPad Prism version 6.00 for Windows, GraphPad Software, La Jolla California USA (www.graphpad.com).

4.3. Results and Discussion

Optimising Antigen-Specific T cell Activation *In Vitro*

A mixed lymphocyte assay was established for the study of DC-T cell interactions. For this, moDCs and T cells were purified from the same donor and co-cultured in a multi-well tissue culture plate. In this thesis, these assays are referred to as Autologous Mixed Lymphocyte Reactions (AMLRs).

T cell activation was induced using two model antigens, purified protein derivative (PPD) from *Mycobacterium tuberculosis* (Mtb) and lysate from *Aspergillus fumigatus* (AF). AF lystate produced the same pattern of T cell response as PPD, however, the intensity of the response was found to be lower compared to PPD. Only the data for PPD is presented.

Initially, both T cell proliferation and cytokine production were considered as measures for T cell activation. Two methods were tested for assessing proliferation of T cells. These were the BrdU (5-bromo-2'-deoxyuridine) proliferation assay and CFSE (Carboxyfluorescein succinimidyl ester) staining. These assays are well-established for measuring cell proliferation and provide a safe (i.e. non-radioactive) and quantitative measure. Cytokine production was measured by enzyme-linked immunosorbant assays (ELISA) using the supernatants collected from the AMLRs.

It was found that T cell proliferation did not give a consistent result for antigen-specific immune activation for all donors. This could have been due to differences in their exposure to Mtb (e.g. vaccination history and exposure to

environmental mycobacteria that cross react with Mtb). For weak-responders, this was probably due to the low frequency of PPD-specific T cells in the samples. It is likely that the proliferation assays were not sensitive enough to measure very low numbers of actively dividing cells.

Cytokines IL-2 and IFN-γ were both found to be good indicators of antigen-specific T cell activation. However, since there was greater variability in IL-2 production, IFN-γ was selected as the readout for T cell activation in this work.

The AMLRs were set up in U-bottom well tissue culture-treated plastic (TCP) plates. The experimental parameters considered during optimisation included the ratio of T cells to moDCs, moDC maturation state and duration of the reaction.

During the preliminary experiments (data not shown) two different ratios of moDCs to T cells were tested, 1:10 and 5:10. This was done with both immature and LPS-matured moDCs. T cells ($CD3^+$) isolated from PBMCs were used directly, without further enrichment, to reflect the natural composition of the T cell population. To determine the appropriate length for the experiments, supernatants were initially sampled between days 3 and 6.

The AMLRs in all of the experiments described in this chapter were set up using a ratio of 1:10 moDCs to T cells, with immature moDCs. Cultures were stimulated with PPD and maintained for 6 days.

Induction of PPD-specific T cell response in conventional cultures

Figure 45 shows the results obtained in static liquid culture, using a conventional U-bottom well TCP format. There was an antigen-specific increase in IFN-γ production (1641.21pg/mL) with PPD stimulation compared to No Antigen (10.53pg/mL) and this was found to be statistically significant (P = 0.0044, **). No increase in IFN-γ was detected with the addition of PPD in the T cell control. Overall, this reaction generated reproducible, PPD-specific activation of T cells. Also, it demonstrated that T cell activation was dependent on the antigen presenting role of moDCs.

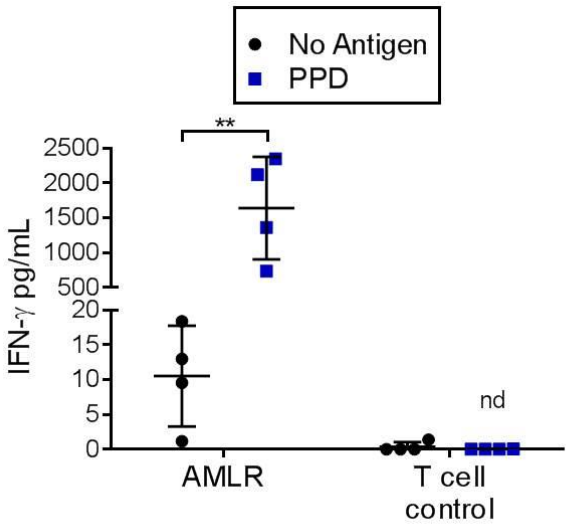

Figure 45. Antigen-specific T cell activation *in vitro*.
IFN-γ production by T cells stimulated with PPD for 6 days. There was a significant increase in IFN-γ secretion with the addition of PPD to AMLRs (P = 0.0044, **, t=4.434, df=6). No antigen-specific IFN-γ production was detected when T cells alone were exposed to PPD (nd = not detected). T tests were performed to determine statistically significant differences. Not significant if P ≥ 0.05 (n=4). Error bars represent standard deviation.

Investigating Antigen-Specific T cell Activation on an ECM Platform

Collagen hydrogels were found to be biocompatible with immune cells and have the potential to increase the physiological relevance of *in vitro* cell culture, as discussed in more detail in Chapter 2 of this thesis.

In this study, a collagen hydrogel was tested for its effects on the induction of antigen-specific immune responses. Six donors were tested and the U-bottom well TCP format was run in parallel with the hydrogel cultures. Three of the donors were found to have high levels of background IFN-γ in unstimulated TCP cultures, they were analysed separately from the three individuals with low levels of background IFN-γ.

PPD-specific T cell activation in the presence of collagen hydrogel

The results from the donors who produced low levels of background IFN-γ are shown in Figure 46. In collagen hydrogel AMLRs, levels of IFN-γ were increased with PPD stimulation (307.47mg/ml), compared to No Antigen (10.93pg/mL); this was found to be statistically significant (P = 0.0352, *). For the TCP control, as expected, the level of IFN-γ produced in PPD-stimulated cultures (326.72pg/mL) was found to be significantly higher compared to No Antigen (12.74pg/mL) (P = 0.0233, *).

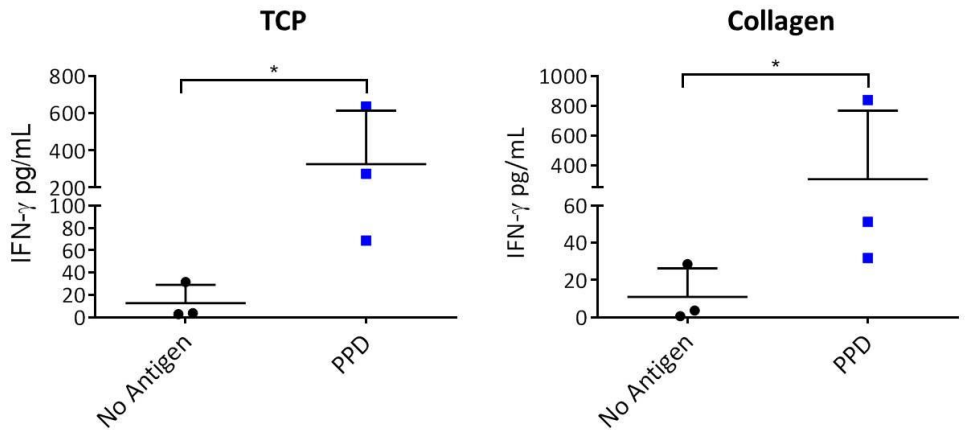

Figure 46. Antigen specific T cell activation on an ECM platform by donors with low background IFN-γ.
TCP: The increase in IFN-γ production in response to PPD stimulation was found to be significant (P = 0.0233, *, t = 6.435, df = 2). Collagen: Production of IFN-γ increased significantly with PPD stimulation (P = 0.0352, *, t = 5.187, df = 2). T tests were used for statistical analysis (n=3). Error bars represent standard deviation.

Figure 47 shows the results from the donors who produced high levels of IFN-γ in the unstimulated TCP condition. In TCP cultures, levels of IFN-γ were raised in response to PPD (2,281.31pg/mL), however this was not found to be significantly different to No Antigen (318.4pg/mL) ($P \geq 0.05$). In the collagen hydrogel cultures from corresponding donors, a PPD-specific increase in IFN-γ was detected (237.185pg/mL) compared to No Antigen (3.57pg/mL) and this was found to be significant (P = 0.0027, **).

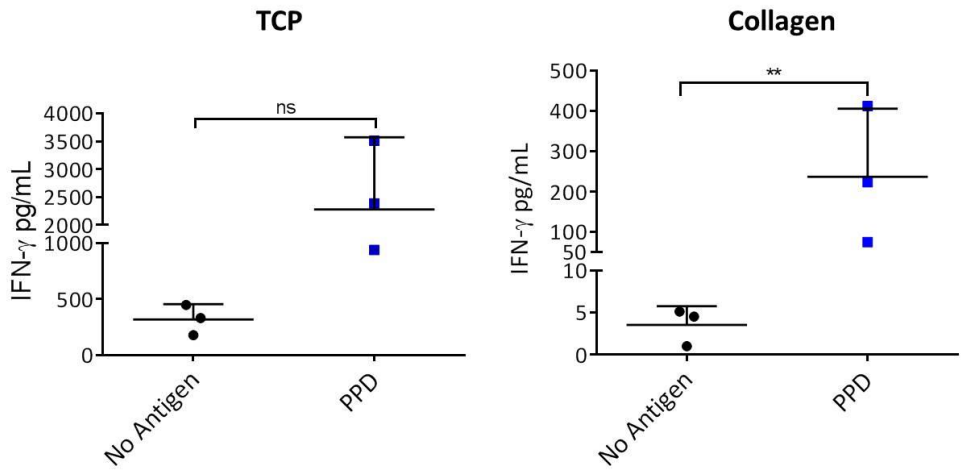

Figure 47. Antigen specific T cell activation on an ECM platform by donors with high background IFN-γ.
TCP: The increase in IFN-γ production in response to PPD stimulation was not found to be significant. Collagen: Production of IFN-γ increased significantly with PPD stimulation (P = 0.0027, **, t = 19.32, df = 2). T tests were used in the statistical analysis (n=3). Error bars represent standard deviation.

All of the donors tested mounted a specific T cell response towards PPD in the context of the collagen hydrogel. Notably, the magnitude of PPD-induced IFN-γ production was lower in collagen cultures than TCP. This may be explained by the tendency of collagen to adsorb proteins, including cytokines, which results in their depletion from the media, as demonstrated in Chapter 2 of this thesis.

This ties-in with the potential anti-inflammatory effects collagen may have through mopping up cytokines. Wiegand et al. demonstrated Type I Collagen bound significant amounts of inflammatory cytokines, including IFN-γ, with anti-inflammatory effects in chronic wounds (Wiegand et al., 2010). In these experiments, such an effect on soluble cytokine concentration could affect the intensity of the T cell response, leading to a reduction in IFN-γ secretion.

An alternative explanation for the lower magnitude of T cell responses in collagen cultures may be due to differences in the spatial organisation of cells. This is because the potential for DC-T cell interactions will determine the overall level of T cell activation.

As demonstrated in Figure 48, cells were densely packed in the centre of the U-bottom wells. This gave rise to a high probability of cell-cell interactions and thus T cell activation. The collagen hydrogels formed a slightly concave surface, due to surface tension around the sides of the wells, but were not as deep as a TCP well. Therefore, the cells were more spread out across the surface the hydrogel. As a result, there were likely to be fewer direct cell-cell interactions. The reduced potential for cell interactions in the hydrogel cultures, compared with TCP, may account for the lower magnitude in T cell activation seen in collagen AMLRs.

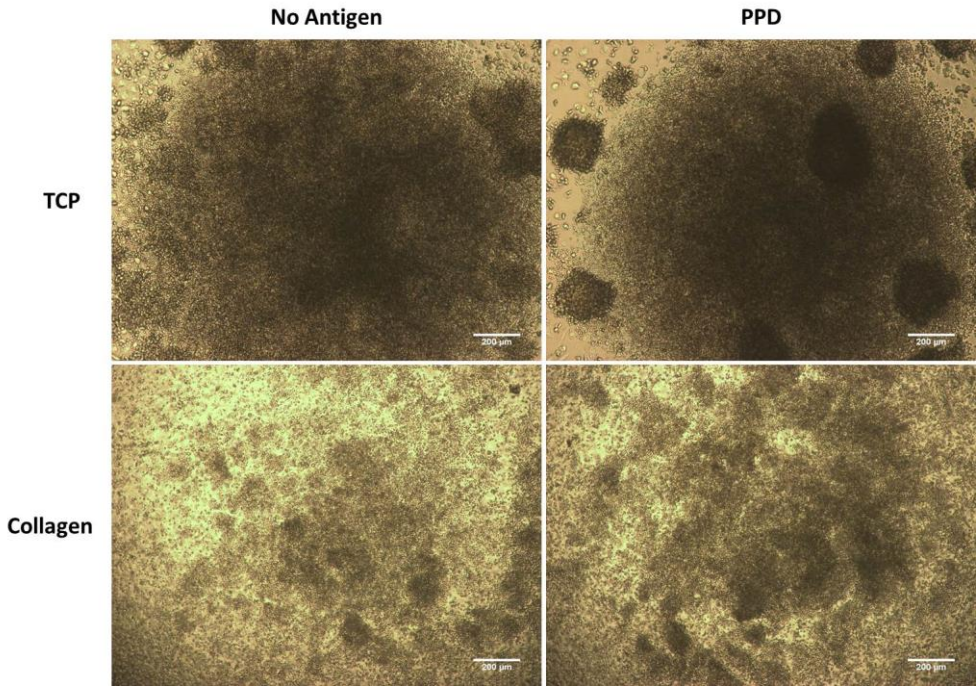

Figure 48. Cell distribution in TCP and collagen hydrogel cultures stimulated with PPD. The U-bottom well of TCP cultures caused cells to settle at a high density in the centre of the cell. This encouraged close cell contacts. With PPD stimulation, significant cell clustering was observed which is indicative of T cell activation. Cells did not pack together at such high densities on the surface of the collagen hydrogel. Therefore, cell-cell contacts were reduced. Less cell clustering was seen with PPD stimulation, compared to TCP. Images were acquired on an Olympus CRX 41 brightfield microscope using a 4X objective, with Infinity Analyse Lumenera software. Scale bars represent 200µm. Images are representative of 3 experiments.

It is worth addressing the variation in the magnitude of IFN-γ production between individual donors. Natural biological variation in the PPD response is common in this type of cell-based assay (Katial et al., 2001). This can be influenced by a range of factors such as donor age and prior antigen exposure, via the environment or vaccination.

For three of the donors, levels of IFN-γ were very high in unstimulated TCP cultures, which was indicative of non-specific immune activation. This can be a result of the basal activation state of the cells, or culture contamination. Interestingly, in collagen cultures for these donors, levels of background IFN-γ were much lower. This reduces the likelihood of contamination being the cause of non-specific activation.

To highlight the differences in the antigen-specific immune response between TCP and collagen, the fold increase in IFN-γ production in response to PPD was calculated. This was done separately for the groups of donors with low and high background IFN-γ. This analysis is shown in Figure 49. Donors with low levels of background IFN-γ were found to have a similar fold increase in PPD-induced IFN-γ production in TCP (44.43) and collagen (38.86) cultures. The fold increase in IFN-γ in response to PPD by donors with high background IFN-γ was relatively low in TCP cultures (8.34). However, the fold increase in the corresponding collagen hydrogel cultures was higher (68.08) and found to be significantly different from TCP (P = 0.0155, *).

This data suggests that culture with collagen hydrogels may be beneficial in terms of reducing non-specific T cell activation, while generating appropriate immune response in the presence of a relevant antigen.

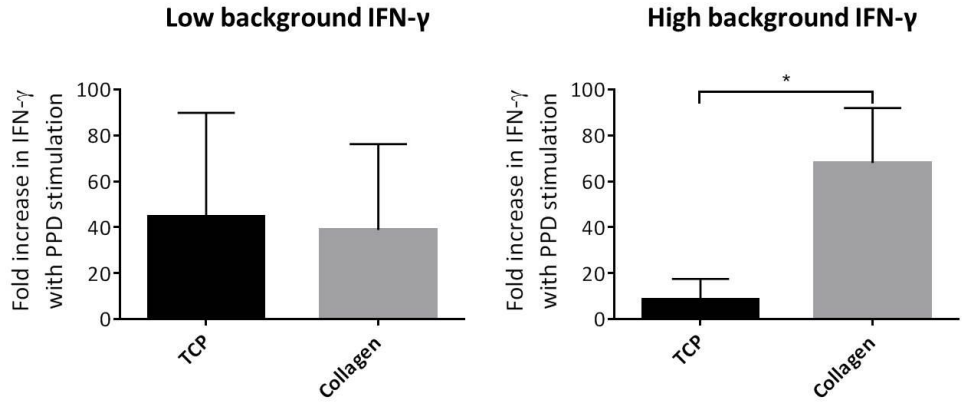

Figure 49. Fold increase in IFN-γ production in response to PPD in TCP and collagen cultures.
When donors produced low levels of background IFN-γ, there was no significant difference in the fold increase in IFN-γ production with antigen stimulation between TCP and collagen cultures. Donors with high background IFN-γ produced a relatively low fold increase in IFN-γ response to PPD. However, on collagen hydrogels, a large fold increase in IFN-γ production with PPD stimulation is seen for the same donors. This was found to be significantly greater than TCP (P = 0.0155, *). Difference not significant if P ≥ 0.05. Statistical analysis was performed using T tests (n=3). Error bars represent standard deviation.

CCL21 Slightly Enhances T Cell Activation in Collagen Cultures.

CCL21 is important for T cell activation as it is known to have a role in cell homing and motility within the lymph node. It has also been shown to modulate key behaviours of dendritic cells and T cells with important implications for the outcome of the immune response. Soluble CCL21 was added to collagen hydrogel AMLRs to investigate whether it had an effect on the magnitude of antigen-specific T cell activation. Three independent donors volunteered for this study.

The results from this experiment are shown in Figure 50. In the presence of CCL21 (+CCL21), IFN-γ production in response to PPD increased for all donors (88.13pg/mL), compared to the unstimulated cultures (9.72pg/mL). For the control reaction (-CCL21), antigen-specific T cell activation was apparent by the increased levels of IFN-γ in PPD stimulated cultures (52.85pg/mL), compared to unstimulated (1.75pg/mL). The increase in IFN-γ production by T cells in response to PPD was significant in both +CCL21 ($P = 0.0107$, *, $t=4.518$ $df=4$) and -CCL21 ($P = 0.0155$, *, $t=4.045$ $df=4$) reactions. The level of PPD-induced IFN-γ secretion appears slightly raised in the presence of CCL21, however, this was not found to be significantly different from -CCL21.

Overall, CCL21 appeared to slightly enhance T cell activation although it was not found to have a significant effect in these assays. *In vivo*, ligand concentration and interactions with other cells and molecules likely contribute to its activity in modulating immune responses. In these experiments, the microenvironment is highly simplified compared to the natural tissue which

could explain the lack of significant difference in T cell responses in the presence of CCL21.

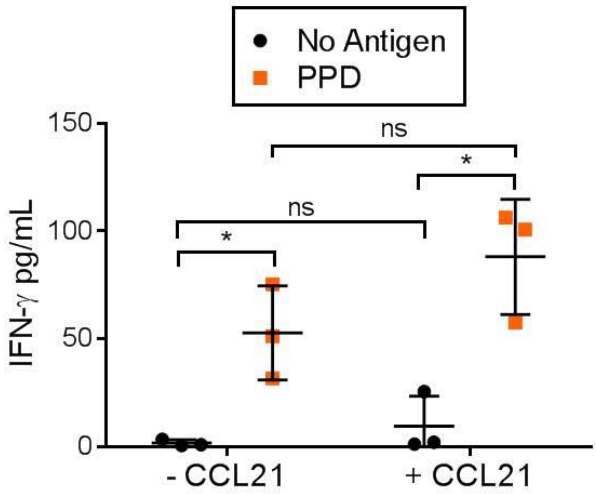

Figure 50. CCL21 slightly enhances T cell activation in collagen hydrogel cultures. IFN-γ production in AMLRs cultured on collagen hydrogels with the addition of CCL21. AMLRs +CCL21 showed a significant increase in IFN-γ with PPD stimulation (P = 0.0107, *, t=4.518 df=4). Antigen-specific increase in IFN-γ for -CCL21 was also found to be significant (P = 0.0155, *, t=4.045 df=4). No significant difference was found in PPD-induced IFN-γ production between -CCL21 and +CCL21 AMLRs. T tests were used to determine statistical significance (n = 3) Not significant if P ≥ 0.05. Error bars represent standard deviation.

Studying Antigen-Specific Immune Responses on a Fluidic Platform

A novel fluidic platform, based on a collagen hydrogel-coated paper scaffold was characterised for immune cell culture applications in Chapter 3 of this thesis. It was utilised in this work to study antigen-specific T cell activation. A comparable static platform, with the same number of cells and volume of media, was set up in parallel with flow experiments. Three new donors were selected for these experiments.

Antigen-specific activation of T cells under static and flow conditions on a paper scaffold-based fluidic platform

The results from the AMLR conducted on the scaffold under static conditions are shown in Figure 51A. A PPD-specific increase in the level of IFN-γ (578.86pg/mL) was found, compared with No Antigen (47.28pg/mL). Although this difference was not found to be significant, the results demonstrated the potential of the paper scaffold for the study of DC-T cell interactions but highlighted that its sensitivity may be limited.

The propensity of the paper scaffold to induce a mature moDC phenotype, as described in Chapter 3 of this thesis, was taken into account in these experiments. Based on the results, the effect of the scaffold on moDC maturation did not result in high levels of non-specific T cell activation

Figure 51B shows the results generated from the platform under flow conditions. IFN-γ production was increased in a PPD-specific fashion, the concentration of IFNγ detected with PPD was 151.64pg/mL, without PPD it was 0.81pg/mL. The increase in IFN-γ in response to PPD was found to be significant under flow conditions ($P = 0.0224$, *).

It should be noted that significantly less IFN-γ was detected in PPD-stimulated AMLRs under flow conditions than the static cultures ($P = 0.0224$, *). There could be a number of reasons for the significant difference in the concentration of PPD-induced IFN-γ detected under static compared to flow conditions. To begin with, the effect of cell death cannot be ruled out as during the

characterisation of the fluidic platform in Chapter 3, cell viability was shown to decrease under flow.

On the flow platform, T cells are able to recirculate the system, therefore, not all of them will be in contact with the DCs in the chamber all of the time. This may lead to reduced cell-cell interactions which would decrease the intensity of the response.

Flow may also have prevented the accumulation of cytokines within the cell culture chamber. Cytokines provide important feedback to elicit and maintain cell activation therefore if they were diluted throughout the system by flow, this could account for a lower magnitude of the cytokine response.

Finally, the silicone-based fluidic tubing, which is only used for the flow system, may also contribute to the reduction in the amount of IFN-γ detected. A limitation of silicone is that due to its hydrophobic nature it has a tendency to absorb proteins.

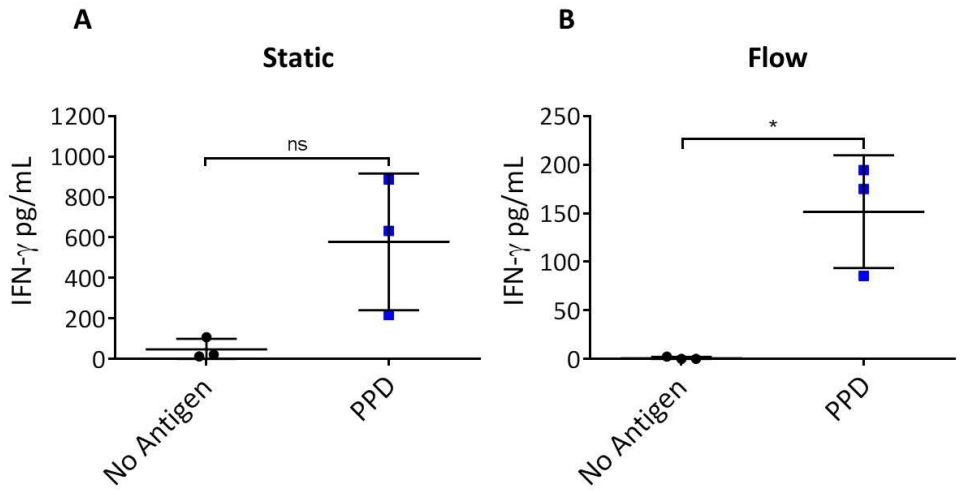

Figure 51. Antigen-specific T cell activation on a paper-based fluidic platform.
Production of IFN-γ from PPD-stimulated AMLR established on paper-based platform under static and flow conditions. A. For the static control, the PPD-specific increase in IFN-γ production was not found to be significant. B. Under flow, IFN-γ production increased significantly in response to PPD (P = 0.0224, *, t=4.566 df=2) (n=3). Error bars represent standard deviation.

The fold difference in PPD-induced IFN-γ production was compared between static and flow, as shown in Figure 52. A much greater fold difference was found between No Antigen and PPD-stimulated cultures under flow (113.06 fold increase), compared with static (20.47 fold increase). A significant difference was found for the fold increase in response to PPD between the static and flow conditions (P = 0.0204, *). These results suggest that, on the paper scaffold platform, flow enhances the sensitivity of the DC-T cell assay to antigen stimulation.

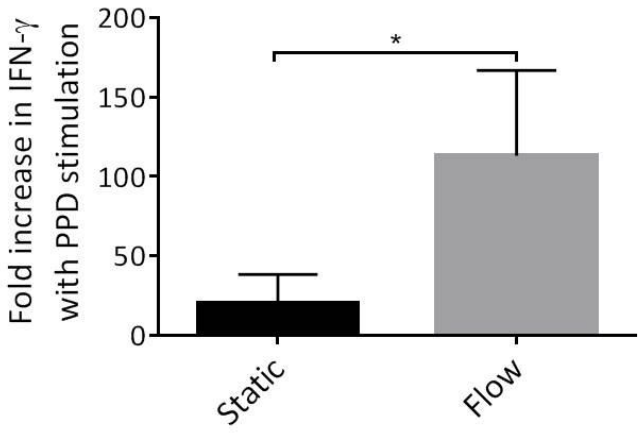

Figure 52. Fold difference in IFN-γ production in response to PPD for static and flow conditions.
The fold difference in PPD-induced IFN-γ production under static conditions (20.47) is significantly less than that found for flow cultures under flow (113.06) (P = 0.204, *, t = 4.796, df = 2). Statistical analysis performed using T tests (n=3) Error bars represent standard deviation.

4.4. Conclusions and Further Work

Establishing biologically relevant assays to study T cell responses *in vitro* is important since it will reduce the requirement for animal testing. Also, with the utilisation of human cells, data will be translatable to human immunology. The limitation of conventional cell culture methods is that they are artificial and not representative of the tissue microenvironment, such as the lymph node, where T cell activation by antigen presenting DCs naturally occurs. Therefore, the development of platforms which mimic the *in vivo* setting is required.

The T cell assay used for this work was robust as antigen stimulation elicited an increase in IFN-γ production by all donors tested. The variation in the magnitude of response between donors was normal for this type of study. Cytokine data can be normalised to account for this variation, however, for this work it was more informative to present the actual concentration of IFN-γ detected in the supernatant for each donor.

The ECM Platform

A collagen hydrogel platform was used to mimic the ECM that T cells are exposed to during antigen presentation in the lymph node. An increase in IFN-γ secretion in response to antigenic stimulation was detected in all collagen hydrogel cultures.

In the collagen hydrogel experiments, the magnitude of PPD-specific IFN-γ production was lower than that in TCP. This could have been due to the propensity of collagen to adsorb proteins, which would directly contribute to the reduction in the concentration of soluble cytokine.

A consequence of IFN-γ sequestration by collagen would be the disruption of the positive feedback loop which is required to elicit and maintain T cell activation. This would dampen the magnitude of the immune response and thus the concentration of IFN-γ would be reduced further.

The fate of IFN-γ could be determined either by digesting the collagen hydrogel and measuring the IFN-γ recovered, or by fluorescent labelling of the collagen hydrogel for IFN-γ.

Additionally, T cells could be treated with Brefeldin A to block cytokine secretion before the end of the experiment, then, fluorescently stained for intracellular IFN-γ. This would allow quantitative analysis of the frequency of antigen-specific T cells and magnitude of the immune response by flow cytometry.

The differences observed between the spatial organisation of cells in TCP and collagen hydrogel cultures are also likely to influence the intensity of the immune response. Investigating the impact of well shape and size on the outcome of immune responses would be interesting. This could be done using microfabrication techniques, by which a range of micro-wells with varying depths and diameters can be made, described in Appendix II of this thesis.

The results from this work suggested that collagen hydrogels may provide a simple method to increase the physiological relevance of T cell activation. It would also be worth investigating the effect of other ECM components, e.g. fibronectin and laminin, and ECM mixtures, on T cell responses to antigen.

The addition of the chemokine, CCL21, to collagen hydrogel cultures appeared to slightly enhance the level of antigen-specific T cell activation but not significantly. Profound effects of CCL21 on immune cells have been described in the literature with specific implications for enhancing T cell activation. The effects of CCL21 *in vitro* could be investigated further through titrating the concentration, creating concentration gradients and immobilisation within the collagen hydrogel.

The Fluidic Platform

T cell activation was induced under flow in an antigen-specific manner. Levels of PPD-induced IFN-γ detected under flow conditions were lower compared to the static counterpart, this could be due to a variety of reasons. Firstly, this may be accounted for by differences in the number of T cell-DC contacts on the flow and static platforms. To address this, the design of the flow device could be modified to ensure all of the T cells are retained within the chamber, while allowing media to circulate.

There is the potential for IFN-γ depletion, either by the collagen hydrogel used to coat the paper scaffold, or the silicone tubing used for the fluidic system. To determine the significance of this, exogenous IFN-γ could be added to the media, in a cell-free system and changes in cytokine concentration monitored over time.

In these experiments, flow was found to increase the sensitivity of the T cell response to antigen, compared to static conditions. Further study into the

impact of the rate of flow on T cell activation using this platform would be insightful.

In conclusion, the data from this work suggest that traditional TCP methods may have a tendency to enhance non-specific T cell activation and exaggerate antigen-specific responses. This may be due to the artificial nature of TCP culture, which could, for example, promote the elicitation of cell activation due to the high cell density and concentration of inflammatory cytokines.

Simple modifications, such as incorporating collagen hydrogel or flow, may generate responses which are more representative of the native tissue setting. Ultimately, however, it is impossible to tell whether the immune response in TCP, collagen hydrogel or fluidic platforms cultures is most representative of *in vivo* T cell activation.

The work presented in this chapter contributes to the establishment of *in vitro* cell culture platforms which aim to reflect the natural microenvironment. By imitating features of the native tissue, it is anticipated that immune cells will respond in a way that is more representative of their *in vivo* counterparts. This has implications for advancing understanding in immunology and improving the accuracy of predicting immune responses to pathogen-derived materials, allergen extracts and therapeutics.

Chapter 5

Investigating Immune Responses to Sensitisers on an ECM Platform

5.1. Introduction

Chapter Overview

Promising progress has been made in establishing immune cell-based methods for the prediction of chemical sensitisation as an alternative to animal testing. However, the current panel of tests available is limited by the lack of emphasis on the value of DC-T cell interactions. In addition, most are performed under conventional cell culture conditions in the absence of biologically relevant cues derived from the extra-cellular microenvironment.

Tissue engineering technologies have the potential to make a great contribution to the development of cell culture by creating more realistic conditions. This could be put into practice in the development of cell culture-based methods for chemical safety testing in order to enhance their biological relevance. This chapter investigates immune cell responses to sensitising chemicals in the context of a collagen hydrogel-based ECM platform.

Properties & Interactions of Sensitisers

Understanding the chemistry and mechanisms through which sensitisers elicit contact hypersensitivity (CHS) responses is important for the development of non-animal tests which predict sensitisation. To induce a CHS response, a sensitiser must successfully negotiate a series of hurdles as depicted in Chapter 1, Figure 2: *Development of Contact Hypersensitivity*, of this thesis. Failure at any single one will put the break on the development of the allergic condition known as allergic contact dermatitis (ACD) (Kimber and Dearman, 2003). The physicochemical properties of chemicals are key to determining their sensitising activity, these include molecular weight, solubility and electrophilic reactivity (Friedmann and Pickard, 2014).

Sensitisers are characterised by having a low molecular weight of less than 500 Daltons, which facilitates their access to the skin (Bos and Meinardi, 2000). The first barrier is the stratum corneum, through which sensitisers penetrate and then partition to the epidermis. The lipid solubility of contact sensitisers also contributes to skin penetration, as lipid-soluble molecules will pass across the stratum corneum more easily than water-soluble ones (Friedmann and Pickard, 2014).

To acquire immunogenicity, most sensitisers form complexes with host peptides, a process termed haptenisation. In terms of the induction of T cell activation *in vitro*, the source of peptide with which sensitisers form immunogenic species is likely to be the serum component, namely albumin, of the cell culture medium.

The stability of the hapten-peptide interaction is important in determining their sensitising activity (Divkovic et al., 2005). However, as shown in Figure 53, there are a variety of possible combinations of high-affinity sensitiser-specific interactions which have the potential to elicit T cell activation.

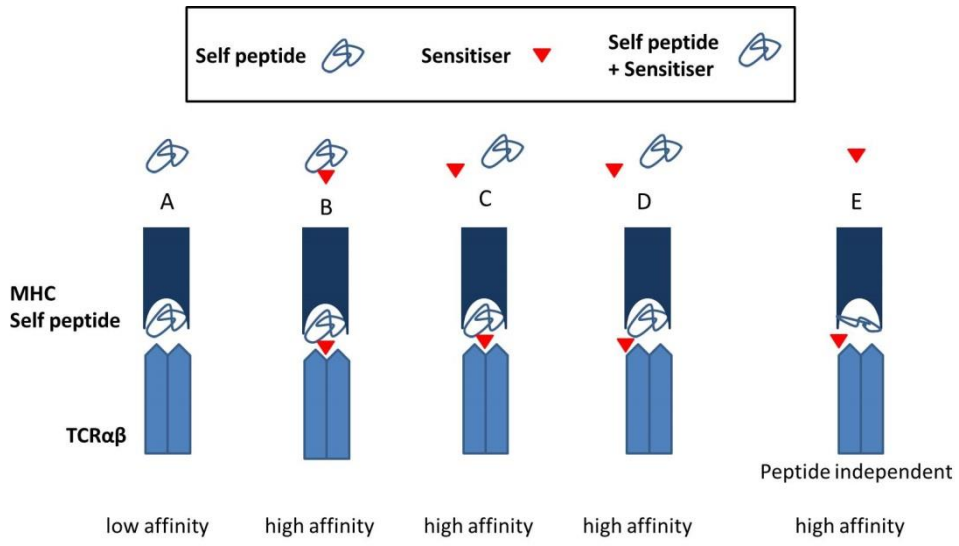

Figure 53. Activation of the TCR by sensitiser-peptide-MHC interactions.
A. The TCR has low affinity for native self-peptide due to negative selection during development in the thymus. B. Covalent modification of self-peptide by sensitiser generates high affinity ligand for TCR. C. Non-covalent interaction of sensitiser with self-peptide generates high affinity TCR ligand. D. Sensitiser binds MHC complex in synergy with self-peptide to form a high affinity TCR ligand. E. Sensitiser bridges MHC and TCR with high affinity, independently of MHC-bound peptide. High affinity MHC-TCR binding induces T cell activation. Modified from Louis-Dit-Sully and Schamel (2014).

Since most sensitisers are electrophiles, covalent bonding is the principle mode by which they interact with host peptides (Figure 53B). The nucleophilic nature of amino acid residues provides reaction sites, with which electrophiles may react through a variety of mechanisms. For example, the reaction of the strong sensitiser, 2,4-Dinitrochlorobenzene (DNCB), with peptide takes place by a classic aromatic nucleophilic substitution (SNAr) mechanism (Aptula et al., 2007). This is illustrated in Figure 54.

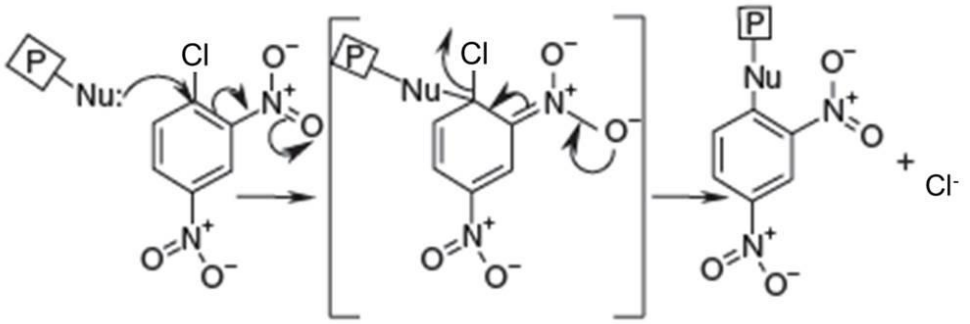

Figure 54. A common predicted reaction mechanism for DNCB with a host peptide.
An aromatic nucleophilic substitution reaction resulting in the covalent modification of host peptide and the generation of a DNCB-specific immunogenic peptide. Nu = nucleophile, P = protein. Modified from Divkovic et al. (2005).

Sensitisers do not necessarily interact with peptides covalently. For metal ions that cause ACD, such as Ni2+, immunogenic determinants arise through the formation of co-ordination bonds with the host peptide (Figure 53 C & D) (Divkovic et al., 2005). It has also been demonstrated that Ni^{2+} might directly bind the TCR and MHC, thereby bridging them with high affinity independently of peptide (Gamerdinger et al., 2003).

Certain chemical sensitisers, including p-phenylendiamine, have been shown to take part in direct, non-covalent interactions with immune receptors (Figure 53E). Although the exact mechanism is controversial, the pharmacological interaction of sensitisers with immune receptors is capable of eliciting T cell responses (Pichler et al., 2006).

Not all chemicals that cause immune sensitisation are inherently reactive before contact with the skin (Gelardi et al., 2001). The weak contact sensitiser, eugenol, is an example of a pro-hapten. Upon application to the skin, it is converted by metabolic enzymes into a reactive species with immune-sensitising activity (Karlberg et al., 2008).

Sensitisers Activate Innate and Cell-Mediated Immunity

Sensitisers induce inflammation through the activation of cellular stress and innate immune responses by cells within the skin. This determines the maturation of dendritic cells, which is a crucial event for the efficient, sensitiser-specific activation of T cells (Kaplan et al., 2012). The severity of the CHS response is conditioned by the level of inflammation caused by the sensitiser (Bonneville et al., 2007).

The specificity of the immune response is determined by the recognition of a sensitiser-(peptide)-MHC complex by the TCR (Louis-Dit-Sully and Schamel, 2014). This takes place within lymph nodes, where T cells are activated in a sensitiser-specific fashion by dendritic cells.

Following activation, clonal expansion of sensitiser-specific T cells takes place, generating effector (T_{EFF}) and effector memory (T_{EM}) T cells. These cells no longer re-circulate LNs and, due to the co-stimulatory signals they receive during priming, acquire a skin-homing phenotype (Dudda et al., 2004). Another subset of T cells, called central memory T cells, also differentiates, these cells re-circulate LNs and ensure a high frequency of sensitiser-specific T cells is maintained (Sallusto et al., 1999).

CHS reactions are essentially effected by $CD8^+$ T cells (Xu et al., 1996, Akiba et al., 2002). $CD4^+$ T helper 1 (Th1), Th17 and regulatory T (Treg) cells have also been implicated in important mediatory roles in the pathology of CHS (Vocanson et al., 2009). Sensitiser-primed effector T cells are rapidly activated

upon repeated contact with the chemical and inflict keratinocyte cytotoxicity at the site of exposure, which results in severe dermatological inflammation.

T Cells as Tools for the Prediction of Sensitisation

The outcome of sensitiser-specific DC-T cell interactions, T cell activation, is arguably one of the most important factors in determining sensitisation, as it indicates the acquisition of specific immunity against a sensitiser and underpins the immune-pathology of ACD.

As demonstrated by the LLNA, T cells are a valuable tool for the prediction of sensitisation. The magnitude of the T cell response correlates with the degree of sensitisation and potency of the sensitiser. The capability to calculate sensitising potency based on the T cell response is a major advantage of the LLNA for chemical safety assessment.

Kimber identified three important characteristics of the T cell response in determining CHS, these are illustrated in Figure 55 (Kimber et al., 2012);

1) Magnitude

The magnitude of the T cell response is dependent on the kinetics, extent and duration of proliferation. Whether the threshold level of activation required for clinically relevant skin sensitisation is reached depends on the extent of the T cell response.

2) Quality

The quality of the T cell response can be described in terms of the balance between effector and regulatory sub-populations. It has been reported that

depletion of the regulatory T cell (Treg) population, characterised by the phenotype $CD4^+$, $CD25^+$, $Foxp3^+$, increased the sensitivity of T cell sensitiser priming assays (Vocanson et al., 2008). However, such manipulations may result in responses which are less reflective of what is expected *in vivo*.

3) Breadth

The breadth of the T cell proliferative response is defined by the level of polyclonal activation. This depends on the number of different T cell epitopes present. Highly reactive chemicals will inflict many peptide modifications, thus generating large numbers of potential T cell epitopes and increasing the chance of T cell activation (Esser et al., 2014).

This also depends on the antigen-specific TCR frequency, which is based on the size and diversity of the TCR pool. The cost of a broad TCR repertoire is having low numbers of cells specific for a given antigen.

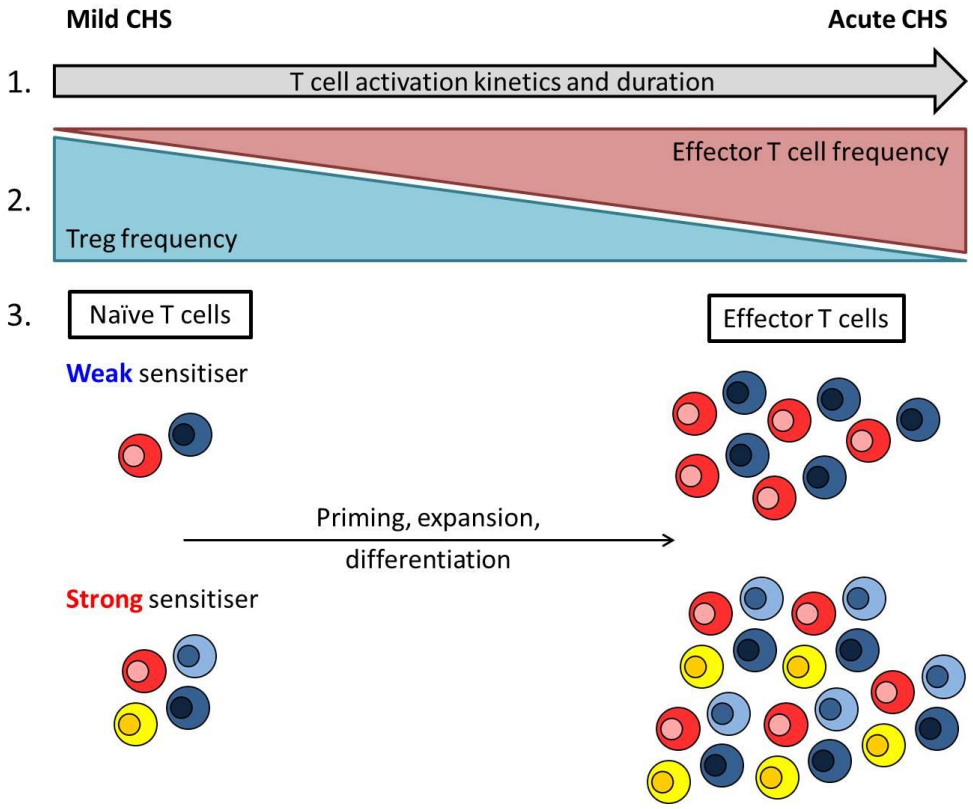

Figure 55. CHS severity is mediated by the extent of the T cell response.
1. Magnitude, determined by duration and kinetics of T cell activation. 2. Quality, depends on the balance of regulatory and effector T cells. 3. Breadth, defined by TCR frequency and level of polyclonal activation. Modified from Esser et al. (2014).

Due to the complexity of the factors that determine T cell responses to sensitisers, the development of *in vitro* assays which measure this aspect of CHS is a challenging task. Various protocols have been developed and tested to assess the T cell response to sensitisers. The most recent assays are composed of co-cultures of purified naïve T cells (i.e. depleted of Tregs) and autologous moDCs. Readouts commonly include T cell proliferation and cytokine detection, either secreted or intracellular, such as IFN-γ (Martin et al., 2010).

Enhancing the Biological Relevance of Immune Sensitisation *In Vitro*

The ECM plays an important role in the modulation of immunological events *in vivo*, from innate inflammatory responses in peripheral tissues (e.g. the skin), to the acquisition of specific immunity in lymphoid tissues (e.g. LNs).

In the context of CHS, sensitiser-induced danger signals derived from the ECM in the epidermis contribute to the activation of DCs (Esser et al., 2012). Since this is crucial for efficient T cell activation, sensitiser-induced DC activation in the context of a relevant ECM may be advantageous for the success of priming naïve T cells *in vitro*.

With regards to T cell-DC interactions, the ECM is known to have important modulatory effects on the outcome of the T cell response in terms of DC antigen presenting capability and cell motility (Garcia-Nieto et al., 2010, Gunzer et al., 2000). This has been described in more detail in Chapters 2 and 4 of this thesis.

Biomaterials are used in tissue engineering to mimic the architectural and biological features of the ECM. There is a wide range of biomaterials available for cell culture applications. The suitability of biomaterials for immune cell culture was characterised and described in detail in Chapter 2 of this thesis.

ECM components are not a common feature of current *in vitro* assays. However, the incorporation of biomaterials could be considered an effective solution to address concerns surrounding the lack of biological relevance of

current immune cell assays for the identification of sensitisers, as highlighted in Chapter 4 of this thesis.

Chapter aims

This chapter brings together the work described so far in this thesis regarding the application of a collagen hydrogel ECM platform for immune cell studies, with the investigation of immune responses to sensitisers. The aim of the work descrived in this chapter was to study the effect of the ECM on immune responses to chemical sensitiser. Using the ECM platform, dendritic cell maturation and T cell activation in response to sensitising chemicals was compared with a conventional cell culture method.

5.2. Materials and Methods

Generation of monocyte-derived dendritic cells

This was done according to the method described in Chapter 2 of this thesis, 2.4. Materials and Methods: *Generation of Monocyte-Derived Dendritic Cells*.

Isolation of T Cells

This was done according to the method described in Chapter 4 of this thesis, 4.4 Materials and Methods: *Isolation of T Cells*.

Preparation of Collagen Hydrogels

The collagen hydrogel was prepared according to the method described in Chapter 2 of this thesis, 2.4. Materials and Methods: *Preparation of Collagen Hydrogels*. The collagen solution was retained on ice until required.

Preparation of Chemical Reagents

All chemicals were purchased from Sigma. Fresh chemical solutions were prepared for each experiment. 50mM stock solutions of DNCB and eugenol were prepared in DMSO. 50mM stocks of SLS were prepared in tissue culture grade water. Further dilutions to achieve concentrations 4X the final test concentration required were carried out in complete RPMI-1640 media.

Pulsing Dendritic Cells with Chemicals

Chemicals were directly applied to monocyte-derived dendritic cells and incubated under standard tissue culture conditions for 24 hours. Cells were then harvested for cell viability and phenotypic analysis, and co-culture experiments.

Co-Culture of Chemical-Pulsed Dendritic Cells with T Cells

This was done according to the method described in Chapter 4 of this thesis, 4.4 Materials and Methods: *Autologous Mixed Lymphocyte Reaction*.

Dendritic Cell Phenotypic Analysis

This was done according to the method described in Chapter 2 of this thesis, 2.4. Materials and Methods: *Dendritic Cell Phenotypic Analysis*.

IFN-γ Detection

Enzyme-linked immunosorbant assays (ELISAs) were used to detect IFN-γ in the supernatants collected from AMLRs. The IFN-γ Duo-set ELISA kit (purchased from R&D systems) was used according to manufacturer's instructions.

LDH cytotoxicity assay

The LDH-Cytotoxicity Assay Kit II (Abnova #KA0786) was carried out according to manufacturer's instructions. Absorbance was measured using the Fluorostar Optima Plate reader, 440nm to 490 nm filter.

This assay is based on the principle that lactate is oxidised by LDH generating NADH. This reacts with a water-soluble tetrazolium salt, causing a colorimetric change. The intensity of the colour can be quantified by a spectrophotometer, or plate reader at OD450nm. The absorbance measurement correlates with the amount of LDH released.

Statistical Analysis

Analysis was carried out using GraphPad Prism version 6.00 for Windows, GraphPad Software, La Jolla California USA (www.graphpad.com).

5.3. Results and Discussion

Dendritic Cell Exposure to Sensitising Chemicals

Sensitiser cytotoxicity

Sensitiser cytotoxicity was determined in order to establish which concentrations to use for moDC exposure. The sensitisers DNCB and eugenol, and the non-sensitising irritant, sodium lauryl sulphate (SLS), were each tested at 4 different concentrations. Cell death was measured after 24 hours of exposure to these reagents using the lactate dehydrogenase (LDH) cytotoxicity assay.

LDH is a cytosolic enzyme, dying cells release LDH into the supernatant as a result of the disruption to their plasma membrane. The LDH cytotoxicity assay is based on the principle that the LDH activity measured in the supernatant correlates with the level of cell death.

It was important to consider that SLS inhibits LDH activity over concentrations of 1mM (Zheng et al., 2002). In this work, the concentration range of SLS did not exceed 0.5mM so that the activity of the LDH cytotoxicity assay was not affected.

In Figure 56, graphs A, B and C show the percentage of cell death measured in moDC cultures following exposure to DNCB, eugenol and SLS respectively.

5µM of DNCB was not found to have significant cytotoxic effects on moDCs (8.9%) compared to untreated cells (1.65%). When cells were exposed to

12.5μM, 25μM and 50μM, the mean cytotoxicity increased to 34.6%, 55.6% and 82.7% respectively. At concentrations of 12.5μM and above, cell death was found to be significantly higher ($P \leq 0.0001$, ****).

The lower concentrations of eugenol, 180μM and 500μM, did not cause significant cytotoxicity, with an average of 6.2% and 15.8% cell death measured for each concentration. Higher concentrations, 1000μM and 1800μM, resulted in increased cell death, with 49.6% and 48.8% measured for each. The increase in cell death at the top concentrations was found to be significant ($P \leq 0.0001$, ****).

The vehicle control in graphs A and B represents 1% DMSO. This was the solvent used in the preparation of DNCB and eugenol and was not found to have a cytotoxic effect on moDCs (2.1%).

SLS applied to moDCs at 7μM and 70μM did not cause significant levels of cytotoxicity, with an average of 0.4% and 4.7% cell death in the respective cultures. At higher concentrations of SLS, 250μM and 500μM, 51.2% and 70.6% cell death was measured for each. These levels of cytotoxicity were found to be highly significant ($P \leq 0.0001$, ****).

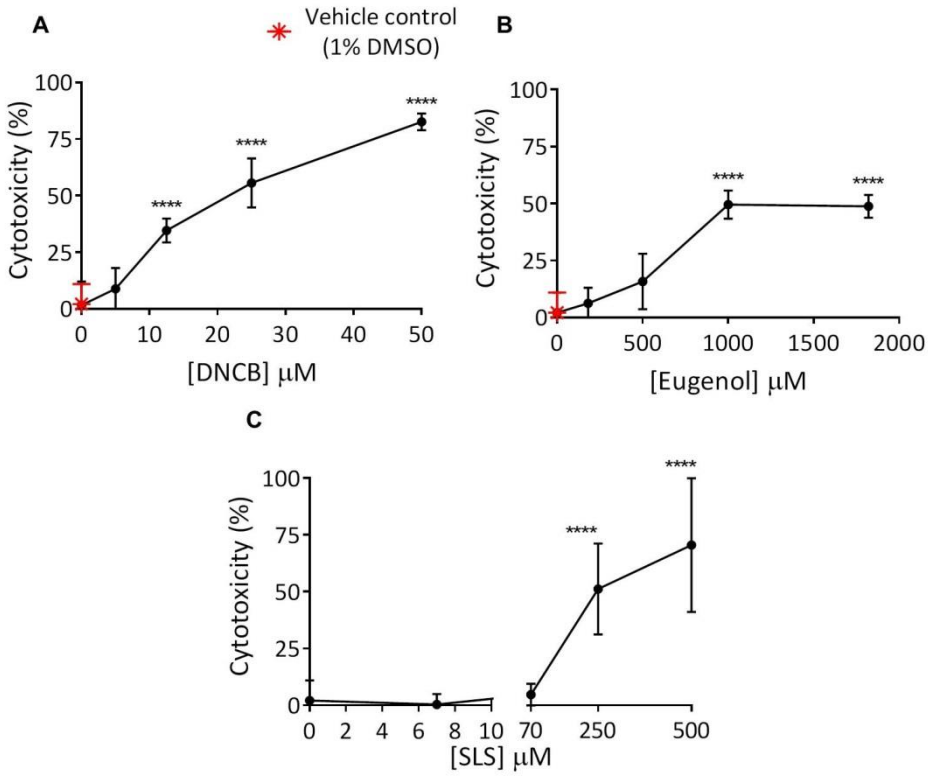

Figure 56. Sensitiser cytotoxicity.
Cell death after 24 hours of exposure to DNCB, eugenol or SLS determined by the LDH cytotoxicity assay. A. DNCB caused significant cytotoxicity at concentrations over 12.5μM ($P \leq 0.0001$, ****). B. There was significant cytotoxicity when eugenol was applied at a concentration of 1mM or higher ($P \leq 0.0001$, ****). C. SLS had significant cytotoxic effects at concentrations of 250μM and above ($P \leq 0.0001$, ****). 1 way ANOVA used to determine statistical significance. Not significant if $P \geq 0.05$ ($n \geq 3$). Error bars represent standard deviation.

The chemical concentrations tested and cytotoxicity data generated from these experiments are summarised in Table 3. This work was used as a basis for the further investigation into immune responses to chemical sensitising agents. A certain level of cytotoxicity can act as an adjuvant, which is a requirement of efficient immune activation. The level of acceptable cytotoxicity in DC sensitiser assays varies between reports but it is usually around 10-20% (Hulette et al., 2005).

Table 3. Summary of sensitiser cytotoxicity.
Summary of the concentration range of chemicals tested and the respective level of cytotoxicity induced, with equivalent wt/vol. *Significant level of cytotoxicity.

DNCB		
µM	µg/mL	Mean Cytotoxicity (%)
5.00	1	8.9
12.50	2.5	*34.6
25.00	5	*55.6
50.00	10	*82.6
Eugenol		
µM	µg/mL	Mean Cytotoxicity (%)
180	30	6.2
500	82	15.8
1000	160	*49.6
1800	300	*48.8
SLS		
µM	µg/mL	Mean Cytotoxicity (%)
7	2	0.4
70	20	4.7
250	72	*51.2
500	144	*70.6

Sensitiser induced moDC phenotypic maturation

The phenotypic response of moDCs to sensitisers was established in conventional TCP culture. This was done based on the expression of the DC maturation markers CD86 and CD54. The increase in the expression of these markers is routinely used for the prediction of sensitisers in the well-established human cell line activation test (hCLAT), which uses the DC-like cell line, THP-1, and also in primary moDC assays.

In these experiments, moDCs were exposed to the strong sensitiser, DNCB, the weak sensitiser, eugenol, and the non-sensitiser, SLS, for 24 hours. Cells were harvested and immunofluorescently labelled for CD54 and CD86, then analysed by flow cytometry.

The results from the analysis of moDC phenotypes following DNCB exposure are shown in Figure 57A, the data is presented as median fluorescent intensity (MFI) for each of the 5 donors tested. Figure 57B shows dot plots generated from flow cytometric analysis of the expression profiles of CD86 and CD54 following DNCB treatment for Donor 1.

Donors 1, 2 and 5, demonstrated an increase in CD86 expression in response to 25μM DNCB. No increase in CD54 was seen for any of the donors in response to DNCB. However, CD54 was found to decrease at concentrations of 25μM, and above, for Donors 1, 2 and 3.

Up-regulation of both CD86 and CD54 to the strong sensitiser DNCB has been reported to be reproducible in DC cell lines and primary DC assays (Nukada et al., 2012, Tuschl et al., 2000). Therefore it was surprising that the expression of CD54 did not positively correlate with CD86 in these experiments.

The absence of response to DNCB observed for Donors 3 and 4 may be due to natural variation. This reflects the lack of sensitivity associated with primary DC assays, a limitation which has also been highlighted by others (Furio et al., 2008).

Notably, sensitiser cytotoxicity has been shown to determine the up-regulation of CD86. Levels of cell death of 10% and above have been shown to induce CD86 (Hulette et al., 2005). In these experiments, the level of cell death in moDC cultures exposed to 10μM DNCB may not have been sufficient to induce the up-regulation of CD86.

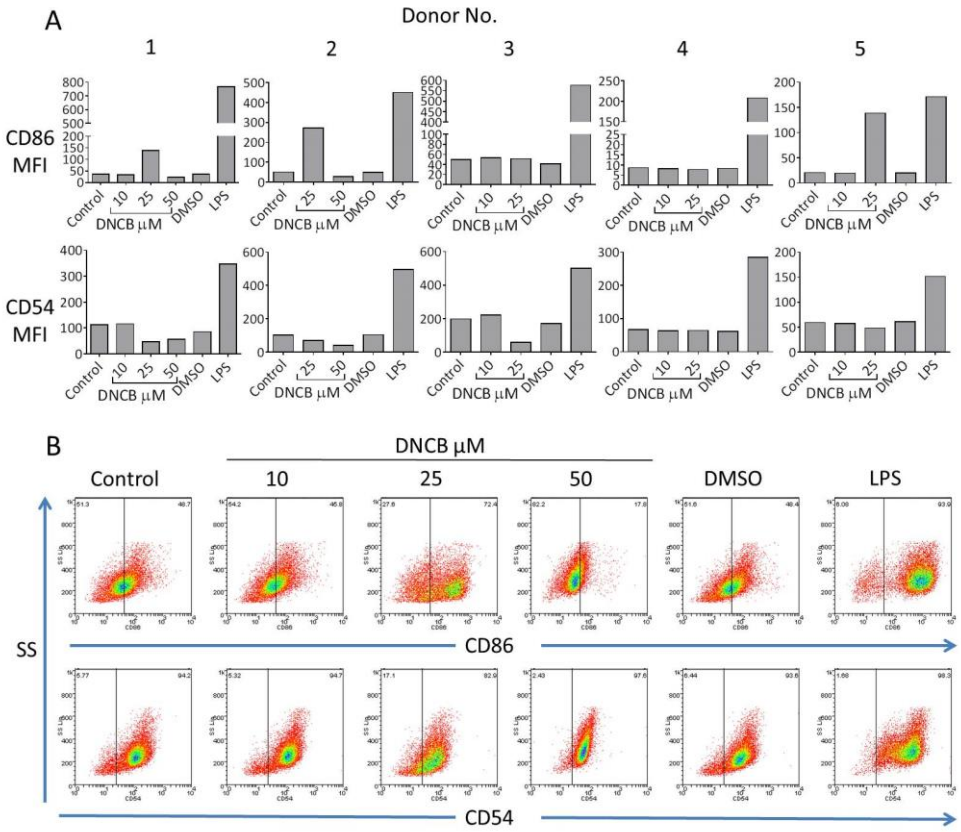

Figure 57. Phenotypic analysis of moDCs treated with DNCB.
A. Median fluorescence intensity of CD86 and CD54 for Donors 1 – 5. Expression of CD86 was seen to be increased in response to 25µM DNCB for Donors 1, 2 and 5. No increase in CD54 was seen in response to DNCB and it decreased for Donors 1, 2 and 3 at concentrations of 25µM and above. B. Dot plots to show the expression profile of CD86 and CD54 for moDCs treated with DNCB from Donor 1.

The analysis of moDCs from 4 individuals exposed to the weakly sensitising agent, eugenol, is shown in Figure 58A. With 250µM eugenol, there was a slight increase in the expression of CD86 for Donors 1 and 4. Donors 2 and 3 did not appear responsive to eugenol. For all of the donors, there was no change in CD54 expression as a result of eugenol exposure. Figure 58B shows the expression profiles of CD86 and CD54 for Donor 4 following treatment of moDCs with eugenol.

Eugenol is weakly sensitising and requires enzymatic conversion to become reactive (Karlberg et al., 2008). It is reasonable not to expect profound effects for eugenol *in vitro* due to the absence of mechanisms for its activation.

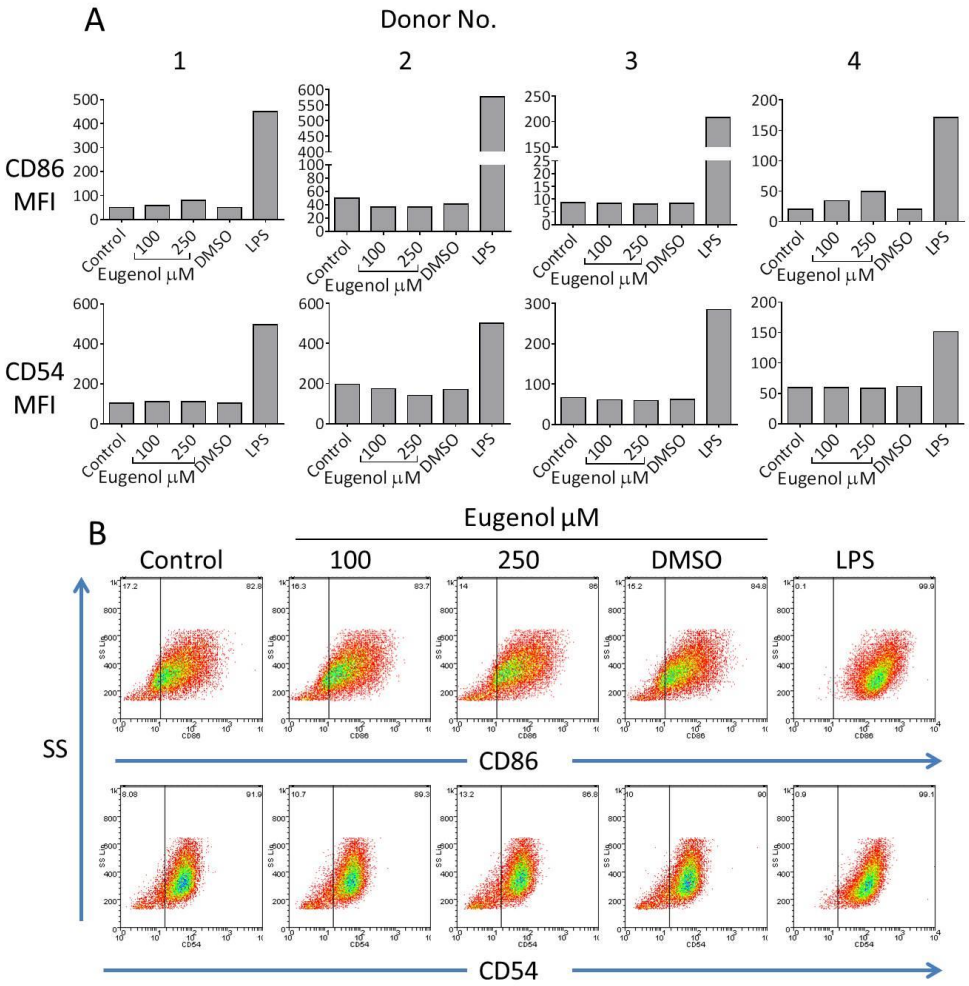

Figure 58. moDC phenotypic analysis following exposure to eugenol.
A. 250µM eugenol induced slight increase in CD86 expression in Donors 1 and 4. No response was observed for Donors 2 and 3. Expression of CD54 was not affected by eugenol for any of the donors tested. B. Dot plots from phenotypic analysis of moDCs from Donor 4 following eugenol treatment.

The analysis of moDCs from 4 donors after treatment with the non-sensitiser, SLS, is shown in Figure 59. The graphs in A show that the expression of CD86 and CD54 was not affected by exposure to SLS. The dot plots in B show the expression profile of CD86 and CD54 by moDCs for Donor 2.

It was reassuring that SLS did not affect the expression of CD86 or CD54 as it is not a sensitiser and is often used as a negative control for *in vitro* and *in vivo* sensitisation studies.

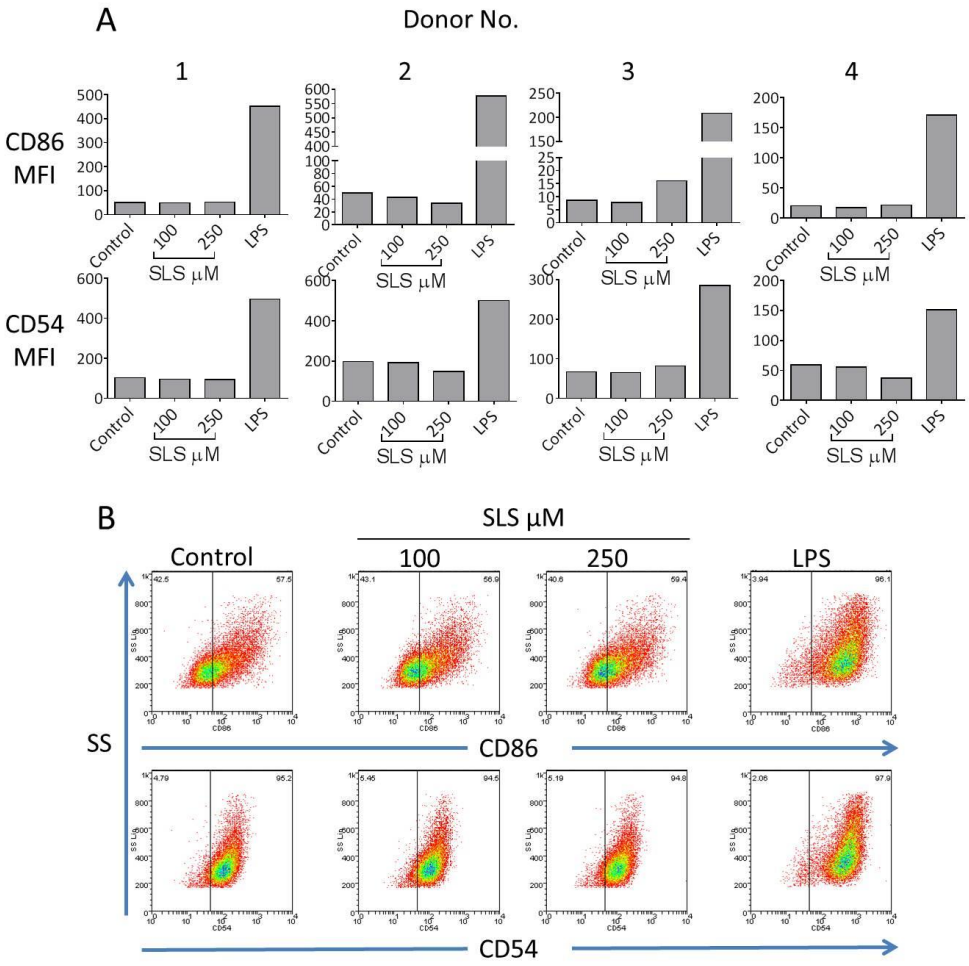

Figure 59. Phenotypic analysis of SLS-treated moDCs.
A. SLS did not affect expression of CD86 or CD54 for any of the 4 donors tested. B. Dot plots from the analysis of CD86 and CD54 expression for Donor 2 after treatment with SLS.

Dendritic Cell Responses to Sensitisers on the ECM Platform

Sensitiser-induced moDC maturation in the context of collagen hydrogels

In-keeping with the theme of this thesis, moDC exposure to sensitisers was performed in the context of collagen hydrogels and compared with responses from TCP cultures.

Figure 60 shows the phenotypic analysis from these experiments of one of the donors. These results were representative of those obtained from 3 individuals tested under the same conditions. In the analysis, the phenotypic response to DNCB, eugenol and SLS in collagen hydrogel cultures was compared to that in TCP.

There was a reproducible increase in CD86 expression in response to 25µM DNCB. The intensity of the increase in CD86 expression was lower on collagen hydrogels, compared to TCP. DNCB did not cause any change in CD54 expression in collagen cultures.

Concentrations of 250µM eugenol induced a slight increase in CD86 expression in collagen cultures. The magnitude of the response was lower in collagen hydrogel cultures than TCP. No response to eugenol was seen based on CD54 expression.

Finally, as expected, the non-sensitiser control, SLS, did not have an effect on CD86 or CD54 expression in collagen cultures.

Compared to TCP, the collagen hydrogel impaired the intensity of the phenotypic response to sensitisers. This was surprising since 'danger' signals derived from other ECM components, such as hyaluronic acid, have been linked with the induction of innate immunity in sensitisation (Esser et al., 2012). It was anticipated that collagen fragments, generated as a result of oxidation by sensitiser-dependent ROS, may have enhanced moDC maturation (Esser et al., 2012, Chen and Nuñez, 2010, Monboisse and Borel, 1992, Hawkins and Davies, 1997).

Certain collagen peptides have been shown to activate innate immunity (Thomas et al., 2007). However, in the same study, different collagen fragments were demonstrated to have anti-inflammatory functions. This suggests collagen peptides may have complex immune-modulatory properties.

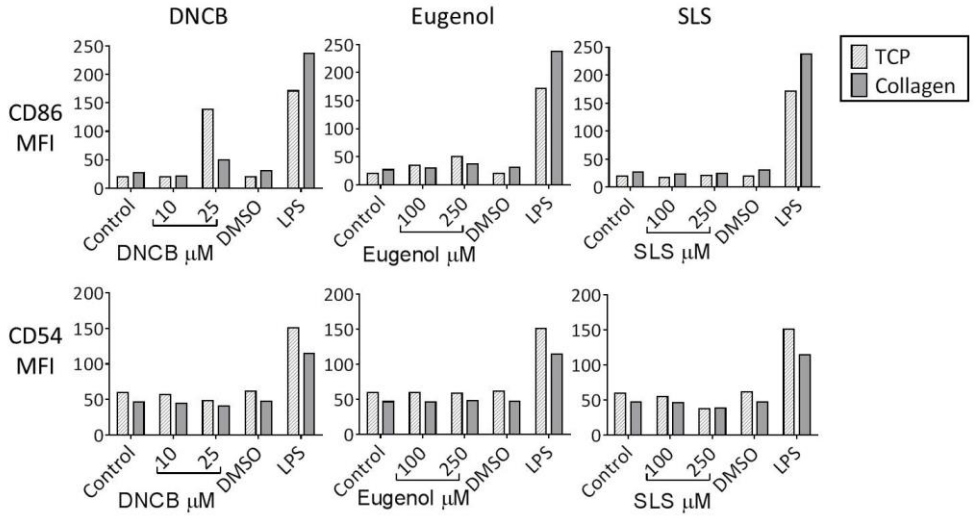

Figure 60. moDC phenotypic responses to sensitisers in collagen hydrogel and TCP cultures.
DNCB. 25μM caused up-regulation of CD86, the magnitude of response was decreased in the presence of collagen. There was no change in CD54 expression. Eugenol. 250μM induced increased CD86 expression, levels of CD86 expression in collagen cultures were lower. CD54 expression remained unchanged. SLS. No effect on CD86 or CD54 expression in TCP and collagen cultures. Data shown from one donor but represents analysis of 3 donors.

Sensitiser-Specific T Cell Activation on the ECM Platform

Activation of T cells by DNCB-pulsed moDCs

To investigate the functional implications of pulsing moDCs with the strong sensitiser, DNCB, their ability to elicit a T cell response was investigated. In keeping with the topic of this chapter, T cell responses to DNCB-treated moDCs were investigated in both in TCP and collagen hydrogel cultures.

Co-culture assays were performed with autologous T cells under similar experimental conditions to those described in Chapter 4 of this thesis and T cell activation was measured by IFN-γ production. moDCs were pulsed with 10μM of the strong sensitiser, DNCB, prior to co-culture with T cells. This concentration was chosen since the level of cytotoxicity caused by higher concentrations resulted in poor cell retrieval.

These experiments were performed with 3 donors, the results for each individual are presented in Figure 61. Out of the three donors, one (Donor 2) mounted a T cell response to DNCB-treated moDCs. For this donor, there was increased production of IFN-γ in TCP cultures with DNCB-pulsed moDCs (1875.6pg/mL), compared to 88.34pg/mL detected in the untreated conditions. For the other two donors (Donors 1 and 3), levels of IFN-γ production were low with no specific effect of sensitiser treatment. On the collagen hydrogel platform, a DNCB-specific T cell response was also detected for Donor 2 based on the raised levels of IFN-γ (1443.04pg/mL). Sensitiser-specific responses were not found for Donors 1 and 3 on collagen hydrogels.

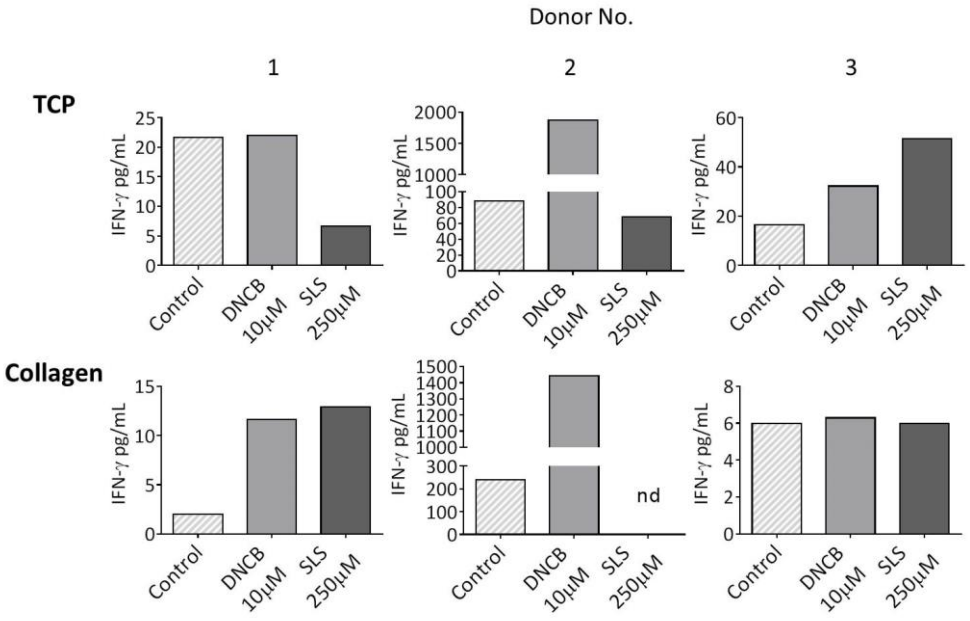

Figure 61. T cell activation by DNCB-modified moDCs.
One out of three donors responded to DNCB. TCP. Donor 2 mounted a T cell response towards DNCB-pulsed moDCs due to the increased levels of IFN-γ detected in these cultures. Collagen. DNCB-specific T cell activation was also observed for Donor2 as IFN-γ production was increased in this condition. T cell activation was not detected for Donors 1 or 3 in either TCP or collagen hydrogel cultures. (nd = not detected).

The possible reasons for the low frequency of T cell responses to DNCB-modified moDCs observed in this investigation are numerous. First, the phenotypic analysis of moDCs pulsed with 10μM DNCB had previously revealed that they did not have increased expression of CD86 or CD54, therefore, they probably would not have had the capacity to activate T cells efficiently.

The presence of memory T cell populations may have influenced T cell activation in this assay. This depends on the individual's prior exposure to sensitiser. The occurrence of exposure to DNCB is expected to be low in the general population. Therefore DNCB-specific memory T cells are expected to be very rare.

Third, the balance of effector and regulatory T cells has important implications in terms of the outcome of T cell responses. Since regulatory T cell populations were not depleted in these assays, they may have contributed to the suppression of T cell activation in response to DNCB-modified moDCs.

Finally, antigen-specific TCR frequency is another factor for consideration. T cells isolated from blood samples only represent a fraction of the total *in vivo* population. This limits the number of TCRs available and therefore the probability of T cell activation, compared to whole-organism studies.

5.4. Conclusions and Further Work

This chapter has described the investigation of moDC maturation and T cell activation in response to chemical sensitisers in the context of a collagen hydrogel platform. To the best of our knowledge, this is the first time such assays have been conducted in the presence of ECM.

Sensitiser-induced moDC maturation on the ECM platform

On the ECM platform, moDC maturation in response to sensitisers was evident based on the increased expression of CD86. The trend in moDC maturation by sensitisers was similar in the presence of collagen hydrogel compared with TCP. However, in collagen hydrogel cultures, the magnitude of the phenotypic response to sensitisers was dampened.

It was postulated that collagen may enhance the immunogenic effects of sensitisers, since DAMPs (derived from the ECM) have been found to have a role in the activation of innate immunity during sensitisation (Esser et al., 2012). This is due to the oxidative effects of the sensitisers on the ECM, which results in degradation and release of ECM fragments.

With regards to collagen fragmentation, certain collagen peptides have also been shown to have anti-inflammatory properties on the innate immune system, which could have contributed to the dampened phenotypic response (Thomas et al., 2007). However, since the release of collagen peptides was not quantified here, the implications of this are difficult to assess.

Analysis of two cell-surface markers was not likely to be sufficient to capture the biological and functional effects of the collagen hydrogel on moDCs in the context of sensitiser exposure. Increasing the range of readouts would give a more detailed insight into moDC responses to sensitisers and the role of the ECM. Alternative measures, such as analysis of different phenotypic markers, such as programmed death-ligand 1 (PD-1), DC immunoreceptor and neutrophil-activating protein-2 (DCIR) (Hitzler et al., 2013); cytokine production, including IL-1β, IL-6 and IL-8; or functional assays, such as endocytosis, could be investigated to this end (dos Santos et al., 2009).

Sensitiser-specific T cell activation on the ECM platform

DNCB-specific T cell activation was elicited by one out of 3 individuals tested. T cell activation is dependent on co-stimulation by DCs, duration of activation, the balance between effector and regulatory T cells, peptide immunogenicity and the frequency of antigen-specific receptors. The impacts of these factors on the outcome of these experiments are considered as follows.

The concentration of DNCB used to pulse moDCs prior to T cell co-culture was not found to induce a mature phenotype. Facilitating the increase in co-stimulatory molecule expression by sensitiser-exposed moDCS could potentially enhance their ability activate T cells. This may be achieved by using higher concentrations of the sensitising agent.

In vivo, T cell priming by chemical sensitisers lasts 10 – 15 days in humans (Vocanson et al., 2009). However, little is known about the kinetics of sensitiser-induced T cell activation *in vitro*. Therefore, the day 6 end point of

this assay may not be optimal for the detection of T cell priming by sensitisers. Further investigation into this aspect of T cell activation would help establish the most appropriate time point at which to monitor the T cell response to sensitisers.

Modifications to the experimental method could be implemented to improve the detection of sensitiser-specific T cell priming. For example, adding a recall response following the initial priming phase would allow for the expansion of sensitiser-specific T cells and re-stimulation would elicit a stronger, specific T cell response.

By directly applying chemicals to cell cultures there was no control over the formation of haptenated peptides (Martin et al., 2010). Other application methods, such as prior formation using a dedicated carrier, such as human serum albumin, could be used to give more control over sensitiser-peptide modification.

This work has outlined the first attempt made at studying immune responses to sensitisers on an ECM platform. The results were encouraging since both innate and adaptive immune responses were mounted in response to sensitisers on the collagen hydrogel.

Overall, it was difficult to quantify the effect of the collagen hydrogel on sensitiser-induced moDC maturation and T cell activation due to suboptimal responses to sensitisers and the high levels of biological variation.

The outcomes of this work reflect the complexity of the molecular and cellular mechanisms involved in the induction of sensitisation. This highlights the complications faced in the development of alternative methods for identifying chemical sensitisers.

Chapter 6

Conclusions

6.1. Summary

This thesis has shown how tissue engineering technologies can be used to develop biomimetic platforms for *in vitro* immunological studies. This was achieved by the development of ECM and flow platforms in order to simulate the extra-cellular microenvironment to which cells are exposed in natural tissues.

Conclusions from studies on the ECM platform

Characterisation of biomaterials to provide a biologically relevant substrate for immune cell culture was important in order to overcome the limitations of conventional methods, which are mostly carried out the absence of ECM. Synthetic biomaterials, thermo-responsive particulate gel and electrospun scaffolds, and naturally-derived biomaterials, GelMA and collagen hydrogels, were tested in this work.

Collagen hydrogel was determined to be a suitable ECM platform for immune cell culture since it supported a high level of cell viability (>75%), did not directly induce inflammatory immune responses and supported the induction of appropriate innate and adaptive immune responses.

Collagen is ubiquitous in all tissues of the body (Parenteau-Bareil et al., 2010). There are several of types of collagen and it can form a variety of 3D matrices, such as sponges, lattices and hydrogels (Glowacki and Mizuno, 2008).

In the lymph node, networks of collagen fibres provide structural support and facilitate the attachment of stromal cells and DCs. It also has an important role in regulating cell adhesion and motility (Wolf et al., 2003). Collagen hydrogels have been used previously for immune cell culture, for example in a study of DC-T cell interactions in 3D reported by Gunzer et al (Gunzer et al., 2000).

In Chapter 4, antigen-specific immunity, elicited in response to the model antigen PPD, was investigated in the context of the collagen hydrogel ECM platform. Compared with conventional methods, which are conducted without ECM, the collagen hydrogel appeared to increase the sensitivity and specificity of antigen-specific immune responses.

Successful T cell activation requires the antigen-specific interaction between MHC-peptide and TCR, engagement of co-stimulatory molecules and inflammatory cytokines (Murphy et al., 2008). More recently, it has become clear that ECM components, namely laminin, fibronectin and collagen, also have important modulatory effects on T cell activation. This is reflected in a number of studies in the literature which reported that the ECM profoundly influenced the outcome of DC-T cell interactions (Gunzer et al., 2000, Garcia-Nieto et al., 2010, Dustin et al., 2001).

Gunzer et al. demonstrated that collagen promotes the motility of DCs and T cells and supports T cell activation. They showed that in suspension, i.e. without ECM, cells formed large clusters dependent on MCH-peptide interactions with TCR. In the presence of a collagen matrix, they found that cells formed smaller clusters while retaining the capability for efficient T cell activation (Gunzer et al., 2000). These observations were similar in terms of the cell distribution, organisation and immune response observed in the experiments described in this work.

The findings from this study and reports by others give rise to the possibility that a collagen ECM determines the threshold for T cell activation (Dustin and de Fougerolles, 2001). This may increase the sensitivity of antigen-specific T cell responses by preventing T cell activation as a result of sub-optimal APC-T cell interactions, according to the strength of the antigen-specific interaction or antigen-presenting efficiency of the DC.

In Chapter 5, an investigation of immune responses to the chemical sensitisers DNCB and eugenol was carried out in the context of the ECM platform. DC maturation following treatment with sensitisers was observed in the presence of the collagen hydrogel. Also, sensitiser-specific T cell activation was detected in conventional cultures and on the ECM platform.

Unlike PPD, no notable difference was found between immune responses to sensitisers on the ECM platform compared with conventional culture methods. This is probably due to the limited sample size, since there was a high level of variation and not all donors mounted a response towards the sensitisers tested.

It is also likely to be a reflection of the complexity of the mechanisms involved in the elicitation of immune responses by sensitisers.

Conclusions from work on the fluidic platform

Chapter 3 describes the development of a fluidic device with a paper-based scaffold for the incorporation of flow into cultures of immune cells. This was done in order to mimic interstitial flow, which cells experience *in vivo* but is not a feature of conventional *in vitro* methods.

The collagen hydrogel-coated paper, which provided the scaffold for cell culture on the fluidic platform, was found to induce moDC maturation based on the expression of cell surface markers. This was the first time this type of scaffold has been used for immunological studies. Hydrogel-coated paper-based scaffolds have recently been described for other cell culture applications, including the generation of an air-liquid interface and investigation of lung tumour cell interactions with fibroblasts (Rahim et al., 2015, Camci-Unal et al., 2016).

Under flow conditions, moDCs cultured on the fluidic platform exhibited high viability, maintained a less-mature phenotype (compared to static) and were responsive to immunological stimulation by LPS.

The fluidic device was implemented in Chapter 4 to study the effect of flow on antigen-specific T cell responses to PPD. Despite the apparent reduction in the intensity of the immune response under flow conditions based on the level of

IFN-γ detected, the sensitivity of antigen-specific T cell activation was higher compared with the static counterpart.

Based on the findings from this work and recent publications, it is clear that shear flow has crucial immune-modulatory effects (Previtera, 2014, Li et al., 2010, Swartz et al., 2008). Elucidation of the mechanisms by which flow regulates inflammatory responses is in the early stages. To date, cell surface receptors and intracellular proteins, particularly those associated with the cytoskeleton, have been implicated in the transduction of flow induced changes in gene expression in immune cells (Makino et al., 2005, Makino et al., 2007). It has been suggested that under homeostatic conditions, physiological stimuli such as flow suppress inflammatory responses. This may explain the less mature moDC phenotype observed on the fluidic platform under the flow conditions.

It is well-established that the maturation state of DCs is critical for the induction of T cell activation. moDCs cultured on the platform under static conditions exhibited a mature phenotype, which would have promoted non-specific T cell activation and exaggerated antigen-specific responses. The effect of flow on moDC maturation state may have increased the threshold for T cell activation, thereby causing antigen-specific T cell activation to be more sensitive under flow conditions.

Future Work

Future work will focus on the applications of ECM and fluidic platforms for the study of cellular immunology. This will include elucidating the mechanisms through which immune cells sense their extracellular environment and how this impacts their behaviour. A better understanding of how environmental factors modulate immune responses will be valuable for the advancement of immune-competent *in vitro* assays which are routinely used for research purposes in academia and industry.

It is anticipated that through enhancing the physiological relevance of *in vitro* cell culture, it will be possible to generate more realistic immune responses, thus improving the reliability of the prediction of immune responses. This will have numerous implications for, but not limited to, optimising strategies for vaccine delivery, identifying novel therapeutic targets for the treatment of cancer and autoimmune diseases, and increasing the efficacy of safety testing. Finally, the ability to produce representative immune responses without resorting to animal models will make a huge contribution to the reduction in the numbers of animals used for research and safety testing.

References

ABE, Y., SUDO, R., IKEDA, M. & TANISHITA, K. 2013. Steady and pulsatile shear stress induce different three-dimensional endothelial networks through pseudopodium formation. *Journal of Biorheology,* 27**,** 38-48.

ACKERMAN, A. L. & CRESSWELL, P. 2004. Cellular mechanisms governing cross-presentation of exogenous antigens. *Nat Immunol,* 5**,** 678-84.

AEBY, P., ASHIKAGA, T., BESSOU-TOUYA, S., SCHEPKY, A., GERBERICK, F., KERN, P., MARREC-FAIRLEY, M., MAXWELL, G., OVIGNE, J. M., SAKAGUCHI, H., REISINGER, K., TAILHARDAT, M., MARTINOZZI-TEISSIER, S. & WINKLER, P. 2010. Identifying and characterizing chemical skin sensitizers without animal testing: Colipa's research and method development program. *Toxicol In Vitro,* 24**,** 1465-73.

AGARWAL, S., WENDORFF, J. H. & GREINER, A. 2008. Use of electrospinning technique for biomedical applications. *Polymer,* 49**,** 5603-5621.

AKIBA, H., KEHREN, J., DUCLUZEAU, M.-T., KRASTEVA, M., HORAND, F., KAISERLIAN, D., KANEKO, F. & NICOLAS, J.-F. 2002. Skin Inflammation During Contact Hypersensitivity Is Mediated by Early Recruitment of CD8+ T Cytotoxic 1 Cells Inducing Keratinocyte Apoptosis. *The Journal of Immunology,* 168**,** 3079-3087.

AKIRA, S., UEMATSU, S. & TAKEUCHI, O. 2006. Pathogen Recognition and Innate Immunity. *Cell,* 124**,** 783-801.

AL GHANAMI, R. C., SAUNDERS, B. R., BOSQUILLON, C., SHAKESHEFF, K. M. & ALEXANDER, C. 2010. Responsive particulate dispersions for reversible building and deconstruction of 3D cell environments. *Soft Matter,* 6**,** 5037-5044.

ALBILLOS, A., HERA AD ADE, L., REYES, E., MONSERRAT, J., MUNOZ, L., NIETO, M., PRIETO, A., SANZ, E. & ALVAREZ-MON, M. 2004. Tumour necrosis factor-alpha expression by activated monocytes and altered T-cell homeostasis in ascitic alcoholic cirrhosis: amelioration with norfloxacin. *J Hepatol,* 40**,** 624-31.

ALBREKT, A.-S., JOHANSSON, H., BÖRJE, A., BORREBAECK, C. & LINDSTEDT, M. 2014. Skin sensitizers differentially regulate signaling pathways in MUTZ-3 cells in relation to their individual potency. *BMC Pharmacology & Toxicology,* 15**,** 5-5.

ANDERSON, J. M., RODRIGUEZ, A. & CHANG, D. T. 2008. Foreign body reaction to biomaterials. *Semin Immunol,* 20**,** 86-100.

ANDREAS, N., CAROLINE, B., LESLIE, F., FRANK, G., KIMBERLY, N., ALLISON, H., HEATHER, I., ROBERT, L., STEFAN, O., HENDRIK, R., ANDREAS, S. & ROGER, E. 2011. The intra- and inter-laboratory reproducibility and predictivity of the KeratinoSens assay to predict skin sensitizers in vitro: results of a ring-study in five laboratories. *Toxicol In Vitro,* 25**,** 733-44.

ANNUNZIATO, F., COSMI, L., LIOTTA, F., MAGGI, E. & ROMAGNANI, S. 2015a. Human T helper type 1 dichotomy: origin, phenotype and biological activities. *Immunology,* 144**,** 343-351.

ANNUNZIATO, F., ROMAGNANI, C. & ROMAGNANI, S. 2015b. The 3 major types of innate and adaptive cell-mediated effector immunity. *Journal of Allergy and Clinical Immunology,* 135**,** 626-635.

APTULA, A. O., ROBERTS, D. W. & PEASE, C. K. 2007. Haptens, prohaptens and prehaptens, or electrophiles and proelectrophiles. *Contact Dermatitis,* 56**,** 54-6.

ARAI, K. I., LEE, F., MIYAJIMA, A., MIYATAKE, S., ARAI, N. & YOKOTA, T. 1990. Cytokines: coordinators of immune and inflammatory responses. *Annu Rev Biochem,* 59**,** 783-836.

AUSTYN, J. M. 1996. New insights into the mobilization and phagocytic activity of dendritic cells. *The Journal of Experimental Medicine,* 183**,** 1287-1292.

BAJAJ, P., SCHWELLER, R. M., KHADEMHOSSEINI, A., WEST, J. L. & BASHIR, R. 2014. 3D Biofabrication Strategies for Tissue Engineering and Regenerative Medicine. *Annual review of biomedical engineering,* 16**,** 247-276.

BALCELLS, M., SUÁREZ, M. F., VÁZQUEZ, M. & EDELMAN, E. R. 2005. Cells in fluidic environments are sensitive to flow frequency. *Journal of Cellular Physiology,* 204**,** 329-335.

BANCHEREAU, J., BRIERE, F., CAUX, C., DAVOUST, J., LEBECQUE, S., LIU, Y.-J., PULENDRAN, B. & PALUCKA, K. 2000.

Immunobiology of Dendritic Cells. *Annual Review of Immunology,* 18**,** 767-811.

BAYRAK, A., PRÜGER, P., STOCK, U. A. & SEIFERT, M. 2013. Absence of Immune Responses with Xenogeneic Collagen and Elastin. *Tissue Engineering. Part A,* 19**,** 1592-1600.

BEG, A. A. 2002. Endogenous ligands of Toll-like receptors: implications for regulating inflammatory and immune responses. *Trends in Immunology,* 23**,** 509-512.

BENTON, J. A., DEFOREST, C. A., VIVEKANANDAN, V. & ANSETH, K. S. 2009. Photocrosslinking of gelatin macromers to synthesize porous hydrogels that promote valvular interstitial cell function. *Tissue Eng Part A,* 15**,** 3221-30.

BERTASSONI, L. E., CECCONI, M., MANOHARAN, V., NIKKHAH, M., HJORTNAES, J., CRISTINO, A. L., BARABASCHI, G., DEMARCHI, D., DOKMECI, M. R., YANG, Y. & KHADEMHOSSEINI, A. 2014. Hydrogel bioprinted microchannel networks for vascularization of tissue engineering constructs. *Lab Chip,* 14**,** 2202-11.

BHANDOOLA, A. & SAMBANDAM, A. 2006. From stem cell to T cell: one route or many? *Nat Rev Immunol,* 6**,** 117-26.

BONNEVILLE, M., CHAVAGNAC, C., VOCANSON, M., ROZIERES, A., BENETIERE, J., PERNET, I., DENIS, A., NICOLAS, J. F. & HENNINO, A. 2007. Skin contact irritation conditions the development and severity of allergic contact dermatitis. *J Invest Dermatol,* 127**,** 1430-5.

BOS, J. D. & MEINARDI, M. M. H. M. 2000. The 500 Dalton rule for the skin penetration of chemical compounds and drugs. *Experimental Dermatology,* 9**,** 165-169.

BOTHAM, P. A., BASKETTER, D. A., MAURER, T., MUELLER, D., POTOKAR, M. & BONTINCK, W. J. 1991. Skin sensitization--a critical review of predictive test methods in animals and man. *Food Chem Toxicol,* 29**,** 275-86.

BREEN, E. C., MCDONALD, M., FAN, J., BOSCARDIN, J. & FAHEY, J. L. 2000. Cytokine gene expression occurs more rapidly in stimulated peripheral blood mononuclear cells from human immunodeficiency virus-infected persons. *Clin Diagn Lab Immunol,* 7**,** 769-73.

BRUSASCA, P. N., COLANGELI, R., LYASHCHENKO, K. P., ZHAO, X., VOGELSTEIN, M., SPENCER, J. S., MCMURRAY, D. N. & GENNARO, M. L. 2001. Immunological Characterization of Antigens Encoded by the RD1 Region of the

Mycobacterium tuberculosis Genome. *Scandinavian Journal of Immunology,* 54**,** 448-452.

CAMCI-UNAL, G., NEWSOME, D., EUSTACE, B. K. & WHITESIDES, G. M. 2016. Fibroblasts Enhance Migration of Human Lung Cancer Cells in a Paper-Based Coculture System. *Adv Healthc Mater,* 5**,** 641-7.

CAO, Y. P., MA, P. C., LIU, W. D., ZHOU, W. Q., TAO, Y., ZHANG, M. L., LI, L. J. & CHEN, Z. Y. 2012. Evaluation of the skin sensitization potential of chemicals in THP-1/keratinocyte co-cultures. *Immunopharmacol Immunotoxicol,* 34**,** 196-204.

CAUX, C., LIU, Y.-J. & BANCHEREAU, J. 1995. Recent advances in the study of dendritic cells and follicular dendritic cells. *Immunology Today,* 16**,** 2-4.

CELLA, M., ENGERING, A., PINET, V., PIETERS, J. & LANZAVECCHIA, A. 1997a. Inflammatory stimuli induce accumulation of MHC class II complexes on dendritic cells. *Nature,* 388**,** 782-787.

CELLA, M., SALLUSTO, F. & LANZAVECCHIA, A. 1997b. Origin, maturation and antigen presenting function of dendritic cells. *Current opinion in immunology,* 9**,** 10-16.

CHAN, B. P. & LEONG, K. W. 2008. Scaffolding in tissue engineering: general approaches and tissue-specific considerations. *European Spine Journal,* 17**,** 467-479.

CHANG, D. T., JONES, J. A., MEYERSON, H., COLTON, E., KWON, I. K., MATSUDA, T. & ANDERSON, J. M. 2008. Lymphocyte/macrophage interactions: biomaterial surface-dependent cytokine, chemokine, and matrix protein production. *J Biomed Mater Res A,* 87**,** 676-87.

CHANG, R., EMAMI, K., WU, H. & SUN, W. 2010. Biofabrication of a three-dimensional liver micro-organ as an in vitro drug metabolism model. *Biofabrication,* 2**,** 045004.

CHAU, D. Y., JOHNSON, C., MACNEIL, S., HAYCOCK, J. W. & GHAEMMAGHAMI, A. M. 2013. The development of a 3D immunocompetent model of human skin. *Biofabrication,* 5**,** 035011.

CHEN, G. Y. & NUÑEZ, G. 2010. Sterile inflammation: sensing and reacting to damage. *Nature reviews. Immunology,* 10**,** 826-837.

CHEN, M. B., SRIGUNAPALAN, S., WHEELER, A. R. & SIMMONS, C. A. 2013. A 3D microfluidic platform incorporating methacrylated gelatin hydrogels to study physiological

cardiovascular cell-cell interactions. *Lab Chip,* 13**,** 2591-2598.

CHEN, Y.-C., LIN, R.-Z., QI, H., YANG, Y., BAE, H., MELERO-MARTIN, J. M. & KHADEMHOSSEINI, A. 2012. Functional Human Vascular Network Generated in Photocrosslinkable Gelatin Methacrylate Hydrogels. *Adv Funct Mater,* 22**,** 2027-2039.

CHO, Y. S., DOBOS, K. M., PRENNI, J., YANG, H., HESS, A., ROSENKRANDS, I., ANDERSEN, P., RYOO, S. W., BAI, G. H., BRENNAN, M. J., IZZO, A., BIELEFELDT-OHMANN, H. & BELISLE, J. T. 2012. Deciphering the proteome of the in vivo diagnostic reagent "purified protein derivative" from Mycobacterium tuberculosis. *Proteomics,* 12**,** 979-91.

CHOI, Y. Y., CHUNG, B. G., LEE, D. H., KHADEMHOSSEINI, A., KIM, J. H. & LEE, S. H. 2010. Controlled-size embryoid body formation in concave microwell arrays. *Biomaterials,* 31**,** 4296-303.

CIMETTA, E., CANNIZZARO, C., JAMES, R., BIECHELE, T., MOON, R. T., ELVASSORE, N. & VUNJAK-NOVAKOVIC, G. 2010. Microfluidic device generating stable concentration gradients for long term cell culture: application to Wnt3a regulation of [small beta]-catenin signaling. *Lab on a Chip,* 10**,** 3277-3283.

COMERFORD, I., HARATA-LEE, Y., BUNTING, M. D., GREGOR, C., KARA, E. E. & MCCOLL, S. R. 2013. A myriad of functions and complex regulation of the CCR7/CCL19/CCL21 chemokine axis in the adaptive immune system. *Cytokine & Growth Factor Reviews,* 24**,** 269-283.

CORSINI, E., GALBIATI, V., MITJANS, M., GALLI, C. L. & MARINOVICH, M. 2013. NCTC 2544 and IL-18 production: A tool for the identification of contact allergens. *Toxicology in Vitro,* 27**,** 1127-1134.

CORSINI, E., MITJANS, M., GALBIATI, V., LUCCHI, L., GALLI, C. L. & MARINOVICH, M. 2009. Use of IL-18 production in a human keratinocyte cell line to discriminate contact sensitizers from irritants and low molecular weight respiratory allergens. *Toxicol In Vitro,* 23**,** 789-96.

COSSON, S., OTTE, E. A., HEZAVEH, H. & COOPER-WHITE, J. J. 2015. Concise review: tailoring bioengineered scaffolds for stem cell applications in tissue engineering and regenerative medicine. *Stem Cells Transl Med,* 4**,** 156-64.

COTTREZ, F. 2011. Development of Sens-IS – an EpiSkin based model for measuring chemical sensitisers potency. *In: Poster at the 8th World Congress on Alternatives, Montreal (Canada).*

CUPEDO, T., STROOCK, A. & COLES, M. 2012. Application of tissue engineering to the immune system: development of artificial lymph nodes. *Front Immunol,* 3**,** 343.

CURTSINGER, J. M. & MESCHER, M. F. 2010. Inflammatory Cytokines as a Third Signal for T Cell Activation. *Current opinion in immunology,* 22**,** 333-340.

D'AMICO, G., BIANCHI, G., BERNASCONI, S., BERSANI, L., PIEMONTI, L., SOZZANI, S., MANTOVANI, A. & ALLAVENA, P. 1998. Adhesion, transendothelial migration, and reverse transmigration of in vitro cultured dendritic cells. *Blood,* 92**,** 207-14.

DE SAINT-VIS, B., VINCENT, J., VANDENABEELE, S., VANBERVLIET, B., PIN, J. J., AÏT-YAHIA, S., PATEL, S., MATTEI, M. G., BANCHEREAU, J., ZURAWSKI, S., DAVOUST, J., CAUX, C. & LEBECQUE, S. A Novel Lysosome-Associated Membrane Glycoprotein, DC-LAMP, Induced upon DC Maturation, Is Transiently Expressed in MHC Class II Compartment. *Immunity,* 9**,** 325-336.

DHANDAYUTHAPANI 2011. Polymeric Scaffolds in Tissue Engineering Application: A Review. *International Journal of Polymer Science,* 2011.

DIVKOVIC, M., PEASE, C. K., GERBERICK, G. F. & BASKETTER, D. A. 2005. Hapten-protein binding: from theory to practical application in the in vitro prediction of skin sensitization. *Contact Dermatitis,* 53**,** 189-200.

DOLATSHAHI-PIROUZ, A., NIKKHAH, M., GAHARWAR, A. K., HASHMI, B., GUERMANI, E., ALIABADI, H., CAMCI-UNAL, G., FERRANTE, T., FOSS, M., INGBER, D. E. & KHADEMHOSSEINI, A. 2014. A combinatorial cell-laden gel microarray for inducing osteogenic differentiation of human mesenchymal stem cells. *Sci Rep,* 4**,** 3896.

DOS SANTOS, G. G., REINDERS, J., OUWEHAND, K., RUSTEMEYER, T., SCHEPER, R. J. & GIBBS, S. 2009. Progress on the development of human in vitro dendritic cell based assays for assessment of the sensitizing potential of a compound. *Toxicol Appl Pharmacol,* 236**,** 372-82.

DUDDA, J. C., SIMON, J. C. & MARTIN, S. 2004. Dendritic Cell Immunization Route Determines CD8+ T Cell Trafficking to Inflamed Skin: Role for Tissue Microenvironment and Dendritic Cells in Establishment of T Cell-Homing Subsets. *The Journal of Immunology,* 172**,** 857-863.

DUSTIN, M. L., ALLEN, P. M. & SHAW, A. S. 2001. Environmental control of immunological synapse formation and duration. *Trends in Immunology,* 22**,** 192-194.

DUSTIN, M. L. & DE FOUGEROLLES, A. R. 2001. Reprogramming T cells: the role of extracellular matrix in coordination of T cell activation and migration. *Curr Opin Immunol,* 13**,** 286-90.

EASTWOOD, D., FINDLAY, L., POOLE, S., BIRD, C., WADHWA, M., MOORE, M., BURNS, C., THORPE, R. & STEBBINGS, R. 2010. Monoclonal antibody TGN1412 trial failure explained by species differences in CD28 expression on CD4+ effector memory T-cells. *British Journal of Pharmacology,* 161**,** 512-526.

EKDAHL, K. N., LAMBRIS, J. D., ELWING, H., RICKLIN, D., NILSSON, P. H., TERAMURA, Y., NICHOLLS, I. A. & NILSSON, B. 2011. Innate immunity activation on biomaterial surfaces: A mechanistic model and coping strategies. *Advanced Drug Delivery Reviews,* 63**,** 1042-1050.

EL-SHERBINY, I. M. & YACOUB, M. H. 2013. Hydrogel scaffolds for tissue engineering: Progress and challenges. *Global Cardiology Science & Practice,* 2013**,** 316-342.

ESSER, P. R., KIMBER, I. & MARTIN, S. F. 2014. Correlation of contact sensitizer potency with T cell frequency and TCR repertoire diversity. *EXS,* 104**,** 101-14.

ESSER, P. R., WOLFLE, U., DURR, C., VON LOEWENICH, F. D., SCHEMPP, C. M., FREUDENBERG, M. A., JAKOB, T. & MARTIN, S. F. 2012. Contact sensitizers induce skin inflammation via ROS production and hyaluronic acid degradation. *PLoS One,* 7**,** e41340.

FLANAGAN, K., MOROZIEWICZ, D., KWAK, H., HÖRIG, H. & KAUFMAN, H. L. 2004. The lymphoid chemokine CCL21 costimulates naïve T cell expansion and Th1 polarization of non-regulatory CD4+ T cells. *Cellular Immunology,* 231**,** 75-84.

FLORES-ROMO, L. 2001. In vivo maturation and migration of dendritic cells. *Immunology,* 102**,** 255-262.

FLYNN, J. L. & CHAN, J. 2001. IMMUNOLOGY OF TUBERCULOSIS. *Annual Review of Immunology,* 19**,** 93-129.

FORSTER, R., DAVALOS-MISSLITZ, A. C. & ROT, A. 2008. CCR7 and its ligands: balancing immunity and tolerance. *Nat Rev Immunol,* 8**,** 362-371.

FÖRSTER, R., SCHUBEL, A., BREITFELD, D., KREMMER, E., RENNER-MÜLLER, I., WOLF, E. & LIPP, M. 1999. CCR7 Coordinates the Primary Immune Response by Establishing Functional Microenvironments in Secondary Lymphoid Organs. *Cell,* 99**,** 23-33.

FRIEDMANN, P. S. & PICKARD, C. 2014. Contact hypersensitivity: quantitative aspects, susceptibility and risk factors. *Exs,* 104**,** 51-71.

FURIO, L., GUEZENNEC, A., DUCARRE, B., GUESNET, J. & PEGUET-NAVARRO, J. 2008. Differential effects of allergens and irritants on early differentiating monocyte-derived dendritic cells. *Eur J Dermatol,* 18**,** 141-7.

GAMERDINGER, K., MOULON, C., KARP, D. R., VAN BERGEN, J., KONING, F., WILD, D., PFLUGFELDER, U. & WELTZIEN, H. U. 2003. A new type of metal recognition by human T cells: contact residues for peptide-independent bridging of T cell receptor and major histocompatibility complex by nickel. *J Exp Med,* 197**,** 1345-53.

GARCIA-NIETO, S., JOHAL, R. K., SHAKESHEFF, K. M., EMARA, M., ROYER, P. J., CHAU, D. Y., SHAKIB, F. & GHAEMMAGHAMI, A. M. 2010. Laminin and fibronectin treatment leads to generation of dendritic cells with superior endocytic capacity. *PLoS One,* 5**,** e10123.

GASTEIGER, G., ATAIDE, M. & KASTENMULLER, W. 2016. Lymph node - an organ for T-cell activation and pathogen defense. *Immunol Rev,* 271**,** 200-20.

GELARDI, A., MORINI, F., DUSATTI, F., PENCO, S. & FERRO, M. 2001. Induction by xenobiotics of phase I and phase II enzyme activities in the human keratinocyte cell line NCTC 2544. *Toxicol In Vitro,* 15**,** 701-11.

GERBERICK, G. F., TROUTMAN, J. A., FOERTSCH, L. M., VASSALLO, J. D., QUIJANO, M., DOBSON, R. L. M., GOEBEL, C. & LEPOITTEVIN, J.-P. 2009. Investigation of Peptide Reactivity of Pro-hapten Skin Sensitizers Using a Peroxidase-Peroxide Oxidation System. *Toxicological Sciences,* 112**,** 164-174.

GERBERICK, G. F., VASSALLO, J. D., BAILEY, R. E., CHANEY, J. G., MORRALL, S. W. & LEPOITTEVIN, J. P. 2004. Development of a peptide reactivity assay for screening contact allergens. *Toxicol Sci,* 81**,** 332-43.

GERMAIN, R. N. 1994. MHC-dependent antigen processing and peptide presentation: Providing ligands for T lymphocyte activation. *Cell,* 76**,** 287-299.

GERMAIN, R. N. 2002. T-cell development and the CD4-CD8 lineage decision. *Nat Rev Immunol,* 2**,** 309-322.

GHAEMMAGHAMI, A. M. 2002. The proteolytic activity of the major house dust mite allergen Der p 1 conditions DCs to produce less IL-12: allergen-induced Th2 bias at the dendritic cell level.

GIANNONE, G. & SHEETZ, M. P. 2006. Substrate rigidity and force define form through tyrosine phosphatase and kinase pathways. *Trends in Cell Biology,* 16**,** 213-223.

GIESE, C., DEMMLER, C. D., AMMER, R., HARTMANN, S., LUBITZ, A., MILLER, L., MULLER, R. & MARX, U. 2006. A human lymph node in vitro--challenges and progress. *Artif Organs,* 30**,** 803-8.

GIESE, C., LUBITZ, A., DEMMLER, C. D., REUSCHEL, J., BERGNER, K. & MARX, U. 2010. Immunological substance testing on human lymphatic micro-organoids in vitro. *J Biotechnol,* 148**,** 38-45.

GIESE, C. & MARX, U. 2014. Human immunity in vitro — Solving immunogenicity and more. *Advanced Drug Delivery Reviews,* 69–70**,** 103-122.

GINHOUX, F. & MERAD, M. 2010. Ontogeny and homeostasis of Langerhans cells. *Immunol Cell Biol,* 88**,** 387-392.

GLOWACKI, J. & MIZUNO, S. 2008. Collagen scaffolds for tissue engineering. *Biopolymers,* 89**,** 338-344.

GOLLA, S., MADIHALLY, S., ROBINSON JR, R. L. & GASEM, K. A. M. 2009. Quantitative structure–property relationship modeling of skin sensitization: A quantitative prediction. *Toxicology in Vitro,* 23**,** 454-465.

GOMEZ-LECHON, M. J., JOVER, R., DONATO, T., PONSODA, X., RODRIGUEZ, C., STENZEL, K. G., KLOCKE, R., PAUL, D., GUILLEN, I., BORT, R. & CASTELL, J. V. 1998. Long-term expression of differentiated functions in hepatocytes cultured in three-dimensional collagen matrix. *J Cell Physiol,* 177**,** 553-62.

GONZALO, J.-A., DELANEY, T., CORCORAN, J., GOODEARL, A., GUTIERREZ-RAMOS, J. C. & COYLE, A. J. 2001. Cutting Edge: The Related Molecules CD28 and Inducible Costimulator Deliver Both Unique and Complementary Signals Required for Optimal T Cell Activation. *The Journal of Immunology,* 166**,** 1-5.

GOODYEAR, M. 2006. Learning from the TGN1412 trial. *BMJ,* 332**,** 677-8.

GORAL, V. N., HSIEH, Y.-C., PETZOLD, O. N., CLARK, J. S., YUEN, P. K. & FARIS, R. A. 2010. Perfusion-based microfluidic device for three-dimensional dynamic primary human hepatocyte cell culture in the absence of biological or synthetic matrices or coagulants. *Lab on a Chip,* 10**,** 3380-3386.

GORDON, S. 2002. Pattern Recognition Receptors: Doubling Up for the Innate Immune Response. *Cell,* 111**,** 927-930.

GRETZ, J. E., ANDERSON, A. O. & SHAW, S. 1997. Cords, channels, corridors and conduits: critical architectural elements facilitating cell interactions in the lymph node cortex. *Immunol Rev,* 156**,** 11-24.

GRETZER, C., GISSELFÄLT, K., LILJENSTEN, E., RYDÉN, L. & THOMSEN, P. 2003. Adhesion, apoptosis and cytokine release of human mononuclear cells cultured on degradable poly(urethane urea), polystyrene and titanium in vitro. *Biomaterials,* 24**,** 2843-2852.

GUERMONPREZ, P., VALLADEAU, J., ZITVOGEL, L., THÉRY, C. & AMIGORENA, S. 2002. ANTIGEN PRESENTATION AND T CELL STIMULATION BY DENDRITIC CELLS. *Annual Review of Immunology,* 20**,** 621-667.

GULD, J., BENTZON, M. W., BLEIKER, M. A., GRIEP, W. A., MAGNUSSON, M. & WAALER, H. 1958. Standardization of a new batch of purified tuberculin (PPD) intended for international use. *Bulletin of the World Health Organization,* 19**,** 845-951.

GUNZER, M., SCHAFER, A., BORGMANN, S., GRABBE, S., ZANKER, K. S., BROCKER, E. B., KAMPGEN, E. & FRIEDL, P. 2000. Antigen presentation in extracellular matrix: interactions of T cells with dendritic cells are dynamic, short lived, and sequential. *Immunity,* 13**,** 323-32.

GUNZER, M., WEISHAUPT, C., HILLMER, A., BASOGLU, Y., FRIEDL, P., DITTMAR, K. E., KOLANUS, W., VARGA, G. & GRABBE, S. 2004. A spectrum of biophysical interaction

modes between T cells and different antigen-presenting cells during priming in 3-D collagen and in vivo. *Blood,* 104**,** 2801-9.

GUO, B. & MA, P. X. 2014. Synthetic biodegradable functional polymers for tissue engineering: a brief review. *Science China Chemistry,* 57**,** 490-500.

HARRINGTON, H., CATO, P., SALAZAR, F., WILKINSON, M., KNOX, A., HAYCOCK, J. W., ROSE, F., AYLOTT, J. W. & GHAEMMAGHAMI, A. M. 2014. Immunocompetent 3D Model of Human Upper Airway for Disease Modeling and In Vitro Drug Evaluation. *Molecular Pharmaceutics,* 11**,** 2082-2091.

HARRY L. IOACHIM, L. J. M. 2009. *Ioachim's Lymph Node Pathology,* Philadelphia, Lippincott Williams and Wilkins.

HART, D. N. J. 1997. Dendritic Cells: Unique Leukocyte Populations Which Control the Primary Immune Response. *Blood,* 90**,** 3245-3287.

HARTY, J. T., TVINNEREIM, A. R. & WHITE, D. W. 2000. CD8+ T Cell Effector Mechanisms in Resistance to Infection. *Annual Review of Immunology,* 18**,** 275-308.

HAWKINS, C. L. & DAVIES, M. J. 1997. Oxidative damage to collagen and related substrates by metal ion/hydrogen peroxide systems: random attack or site-specific damage? *Biochimica et Biophysica Acta (BBA) - Molecular Basis of Disease,* 1360**,** 84-96.

HAYDEN, M. S. & GHOSH, S. 2008. Shared Principles in NF-kB Signaling. *Cell,* 132**,** 344-362.

HITZLER, M., BERGERT, A., LUCH, A. & PEISER, M. 2013. Evaluation of selected biomarkers for the detection of chemical sensitization in human skin: A comparative study applying THP-1, MUTZ-3 and primary dendritic cells in culture. *Toxicol In Vitro,* 27**,** 1659-1669.

HOFFMAN, A. S. 2013. Stimuli-responsive polymers: Biomedical applications and challenges for clinical translation. *Advanced Drug Delivery Reviews,* 65**,** 10-16.

HONDA, T., NAKAJIMA, S., EGAWA, G., OGASAWARA, K., MALISSEN, B., MIYACHI, Y. & KABASHIMA, K. 2010. Compensatory role of Langerhans cells and langerin-positive dermal dendritic cells in the sensitization phase of murine contact hypersensitivity. *J Allergy Clin Immunol,* 125**,** 1154-1156.e2.

HORLOCK, C., SHAKIB, F., MAHDAVI, J., JONES, N. S., SEWELL, H. F. & GHAEMMAGHAMI, A. M. 2007. Analysis of proteomic profiles and functional properties of human peripheral blood myeloid dendritic cells, monocyte-derived dendritic cells and the dendritic cell-like KG-1 cells reveals distinct characteristics. *Genome Biol,* 8**,** R30.

HUANG, C., SOENEN, S. J., REJMAN, J., LUCAS, B., BRAECKMANS, K., DEMEESTER, J. & DE SMEDT, S. C. 2011. Stimuli-responsive electrospun fibers and their applications. *Chem Soc Rev,* 40**,** 2417-34.

HUGHES, C. S., POSTOVIT, L. M. & LAJOIE, G. A. 2010. Matrigel: a complex protein mixture required for optimal growth of cell culture. *Proteomics,* 10**,** 1886-90.

HULETTE, B. C., RYAN, C. A., GILDEA, L. A. & GERBERICK, G. F. 2005. Relationship of CD86 surface marker expression and cytotoxicity on dendritic cells exposed to chemical allergen. *Toxicology and Applied Pharmacology,* 209**,** 159-166.

HUTSON, C. B., NICHOL, J. W., AUBIN, H., BAE, H., YAMANLAR, S., AL-HAQUE, S., KOSHY, S. T. & KHADEMHOSSEINI, A. 2011. Synthesis and characterization of tunable poly(ethylene glycol): gelatin methacrylate composite hydrogels. *Tissue Eng Part A,* 17**,** 1713-23.

HWANG, Y.-S., CHUNG, B. G., ORTMANN, D., HATTORI, N., MOELLER, H.-C. & KHADEMHOSSEINI, A. 2009. Microwell-mediated control of embryoid body size regulates embryonic stem cell fate via differential expression of WNT5a and WNT11. *Proceedings of the National Academy of Sciences,* 106**,** 16978-16983.

INAMDAR, N. K. & BORENSTEIN, J. T. 2011. Microfluidic cell culture models for tissue engineering. *Current Opinion in Biotechnology,* 22**,** 681-689.

JEONG, E. & LEE, J. Y. 2011. Intrinsic and extrinsic regulation of innate immune receptors. *Yonsei Med J,* 52**,** 379-92.

JOHANSSON, H., ALBREKT, A.-S., BORREBAECK, C. A. K. & LINDSTEDT, M. 2013. The GARD assay for assessment of chemical skin sensitizers. *Toxicology in Vitro,* 27**,** 1163-1169.

JOHNSON, P. C., MIKOS, A. G., FISHER, J. P. & JANSEN, J. A. 2007. Strategic directions in tissue engineering. *Tissue Eng,* 13**,** 2827-37.

JUNG, J. & OH, J. 2014. Swelling characterization of photo-cross-linked gelatin methacrylate spherical microgels for bioencapsulation. *e-Polymers.*

KANDAROVA, H., LIEBSCH, M., GERNER, I., SCHMIDT, E., GENSCHOW, E., TRAUE, D. & SPIELMANN, H. 2005. The EpiDerm test protocol for the upcoming ECVAM validation study on in vitro skin irritation tests--an assessment of the performance of the optimised test. *Altern Lab Anim,* 33**,** 351-67.

KANE, L. P., LIN, J. & WEISS, A. 2000. Signal transduction by the TCR for antigen. *Current Opinion in Immunology,* 12**,** 242-249.

KANTA, J. 2015. Collagen matrix as a tool in studying fibroblastic cell behavior. *Cell Adh Migr,* 9**,** 308-16.

KAPLAN, D. H., IGYARTO, B. Z. & GASPARI, A. A. 2012. Early immune events in the induction of allergic contact dermatitis. *Nat Rev Immunol,* 12**,** 114-24.

KARLBERG, A. T., BERGSTROM, M. A., BORJE, A., LUTHMAN, K. & NILSSON, J. L. 2008. Allergic contact dermatitis--formation, structural requirements, and reactivity of skin sensitizers. *Chem Res Toxicol,* 21**,** 53-69.

KARP, J. M., YEH, J., ENG, G., FUKUDA, J., BLUMLING, J., SUH, K.-Y., CHENG, J., MAHDAVI, A., BORENSTEIN, J., LANGER, R. & KHADEMHOSSEINI, A. 2007. Controlling size, shape and homogeneity of embryoid bodies using poly(ethylene glycol) microwells. *Lab on a Chip,* 7**,** 786-794.

KASHIPAZ, M. R. A., HUGGINS, M. L., POWELL, R. J. & TODD, I. 2002. Human autologous mixed lymphocyte reaction as an in vitro model for autoreactivity to apoptotic antigens. *Immunology,* 107**,** 358-365.

KATAKAI, T., HARA, T., LEE, J. H., GONDA, H., SUGAI, M. & SHIMIZU, A. 2004. A novel reticular stromal structure in lymph node cortex: an immuno-platform for interactions among dendritic cells, T cells and B cells. *Int Immunol,* 16**,** 1133-42.

KATIAL, R. K., HERSHEY, J., PUROHIT-SETH, T., BELISLE, J. T., BRENNAN, P. J., SPENCER, J. S. & ENGLER, R. J. M. 2001. Cell-Mediated Immune Response to Tuberculosis Antigens: Comparison of Skin Testing and Measurement of In Vitro Gamma Interferon Production in Whole-Blood Culture. *Clinical and Diagnostic Laboratory Immunology,* 8**,** 339-345.

KHAN, R. & KHAN, M. H. 2013. Use of collagen as a biomaterial: An update. *Journal of Indian Society of Periodontology,* 17**,** 539-542.

KIMBER, I., BASKETTER, D. A., BERTHOLD, K., BUTLER, M., GARRIGUE, J. L., LEA, L., NEWSOME, C., ROGGEBAND, R., STEILING, W., STROPP, G., WATERMAN, S. & WIEMANN, C. 2001. Skin sensitization testing in potency and risk assessment. *Toxicol Sci,* 59**,** 198-208.

KIMBER, I. & DEARMAN, R. J. 2003. What makes a chemical an allergen? *Annals of Allergy, Asthma & Immunology,* 90**,** 28-31.

KIMBER, I., DEARMAN, R. J., BASKETTER, D. A., RYAN, C. A. & GERBERICK, G. F. 2002. The local lymph node assay: past, present and future. *Contact Dermatitis,* 47**,** 315-28.

KIMBER, I., MAXWELL, G., GILMOUR, N., DEARMAN, R. J., FRIEDMANN, P. S. & MARTIN, S. F. 2012. Allergic contact dermatitis: A commentary on the relationship between T lymphocytes and skin sensitising potency. *Toxicology,* 291**,** 18-24.

KLEINMAN, H. K., PHILP, D. & HOFFMAN, M. P. 2003. Role of the extracellular matrix in morphogenesis. *Curr Opin Biotechnol,* 14**,** 526-32.

KNIGHT, C. G., MORTON, L. F., PEACHEY, A. R., TUCKWELL, D. S., FARNDALE, R. W. & BARNES, M. J. 2000. The collagen-binding A-domains of integrins alpha(1)beta(1) and alpha(2)beta(1) recognize the same specific amino acid sequence, GFOGER, in native (triple-helical) collagens. *J Biol Chem,* 275**,** 35-40.

KNUPP, C. & SQUIRE, J. M. 2003. Molecular packing in network-forming collagens. *ScientificWorldJournal,* 3**,** 558-77.

KOHANE, D. S. & LANGER, R. 2008. Polymeric Biomaterials in Tissue Engineering. *Pediatr Res,* 63**,** 487-491.

LANZAVECCHIA, A. & SALLUSTO, F. 2001. The instructive role of dendritic cells on T cell responses: lineages, plasticity and kinetics. *Current Opinion in Immunology,* 13**,** 291-298.

LEE, E. J., KASPER, F. K. & MIKOS, A. G. 2014. Biomaterials for Tissue Engineering. *Annals of biomedical engineering,* 42**,** 323-337.

LEIN, A. D. & VON REYN, C. F. 1997. In Vitro Cellular and Cytokine Responses to Mycobacterial Antigens: Application to Diagnosis of Tuberculosis Infection and

Assessment of Response to Mycobacterial Vaccines. *The American Journal of the Medical Sciences,* 313**,** 364-371.

LEON, B. & ARDAVIN, C. 2008. Monocyte-derived dendritic cells in innate and adaptive immunity. *Immunol Cell Biol,* 86**,** 320-324.

LEWIS, J. S., DOLGOVA, N. V., CHANCELLOR, T. J., ACHARYA, A. P., KARPIAK, J. V., LELE, T. P. & KESELOWSKY, B. G. 2013. The effect of cyclic mechanical strain on activation of dendritic cells cultured on adhesive substrates. *Biomaterials,* 34**,** 9063-70.

LEWIS, J. S., ROY, K. & KESELOWSKY, B. G. 2014. Materials that harness and modulate the immune system. *Mrs Bulletin,* 39**,** 25-34.

LI, Y. C., CHEN, B. M., WU, P. C., CHENG, T. L., KAO, L. S., TAO, M. H., LIEBER, A. & ROFFLER, S. R. 2010. Cutting Edge: mechanical forces acting on T cells immobilized via the TCR complex can trigger TCR signaling. *J Immunol,* 184**,** 5959-63.

LIU, Y.-J. 2005. IPC: Professional Type 1 Interferon-Producing Cells and Plasmacytoid Dendritic Cell Precursors. *Annual Review of Immunology,* 23**,** 275-306.

LIVAK, K. J. & SCHMITTGEN, T. D. 2001. Analysis of Relative Gene Expression Data Using Real-Time Quantitative PCR and the 2−ΔΔCT Method. *Methods,* 25**,** 402-408.

LORTAT-JACOB, H., KLEINMAN, H. K. & GRIMAUD, J. A. 1991. High-affinity binding of interferon-gamma to a basement membrane complex (matrigel). *Journal of Clinical Investigation,* 87**,** 878-883.

LOUIS-DIT-SULLY, C. & SCHAMEL, W. W. A. 2014. Activation of the TCR Complex by Small Chemical Compounds. *In:* MARTIN, F. S. (ed.) *T Lymphocytes as Tools in Diagnostics and Immunotoxicology.* Basel: Springer Basel.

LUTZ, M. B. & SCHULER, G. 2002. Immature, semi-mature and fully mature dendritic cells: which signals induce tolerance or immunity? *Trends in Immunology,* 23**,** 445-449.

LYNN, A. K., YANNAS, I. V. & BONFIELD, W. 2004. Antigenicity and immunogenicity of collagen. *Journal of Biomedical Materials Research Part B: Applied Biomaterials,* 71B**,** 343-354.

MACEWAN, D. J. 2002. TNF receptor subtype signalling: Differences and cellular consequences. *Cellular Signalling,* 14**,** 477-492.

MACKIN, L. A. 1998. Screening for tuberculosis in the primary care setting. *Lippincotts Prim Care Pract,* 2**,** 599-610; quiz 611-3.

MAKINO, A., GLOGAUER, M., BOKOCH, G. M., CHIEN, S. & SCHMID-SCHÖNBEIN, G. W. 2005. Control of neutrophil pseudopods by fluid shear: role of Rho family GTPases. *American Journal of Physiology - Cell Physiology,* 288**,** C863-C871.

MAKINO, A., SHIN, H. Y., KOMAI, Y., FUKUDA, S., COUGHLIN, M., SUGIHARA-SEKI, M. & SCHMID-SCHONBEIN, G. W. 2007. Mechanotransduction in leukocyte activation: a review. *Biorheology,* 44**,** 221-49.

MARSLAND, B. J., BÄTTIG, P., BAUER, M., RUEDL, C., LÄSSING, U., BEERLI, R. R., DIETMEIER, K., IVANOVA, L., PFISTER, T., VOGT, L., NAKANO, H., NEMBRINI, C., SAUDAN, P., KOPF, M. & BACHMANN, M. F. 2005. CCL19 and CCL21 Induce a Potent Proinflammatory Differentiation Program in Licensed Dendritic Cells. *Immunity,* 22**,** 493-505.

MARTIN, S. F. 2004. T lymphocyte-mediated immune responses to chemical haptens and metal ions: implications for allergic and autoimmune disease. *Int Arch Allergy Immunol,* 134**,** 186-98.

MARTIN, S. F., DUDDA, J. C., BACHTANIAN, E., LEMBO, A., LILLER, S., DURR, C., HEIMESAAT, M. M., BERESWILL, S., FEJER, G., VASSILEVA, R., JAKOB, T., FREUDENBERG, N., TERMEER, C. C., JOHNER, C., GALANOS, C. & FREUDENBERG, M. A. 2008. Toll-like receptor and IL-12 signaling control susceptibility to contact hypersensitivity. *Journal of Experimental Medicine,* 205**,** 2151-2162.

MARTIN, S. F., ESSER, P. R., SCHMUCKER, S., DIETZ, L., NAISBITT, D. J., PARK, B. K., VOCANSON, M., NICOLAS, J. F., KELLER, M., PICHLER, W. J., PEISER, M., LUCH, A., WANNER, R., MAGGI, E., CAVANI, A., RUSTEMEYER, T., RICHTER, A., THIERSE, H. J. & SALLUSTO, F. 2010. T-cell recognition of chemicals, protein allergens and drugs: towards the development of in vitro assays. *Cell Mol Life Sci,* 67**,** 4171-84.

MEHLING, A., ERIKSSON, T., ELTZE, T., KOLLE, S., RAMIREZ, T., TEUBNER, W., VAN RAVENZWAAY, B. & LANDSIEDEL, R. 2012. Non-animal test methods for predicting skin sensitization potentials. *Arch Toxicol,* 86**,** 1273-95.

MENON, G. K., CLEARY, G. W. & LANE, M. E. 2012. The structure and function of the stratum corneum. *International Journal of Pharmaceutics,* 435**,** 3-9.

MERAD, M., SATHE, P., HELFT, J., MILLER, J. & MORTHA, A. 2013. The Dendritic Cell Lineage: Ontogeny and Function of Dendritic Cells and Their Subsets in the Steady State and the Inflamed Setting. *Annual review of immunology,* 31**,** 10.1146/annurev-immunol-020711-074950.

MIRONI-HARPAZ, I., WANG, D. Y., VENKATRAMAN, S. & SELIKTAR, D. 2012. Photopolymerization of cell-encapsulating hydrogels: Crosslinking efficiency versus cytotoxicity. *Acta Biomaterialia,* 8**,** 1838-1848.

MITEVA, D. O., RUTKOWSKI, J. M., DIXON, J. B., KILARSKI, W., SHIELDS, J. D. & SWARTZ, M. A. 2010. Transmural flow modulates cell and fluid transport functions of lymphatic endothelium. *Circ Res,* 106**,** 920-31.

MIYAKAWA, N., NISHIKAWA, M., TAKAHASHI, Y., ANDO, M., MISAKA, M., WATANABE, Y. & TAKAKURA, Y. 2011. Prolonged circulation half-life of interferon gamma activity by gene delivery of interferon gamma-serum albumin fusion protein in mice. *J Pharm Sci,* 100**,** 2350-7.

MOCAN, E., TAGADIUC, O. & NACU, V. 2011. Aspects of collagen isolation procedure. *Clin. Res. Studies,* 2**,** 3-5.

MOELLER, H.-C., MIAN, M. K., SHRIVASTAVA, S., CHUNG, B. G. & KHADEMHOSSEINI, A. 2008. A microwell array system for stem cell culture. *Biomaterials,* 29**,** 752-763.

MOGENSEN, T. H. 2009. Pathogen Recognition and Inflammatory Signaling in Innate Immune Defenses. *Clinical Microbiology Reviews,* 22**,** 240-273.

MONBOISSE, J. C. & BOREL, J. P. 1992. Oxidative damage to collagen. *Exs,* 62**,** 323-7.

MORGAN, M. J. & LIU, Z.-G. 2011. Crosstalk of reactive oxygen species and NF-κB signaling. *Cell Research,* 21**,** 103-115.

MOSER, M. 2003. Dendritic Cells in Immunity and Tolerance—Do They Display Opposite Functions? *Immunity,* 19**,** 5-8.

MOTTA, J. M. & RUMJANEK, V. M. 2016. Sensitivity of Dendritic Cells to Microenvironment Signals. *J Immunol Res,* 2016**,** 4753607.

MURPHY, K., TRAVERS, P., WALPORT, M. & JANEWAY, C. 2008. *Janeway's immunobiology,* New York, Garland Science.

NATSCH, A. 2010. The Nrf2-Keap1-ARE toxicity pathway as a cellular sensor for skin sensitizers--functional relevance and a hypothesis on innate reactions to skin sensitizers. *Toxicol Sci,* 113**,** 284-92.

NATSCH, A. & EMTER, R. 2008. Skin sensitizers induce antioxidant response element dependent genes: application to the in vitro testing of the sensitization potential of chemicals. *Toxicol Sci,* 102**,** 110-9.

NEZU, T. & WINNIK, F. M. 2000. Interaction of water-soluble collagen with poly(acrylic acid). *Biomaterials,* 21**,** 415-419.

NIKKHAH, M., ESHAK, N., ZORLUTUNA, P., ANNABI, N., CASTELLO, M., KIM, K., DOLATSHAHI-PIROUZ, A., EDALAT, F., BAE, H., YANG, Y. & KHADEMHOSSEINI, A. 2012. Directed endothelial cell morphogenesis in micropatterned gelatin methacrylate hydrogels. *Biomaterials,* 33**,** 9009-9018.

NOORDEGRAAF, M., FLACHER, V., STOITZNER, P. & CLAUSEN, B. E. 2010. Functional redundancy of Langerhans cells and Langerin+ dermal dendritic cells in contact hypersensitivity. *J Invest Dermatol,* 130**,** 2752-9.

NUKADA, Y., ASHIKAGA, T., MIYAZAWA, M., HIROTA, M., SAKAGUCHI, H., SASA, H. & NISHIYAMA, N. 2012. Prediction of skin sensitization potency of chemicals by human Cell Line Activation Test (h-CLAT) and an attempt at classifying skin sensitization potency. *Toxicol In Vitro,* 26**,** 1150-60.

OECD 2012. The Adverse Outcome Pathway for Skin Sensitisation Initiated by Covalent Binding to Proteins. Part 2: Use of the AOP to Develop Chemical Categories and Integrated Assessment and Testing Approaches. Series on Testing and Assessment No. 168. ENV/JM/MONO(2012)/PART2.

OVSIANIKOV, A., DEIWICK, A., VAN VLIERBERGHE, S., DUBRUEL, P., MÖLLER, L., DRÄGER, G. & CHICHKOV, B. 2011. Laser Fabrication of Three-Dimensional CAD Scaffolds from Photosensitive Gelatin for Applications in Tissue Engineering. *Biomacromolecules,* 12**,** 851-858.

PAMPALONI, F., REYNAUD, E. G. & STELZER, E. H. 2007. The third dimension bridges the gap between cell culture and live tissue. *Nat Rev Mol Cell Biol,* 8**,** 839-45.

PARENTEAU-BAREIL, R., GAUVIN, R. & BERTHOD, F. 2010. Collagen-Based Biomaterials for Tissue Engineering Applications. *Materials,* 3**,** 1863.

PATLEWICZ, G., APTULA, A. O., URIARTE, E., ROBERTS, D. W., KERN, P. S., GERBERICK, G. F., KIMBER, I., DEARMAN, R. J., RYAN, C. A. & BASKETTER, D. A. 2007. An evaluation of selected global (Q)SARs/expert systems for the prediction of skin sensitisation potential. *SAR and QSAR in Environmental Research,* 18**,** 515-541.

PEELA, N., SAM, F. S., CHRISTENSON, W., TRUONG, D., WATSON, A. W., MOUNEIMNE, G., ROS, R. & NIKKHAH, M. 2016. A three dimensional micropatterned tumor model for breast cancer cell migration studies. *Biomaterials,* 81**,** 72-83.

PEISER, M., TRALAU, T., HEIDLER, J., API, A. M., ARTS, J. H., BASKETTER, D. A., ENGLISH, J., DIEPGEN, T. L., FUHLBRIGGE, R. C., GASPARI, A. A., JOHANSEN, J. D., KARLBERG, A. T., KIMBER, I., LEPOITTEVIN, J. P., LIEBSCH, M., MAIBACH, H. I., MARTIN, S. F., MERK, H. F., PLATZEK, T., RUSTEMEYER, T., SCHNUCH, A., VANDEBRIEL, R. J., WHITE, I. R. & LUCH, A. 2012. Allergic contact dermatitis: epidemiology, molecular mechanisms, in vitro methods and regulatory aspects. Current knowledge assembled at an international workshop at BfR, Germany. *Cell Mol Life Sci,* 69**,** 763-81.

PHILIP, R. & EPSTEIN, L. B. 1986. Tumour necrosis factor as immunomodulator and mediator of monocyte cytotoxicity induced by itself, gamma-interferon and interleukin-1. *Nature,* 323**,** 86-9.

PICHLER, W. J., BEELER, A., KELLER, M., LERCH, M., POSADAS, S., SCHMID, D., SPANOU, Z., ZAWODNIAK, A. & GERBER, B. 2006. Pharmacological interaction of drugs with immune receptors: the p-i concept. *Allergol Int,* 55**,** 17-25.

PLACE, E. S., EVANS, N. D. & STEVENS, M. M. 2009. Complexity in biomaterials for tissue engineering. *Nat Mater,* 8**,** 457-470.

POLTORAK, M. P. & SCHRAML, B. U. 2015. Fate Mapping of Dendritic Cells. *Frontiers in Immunology,* 6**,** 199.

PÖRTNER, R. & GIESE, C. 2006. An Overview on Bioreactor Design, Prototyping and Process Control for Reproducible Three-Dimensional Tissue Culture. *Drug Testing in vitro.* Wiley-VCH Verlag GmbH & Co. KGaA.

PREVITERA, M. L. 2014. Mechanotransduction in the Immune System. *Cellular and Molecular Bioengineering,* 7**,** 473-481.

RAHIM, R., MANUEL, O., AMY, D., TEJASVI, P., MEHMET, R. D., ALI, K., AMIR, G. & BABAK, Z. 2015. A Janus-paper PDMS platform for air–liquid interface cell culture applications. *Journal of Micromechanics and Microengineering,* 25**,** 055015.

RANDOLPH, G. J., ANGELI, V. & SWARTZ, M. A. 2005. Dendritic-cell trafficking to lymph nodes through lymphatic vessels. *Nature Reviews Immunology,* 5**,** 617-628.

REISER, H. & SCHNEEBERGER, E. E. 1996. Expression and function of B7-1 and B7-2 in hapten-induced contact sensitivity. *European Journal of Immunology,* 26**,** 880-885.

REIZIS, B., BUNIN, A., GHOSH, H. S., LEWIS, K. L. & SISIRAK, V. 2011. Plasmacytoid Dendritic Cells: Recent Progress and Open Questions. *Annual review of immunology,* 29**,** 163-183.

REMES, A. & WILLIAMS, D. F. 1992. Immune response in biocompatibility. *Biomaterials,* 13**,** 731-43.

REUTER, H., SPIEKER, J., GERLACH, S., ENGELS, U., PAPE, W., KOLBE, L., SCHMUCKER, R., WENCK, H., DIEMBECK, W., WITTERN, K. P., REISINGER, K. & SCHEPKY, A. G. 2011. In vitro detection of contact allergens: development of an optimized protocol using human peripheral blood monocyte-derived dendritic cells. *Toxicol In Vitro,* 25**,** 315-23.

RICHTER, A., SCHMUCKER, S. S., ESSER, P. R., TRASKA, V., WEBER, V., DIETZ, L., THIERSE, H. J., PENNINO, D., CAVANI, A. & MARTIN, S. F. 2012. Human T cell priming assay (hTCPA) for the identification of contact allergens based on naive T cells and DC - IFN-gamma and TNF-alpha readout. *Toxicol In Vitro*.

RIZVI, I., GURKAN, U. A., TASOGLU, S., ALAGIC, N., CELLI, J. P., MENSAH, L. B., MAI, Z., DEMIRCI, U. & HASAN, T. 2013. Flow induces epithelial-mesenchymal transition, cellular heterogeneity and biomarker modulation in 3D ovarian

cancer nodules. *Proceedings of the National Academy of Sciences*.

RONKINA, N., MENON, M. B., SCHWERMANN, J., TIEDJE, C., HITTI, E., KOTLYAROV, A. & GAESTEL, M. 2010. MAPKAP kinases MK2 and MK3 in inflammation: complex regulation of TNF biosynthesis via expression and phosphorylation of tristetraprolin. *Biochem Pharmacol,* 80**,** 1915-20.

ROSSO, F., GIORDANO, A., BARBARISI, M. & BARBARISI, A. 2004. From Cell–ECM interactions to tissue engineering. *Journal of Cellular Physiology,* 199**,** 174-180.

ROSTAM, H. M., SINGH, S., VRANA, N. E., ALEXANDER, M. R. & GHAEMMAGHAMI, A. M. 2015. Impact of surface chemistry and topography on the function of antigen presenting cells. *Biomater Sci,* 3**,** 424-41.

ROYER, P.-J., EMARA, M., YANG, C., AL-GHOULEH, A., TIGHE, P., JONES, N., SEWELL, H. F., SHAKIB, F., MARTINEZ-POMARES, L. & GHAEMMAGHAMI, A. M. 2010. The Mannose Receptor Mediates the Uptake of Diverse Native Allergens by Dendritic Cells and Determines Allergen-Induced T Cell Polarization through Modulation of IDO Activity. *The Journal of Immunology,* 185**,** 1522-1531.

RUDOLPH, M. G., STANFIELD, R. L. & WILSON, I. A. 2006. How TCRs bind MHCs, peptides, and coreceptors. *Annu Rev Immunol,* 24**,** 419-66.

SAINI, H., NAVAEI, A., VAN PUTTEN, A. & NIKKHAH, M. 2015. 3D cardiac microtissues encapsulated with the co-culture of cardiomyocytes and cardiac fibroblasts. *Adv Healthc Mater,* 4**,** 1961-71.

SALLUSTO, F. & LANZAVECCHIA, A. 1994. Efficient presentation of soluble antigen by cultured human dendritic cells is maintained by granulocyte/macrophage colony-stimulating factor plus interleukin 4 and downregulated by tumor necrosis factor alpha. *The Journal of Experimental Medicine,* 179**,** 1109-1118.

SALLUSTO, F., LENIG, D., FORSTER, R., LIPP, M. & LANZAVECCHIA, A. 1999. Two subsets of memory T lymphocytes with distinct homing potentials and effector functions. *Nature,* 401**,** 708-712.

SCHILDBERGER, A., ROSSMANITH, E., EICHHORN, T., STRASSL, K. & WEBER, V. 2013. Monocytes, Peripheral Blood Mononuclear Cells, and THP-1 Cells Exhibit Different

Cytokine Expression Patterns following Stimulation with Lipopolysaccharide. *Mediators of Inflammation,* 2013**,** 697972.

SCHMIDT, M., RAGHAVAN, B., MULLER, V., VOGL, T., FEJER, G., TCHAPTCHET, S., KECK, S., KALIS, C., NIELSEN, P. J., GALANOS, C., ROTH, J., SKERRA, A., MARTIN, S. F., FREUDENBERG, M. A. & GOEBELER, M. 2010. Crucial role for human Toll-like receptor 4 in the development of contact allergy to nickel. *Nat Immunol,* 11**,** 814-9.

SCHNEIDER, C. A., RASBAND, W. S. & ELICEIRI, K. W. 2012. NIH Image to ImageJ: 25 years of image analysis. *Nat Meth,* 9**,** 671-675.

SCHNUCH, A., WESTPHAL, G., MOSSNER, R., UTER, W. & REICH, K. 2011. Genetic factors in contact allergy--review and future goals. *Contact Dermatitis,* 64**,** 2-23.

SCHRAML, B. U. & REIS E SOUSA, C. 2015. Defining dendritic cells. *Current Opinion in Immunology,* 32**,** 13-20.

SCHULTZ, H. S., NITZE, L. M., ZEUTHEN, L. H., KELLER, P., GRUHLER, A., PASS, J., CHEN, J., GUO, L., FLEETWOOD, A. J., HAMILTON, J. A., BERCHTOLD, M. W. & PANINA, S. 2015. Collagen Induces Maturation of Human Monocyte-Derived Dendritic Cells by Signaling through Osteoclast-Associated Receptor. *The Journal of Immunology Author Choice,* 194**,** 3169-3179.

SHARMA, N. S., JINDAL, R., MITRA, B., LEE, S., LI, L., MAGUIRE, T. J., SCHLOSS, R. & YARMUSH, M. L. 2011. Perspectives on Non-Animal Alternatives for Assessing Sensitization Potential in Allergic Contact Dermatitis. *Cellular and Molecular Bioengineering,* 5**,** 52-72.

SHARQUIE, I. K., AL-GHOULEH, A., FITTON, P., CLARK, M. R., ARMOUR, K. L., SEWELL, H. F., SHAKIB, F. & GHAEMMAGHAMI, A. M. 2013. An investigation into IgE-facilitated allergen recognition and presentation by human dendritic cells. *BMC Immunology,* 14**,** 54-54.

SHIN, H. J., LEE, C. H., CHO, I. H., KIM, Y. J., LEE, Y. J., KIM, I. A., PARK, K. D., YUI, N. & SHIN, J. W. 2006. Electrospun PLGA nanofiber scaffolds for articular cartilage reconstruction: mechanical stability, degradation and cellular responses under mechanical stimulation in vitro. *J Biomater Sci Polym Ed,* 17**,** 103-19.

SHIN, S. R., JUNG, S. M., ZALABANY, M., KIM, K., ZORLUTUNA, P., KIM, S. B., NIKKHAH, M., KHABIRY, M., AZIZE, M., KONG, J.,

WAN, K.-T., PALACIOS, T., DOKMECI, M. R., BAE, H., TANG, X. & KHADEMHOSSEINI, A. 2013. Carbon-Nanotube-Embedded Hydrogel Sheets for Engineering Cardiac Constructs and Bioactuators. *ACS Nano,* 7**,** 2369-2380.

SILL, T. J. & VON RECUM, H. A. 2008. Electrospinning: Applications in drug delivery and tissue engineering. *Biomaterials,* 29**,** 1989-2006.

SILVA, A. L., ROSALIA, R. A., VARYPATAKI, E., SIBUEA, S., OSSENDORP, F. & JISKOOT, W. 2015. Poly-(lactic-co-glycolic-acid)-based particulate vaccines: Particle uptake by dendritic cells is a key parameter for immune activation. *Vaccine,* 33**,** 847-54.

SLAUGHTER, B. V., KHURSHID, S. S., FISHER, O. Z., KHADEMHOSSEINI, A. & PEPPAS, N. A. 2009. Hydrogels in Regenerative Medicine. *Advanced Materials,* 21**,** 3307-3329.

SLOANE, J. A., BLITZ, D., MARGOLIN, Z. & VARTANIAN, T. 2010. A clear and present danger: endogenous ligands of Toll-like receptors. *Neuromolecular Med,* 12**,** 149-63.

SNIJDER, B. & PELKMANS, L. 2011. Origins of regulated cell-to-cell variability. *Nat Rev Mol Cell Biol,* 12**,** 119-125.

STACHOWIAK, A. N. & IRVINE, D. J. 2008. Inverse opal hydrogel-collagen composite scaffolds as a supportive microenvironment for immune cell migration. *J Biomed Mater Res A,* 85**,** 815-28.

STEBBINGS, R., POOLE, S. & THORPE, R. 2009. Safety of biologics, lessons learnt from TGN1412. *Current Opinion in Biotechnology,* 20**,** 673-677.

STEINMAN, R. M. 1991. The dendritic cell system and its role in immunogenicity. *Annual review of immunology,* 9**,** 271-296.

STRANFORD, S. & RUDDLE, N. H. 2012. Follicular dendritic cells, conduits, lymphatic vessels, and high endothelial venules in tertiary lymphoid organs: Parallels with lymph node stroma. *Front Immunol,* 3**,** 350.

SWARTZ, M. A. & FLEURY, M. E. 2007. Interstitial Flow and Its Effects in Soft Tissues. *Annu Rev Biomed Eng,* 9**,** 229-256.

SWARTZ, M. A., HIROSUE, S. & HUBBELL, J. A. 2012. Engineering Approaches to Immunotherapy. *Science Translational Medicine,* 4**,** 148rv9-148rv9.

SWARTZ, M. A., HUBBELL, J. A. & REDDY, S. T. 2008. Lymphatic drainage function and its immunological implications:

from dendritic cell homing to vaccine design. *Semin Immunol,* 20**,** 147-56.

SZOT, C. S., BUCHANAN, C. F., FREEMAN, J. W. & RYLANDER, M. N. 2011. 3D in vitro bioengineered tumors based on collagen I hydrogels. *Biomaterials,* 32**,** 7905-7912.

TAKAHASHI, H., MATSUZAKA, N., NAKAYAMA, M., KIKUCHI, A., YAMATO, M. & OKANO, T. 2012. Terminally Functionalized Thermoresponsive Polymer Brushes for Simultaneously Promoting Cell Adhesion and Cell Sheet Harvest. *Biomacromolecules,* 13**,** 253-260.

TAKEUCHI, O. & AKIRA, S. 2010. Pattern Recognition Receptors and Inflammation. *Cell,* 140**,** 805-820.

TARAVEL, M. N. & DOMARD, A. 1993. Relation between the physicochemical characteristics of collagen and its interactions with chitosan: I. *Biomaterials,* 14**,** 930-8.

TAZI, K. A., QUIOC, J.-J., SAADA, V., BEZEAUD, A., LEBREC, D. & MOREAU, R. 2006. Upregulation of TNF-alpha production signaling pathways in monocytes from patients with advanced cirrhosis: Possible role of Akt and IRAK-M. *Journal of Hepatology,* 45**,** 280-289.

TEN BROEKE, T., WUBBOLTS, R. & STOORVOGEL, W. 2013. MHC Class II Antigen Presentation by Dendritic Cells Regulated through Endosomal Sorting. *Cold Spring Harbor Perspectives in Biology,* 5**,** a016873.

THÉRY, C. & AMIGORENA, S. 2001. The cell biology of antigen presentation in dendritic cells. *Current Opinion in Immunology,* 13**,** 45-51.

THOMAS, A. H., EDELMAN, E. R. & STULTZ, C. M. 2007. A BRIEF COMMUNICATION: Collagen Fragments Modulate Innate Immunity. *Experimental Biology and Medicine,* 232**,** 406-411.

THYSSEN, J. P., LINNEBERG, A., MENNE, T. & JOHANSEN, J. D. 2007. The epidemiology of contact allergy in the general population--prevalence and main findings. *Contact Dermatitis,* 57**,** 287-99.

THYSSEN, J. P., LINNEBERG, A., ROSS-HANSEN, K., CARLSEN, B. C., MELDGAARD, M., SZECSI, P. B., STENDER, S., MENNE, T. & JOHANSEN, J. D. 2013. Filaggrin mutations are strongly associated with contact sensitization in individuals with dermatitis. *Contact Dermatitis,* 68**,** 273-6.

TIBBITT, M. W. & ANSETH, K. S. 2009. Hydrogels as extracellular matrix mimics for 3D cell culture. *Biotechnol Bioeng,* 103**,** 655-663.

TIRELLA, A., MARANO, M., VOZZI, F. & AHLUWALIA, A. 2008. A microfluidic gradient maker for toxicity testing of bupivacaine and lidocaine. *Toxicology in Vitro,* 22**,** 1957-1964.

TOMEI, A. A., SIEGERT, S., BRITSCHGI, M. R., LUTHER, S. A. & SWARTZ, M. A. 2009. Fluid flow regulates stromal cell organization and CCL21 expression in a tissue-engineered lymph node microenvironment. *J Immunol,* 183**,** 4273-83.

TSENG, S.-Y. & DUSTIN, M. L. 2002. T-cell activation: a multidimensional signaling network. *Current Opinion in Cell Biology,* 14**,** 575-580.

TUSCHL, H., KOVAC, R. & WEBER, E. 2000. The expression of surface markers on dendritic cells as indicators for the sensitizing potential of chemicals. *Toxicol In Vitro,* 14**,** 541-9.

UCHINO, T., TAKEZAWA, T. & IKARASHI, Y. 2009. Reconstruction of three-dimensional human skin model composed of dendritic cells, keratinocytes and fibroblasts utilizing a handy scaffold of collagen vitrigel membrane. *Toxicol In Vitro,* 23**,** 333-7.

VAIDYANATHAN, J., CHINNASWAMY, K. & VAIDYANATHAN, T. K. 2003. Biomimetic recognition and immunochemical assay of ligand binding to collagen. *J Adhes Dent,* 5**,** 7-17.

VALLABHAPURAPU, S. & KARIN, M. 2009. Regulation and function of NF-kappaB transcription factors in the immune system. *Annu Rev Immunol,* 27**,** 693-733.

VAN DEN BULCKE, A. I., BOGDANOV, B., DE ROOZE, N., SCHACHT, E. H., CORNELISSEN, M. & BERGHMANS, H. 2000. Structural and rheological properties of methacrylamide modified gelatin hydrogels. *Biomacromolecules,* 1**,** 31-8.

VAN DER REST, M. & GARRONE, R. 1991. Collagen family of proteins. *FASEB J,* 5**,** 2814-23.

VAN DER VEEN, J., W., VANDEBRIEL, ROB, J., VAN LOVEREN, HANK AND EZENDAM, JANINE. 2011. *Keratinocytes, Innate Immunity and Allergic Contact Dermatitis - Opportunities for the Development of In Vitro Assays to Predict the Sensitizing Potential of Chemicals*, InTech.

VAN DUINEN, V., TRIETSCH, S. J., JOORE, J., VULTO, P. & HANKEMEIER, T. 2015. Microfluidic 3D cell culture: from tools to tissue models. *Current Opinion in Biotechnology,* 35**,** 118-126.

VILLADANGOS, J. A. 2001. Presentation of antigens by MHC class II molecules: getting the most out of them. *Mol Immunol,* 38**,** 329-46.

VOCANSON, M., CLUZEL-TAILHARDAT, M., POYET, G., VALEYRIE, M., CHAVAGNAC, C., LEVARLET, B., COURTELLEMONT, P., ROZIÈRES, A., HENNINO, A. & NICOLAS, J.-F. 2008. Depletion of Human Peripheral Blood Lymphocytes in CD25+ Cells Allows for the Sensitive In Vitro Screening of Contact Allergens. *Journal of Investigative Dermatology,* 128**,** 2119-2122.

VOCANSON, M., HENNINO, A., ROZIERES, A., POYET, G. & NICOLAS, J. F. 2009. Effector and regulatory mechanisms in allergic contact dermatitis. *Allergy,* 64**,** 1699-714.

VON ANDRIAN, U. H. & MEMPEL, T. R. 2003. Homing and cellular traffic in lymph nodes. *Nat Rev Immunol,* 3**,** 867-78.

WAJANT, H., PFIZENMAIER, K. & SCHEURICH, P. 2003. Tumor necrosis factor signaling. *Cell Death Differ,* 10**,** 45-65.

WANG, W., LIANG, H., CHEIKH AL GHANAMI, R., HAMILTON, L., FRAYLICH, M., SHAKESHEFF, K. M., SAUNDERS, B. & ALEXANDER, C. 2009. Biodegradable Thermoresponsive Microparticle Dispersions for Injectable Cell Delivery Prepared Using a Single-Step Process. *Advanced Materials,* 21**,** 1809-1813.

WANNER, R. & SCHREINER, M. 2008. An in vitro assay to screen for the sensitizing potential of xenobiotics. *ALTEX,* 25**,** 115-20.

WATANABE, H., GEHRKE, S., CONTASSOT, E., ROQUES, S., TSCHOPP, J., FRIEDMANN, P. S., FRENCH, L. E. & GAIDE, O. 2008. Danger signaling through the inflammasome acts as a master switch between tolerance and sensitization. *J Immunol,* 180**,** 5826-32.

WIEGAND, C., SCHONFELDER, U., ABEL, M., RUTH, P., KAATZ, M. & HIPLER, U. C. 2010. Protease and pro-inflammatory cytokine concentrations are elevated in chronic compared to acute wounds and can be modulated by collagen type I in vitro. *Arch Dermatol Res,* 302**,** 419-28.

WILLARD-MACK, C. L. 2006. Normal structure, function, and histology of lymph nodes. *Toxicol Pathol,* 34**,** 409-24.

WILLIAMS, A., PEH, C. A. & ELLIOTT, T. 2002. The cell biology of MHC class I antigen presentation. *Tissue Antigens,* 59**,** 3-17.

WILLIAMS, C. G., MALIK, A. N., KIM, T. K., MANSON, P. N. & ELISSEEFF, J. H. 2005. Variable cytocompatibility of six cell lines with photoinitiators used for polymerizing hydrogels and cell encapsulation. *Biomaterials,* 26**,** 1211-1218.

WILLIAMS, D. F. 2008. On the mechanisms of biocompatibility. *Biomaterials,* 29**,** 2941-53.

WILLIAMS, D. F. 2014. There is no such thing as a biocompatible material. *Biomaterials,* 35**,** 10009-14.

WOLF, K., MULLER, R., BORGMANN, S., BROCKER, E. B. & FRIEDL, P. 2003. Amoeboid shape change and contact guidance: T-lymphocyte crawling through fibrillar collagen is independent of matrix remodeling by MMPs and other proteases. *Blood,* 102**,** 3262-9.

WOOLF, E., GRIGOROVA, I., SAGIV, A., GRABOVSKY, V., FEIGELSON, S. W., SHULMAN, Z., HARTMANN, T., SIXT, M., CYSTER, J. G. & ALON, R. 2007. Lymph node chemokines promote sustained T lymphocyte motility without triggering stable integrin adhesiveness in the absence of shear forces. *Nat Immunol,* 8**,** 1076-1085.

XU, H., DIIULIO, N. A. & FAIRCHILD, R. L. 1996. T cell populations primed by hapten sensitization in contact sensitivity are distinguished by polarized patterns of cytokine production: interferon gamma-producing (Tc1) effector CD8+ T cells and interleukin (Il) 4/Il-10-producing (Th2) negative regulatory CD4+ T cells. *J Exp Med,* 183**,** 1001-12.

YANAGAWA, Y. & ONOE, K. 2003. CCR7 ligands induce rapid endocytosis in mature dendritic cells with concomitant up-regulation of Cdc42 and Rac activities. *Blood,* 101**,** 4923-9.

YANG, H., KRUH-GARCIA, N. A. & DOBOS, K. M. 2012. Purified protein derivatives of tuberculin – past, present, and future. *FEMS Immunology & Medical Microbiology,* 66**,** 273-280.

YOSHIDA, M. & BABENSEE, J. E. 2004. Poly(lactic-co-glycolic acid) enhances maturation of human monocyte-derived

dendritic cells. *Journal of Biomedical Materials Research Part A,* 71A**,** 45-54.

YOUNES, H. M. & AMSDEN, B. G. 2002. Interferon-γ therapy: Evaluation of routes of administration and delivery systems. *Journal of Pharmaceutical Sciences,* 91**,** 2-17.

ZHENG, Y. B., MENG, F. G., CHEN, B. Y. & WANG, X. C. 2002. Inactivation and conformational changes of lactate dehydrogenase from porcine heart in sodium dodecyl sulfate solutions. *Int J Biol Macromol,* 31**,** 97-102.

ZHU, J. 2010. Bioactive Modification of Poly(ethylene glycol) Hydrogels for Tissue Engineering. *Biomaterials,* 31**,** 4639-4656.

ZOU, G. M. & TAM, Y. K. 2002. Cytokines in the generation and maturation of dendritic cells: recent advances. *Eur Cytokine Netw,* 13**,** 186-99.

ZUNIGA-PFLUCKER, J. C. & LENARDO, M. J. 1996. Regulation of thymocyte development from immature progenitors. *Curr Opin Immunol,* 8**,** 215-24.

Appendix I

Supplementary data for TNF-alpha PCR

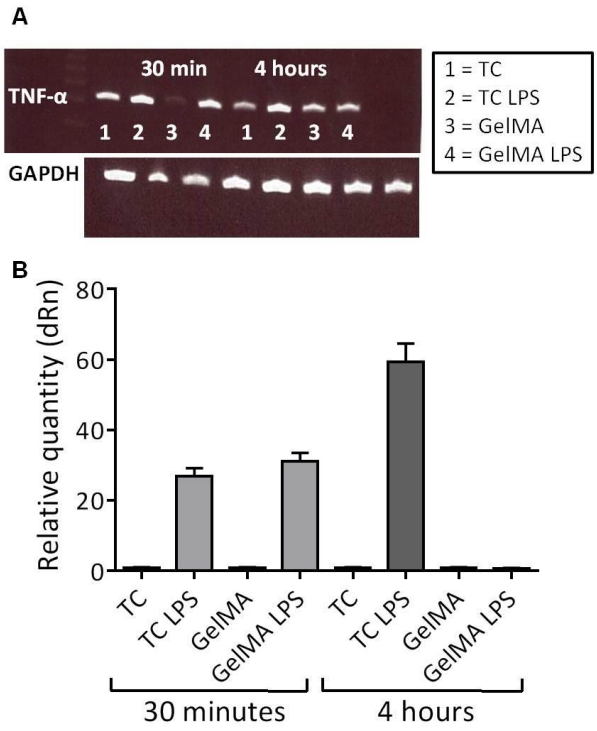

A. Measurement of TNF-α gene expression by conventional ethidium gel-based RT PCR for donor 1. After 30 minutes, band intensity shows up-regulation of TNF-α in TC and GelMA LPS-stimulations. At 4 hours, TNF-α expression is reduced in the stimulated GelMA conditions but up-regulation of expression is maintained in the LPS stimulated TC condition.

B. Analysis of TNF-α expression by real time quantitative PCR for donor 2.TNF-α expression is up-regulated within 30 minutes of stimulation by LPS in both TC and GelMA cultures. After 4 hours, expression is maintained in stimulated TC cultures, however, in the LPS-stimulated GelMA cultures expression is diminished.

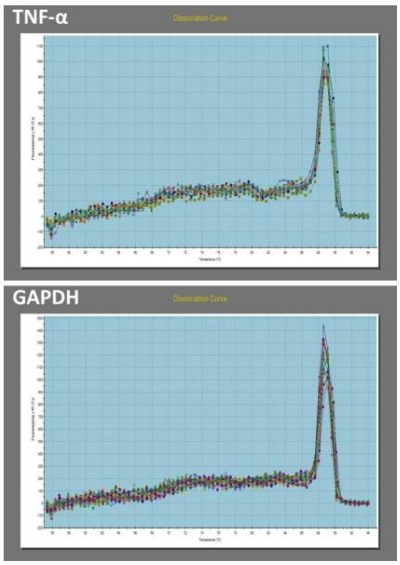

Melt curves from TNF-α and GAPDH quantitative real-time PCR. For each, the single peak is indicative of a specific PCR product.

Appendix II

Microfabrication Technique

Micro-patterning techniques provide a useful way to generate a variety of surface topographies, which can be used for cell culture applications. The advantage of micro-patterning techniques is that they are inexpensive and convenient, whilst giving a fine degree of control over dimensions and a high level of precision over the geometric features.

Micro-scale wells (microwells) produced using micro-patterning methods have previously been used to investigate the effect of well size on cell behaviour. The research in this area concentrated on embryonic stem cell body homogeneity and differentiation (Hwang et al., 2009, Choi et al., 2010).

In relation to the research presented in this thesis, microwell platforms have been identified as potentially valuable tools for studying the effect of well depth and diameter on DC-T cell interactions and subsequent T cell activation. The data presented in Chapter 4 of this thesis suggested that differences in the distribution of cells between the U-bottom TCP wells and the collagen hydrogel affected the outcome of the T cell response.

A customised array of microwells of varying diameter and depth was produced. Microwells were fabricated from poly(ethylene glycol) diacrylate (PEGDA), using a photolithography micro-patterning method as illustrated in Figure i. PEGDA is cell-repellent, thus reducing the cell interactions with the substrate

in order to focus on the effect of the geometry of the microenvironment on cell behaviour.

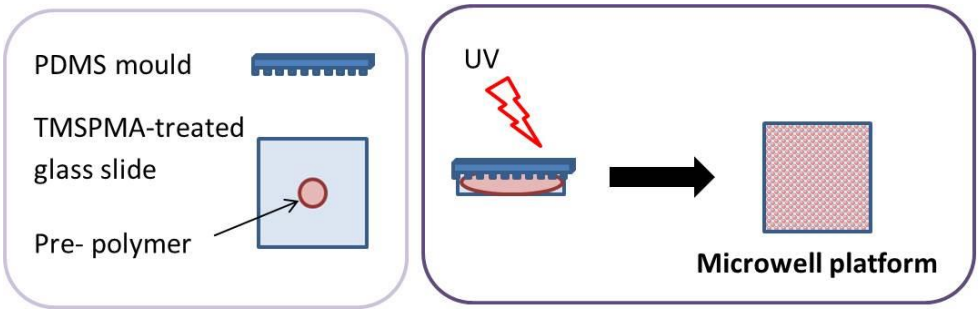

Figure i. Schematic representation of microwell fabrication by photolithography.
A drop of pre-polymer solution is applied to a TMSPMA-functionalised glass slide. A PDMS mould is put on top of the polymer solution and exposed to UV to photo-cross link the polymer giving rise to a micropatterned surface.

To investigate the precision of the fabrication technique and examine the integrity of the microwell structures, samples were analysed by environmental scanning electron microscopy (eSEM). eSEM is useful as it does not require sample dehydration, thereby allowing one to obtain high resolution images of hydrated structures, such as micro-patterned hydrogels.

Figure ii shows representative micrographs taken by eSEM. The microwell patterns were robust and consistent. This demonstrated the reproducibility of the technique for the fabrication of precisely micro-patterned platforms. Overall, the microwells showed great promise for cell culture applications as a vast range of dimensions can be produced depending on the application. They can provide a defined microenvironment with precise dimensions which gives a high level of experimental control.

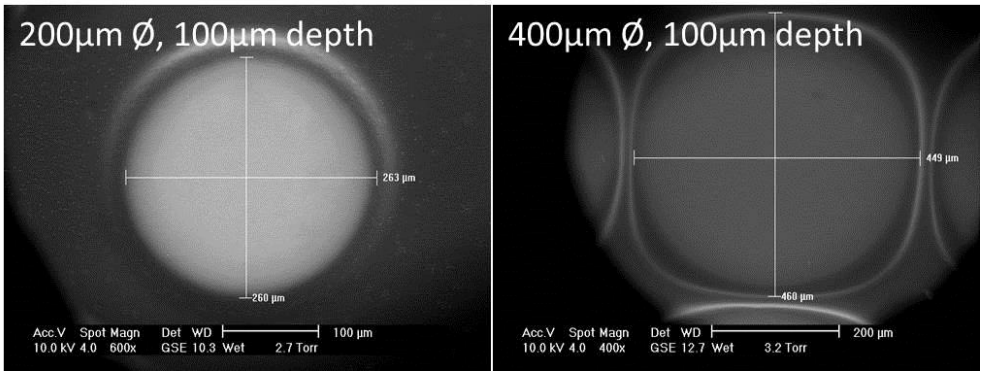

Figure ii. Microwell characterisation by eSEM.
Analysis of microwell structures demonstrated a robust and consistent microwell pattern generated using a photolithography micro-patterning method. eSEM was performed using a FEI Quanta 650 ESEM system.

Microwell Fabrication – Materials and Method

The method for microwell fabrication has been described previously (Karp et al., 2007, Hwang et al., 2009, Moeller et al., 2008). PDMS stamps were used to mould the microwells, the stamps were made by pouring a mixture (10:1) of Sylgard 184 silicone elastomer base solution and curing agent (purchased from Dow Corning) onto a negative template in a petri dish. This was then put into a vacuum chamber for 1 hours to remove air bubbles. Finally, it was transferred to an oven, set at 80°C, for 2 hours to cure.

Hydrogel microwells were fabricated from Poly(ethylene glycol 1000 Dimeth-acrylate) (purchased from polysciences). A 0.5% w/v photoinitiator solution (Irgacure 2959) was prepared in PBS. Then a 10% w/v PEGDA solution was made in the 0.5% photoinitiator solution. A 15µL drop of PEGDA monomer solution was dispensed onto a TMSPMA-functionalised glass slide, a PDMS stamp was then placed on top. The PEGDA was photo cross-linked by exposure to UV light (180 seconds, 850mW, 8.5cm). Finally, slides were submerged in PBS to wash away excess un-polymerised solution and allow gels to swell to a uniform shape.